UNIVERSITÀ DEGLI STUDI DI PADOVA

Dipartimento di Fisica e Astronomia "Galileo Galilei"

Master Degree in Physics

Final Dissertation

Perturbative Unitarity Constraints on Dark Matter Theories with Vector Portals

Thesis supervisor

Prof./Dr. Francesco D'Eramo

Thesis co-supervisor

Prof./Dr. Natascia Vignaroli

Candidate

Matteo Pio Narcisi

Academic Year 2022/2023

Contents

Introduction

The complete picture of phenomena and particles governing our Universe is far from being clear. Not too long ago we found out that the visible sector of particle physics corresponds to a mere 5% of the total energy budget. In fact recent data suggest that the major components of this budget are dark matter (25%) and dark energy (70%), both of which are nearly completely unknown to us in their composition and structure.
This kind of knowledge is relatively recent, in fact, the whole concept of dark matter is as old as the beginning of the 20th century when it was formulated after the revolutionary researches of the Caltech professor Fritz Zwicky in the 1930's. Anyways today we possess different types of evidence about the existence of dark matter at different scales: galactic, galaxy cluster and cosmological.
Before talking about these three sectors, it could be of purely intellectual interest to delve a little bit more into the historical aspect of the conceptual formulation of dark matter.
Throughout history numerous philosophers speculated about the existence of planets, galaxies or cosmological systems that were too far away from us or too dim to be detected by us, becoming indeed invisible to our searches.
A valiant force that, during the centuries, has come in help to unveil potentially existing cosmological systems that, for some reason, were invisible to us is the gravitational interaction.
A classic example of this situation is the discovery of the planet Neptune by the astronomers Urbain Le Verrier and John Couch Adams [5] . Both of them were able to identify anomalies in the trajectory of Uranus confronting the results of the application of Newton's laws and the observational evidence. It came out that the anomaly was to be attributed to the presence of an additional planet with a non-trivial mass that was influencing Uranus' motion with its gravitational field.
The discovery of Neptune is an evident example of how the laws of gravity are able to spot the presence of what could be invisible structures to our eyes.
Thanks to his previous intuitions on Neptune, Le Verrier tried to explain the anomalous path of Mercury around the Sun with, yet again, another invisible planet called "Vulcan". It was here that his fortune came to an end since it would require Einstein's General Relativity theory to explain Mercury's orbit.
Even though wrongful, this is another example of the power of gravitational force as an instrument to shed light into the darkness of astronomical data.
This is crucial since even to the present day, almost the totality of proof in our hands concerning dark matter displays a gravitational nature. For this type of matter considered collisionless and weakly interacting with light, gravity is the only interaction that allows us to unveil its presence. In the following section, we will examine more clearly the

complete meaning of these sentences.
To complete this historical framework, it is curious to notice that in the late 19th century doubts about the presence of dark regions in the sky began spreading in astronomical circles. After the invention of astronomical photography, it was observed the presence of dark regions inside stellar fields that enticed the idea of the existence of an undiscovered type of matter along the line of sight responsible for the absorption of light.
It was not until some decade later that the concept of dark matter assumed the conceptual frame that still possesses to this day, by the hands of a few pioneers like Zwicky and Vera Rubin.
The aim of this master thesis is, as the title suggests, to analyze and discuss dark matter theories with a Z' vector portal and, in particular, the constraints coming from the analysis of perturbative unitarity. The structure of the thesis is the following. In the first chapter, we will proceed to examine the main evidence of the existence of dark matter, starting from Zwicky's discovery and we will try to outline constraints coming from both experimental measures and theoretical predictions in order to narrow the field on what really is dark matter.
Then in the second chapter we will provide a description of the main particle candidates to constitute dark matter in WIMPs and we will try to draw an inclusive picture of the major research fields in which our efforts on finding dark matter are concentrated.
The third and fourth chapters will be focused on Z' vector dark matter models and their perturbative unitarity constraints, the most important part.

Chapter 1

Evidence of dark matter

1 Zwicky's discovery

Even though this would be more of a cluster scale proof, for chronological reasons we start the conversation about dark matter talking about the man who first found out about his existence. As said shortly before, the introduction of dark matter in the scientific community is to be attributed to Fritz Zwicky who, like other physicists of that time, focused his observation on the Coma cluster, which had the peculiarity of presenting a strong central condensation and a tendency towards the spherical symmetry. It was the latter and very peculiar trait that got Zwicky more into this atypical cluster.

The originality in Zwicky's approach was to apply the virial theorem in a context so far from thermodynamics like that of a group of galaxies. He was not the first to use this theorem outside the normal area of expertise. Henry Poincarè had applied it to astronomy a couple of decades earlier, but the Caltech professor was, to the best of our knowledge, the first one to employ it to calculate the mass of the galaxies.
He first noticed large velocity dispersion in the galaxies composing the Coma cluster, typically more than 1000 km/s. Despite the velocity gap between galaxies, the system had not fallen apart: some kind of force was keeping it together. Even though this was undoubtedly a breakthrough, it was not considered big news at the time, since large differences in velocities of galaxies present in Coma compared to other clusters had already been observed by Hubble years prior.

Of course, pysicists first guess in order to explain the existence of this cluster was gravity: the strength of this interaction had to be responsible for the boundness of the system. Zwicky's work and discovery was the demonstration that, to hold the system together, the amount of mass required had to be orders of magnitude superior to that inferred by luminous measurements.
First, he counted approximately the number of galaxies in the cluster, so to extrapolate its mass, obtaining as a result a number close to 800. He took, as suggested by Hubble, the average mass of a galaxy to be of the order of $10^9 M_\odot$.
He then proceeded to indagate the luminosity of the cluster and presented a mass-to-light

Figure 1.1: Mosaic of the Coma cluster from [31]

factor of about $\frac{M}{L} \sim 400\frac{M_\odot}{L_\odot}$. Thanks to a conversion factor fixed by experiments, he obtained a result in terms of the mass of the Coma cluster inferred by electromagnetic measurements

$$M_{Coma}^{(vis)} \simeq 1,6 \times 10^{42} kg. \tag{1.0.1}$$

To obtain a second term of comparison, he proceeded to calculate the same value of mass with the virial theorem. In its simplest form it states that in a system in kinetic equilibrium:

$$T = -\frac{1}{2}U \tag{1.0.2}$$

where T and U are respectively the kinetic energy and the gravitational potential of the system.
He assumed spherical symmetry and kinetic equilibrium for Coma, properties that were supported by observation, and proceeded to calculate the two terms of the equation. For the kinetic energy he used the simple formula

$$T = \sum_i \frac{1}{2} m_i v_i^2. \tag{1.0.3}$$

He assumed that the galaxies have approximately the same mass m_{gal} and made use of the average velocity defined as

$$< v^2 >= \frac{\sum_i v_i^2}{N_{gal}} = \frac{\sum_i m_i v_i^2}{m_{gal} N_{gal}} = \frac{2T}{M_{Coma}}. \tag{1.0.4}$$

This quantity can be easily obtained by measurements of simple Doppler effects.
For what concerns the gravitational potential, it can be written as

$$U = -\sum_{i<j} \frac{G m_i m_j}{r_{ij}} = -\frac{3}{5}\frac{G M_{Coma}^2}{R_{Coma}} \tag{1.0.5}$$

if one makes use of the spherical symmetry and of the total mass of the cluster M_{Coma}. Using the data he had collected, Zwicky estimated the Coma mass as

$$M_{Coma}^{(grav)} = \frac{5}{3}\frac{R_{Coma} < v^2 >}{G} \simeq 2,4 \times 10^{44} kg. \tag{1.0.6}$$

Even at this point is pretty clear that

$$M_{Coma}^{(grav)} >> M_{Coma}^{(vis)}. \tag{1.0.7}$$

The easiest hypothesis that could be made to explain such a discrepancy is the presence of additional dark mass. Indeed Zwicky presented to the scientific community in 1937 the results of his work and the final hypothesis, which by the time was more of a gamble, talking about "*dunkle materie*" [52] or dark matter and, with little if any surprise, was largely ignored by the rest of the physicists.
Zwicky's findings, although misregarded, were revolutionary and are considered still in the present days as the most overwhelming evidence of the presence of Dark Matter in the Universe.

2 Galactic scale

Let's move on to galactic scales. We present maybe the most striking proof of DM existence after Zwicky's one. This discovery also happened chronologically after the one that we have just described and, even though at completely different scales, it only confirmed and added validity to Zwicky's claims.

2.1 Spiral galaxies

We find ourselves decades later, in the 1970's when another incredible discovery came with the work of Vera Rubin and her research group. Together they used the improved technologies of those years to observe galactic velocities far away from the galactic center. What was found was quite unexpected: the rotation curves of galaxies expressed a $flat$ behavior far beyond the extent of the visible galactic disk.
Even in this case, the math is quite simple: one can use Newton's laws to calculate the circular velocity of stars orbiting due to the weakness of gravity [44] [2].
By getting the acceleration experienced by a probe star from the equation of motion, one can see that

$$\frac{v^2}{r} = \frac{GM(r)}{r^2} \tag{2.1.1}$$

this leads to

$$v(r) = \sqrt{\frac{GM(r)}{r}} \tag{2.1.2}$$

If one looks at the mathematical form of the velocity he can see that for radii inside the galactic radius, it will be proportional to r as one can express M as $M(r) = \frac{4}{3}\pi r^3 \rho(r)$, with $\rho(r)$ the density of matter.
So inside the galaxy, where $M(r) \propto r^3$, with the density approximately constant, the

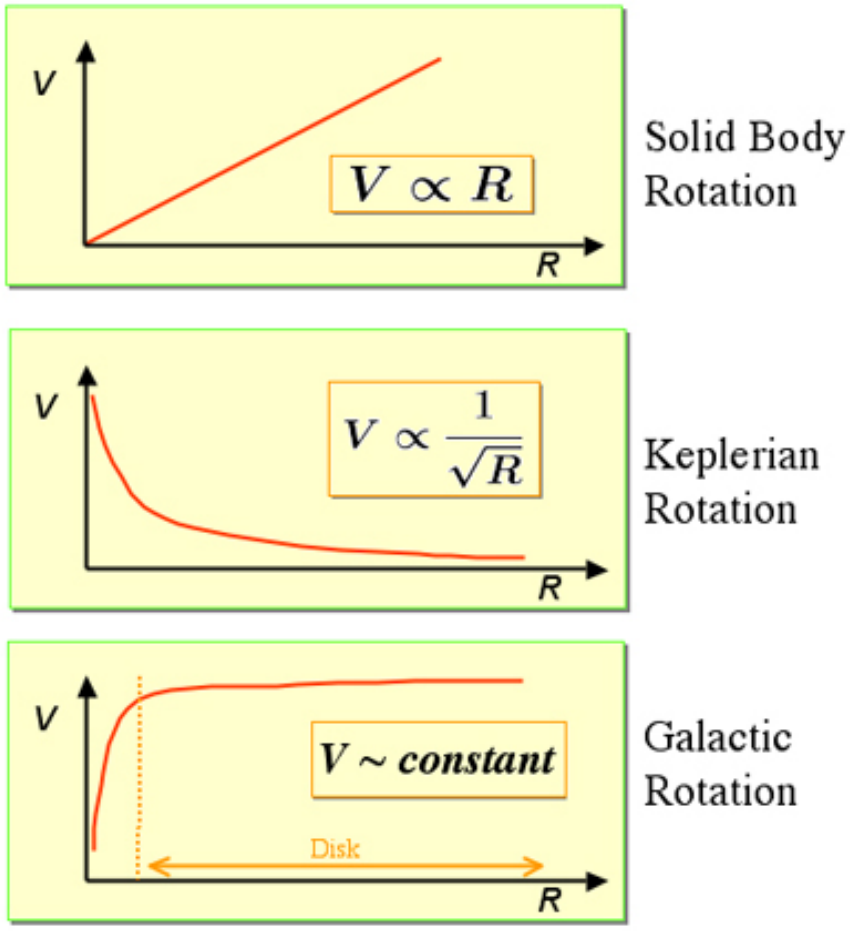

Figure 1.2: rotation curves of respectively: a solid body, the solar system and a spiral galaxy from [27]

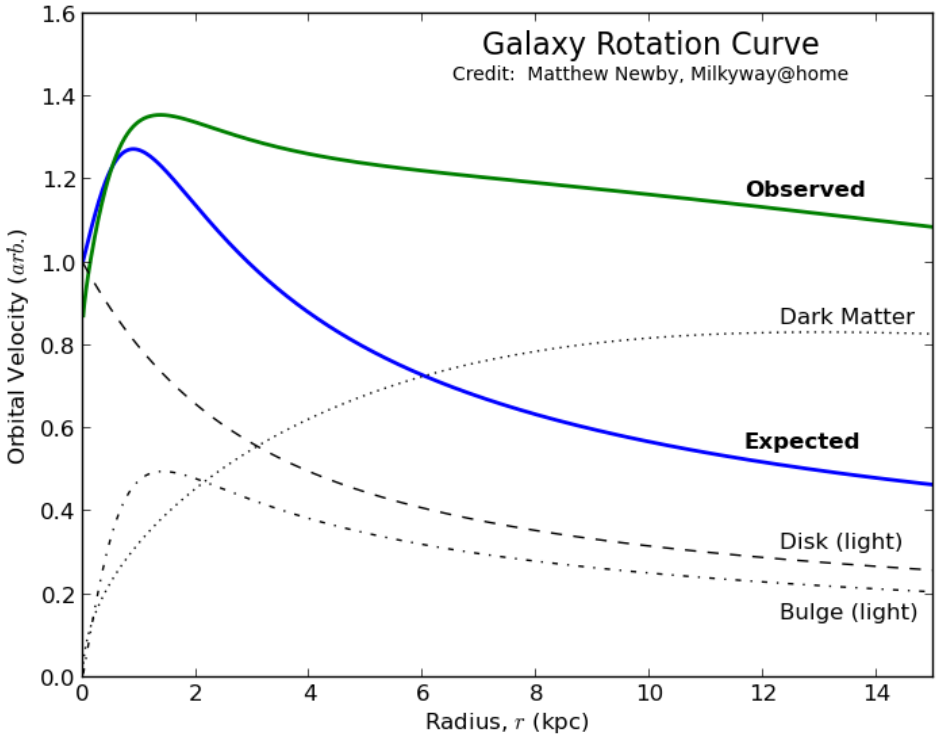

Figure 1.3: An example of the flat behavior of the rotation curve. From [34]

formula will give us the already cited proportionality. Outside the galactic radius, the mass of the galaxy is saturated and $M(r)$ will not change since all the mass is inside the galaxy. This means that $v(r)$ would be solely proportional to $\frac{1}{\sqrt{r}}$.

$$v(r) \propto \begin{cases} r & r << r_{gal} \\ r^{-\frac{1}{2}} & r >> r_{gal} \end{cases} \tag{2.1.3}$$

What was incredible was to find a flat behavior in which $v(r)$ remains almost constant even at distances far away from the galactic center. In 1980 they published their result to support Zwicky's thesis about the additional mass of the galaxies.

Today we are able to obtain precise measurements of the velocity of stars in spiral galaxies with the help of observation of the Doppler shift of the 21 cm line transition of hyperfine hydrogen. Moreover, spherical symmetry can be employed due to most of the matter in spiral galaxies being concentrated in the center. This is a strong approximation but gives us the same qualitative results.
It is to take account of the fact that even with the fast technological progress of the last decades, the result obtained for the galactic rotation curves do not change, showing regions with the anomalous $flat$ behavior stretching for hundreds of parsec away from the galactic center.
A way to explain this is MOND [25] , an acronym that stands for MOdified Newtonian Dynamics. The idea here is to slightly correct Newton's second law $F = ma$ with a factor μ to get $F = ma\mu(a)$, where μ is usually close to unity apart from cases of small acceleration where $\mu \propto \frac{a}{a_0}$.

This way the gravitation law is modified and for a star outside a galaxy of mass M

$$F = \frac{GMm}{r^2} = ma\mu \tag{2.1.4}$$

and in the low acceleration limit with $a << a_0$

$$a = \frac{\sqrt{GMa_0}}{r}. \tag{2.1.5}$$

Following the above procedure, we equate this to the centrifugal acceleration

$$\frac{\sqrt{GMa_0}}{r} = \frac{v^2}{r} \implies v = (GMa_0)^{\frac{1}{4}} \tag{2.1.6}$$

recovering the behavior we have already seen but without the use of additional matter.
Although in agreement with observation, MOND is not able to explain other evidence for dark matter, like the one at cluster scales or CMB anisotropies, so this characteristical pattern can only be explained using additional matter.

2.2 Elliptical galaxies

We can't measure rotation curves for elliptical galaxies, which are not flat like spiral galaxies. Instead, we can study the mass-to-light ratio of elliptical galaxies with gravitational lensing [6], a method that we'll explain in the next section. As the galaxy passes between us and a quasar, the light from the quasar is bent by the gravity of the galaxy. If the galaxy is directly between us and the quasar, the quasar appears to be smeared out in a ring around the galaxy, usually called an Einstein ring.
Alternatively one can use the virial theorem in the exact same way operated by Zwicky. Also in this case it appears that there is an excess of matter compatible with that found in the case of spiral galaxies.

3 The scale of galaxy clusters

Earlier we have extensively discussed Zwicky's findings on the Coma cluster and of how $\frac{M}{L} \sim 400\frac{M_\odot}{L_\odot}$, showing an exceeding ratio with respect to the solar neighborhood of two odrers of magnitude.
With the knowledge of Friedman's equations on our side, we can write an equation for the Hubble parameter

$$H^2 = \frac{8\pi G}{3}\rho - \frac{kc^2}{a^2} \tag{3.0.1}$$

where ρ is the energy density, k is the curvature factor, c is the speed of light and a the scale factor. In a flat Universe (ours appears to be close to flat from the recent measurements) $k \sim 0$, so we can write an equation for the critical energy density

$$\rho_C = \frac{3H(t)^2}{8\pi G} \tag{3.0.2}$$

and introduce a new factor Ω

$$\Omega = \frac{\rho(t)}{\rho_C(t)} \tag{3.0.3}$$

for each species present in the Universe.
For dark matter today, thanks to measurements at cluster scales, we can safely say that the total Ω for matter, baryonic and dark, is

$$\Omega_M \sim 0,2 - 0,3. \tag{3.0.4}$$

Before starting to talk about dark matter in this sector though, it is convenient to clarify that a cluster is composed of

- galaxies: spotted through optical observations
- intergalactic gas: plasma at high temperature that emits x-rays by thermal bremsstrahlung. The gas does not fall inside the galaxies but fills the cluster.

Here it is convenient to apply, for the intergalactic gas, the equation

$$\frac{dP(r)}{dr} = -\frac{GM(r)\rho(r)}{r^2} \tag{3.0.5}$$

since we are considering a system in hydrostatic equilibrium with spherical symmetry.
We are equating the contribution of the pressure of the gas to the one of the gravitational force.
Here P and ρ indicate pressure and energy density respectively, while $a(r)$ is the gravitational acceleration of the gas at radius r.
Considering the equation of state for a gas we can relate pressure and temperature through

$$P = k(\sum_i n_i)T = k\frac{\rho}{\mu m_P}T \tag{3.0.6}$$

with m_P the mass of the proton and μ the average molecular weight fixed approximately at $\mu \simeq 0,6$. We can manipulate these expressions in the final formula and solve for $M(r)$

$$\frac{d\log(\rho)}{d\log(r)} + \frac{d\log(T)}{d\log(r)} = -\frac{r}{T}(\frac{\mu m_P}{k})\frac{GM(r)}{r^2} \tag{3.0.7}$$

The temperature of the cluster is approximately constant outside the cores, plus the density profile of the gas observed is a power law at large radii.
It can be calculated that

$$kT \approx (1,3 - 1,8)keV\big(\frac{M_b}{10^{14}M_\odot}\big)\big(\frac{1Mpc}{r}\big) \tag{3.0.8}$$

with M_b equal to the contribution of the baryonic matter only[6].
Even in this case, the disparity between the expectations and what is found in the experiments suggests the presence of additional non-baryonic matter.

3.1 Gravitational lensing

Another powerful instrument at these scales is gravitational lensing. Einstein's general theory of relativity describes how mass concentrations distort the space around them. A gravitational lens can occur when a huge amount of matter, like a cluster of galaxies, creates a gravitational field that distorts the light from distant galaxies that are behind it but in the same line of sight. If an observer was located at the correct distance, the deflected light rays from around the celestial object would converge to make a magnified image. This is a phenomenon known as strong gravitational lensing.
In a weak gravitational lens, light rays are not deflected enough to magnify the image, instead they introduce subtle distortions.
The simplest type of gravitational lensing occurs when there is a single concentration of matter at the center, such as the dense core of a galaxy. The light of another distant galaxy is redirected around this core, often producing multiple images of the background galaxy.
More complex gravitational lensing arises in observations of massive clusters of galaxies. Background galaxies are lensed by the cluster and their images often appear as short, thin "lensed arcs" around the external border of the cluster.
The distribution of lensed images reflects the distribution of all matter, both visible and dark.
Several distorted images distribute around the so-called Einstein circle which possesses the property being related to the mass giving deflection through its angular radius

$$\theta_E = \sqrt{\frac{4GM}{c^2}\frac{(D_S - D_L)}{D_S D_L}} \tag{3.1.1}$$

where M is the lens' mass, D_L is the distance of the lens and D_S is the distance of the source of light rays[2].
Gravitational lensing suggests that only $10\% - 20\%$ of the total mass is visible, the rest is dark.

3.2 Bullet cluster

The biggest challenge of indirect dark matter observations has been the spatial coincidence of DM and baryonic matter. Indeed of all the examples we have just presented, no one shows any kind of separation between baryonic and dark matter, they blend in an undistinguishable unique entity. A system in which DM and baryons were spatially segregated is ideal for such a study.
Galaxy mergers are some of the most violent events in the universe. Galaxies are made up of stars, gas and plasma for less than 10% of their matter budget, the rest should be only dark matter. During collisions, stars rarely collide, the gas and plasma interact through gravity as well as electromagnetic friction-like interactions, and the dark matter is expected to be collisionless and pass right through at high velocities. Once the merger has taken place (over a period of a few million years), an interesting result is seen. The Bullet Cluster, discovered in 1998, is the prototypical example of galaxy merger [23] .

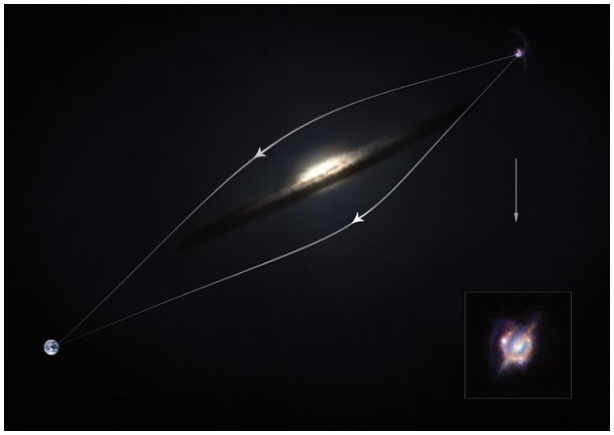

Figure 1.4: Strong gravitational field cause light that passes by to be deflected.The distant source appear distorted, but brighter, forming characteristic rings of light, known as Einstein rings. From [26]

Figure 1.5: Galaxy cluster Abell 370 composed of several hundreds of galaxies. The blue arcs are distorted images of remote galaxies behind the cluster. From [32]

In a merger the stars would almost always pass by one another without individual stellar collisions and would emerge as separate systems, in fact they can be considered as a collisionless system. The more abundant gas atoms in each system, however, are bound to collide with their counterparts in the other system the moment they crash.

If we consider the scenario in which there is no DM in the Universe, then the source of the gravitational force in this system would be the intergalactic gas in the middle of the picture, since, in terms of mass, the gas dominates over the stars by a factor of ten. This means that we would observe the direction of gravitational interactions to be pointing towards the middle of Figure 1.6, where all the intergalactic gas is concentrated.
Instead, if dark matter dominates, then it will completely disregard collisions and it will behave as stars do and appear in two separate lumps in the right and left corners of the image. Then we would observe the gravitational force to be pointing toward dark matter direction, which is the center of the two stellar systems.
By looking at the orbital velocities of the stars, one can easily determine the direction of gravity, and observers found that it is clearly pointing toward the centers of the blue patches, the centers of the two stellar systems, and not toward the gas in between them.

We can see from Figure 1.6 the hot gas which assumes this characteristic pink shade right in the center of the picture and contains the majority of baryonic matter. In fact the bullet-shaped mass on the near right is nothing but hot gas from one cluster, which is gone through the intergalactic gas of the other cluster during the collision. Here we can see the galaxies with different colors, mostly orange and white. The interesting part instead are the blue areas which is where astronomers find most of the mass in the clusters. We can use gravitational lensing in order to extrapolate the mass concentration and, to our surprise, the result is that the majority of the mass is clearly concentrated in the blue areas and is separated from the baryonic matter in the pink area. This is not only clear

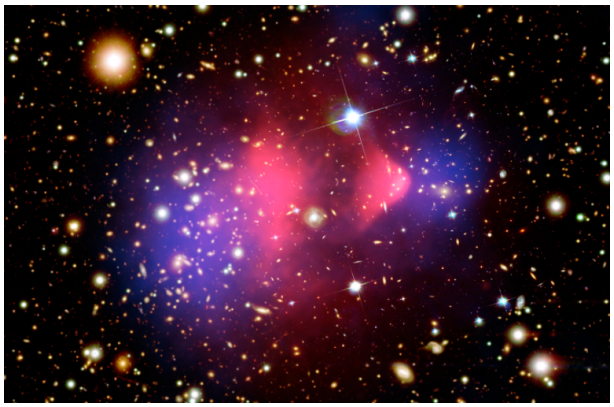

Figure 1.6: Composite image of the Bullet cluster. Red: hot gas observed by the Chandra X-Ray Observatory. Blue: major part of the mass deduced from gravitational lensing. From [36]

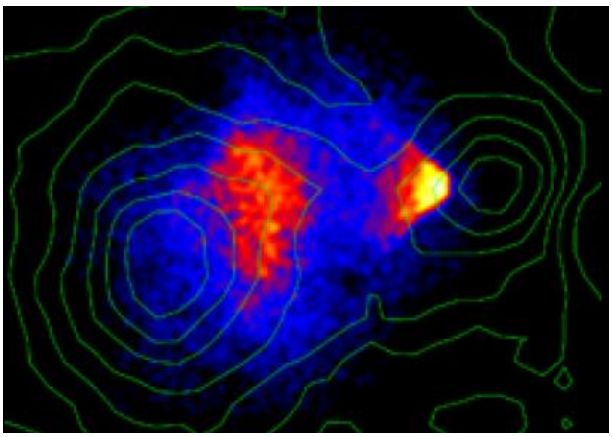

Figure 1.7: Bullet cluster, mass density contours, in green, obtained through weak lensing, superimposed over photograph. From [29]

proof that there is a different kind of non-baryonic matter, but also that it is dominating in quantity with respect to the baryonic one.

Another precious hint lies here on the true nature of dark matter. Because it is composed of baryonic matter, the intergalactic gas from the two clusters cannot help but collide with each other, thus slowing down and accumulating near the collision area. Instead dark matter, which is assumed to be collisionless, clearly comes out of the collision unfazed. By avoiding completely the crash, dark matter separates completely from the intergalactic gas during the collision and it is able to create the blue area that we have seen, gifting us with this amazing opportunity to observe it alone. If hot gas was the most massive component in the clusters, as proposed by alternative theories of gravity, such an effect would not be seen. Instead, this result shows that dark matter is required.
This is clear disproof of theories that suggests that dark matter doesn't exist, like MOND.

4 Cosmological scales

CMB is a unique and unreplaceable tool. It was emitted approximately at $t \simeq 10^5 yr$ after the Big Bang and its distribution look like the one of a black body in thermal equilibrium. It was produced at *last scattering surface* when matter and radiation decoupled, the Universe became transparent to radiation. From that point in time, photons' mean free path stretched and can be observed today coming from every direction in the sky at a temperature

$$T_{CMB} \simeq 2,73K \simeq 2,4 \times 10^{-4} eV \tag{4.0.1}$$

CMB is essentially a picture of how the Universe was at its emission. It can serve in innumerable ways to us as an instrument to be confronted with our predictions about the evolution of the Universe. We do not possess any consistent data about the Universe prior to CMB emission, this adds to the already stressed importance of this distribution. Cosmic Microwave Background(as CMB stands for) was postulated in 1948 by Ralph Alpher and Robert Herman, but was only detected accidentally in 1964 by Arno Penzias

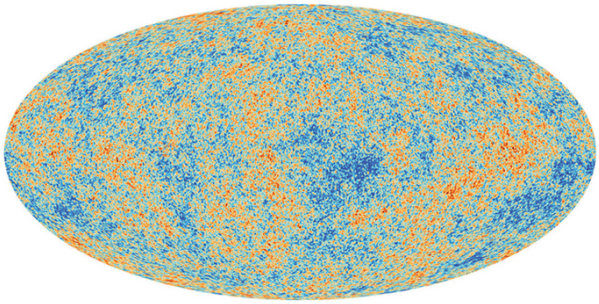

Figure 1.8: Full-sky map of the tiny temperature anisotropies of the CMB. From [35]

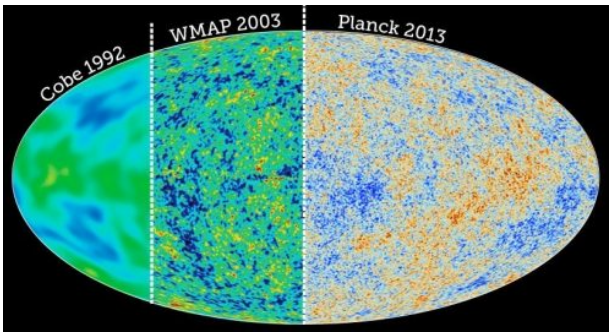

Figure 1.9: Resolution of the CMB maps for all three satellites. From [39]

and Robert Wilson who were working with a simple radio antenna in New Jersey. This fortunate event awarded the Nobel prize.
The first space mission specifically designed to study the cosmic microwave background (CMB) was the Cosmic Background Explorer (COBE), launched by NASA in 1989. The measurements show a spectrum that conforms extremely precisely to a black body with error bars that have to be multiplied by a factor of 400 not to be visible in the plot.
CMB is almost isotropic. The reason for the use of the word *almost* is the fact that it exhibits fluctuations in temperature of the order of $\frac{\Delta T}{T} \sim 10^{-5}$.

All data we collected at smaller scales would not provide us with precise information about the total amount of dark matter in the Universe, this comes from the analysis of the CMB and its power spectrum.

Indeed the study of CMB anisotropies allows us to put stringent constraints on cosmological parameters. Let's expand in spherical harmonics temperature fluctuations

$$\delta T(\theta, \phi) = \sum_{l=2}^{\inf} \sum_{m=-l}^{l} a_{lm} Y_{lm}(\theta, \phi) \tag{4.0.2}$$

where $Y_{lm}(\theta, \phi)$ are spherical harmonics and θ and ϕ cover the solid angle.
Here the sum starts at 2 because the term with $l = 0$ is the monopole contribution that sets the overall temperature of CMB and is of no interest to us. The term with $l = 1$ gives us the dipole contribution which in turn depends on the Earth's movement around the rest frame of CMB and is again of no use to us.
We can call c_l the variance of the factor a_{lm}

$$c_l =< |a_{lm}^2| > \frac{1}{2l+1} \sum_{m=-l}^{l} |a_{lm}^2|. \tag{4.0.3}$$

c_l depends only on l because of isotropy. The power spectrum reads

$$< \delta T(\theta_i, \phi_i) \delta T(\theta_j, \phi_j) >= \sum_l (2l+1) c_l P_l(cos\theta_{ij}) \tag{4.0.4}$$

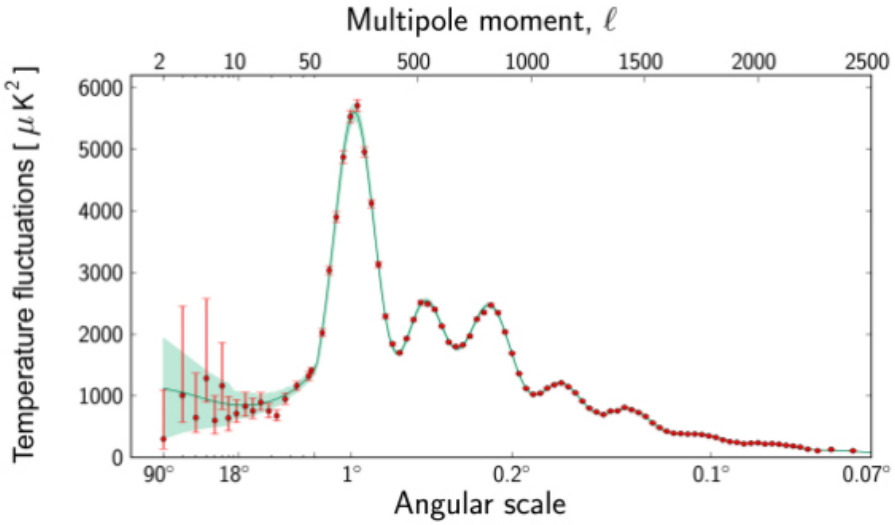

Figure 1.10: CMB power spectrum from [37]

with $P_l(cos\theta_{ij})$ being the Legendre polynomials evaluated at the angle between the directions i and j. If one assumes the fluctuations to be gaussian as it appears to be the case with recent measurements, it can be seen that all information about CMB is compressed inside this power spectrum.
We are interested in the behavior of c_l as function of l, but usually what is plotted is

$$(2l+1)\frac{c_l}{2\pi}. \tag{4.0.5}$$

NASA's second-generation space mission, the Wilkinson Microwave Anisotropy Probe (WMAP) was launched in 2001 to study these very small fluctuations in much more detail. Finally, ESA's Planck was launched in 2009 to study the CMB in even greater detail than ever before. It covers a wider frequency range in more bands and at a higher sensitivity than WMAP, making it possible to make a much more accurate separation of all of the components of the submillimeter and microwave wavelength sky. This reveals the CMB and its tiny fluctuations in much greater detail and precision than previously achieved.
CMB power spectrum is affected in different ways by baryonic matter and dark matter, thus making it possible for us to separate the two contributions and get estimates of the abundances of these two quantities [21] [6].
At the time of CMB formation, the Universe was filled with photons, neutrinos, electrons, protons and dark matter. Electrons and protons try to combine and form hydrogen atoms, but the pressure exerted by photons would break their bond. Photons can interact with electrons by means of coulomb and Compton scattering and the overall effect of the interactions is an oscillatory motion where the radiation pressure depends on the speed of sound in the primordial plasma. Presence of baryonic matter affects this value, keeping it smaller than $c_s = \frac{c}{\sqrt{3}}$, the value assumed in a pure photonic gas.
Dark matter is believed to be decoupled from the primordial plasma by this time, so it would interact only gravitationally, thus not contributing to the radiation pressure.
With the power spectrum one is able to spot both the overall amount of matter and that

of baryonic one, with values at the present time of

$$\begin{cases} \Omega_M h^2 = 0,1428 \pm 0,0011 \\ \Omega_b h^2 = 0,02233 \pm 0,00015 \end{cases} \tag{4.0.6}$$

with h being a number $h \simeq 0,7$. So for dark matter we have

$$\Omega_{DM} h^2 = 0,1198 \pm 00012 \tag{4.0.7}$$

Here one can see dark matter presence at the time of CMB formation and that the amount of Dark matter in the universe at that time was more or less five times the one of common baryonic matter.

4.1 Numerical simulations

Before talking about the numerical simulations we first need to introduce the cosmological principle, which constitutes the basis for cosmology.
It states that, at large scales, our Universe is homogeneous and isotropic. Here by large scales we mean hundreds of Mpc. Homogeneity is confirmed by studies on galactic distributions and, as we have already seen, isotropy is clearly observed in CMB analysis.
There are also philosophical reasons that support the cosmological principle, like the fact that the Universe should appear the same to observers located in different places, as there is no reason to suppose the opposite.
We have already talked about the time when CMB is emitted and atoms form and experience gravity. At this point, matter will experience two different and opposite effects. For starters, it will feel the gravitational interaction, as we said, which will drag particles together and be responsible for their fall in a dense core. Secondly, we have to take into account the fact that Universe is expanding, this is responsible for the separation of large structures, that will be affected by the stretching of the very fabric of the Universe. Obviously these two effects are antagonists and the Universe as we observe it today will be the final product of a long, still-lasting process, that has these forces as main dance partners.
Thanks to the cosmological principle we were able to create a model able to explain cosmological observations which we refer to as ΛCDM. Here Λ identifies the dark energy component of our Universe which covers approximately 70% of the total energy budget and CDM stands for *cold dark matter*, a model of Dark matter with the features that better fit the observations, as we will see in the next chapter.

Here, as we have also seen previously, dark matter is considered collisionless, contrary to baryonic matter which interacts with itself. This is a very important feature, that will help us distinguish between visible and dark matter in our simulations.
Perhaps the most widely-used N-body simulation of cosmological structure formation to date has been the Millennium Simulation, which followed more than ten billion particles within a simulation volume of $(500h^{-1}Mpc)^3$[8].
Dark matter in Millenium simulation is analyzed as a function of redshift ad cosmological time. The simulation starts with a uniformly distributed matter density in the primordial

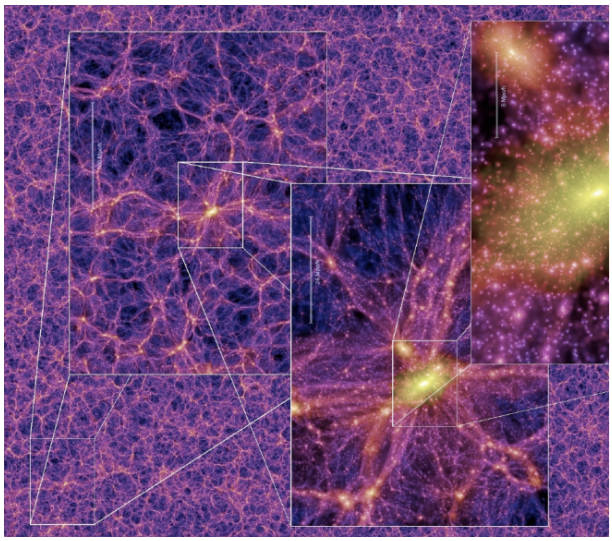

Figure 1.11: The Millennium Simulation: a n-body calculation of the formation of large-scale and galaxy-sized structures via hierarchical clustering of primordial quantum density fluctuations that have been stretched by the expansion of the Universe and increased in contrast by self-gravity. From [30]

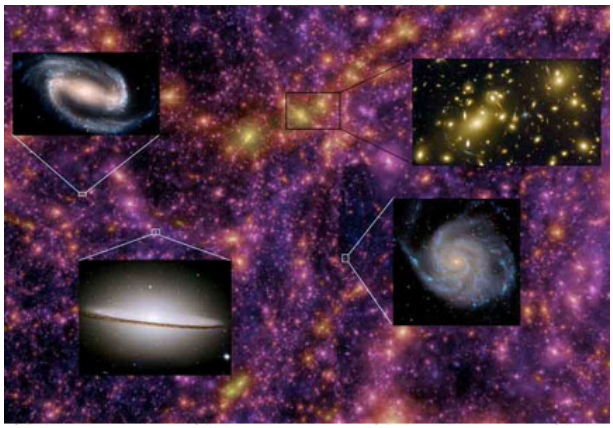

Figure 1.12: Galaxy formation obtained by studying the physics of baryonic galaxies as embedded in the dark matter hierarchy represented here by the Millennium Simulation. From [30]

cosmos, then gravity starts to play its role by creating centers of mass. As time passes one can clearly see the formation of matter filaments with a high number of structures formed.
The goal for these simulations is to be compared to the actual data observed, but for this to be the case, one would need a large statistic.
What is observed is that simulations reproduce a set of data very similar to what is found in the experiments, with a good agreement between the ΛCDM model and the observations.
In particular, it can be seen that the fraction between baryonic mass and the total mass is

$$\frac{baryonic\ mass}{total\ mass} \sim 15\% \tag{4.1.1}$$

in great agreement with what we have seen previously [2][6].

4.2 BBN

Big Bang Nucleosynthesis can actually be an indirect constraint for dark matter. BBN is one of the best proofs we possess for the Big Bang theory, it allows us to predict the abundances of light nuclei in the universe with great accuracy. The process of nuclei formation strongly depends on the primordial plasma content, so it is obvious that the amount of nuclei formed has its main dependence on the amount of baryon matter present in the primordial plasma. Thanks to this information, combined to the observed abundances of light elements in the Universe, we are able to track the percentage of baryon matter present in the Universe at the time when BBN took place. Confronting the result with the total amount of matter, one can clearly see that there is a solid discrepancy between the two values explainable with the presence of dark matter.
In particular, BBN gives precise a result regarding the quantity baryon-to-photon ratio

$$\eta = \frac{n_b}{n_\gamma} \tag{4.2.1}$$

where n_b and n_γ represent baryon and photon number densities. in particular one can see that for baryons

$$\Omega_b = \frac{\rho_b}{\rho_{crit}} = \frac{m_p n_b}{\rho_{crit}} = \frac{\eta n_\gamma m_p}{\rho_{crit}} \tag{4.2.2}$$

with m_p mass of the proton. With CMB analysis one can estimate $n_\gamma = 410.5 cm^{-3}$, the measurements give

$$5.8 \times 10^{-10} \leq \eta \leq 6.6 \times 10^{-10} \quad \Longrightarrow \quad 0.021 \leq \Omega_b h^2 \leq 0.024. \tag{4.2.3}$$

The fact that with other experiments we reach a bound for the total amount of matter

$$\Omega_M \simeq 0,14 \tag{4.2.4}$$

just adds another proof to our thesis on dark matter existence[15].
On the other side, there are various effects that influence the light element abundances. Of particular relevance is the expansion rate H of the Universe during the time of BBN, as it determines at which point in time protons and neutrons fall out of thermodynamic

equilibrium and hence sets the ratio of the corresponding number densities[40]. The Hubble rate, in turn, is fully determined by the total energy density, which receives contributions from all particles, including those beyond the SM. In particular, even fully decoupled dark sectors can be probed via their effect on the expansion rate. This is how we can be sure, even if indirectly, of the presence of dark matter thanks to this highly precise constraint.

5 What do we actually know about Dark Matter?

Aside from the gravitational evidence of dark matter, we do not know much about its particle structure. No matter how much we search, there is no solid clue about its properties. There is a series of bounds in our hands though [10] [3], which gives more clarity on what dark matter *cannot* be, cutting on the range of possible models and reducing the otherwise almost endless list of dark matter particle wannabes.

5.1 Dark matter is stable

In chronological terms the first picture we have of the early Universe is CMB. It is the oldest, most precise dataset in our hands that draws an accurate report about what was happening 300000 years circa after the Big Bang. We have seen, from power spectrum analysis, that dark matter was present in the Universe at the time of CMB formation. It is also present today in halos around galaxies and, during all these billion years between CMB emission and now, it has helped shape the Universe as we see it. So the conclusion comes spontaneously to mind: dark matter is stable or, at least, it must not decay over the Universe lifetime

$$\tau_{DM} \geq 14\ Gyr \simeq 4 \times 10^{17} sec \tag{5.1.1}$$

Moreover, this bound becomes more stringent when we consider BBN. In fact dark matter decays or annihilations could have an enormous impact on BBN by injecting into the primordial plasma more SM particles, which in turn, affect light elements' abundances. As an example, DM decay in pions $\pi^{\pm}$ could cause the exchange

$$\pi^- + p \rightarrow \pi^0 + n \tag{5.1.2}$$

which increases the fraction $\frac{n}{p}$, thus influencing helium mass fraction.
One more at it is that the decay into electromagnetically interacting particles that rises the previous constraint. The injection of photons could impact CMB formation and this puts a higher bound on DM lifetime

$$\tau_{DM} \geq 10^{25-29} sec. \tag{5.1.3}$$

5.2 Optical darkness

Dark matter is not observed at all, thus the dark matter particles must have very weak electromagnetic interactions. This does not mean that the electric charge and electric and magnetic dipole moments vanish, they can exist but are forced to be very small.

$$q_{DM} \simeq \begin{cases} 10^{-6} & m_{DM} = 10GeV \\ 10^{-4} & m_{DM} = 10TeV \end{cases} \tag{5.2.1}$$

These constraints were put looking for bound states DMe^- in experiments on heavy hydrogen.
An important consequence of this is that the dark matter can not cool by radiating photons, and thus will not collapse to the center of galaxies as the baryons do, by radiating their energy away electromagnetically. In other words, the dark matter is very nearly dissipationless.

5.3 Collisionlessness

Limits on DM self-interactions are taken from Bullet cluster studies. Here we saw DM and visible matter disentangled for the first time. Baryonic matter is highly interactive, during the merger Standard Model particles interact with each other, the gas gets hotter and emits X-rays. Dark matter, on the other hand, just passes through anything else, just like stars do and can be detected, through gravitational lensing, forming the two main mass densities outside the gas region. This behavior generates constraint on DM self-interaction cross section

$$\frac{\sigma_{self}}{m} \leq \frac{1cm^2}{g} \simeq \frac{2barn}{GeV} \simeq 10^{-24}\frac{cm^2}{TeV} \tag{5.3.1}$$

Even though it appears as a small number, this is still huge compared to, for example, neutron capture cross section of uranium, which is a few barns. Or 50 mb is a typical QCD cross section like the one for pp scattering.

5.4 Coldness

Dark matter models can be divided into three main categories: hot, cold and warmth, as we'll see in the next chapter, according to whether or not DM was relativistic at the time of decoupling.
The difference lies in the consequences that different types of DM have on structure formation. Baryonic perturbations cannot form before CMB emission. Prior to that time, photon interactions with visible matter were too frequent with the result of erasing whatever bound state was formed between baryons. After CMB emission, baryon could originate perturbations, little clots of matter which had the potential to grow and form large scale structures we observe today. In order to do that baryonic matter had to fall in DM potential wells, which in turn had to be already formed by the time of recombination. Here the difference between models comes to play. For hot dark matter models, we have DM particles relativistic at their decoupling. Now if the dark matter particles have significant velocities, then the small scale structures could be erased. In this case inhomogeneities would not be the seeds for large scale structures formations and would not originate the Universe as we see it. For this not to occur, the particles must be sufficiently non-relativistic temperature of the universe was roughly 1 keV. Only in this case inhomogeneities would survive. Cold dark matter and warm dark matter models only can explain what we see today.

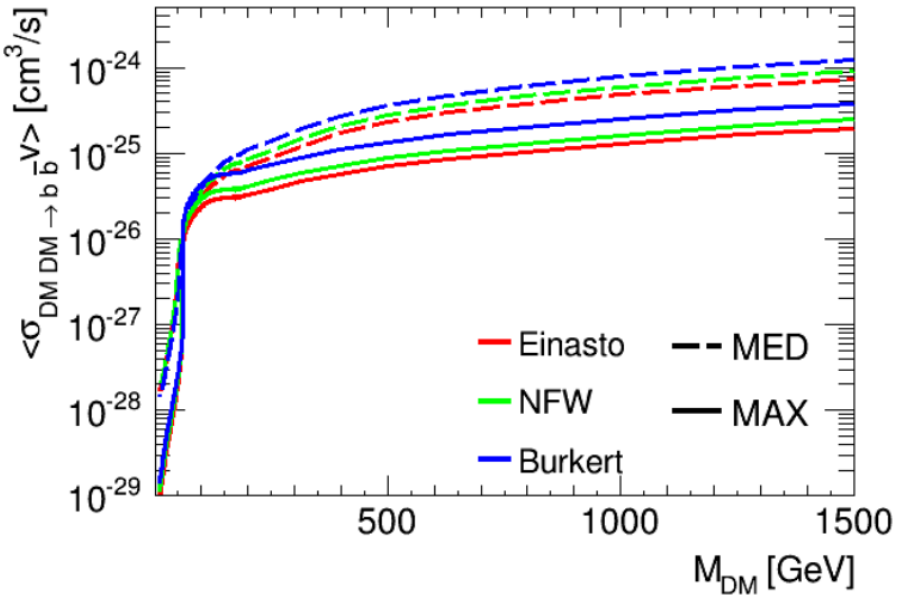

Figure 1.13: 95% C.L. upper limit of dark matter annihilation cross section into bb^- (left) and W^+W^- (right) as a function of the dark matter mass, derived from AMS-02 antiproton data, for different choices of dark matter profiles (Einasto, Burkert, NFW) and propagation models (MED, MAX). From [28]

5.5 Density profile

Numerical simulations have, amongst all the advantages, that of providing us with galactic distribution function $\rho(r)$ that encodes the behavior of dark matter halos around spiral galaxies. In particular the most famous and best-fitting functions are

$$\begin{cases} NFW: & \rho_{DM}^{NFW} = \rho_s \frac{r_s}{r}(1+\frac{r}{r_s})^{-2} \\ Einasto: & \rho_{DM}^{Einasto} = \rho_s \exp\left(-\frac{2}{\alpha}[(\frac{r}{r_s})^{\alpha}-1]\right) \\ Isothermal: & \rho_{DM}^{Iso} = \frac{\rho_s}{1+(\frac{r}{r_s})^2} \\ Burket: \rho_{DM}^{Burk} = & \frac{\rho_s}{(1+\frac{r}{r_s})(1+(\frac{r}{r_s})^2)} \end{cases} \tag{5.5.1}$$

with $\alpha = 0,17$ in Einasto's. In all models r_s is the characteristic radius and depends on the particular galaxy considered, as well as any ρ_i. All these are the result of N-body simulations, where we can keep track of all bodies with their interactions (only gravitational for DM in this case) as they form larger structures.
Here in Figure 1.13 is shown a comparison of NFW, Einasto and Burket. Notice that the isothermal profile goes like r^{-2}, thus respecting what we have previously seen for spiral galaxies' rotation curves. Also take into account that in some profiles $r \to 0$ brings divergence, thus are not likely to represent accurately DM distribution towards the galactic center.

5.6 Velocity distribution

Since no DM particle has been observed yet, also its velocity distribution is not known. What has been hypothesized is that it has a truncated Maxwellian, also known as Standard Halo Model:

$$f(v) = \begin{cases} \frac{1}{N_{esc}}(\frac{3}{2\pi\sigma_v^2})^{\frac{3}{2}} e^{\frac{-3v^2}{2\sigma_v^2}} & : |v| < v_{esc} \\ 0 & : otherwise \end{cases} \tag{5.6.1}$$

where the normalization constant $\frac{1}{N_{esc}}$ has been chosen so that $\int f(v)dv = 1$.
Here we can notice the obvious fact that if DM acquires a velocity superior to the escape one v_{esc}, it evaporates.
σ_v is velocity dispersion, $v_0 = \sqrt{\frac{2}{3}}\sigma_v \sim 235km/s$ is the most probable velocity.
We can also estimate dark matter velocity for Milky Way's halo with the virial theorem as we have shown previously

$$2T + U = 0 \tag{5.6.2}$$

then with

$$\begin{cases} U = -\frac{3}{5}\frac{GM_{halo}^2}{R_{halo}} \\ T = \frac{1}{2}M_{halo}v^2 \end{cases} \tag{5.6.3}$$

to obtain (obviously this is an approximated result)

$$v \simeq (\frac{3}{5}\frac{GM_{halo}}{R_{halo}}). \tag{5.6.4}$$

5.7 Mass

Here the problem is renovated as we have not yet identified any DM particle, so we have no substantial data on its mass. Anyway we can still impose some bounds based on the nature of this particle.
First of all the mass cannot assume arbitrarily high values, as, at some point, quantum gravity effects will not be negligible. For example for masses

$$m \geq M_{PL} \tag{5.7.1}$$

with M_{PL} Plank mass, the particle's wavelength would be smaller than its Swartzshild radius

$$\frac{2\pi}{M} \leq \frac{2m}{M_{PL}^2} \tag{5.7.2}$$

turning into a black hole. Thus we can safely impose that

$$m \leq M_{PL}. \tag{5.7.3}$$

Then a distinction has to be made whether the particle is a boson or fermion. In both cases what comes to help are studies on dwarf galaxies. Dwarf galaxies are one of the most important instruments for DM study, as they have relatively small mass and they have larger DM mass fraction than other bigger galaxies to be held together.

Bosonic

Here we can store almost an infinite number of particles in the same state. Bose-Einstein statistic imposes a distribution function for these kinds of particles

$$f(E) = \frac{g}{\exp\left(\frac{(E-\mu)}{T}\right) - 1} \tag{5.7.4}$$

with g number of degrees of freedom of the system, E being its energy, μ the chemical potential and T the temperature.
We can put bounds on dwarf galaxies by studying their de-Broglie wavelength

$$\lambda = \frac{2\pi}{m_{DM} v}. \tag{5.7.5}$$

We can constrain this quantity to be smaller than the galactic radius

$$\lambda \leq R_d \simeq 1kpc \simeq 3 \times 10^{19} m \tag{5.7.6}$$

to obtain a bound on DM particle mass

$$m_{DM} \geq 10^{-22} eV. \tag{5.7.7}$$

Of course this is a lower bound because if DM particle's mass would be lower than this then its wavelength would be bigger than the galactic radius.

Fermionic

The same cannot be said for fermions, which are ruled by Pauli's exclusion principle. Here even the statistic is quite different

$$f(E) = \frac{g}{\exp\left(\frac{(E-\mu)}{T}\right) + 1}. \tag{5.7.8}$$

Because of Pauli exclusion principle, fermions are constrained to fill up all energetic levels, starting from the ground state, but there cannot be two fermions with the same quantum numbers inside a level. This results in a simplification of the distribution function, which now becomes

$$g \begin{cases} 1 & : E << \mu \\ 0 & : E >> \mu. \end{cases} \tag{5.7.9}$$

Here the $\leq$ comes from the impossibility, by Pauli's principle, of casting more than one fermion inside a unit volume of the phase space.
This implies that, in order to calculate the galaxy mass, we run into the bound

$$M_{halo} = m_{ferm} V \int f(p) d^3p \leq m_{ferm} V \int d^3p \sim m_{ferm} R_{halo}^3 (m_{ferm} v)^3 \tag{5.7.10}$$

with $V = \frac{4}{3}\pi R^3$ is the volume of a spherical halo of dark matter and m_{ferm} is of course the mass of fermionic dark matter.
We have already calculated the escape velocity of the system as

$$v = (\frac{2GM}{R})^{\frac{1}{2}} \tag{5.7.11}$$

so we can substitute this result and obtain the bound

$$m_{ferm} \geq (G^3 M_{halo} R_{halo}^3)^{-\frac{1}{8}} \tag{5.7.12}$$

This in turn gets us the numerical result, depending of course on the particular example we are considering,

$$m_{ferm} \geq (10 - 100)eV. \tag{5.7.13}$$

One can take as an example a dwarf galaxy phase space density, with data in our possess on M_{halo} and R_{halo}, to obtain

$$m_{ferm} \geq 0,7keV \tag{5.7.14}$$

Of course after all we have said about Pauli's exclusion principle influencing fermionic distribution, it is obvious *a posteriori* to have found a bound on masses for this kind of particles far greater than what we have seen for bosons.

5.8 Conclusions

The question of what really is dark matter is still open since it has been theorized by Zwicky in the now distant 1937. Dark matter not only shapes the Universe we live in but also without its existence there also would be no life. We have had the opportunity to study fluctuation in the spectrum of the CMB and we have seen that they amount to an amplitude of 10^{-5} revealing that the Universe was still quite homogeneous by the time of its emission.
This of course raises the genuine question if after CMB emission, baryonic matter fluctuation could have grown forming the Universe we see today all by themselves, with no help whatsoever of dark matter.
Turns out that the answer to this question is negative. The perturbations will grow and, thanks to Friedman's laws we are able to study the dependence of their energy density on the scale factor. We remind the reader briefly just Friedman's equations:

$$\begin{cases} \frac{\dot{a}}{a}^2 = \frac{\rho}{3M_{PL}^2} - \frac{k}{a^2} \\ \dot{\rho} = -3H(\rho + p) \\ \frac{\ddot{a}}{a} = -\frac{1}{6M_{PL}^2}(\rho + 3p) \end{cases} \tag{5.8.1}$$

with k being the curvature constant, M_{PL} Plank's mass, $H = \frac{\dot{a}}{a}$ and a is the scale factor. Here one can see that we omitted any cosmological constant Λ, which in fact was added by hand. To solve this system one can use the equation of state

$$p = w\rho \tag{5.8.2}$$

with

$$w = \begin{cases} \frac{1}{3} & radiation \\ 0 & Non\ \ relativistic\ matter \\ -1 & Vacuum\ energy/Cosmological\ constant \end{cases} \tag{5.8.3}$$

Now one can obtain, through some manipulation, the energy density dependence on the scale factor

$$\rho \propto \begin{cases} a^{-4} & Radiation \\ a^{-3} & Non\ relativistic\ matter \\ const & Vacuum\ energy/Cosmological\ constant \end{cases} \tag{5.8.4}$$

At a temperature of approximately $T \simeq 0,8eV$ the Universe became matter dominated, this means that

$$\frac{\delta\rho}{\rho} \propto \begin{cases} ln(a) & radiation\ domination \\ a & matter\ domination \end{cases} \tag{5.8.5}$$

Before matter-radiation equality the perturbation growth is clearly negligible, so if the Universe was only made of baryonic matter, perturbation would experience linear growth only after CMB emission. In fact before recombination, matter and radiation were coupled, thus sharing the same perturbations with amplitude $\propto 10^{-5}$. Being coupled to radiation means that perturbation growth will be negligible unitill recombination. After that perturbations will grow linearly. Now we can calculate perturbation growth from recombination till the present with the simple equation

$$\frac{\delta\rho}{\rho}_{today} \simeq \frac{\delta\rho}{\rho}_{rec} \frac{a_0}{a_{rec}} \simeq 10^{-5} \times 10^3 = 10^{-2} \tag{5.8.6}$$

thus not explaining the highly inhomogeneous universe that we see today with $\delta\rho >> \rho$ [51].

The point is that we need some decoupled matter that will enable the perturbations to grow non-linearly. Dark matter serves this scope excellently. It has been hypnothized that dark matter was already decoupled long before recombination time and that by this time it would already have formed the potential wells in which baryonic matter will eventually fall after CMB emission, thus creating the structures that we see today.

This is another striking feature of dark matter and of the fact that we need it desperately to explain our Universe's characteristics.

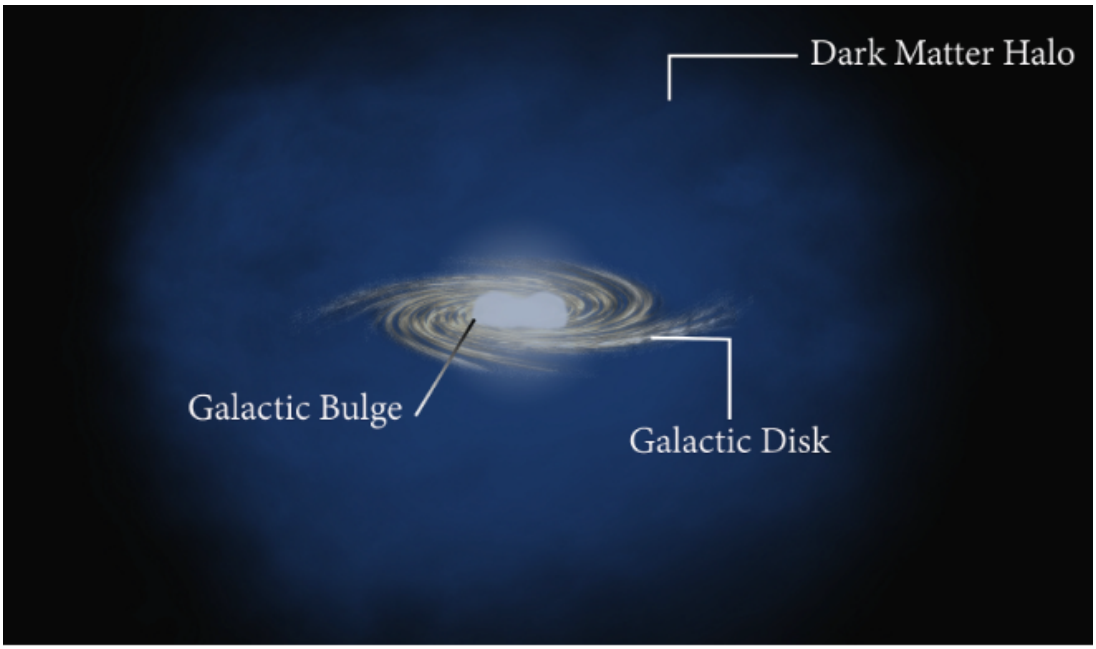

Figure 1.14: dark matter halo representation from [33]

Chapter 2

History of WIMPS

As we said in the previous chapter, there is plenty of models to describe dark matter, but they can be divided into two major categories: hot and cold dark matter. The difference lies in how relativistic they were at the time of their decoupling. Decoupling is a process in which particles that were in thermal equilibrium with primordial plasma lose this condition as a consequence of the expansion of the Universe.
We imagine the primordial plasma as a mixture of the fundamental constituents of the Universe which are in thermal equilibrium. This is of course ensured by the collisions between particles, which guarantee energetic exchanges between different species. The point is that even here we find ourselves in the middle of two opposite factors. One side is occupied by the number of interactions N that a species i has, the more interaction, the better for thermal equilibrium. On the other side, the Universe's expansion stretches space, making it difficult for particles to find each other.
We can formalize the number of interactions of the species i as

$$N_i = \int_{t_1}^{t_2} dt\Gamma \tag{0.0.1}$$

which implies, using the relation between time and temperature

$$N_i = \int_{T1}^{T2} dT \frac{dt}{dT}\Gamma(T) \tag{0.0.2}$$

which transforms in

$$N_i = \int_{T1}^{T2} \frac{dT}{T}\frac{\Gamma(T)}{H(T)} \tag{0.0.3}$$

if one notices that deriving by the time the condition for conservation of entropy Ta, one obtains $\frac{dT}{T} = -HT$.
Now if we choose an infinitesimal temperature interval, we can see that the condition of decoupling can be imposed whether or not there are collisions in the time interval of the first integral. In particular this means that

$$\begin{cases} \frac{\Gamma(T)}{H(T)} \geq 1 & \textit{species coupled} \\ \\ \frac{\Gamma(T)}{H(T)} \leq 1 & \textit{species decoupled.} \end{cases} \tag{0.0.4}$$

Now for what concerns dark matter, we can already introduce

$$\Gamma(T) = n_\chi < \sigma v > \tag{0.0.5}$$

with n_χ being the number density of the particular dark matter model we are considering and $< \sigma v >$ being the thermal averaged cross section with v the particle's velocity.
The difference we have talked about comes with n_χ assuming different forms in the cases $m_\chi \geq T$ (non-relativistic) or the opposite one, in which dark matter is relativistic. In particular if at the time of decoupling, which we refer to as $freeze\ out\ time$, the former (or the latter) condition is realized, we talk about cold(hot) dark matter.
The hot models have been studied and it has been seen that they cannot explain the Universe, in particular the large structures present today. In fact, relativistic particles, having more kinetic energy, are able of covering bigger distances in the primordial Universe than the non-relativistic ones. After decoupling they spread, or $free\ stream$, across the universe and they destroy the matter perturbations that were forming at that time. In their motion, DM particles diffuse in underdense regions and completely erase cosmological perturbations before the time that they can grow linearly, which, as we have already seen, is the time of matter-radiation equality.
Having ruled out Hot dark matter models, we can focus on Cold Dark Matter. In fact, the present cosmological model, which is what we believe to be the closest to explain reality, is called ΛCDM, referring to these kinds of dark matter models.
Amongst Cold Dark Matter models there is a class called $WIMPS$ which stands for $Weakly\ Interacting\ Massive\ Particles$ that have the quality of being able to reproduce the correct relic density that we have already shown in the previous section. We analyze the WIMP model in the following sections.

1 CDM at decoupling

We have already seen the condition for decoupling to be

$$\Gamma(T) \simeq H(T) \tag{1.0.1}$$

with $H(T)$ Hubble factor. Now we know that

$$H(T)^2 = \frac{\rho}{3M_{PL}^2} \tag{1.0.2}$$

and that $\Gamma = n_\chi < \sigma v >$. For a non-relativistic species it can be demonstrated that

$$\rho = g_*(T)\frac{\pi}{30}T^4 \tag{1.0.3}$$

with $g_*(T)$ primordial plasma's degrees of freedom at temperature T.
This means that at decoupling or, as we say at freeze-out,

$$H(T_{FO}) \simeq \frac{T_{FO}^2}{M_{PL}} \tag{1.0.4}$$

where FO stands for freeze out.

For a non-relativistic matter distribution, it can be proved that

$$n_\chi = g_\chi(\frac{m_\chi T}{2\pi})^{\frac{3}{2}} \exp\Big(-\frac{m_\chi}{T}\Big) \tag{1.0.5}$$

with g_χ the particle degrees of freedom. This allows us to obtain an approximated formula for $\Gamma(T_{FO})$ at decoupling in

$$\Gamma(T_{FO}) \simeq \sigma_A^{NR}(T_{FO})(\frac{m_\chi T}{2\pi})^{\frac{3}{2}} \exp\Big(-\frac{m_\chi}{T}\Big) \tag{1.0.6}$$

By equating the two terms of H and Γ we can obtain an approximated formula for decoupling in

$$\sigma_A^{NR}(T_{FO})(\frac{m_\chi T_{FO}}{2\pi})^{\frac{3}{2}} \exp\left(-\frac{m_\chi}{T_{FO}}\right) \simeq \frac{T_{FO}^2}{M_{PL}} \tag{1.0.7}$$

The exponential factor and T_{FO}^2 will meet when the argument of the exponential is actually not very large. Actually we will see that $\frac{m}{T_{FO}} = O(10)$. Here we can use $T_{FO} \simeq m$ in order to prove an important result:

$$n_\chi(T_{FO}) \simeq \frac{T_{FO}^2}{\sigma_A^{NR}(T_{FO})}. \tag{1.0.8}$$

Then we know that after decoupling, the number density decreases as T^3 due to Universe expansion so that

$$n_\chi(T) = n_\chi(T_{FO})(\frac{T^3}{T_{FO}^3}) \tag{1.0.9}$$

In order to obtain the DM density, we just have to multiply this expression for DM mass, given that we are in a non-relativistic regime. So what we obtain is a formula of this kind:

$$\rho(T) = mn(T) \simeq \frac{m^3}{\sigma_A^{NR}(T_{FO})}\frac{T^3}{m^3} = \frac{T^3}{\sigma_A^{NR}(T_{FO})} \tag{1.0.10}$$

and this just proves that the relic density is only inversely proportional to the non-relativistic elastic cross section [21].

Let's go back to our mission to recover DM relic density formula now. In order to do that, we need to solve Boltzmann equation for dark matter.

2 Boltzmann equation

This is such an important element that dark matter study would be almost impossible without it. Without further ado, let's dive straight into it. Boltzmann equation assumes the general form [44]

$$L[f] = C[f.] \tag{2.0.1}$$

Here L and C represent respectively Liouville and collision operators for dark matter particles distributed according to the function f, which in general depends itself on the phase space $f(x^\mu, p^\mu)$.

The first operator describes the spacetime geometry influencing the phase space evolution, the latter keeps track of all particle interactions.
In the relativistic case

$$L[f] = \frac{df}{dx^a}\frac{dx^a}{d\lambda} + \frac{df}{dp^a}\frac{dp^a}{d\lambda} \tag{2.0.2}$$

with λ being the affine parameter that parametrizes the trajectory followed by a given particle. Now using the fact that $\frac{dx^\alpha}{d\lambda} = p^\alpha$ combined with the geodesic equation $\frac{dp^\alpha}{d\lambda} + \Gamma^\alpha_{\beta\gamma}p^\beta p^\gamma = 0$ and that $g_{ab}p^a p^b = p^2 = -m^2$, we can obtain

$$L[f] = \frac{df}{dx^a}\frac{dx^a}{d\lambda} - \Gamma^a_{bc}p^b p^c\frac{df}{dp^a} = \Big(p^a\frac{d}{dx^a} - \Gamma^a_{bc}p^b p^c\frac{d}{dp^a}\Big)f. \tag{2.0.3}$$

Here of course Γ^a_{bc} is the Christoffel symbol which obeys to

$$\Gamma^a_{bc} = \frac{1}{2}g^{ad}\Big(\frac{dg_{bd}}{dx^c} + \frac{dg_{bc}}{dx^b} - \frac{dg_{bc}}{dx^d}\Big). \tag{2.0.4}$$

From here we have to impose the properties of homogeneity and isotropy. The former reduces the space-time coordinates dependence only on time

$$p^a\frac{d}{dx^a} = E\frac{d}{dt} \tag{2.0.5}$$

while the second implies that f can only depend on the modulus of spatial momentum or, equivalently, on energy. For what concerns Christoffel symbols, we can examine the Friedmann-Robertson-Walker metric to see that the only few left are

$$\Gamma^0_{ij} = a\dot{a}\delta_{ij} \qquad and \qquad \Gamma^i_{0j} = \Gamma^j_{0i} = \frac{\dot{a}}{a}\delta^i_j. \tag{2.0.6}$$

All of this combines in the (almost) final form of the Liouville operator

$$L[f] = E\frac{df}{dt} - \Gamma^0_{ij}p^i p^j\frac{df}{dE} = E\frac{df}{dt} - H\delta_{ij}p^i p^j a^2\frac{df}{dE} = E\frac{df}{dt} - Hp^2\frac{df}{dE} \tag{2.0.7}$$

So now the Boltzmann equation has become

$$E\frac{df}{dt} - Hp^2\frac{df}{dE} = C[f(t,E)] \tag{2.0.8}$$

Let's multiply both members by the factor $\frac{g}{(2\pi)^3E}\int d^3p$

$$\frac{g}{(2\pi)^3}\int d^3p\frac{df}{dt} - \frac{g}{(2\pi)^3}\int d^3p\; Hp^2\frac{df}{dE} = \frac{g}{(2\pi)^3E}\int d^3p\; C[f(t,p)] \tag{2.0.9}$$

We can already notice that the first factor on the left-handed side corresponds to $\dot{n}$, then we can use the conservation of energy formula $EdE = pdp$ in the second term to see that

$$\begin{gathered}\frac{g}{(2\pi)^3}\int d^3p\; Hp^2\frac{df}{dE} = \frac{g}{(2\pi)^3}H\int dp\;\frac{p^4}{E}\frac{df}{dE}\int d\Omega = \\ \frac{g}{(2\pi)^3}H\int dpp^3\frac{df}{dp}\int d\Omega = \frac{g}{(2\pi)^3}H([p^3f]_0^\infty - 3\int dpp^2 f)\int d\Omega\end{gathered} \tag{2.0.10}$$

since the first term in the brackets vanishes at 0 and at ∞ as well for a distribution function, we can isolate, from the second term in the brackets, the factor $-3Hn(t)$ to form the Boltzmann equation

$$\dot{n} + 3Hn = \frac{g}{(2\pi)^3 E} \int d^3p\, C[f(t,p)]. \tag{2.0.11}$$

Now it's time to present the RHS with its appropriate mathematical form:

$$\begin{aligned} &\frac{g}{(2\pi)^3 E} \int d^3p\, C[f(t,p)] = \int d\Pi_1 d\Pi_2 d\Pi_3 d\Pi_4 (2\pi)^4 \delta(p_1 + p_2 + p_3 + p_4) \times \\ &[|M_{3+4 \Longrightarrow 1+2}|^2 f_3 f_3 (1 \pm f_1)(1 \pm f_2) - |M_{1+2 \Longrightarrow 3+4}|^2 f_1 f_2 (1 \pm f_3)(1 \pm f_4)] \end{aligned} \tag{2.0.12}$$

Here $d\Pi_i = \frac{g}{(2\pi)^3 E} d^3p_i$ is the phase space factor for the i species and $M_{i+j \Longrightarrow m+n}$ is the amplitude for the processes that, in this case, create and destroy species 1, as one can deduce from the opposite signs before them. Moreover, the factors $1 \pm f_i$ represent the *Bose enhancing factor* and the *Pauli blocking term*. Because of the different statistics, in fact, bosons will be prone to accumulation, hence favoring the production of species 1, fermions however will experience the repulsion coming from Pauli exclusion principle, thus slowing down the reaction.
Here we can make a number of assumptions in order to simplify the RHS:

- take the two amplitudes to be equal
- suppose kinetic equilibrium, in order to use the Fermi-Dirac and Bose-Einstein well known distribution functions $f_{FD(BE)} = \frac{1}{e^{\frac{E-\mu}{T}} + (-)1}$
- suppose $E - \mu > T$ in order to suppress Bose enhancing factor and Pauli blocking term. In this case we have $f \simeq e^{\frac{\mu}{T}} e^{-\frac{E}{T}} = e^{\frac{\mu}{T}} f_{EQ}$. Here f_{EQ} represent the distribution function assumed by the system is one suppose chemical equilibrium too, hence neglecting all the μ_i.

This way the RHS becomes

$$\int d\Pi_1 d\Pi_2 d\Pi_3 d\Pi_4 (2\pi)^4 \delta(p_1 + p_2 + p_3 + p_4)(f_3 f_4 - f_1 f_2)|M|^2 \tag{2.0.13}$$

We can use energy conservation here to see that the factor between brackets can be written as

$$e^{-\frac{E_1+E_2}{T}} (e^{\frac{\mu_3}{T}} e^{\frac{\mu_4}{T}} - e^{\frac{\mu_1}{T}} e^{\frac{\mu_2}{T}}) \tag{2.0.14}$$

which can be easily rewritten as

$$e^{-\frac{E_1+E_2}{T}} \left(\frac{n_3(t) n_4(t)}{n_3(t)^{eq} n_4(t)^{eq}} - \frac{n_1(t) n_2(t)}{n_1(t)^{eq} n_2(t)^{eq}} \right) \tag{2.0.15}$$

In fact, since $n(t) = \frac{g}{(2\pi)^3} f$ one can see that

$$\frac{g}{(2\pi)^3} \int d^3p f = \frac{g}{(2\pi)^3} \int d^3p e^{\frac{\mu}{T}} e^{-\frac{E}{T}} = \frac{g}{(2\pi)^3} \int d^3p e^{\frac{\mu}{T}} f_{EQ} = e^{\frac{\mu}{T}} n_{EQ}(t). \tag{2.0.16}$$

Now we obtain

$$\begin{aligned} \dot{n_1} + 3Hn_1(t) = \int d\Pi_1 d\Pi_2 d\Pi_3 d\Pi_4 (2\pi)^4 \delta(p_1 + p_2 + p_3 + p_4) \times \\ |M|^2 e^{-\frac{E_1+E_2}{T}} \Big(\frac{n_3(t) n_4(t)}{n_3(t)^{eq} n_4(t)^{eq}} - \frac{n_1(t) n_2(t)}{n_1(t)^{eq} n_2(t)^{eq}} \Big) \end{aligned} \tag{2.0.17}$$

Let's introduce the thermally averaged cross section

$$< \sigma v >= \frac{\int d\Pi_1 d\Pi_2 d\Pi_3 d\Pi_4 (2\pi)^4 \delta(p_1 + p_2 + p_3 + p_4) |M|^2 e^{-\frac{E_1+E_2}{T}}}{n_1^{EQ} n_2^{EQ}} \tag{2.0.18}$$

this enables us to rewrite the Boltzmann equation as

$$\dot{n_1} + 3Hn_1(t) = n_1^{EQ} n_2^{EQ} < \sigma v > \Big(\frac{n_3(t) n_4(t)}{n_3(t)^{eq} n_4(t)^{eq}} - \frac{n_1(t) n_2(t)}{n_1(t)^{eq} n_2(t)^{eq}} \Big). \tag{2.0.19}$$

This is the final and most general form of the Boltzmann equation, now we are ready to use it with dark matter.
Suppose now to analyze the process $\chi\bar{\chi} \to \psi\bar{\psi}$ with χ and ψ the only two particle species considered. Then if at the beginning $n_\psi = n_{\bar{\psi}}$ and $n_\chi = n_{\bar{\chi}}$ and if ψ is in thermal equilibrium with the plasma, the Boltzmann equation can be written as

$$\dot{n_\chi} + 3Hn_\chi =< \sigma v > [(n_\chi^{eq})^2 - (n_\chi)^2] \tag{2.0.20}$$

One precious piece of information we can extract by just looking at this is whether or not the species are coupled or not. In fact, if we use $\frac{\partial}{\partial t} \simeq H$, which is just a rough approximation in a qualitative analysis that we hope leads just to a likewise rough esteem, we can see that

$$\begin{cases} \dot{n_\chi} + 3Hn_\chi \propto Hn_\psi \\ n_\chi \Gamma \simeq n_\chi n_\chi < \sigma v >=< \sigma v > [(n_\chi^{eq})^2 - (n_\chi)^2] \end{cases} \tag{2.0.21}$$

From here one can separate two opposite cases

- In the case of $\Gamma >> H$ this refers to an important particle ψ interaction rate, which leads quickly to particles reaching thermal equilibrium, hence annihilating completely the second equation of the couple
- In the opposite case where $H >> \Gamma$ this configuration is characterized by a strongly reduced interaction rate, which in turn, again nullifies the second equation and, more generally, the RHS of the Boltzmann equation.

Just for curiosity purposes, we can indagate what happens in the case where the RHS of the Boltzmann equation is placed to 0. In this case, Boltzmann equation assumes the form

$$\dot{n_\psi} + 3Hn_\chi = 0 \tag{2.0.22}$$

We can easily see that

$$\frac{d}{dt}(n_\chi a^3) = a^3 \frac{dn}{dt} + 3na^2 \frac{da}{dt} = a^3 (\frac{dn}{dt} + 3Hn) \tag{2.0.23}$$

which is equal to LHS of the Boltzmann equation, apart from the multiplicative factor. This is consistent with what we know about the number density function, which, in absence of collisions, scales as a^{-3}. Now that we have satisfied our curiosity with this little digression, we can carry on with our analysis of the Boltzmann equation.
Before moving on, it is interesting to examine an important mechanism capable to influence WIMPs relic density.

3 Boltzmann equation for cold relics

Let's now apply the Boltzmann equation to the case of WIMP dark matter. For this purpose we will suppose the existence of two particles χ and ψ connected through the process $\chi\bar{\chi} \to \psi\bar{\psi}$ which is the only one happening. This is a simple scenario that will enable us to reconstruct n_ψ starting from Boltzmann equations. Suppose that we start from a situation purely symmetric in which $n_\psi = n_{\bar{\psi}}$ and that $n_\chi = n_{\bar{\chi}}$, so that there is no matter-antimatter asymmetry. Then suppose ψ to be in thermal equilibrium with the primordial plasma. This condition, as we have already seen in the beginning of this chapter, is achieved through a significant interaction rate with the plasma after their production. Thermal equilibrium of course implies $n_\psi = n_\psi^{eq}$. Finally, the last assumption is that ψ are taken to be massive and stable so that decays are out of the picture [44].
With all of this behind us, we can proceed to write the Boltzmann equation which takes the following form through all of the above assumptions

$$\dot{n_\chi} + 3Hn_\chi =< \sigma v > [(n_\chi^{eq})^2 - (n_\chi)^2] \tag{3.0.1}$$

Since we are analyzing a species which has to be non-relativistic at decoupling, its number density at equilibrium would be of the form

$$n_{\chi,eq} = g_\chi (\frac{m_\chi T}{2\pi})^{\frac{3}{2}} e^{-\frac{m_\chi}{T}} \tag{3.0.2}$$

with of course g_χ its number of degrees of freedom.
Usually, just the appearance of it would suggest that in absence of other effects, the number density would become exponentially suppressed very fast, leaving us with a negligible abundance. Since this is not the case, provided that we have observed that nearly 70% of matter in the Universe is dark, there is going to be for sure an antagonist effest to reduce the dilution of the number density. The answer will surely lie in the Universe's expansion, which will progressively pull particles apart, thus eventually completely shutting down their interaction. This is the process leading to the freeze-out, as we have already had the opportunity to get in touch with. In fact for sufficiently small temperatures, the annihilation term $< \sigma v >$ becomes negligible compared to $H = \sqrt{\frac{\rho}{3M_{PL}^2}}$, which is responsible for particle dilution, thus bringing the freeze-out.
Let's study Boltzmann equation now. In order to do that let's lean on comoving quantities in order to avoid the relations to Universe expansion. Introducing $Y = \frac{n_\chi}{s}$. This is something that we have already encountered previously and, as we have already explained, s represents the entropy density per comoving volume, so we know that scales

like a^{-3}, balancing the same n_χ scaling. Boltzmann equation transforms in the following way

$$\frac{dY}{dt} = - < \sigma v_{rel} > s(Y^2 - Y_{eq}^2) \tag{3.0.3}$$

as one can easily see that, being sa^3 the total entropy in a comoving volume constant,

$$\frac{dY}{dt} = \frac{d}{dt}\frac{n_\chi a^3}{sa^3} = \frac{1}{sa^3}\frac{d(na^3)}{dt} = \frac{1}{s}(\frac{dn_\chi}{dt} + 3hn_\chi). \tag{3.0.4}$$

As it is naturally understood Y_{eq} is the comoving number density at thermal equilibrium. Now reintroduce $x = \frac{m_\chi}{T}$ and look at entropy conservation. It can be demonstrated that, as we have already seen, $s = \frac{2\pi^2}{45} g_{*s} t^3$, hence the conservation of entropy in a comoving volume implies $g_{*s} T^3 a^3 = const.$ If we neglect the dependence on g_{*s} that can be assumed to be constant if we consider its temperature dependence to be weak compared to the other two factors, then conservation of entropy reads

$$Ta = const \tag{3.0.5}$$

leading to

$$\frac{dT}{T} + \frac{da}{a} = 0 \tag{3.0.6}$$

hence implying that, through time derivation,

$$\frac{dT}{dt} = -HT. \tag{3.0.7}$$

Using $m_\chi = xT$ we can see that

$$xdT + Tdx = 0 \tag{3.0.8}$$

and using all of the above in the Boltzmann equation, we can recast it in the following form

$$\frac{dY}{dt} = \frac{dY}{dx}\frac{dx}{dT}\frac{dT}{dt} = \frac{dY}{dx}\frac{x}{T}HT = \frac{dY}{dx}H \tag{3.0.9}$$

so finally the Boltzmann equation reads

$$\frac{dY}{dx} = - < \sigma v_{rel} > \frac{s}{Hx}[Y^2 - Y_{eq}^2]. \tag{3.0.10}$$

This gives us the opportunity of analyzing the Boltzmann equation in different regimes, since this equation cannot be completely solved analytically. We will then match the results at freeze-out

Since we are talking about WIMPs, we again stress the fact that they are non-relativistic at decoupling, so $T_{FO} \leq m_\chi$ hence giving $x_{FO} \geq 1$. If we analyze the temperature dependence of both H and s we'll clearly see that $H \propto x^{-2}$ and $s \propto x^{-3}$. We can express this by simply putting $H = H(x=1)x^{-2}$ and $s = s(x=1)x^{-3}$. Boltzmann equation now shows the form

$$\frac{dY}{dx} = -\frac{\lambda}{x^2}[Y^2 - Y_{eq}^2] \tag{3.0.11}$$

with

$$\lambda = \frac{s(x=1) < \sigma v_{rel} >}{H(x=1)} \tag{3.0.12}$$

being a constant.
There is no analytic solution to this kind of equation, but we can study Y behavior in order to hope for a numerical one. Remember that for $\Gamma >> H$ we have a sufficient number of collisions that keep DM and primordial bath particles in thermal equilibrium. The opposite happens when $\Gamma << H$. In this situation, the Universe expansion has brought DM particles too far apart, so they cannot meet each other in order to annihilate. This situation is responsible for the DM freeze-out and its fall out of thermal equilibrium. Let's restate this using Y. The two situations can be summarized in the equation

$$Y(x \leq x_f) \simeq Y_{eq}(x) \qquad and \qquad Y(x \geq x_f) \simeq Y_{eq}(x_f) \tag{3.0.13}$$

with x_f at freeze-out. In the cold dark matter case, Y decreases exponentially before freeze-out. Then, after freeze-out, abundance is larger than what it would be if DM were to be at equilibrium. More clearly

$$Y_{eq}(x_f) > Y_{eq}(x > x_f). \tag{3.0.14}$$

This observation can lead us to an approximate solution for Y_{today} in the Boltzmann equation

$$\frac{1}{Y_{today}} - \frac{1}{Y_f} = \frac{\lambda}{x_f} \longrightarrow Y_{today} \simeq \frac{x_f}{\lambda} \tag{3.0.15}$$

being $Y_f >> Y_{today}$.
With this, we can arrive at a formula for Ω_χ:

$$\Omega_\chi h^2 = \frac{m s_{today} Y_{today}}{\frac{\rho_{crit}}{h^2}} \tag{3.0.16}$$

4 Numerical estimation

Now we need to estimate numerically $\Omega_\chi h^2$ and compare it to the value we obtained from the experiments. To achieve this, we take into consideration the same line of reasoning we employed in a few sections above when comparing Γ and H at freeze-out. In particular let's use for Γ:

$$\Gamma = n_\chi^{eq} < \sigma v >= g_\chi (\frac{m_\chi T}{2\pi})^{\frac{3}{2}} \exp\Big(-\frac{m_\chi}{T}\Big) < \sigma v > \tag{4.0.1}$$

and the complete formula for H:

$$H^2 = \frac{\rho}{3M_{PL}^2} \tag{4.0.2}$$

with

$$\rho = g_*(T)\frac{\pi}{30}T^4 \tag{4.0.3}$$

If we consider the situation at freeze-out with $x_{FO} = \frac{m}{T_{FO}}$ and just compare the two expressions for H and Γ, reshaping everything as a function of x_{FO} we obtain something of the kind:

$$\frac{\exp(-x_{FO})}{x_{FO}^{\frac{1}{2}}} \simeq \frac{3\sqrt{5}}{2\pi^{\frac{5}{2}}} \frac{g_\chi}{g_*^{\frac{1}{2}}(x_{FO})} m_\chi M_{PL} \tag{4.0.4}$$

that can be reacasted in

$$\frac{\exp(-x_{FO})}{x_{FO}^{\frac{1}{2}}} \simeq \frac{3\sqrt{5}}{2\pi^2}\frac{g_\chi}{g_*^{\frac{1}{2}}(x_{FO})}m_\chi M_{PL} \tag{4.0.5}$$

What we want to achieve is just a qualitative estimate of x_{FO}, so by leaving only the exponential term on the left side and taking the logarithm of both members, we come up with a benchmark value [44] of

$$x_{FO} \simeq -\ln\left(\frac{3\sqrt{5}}{2\pi^2}M_{PL}\right) = O(10) \tag{4.0.6}$$

Here there is a little detail to notice for the factor $< \sigma v_{rel} >$. There are some approximations we can make even though we do not know the specific form of this factor. Using a wave expansion for the solution of the Schroedinger equation, one can see, after a few manipulations, that even the scattering cross section can be approximated into a sum of different factors in the small velocities regime. In fact the most important ones are the so-called $s-wave$ and $p-wave$ which are respectively the first and the second factor in the expression below, which are constants.

$$< \sigma v_{rel} > \sim a + bv^2 + ... \tag{4.0.7}$$

In the following, the result we obtain is calculated for s-wave processes, that involve only the first factor in the approximation above.
With WIMPs being weakly interacting, we can use a cross section of the kind $< \sigma v > \sim \frac{\alpha^2}{m^2}$.
For a weak scale particle we can use $\alpha \sim 0.01$ and $m_\chi \sim 100\ GeV$.
We employ the previoulsy obtained result $Y_0 \sim \frac{x_{FO}}{\lambda}$.

Moreover, thanks to recent experiments we can safely use

$$\begin{cases} \rho_{crit}(t_0) \simeq 1,05 \times 10^{-5} h^2\ GeV\ cm^{-3} \\ s_0 \simeq 2891,2\ cm^{-3} \end{cases} \tag{4.0.8}$$

Taking all of this into consideration and using $x_{FO} = 10$ we arrive finally at the formula

$$\Omega_\chi = \frac{m_\chi s_0 Y_0}{\rho_{crit}} \to \Omega_\chi h^2 \sim \frac{10^{-26} cm^3/s}{< \sigma v >} \simeq 0,1(\frac{0,01}{\alpha})^2(\frac{m}{100\ GeV})^2 \tag{4.0.9}$$

obtaining the right order of magnitude suggested by Plank and WMAP [44].

5 WIMPs

So what is it with WIMPs that makes them such a great candidate in the role of dark matter particle? First of all it must be said that any given model must be confronted with the solid value already obtained of $\Omega_\chi h^2 \simeq 0,12$. Looking for WIMPs, as the name suggests, we must employ cross section typical of weak interactions that in general

gravitate around a scale of $1pb$ as we have already seen. Then we suppose that this kind of dark matter decouples in a regime where $g_* \simeq g_{*s}$. This is not a terrible approximation if we consider high temperatures, which is the case in the early Universe. Now making use of the value $x_{FO} \simeq 25$ we can obtain

$$\Omega_\chi h^2 \simeq 0,12(\frac{106,75}{g_*(T_{FO})})^{\frac{1}{2}}(\frac{0,7pb}{<\sigma v_{rel}>}) \tag{5.0.1}$$

thus revealing that particles with cross section typical of weak interaction(of the order of the pico barn) can reach a value for the relic density very similar to the one we are looking for. This is referred to as "The WIMP miracle", as the correct result for $\Omega_\chi h^2$ is reached for m_χ in the GeVs-to-Tev range.
The first WIMP consisted in a 4^{th} generation Dirac neutrino which, for $m_\nu > MeV$, is non relativistic at decoupling [21], thus entering the case just studied. Here a little clarification needs to be done on the form that the cross section assumes depending on the particle that mediates the interaction. Since the particle considered, the interaction would be mediated by the Z boson, which will provide the $\Omega_\chi h^2$ plot the classic V-shape that comes with it at the resonance for $m_\nu \sim \frac{M_Z}{2}$. Then whether we find ourselves in the regime $m_\nu < M_Z$ or $m_\nu > M_Z$, the cross section will assume different shapes. In the first case, the cross section will assume the characteristic form that we encountered studying weak interactions

$$<\sigma v_{rel}> \sim G_F^2 m_\nu^2 \simeq (\frac{m_\nu}{GeV})^2 10^{-26}\frac{cm^3}{s} \tag{5.0.2}$$

with G_F Fermi's constant. In the opposite case, the cross section will resemble more the one of electromagnetic processes

$$<\sigma v_{rel}> \sim \frac{\alpha^2}{m_\nu^2} \simeq (\frac{m_\nu}{TeV})^{-2} 10^{-26}\frac{cm^3}{s} \tag{5.0.3}$$

thus proving our previous claim that a mass between GeV and TeV will grant us the relic density that we are seeking.
In all fairness this is not much of a miracle, because one can still achieve the correct relic density with a really weak coupling $\alpha << 1$ but keeping fixed $\frac{\alpha}{m}$, thus allowing for a wider variety of masses to reach the result we want.
In the following section, we are going to analyze WIMPs behavior in the early Universe making use of a powerful tool in Boltzmann equations, which will grant us more precise results.

6 DM searches

Right now there are three major sectors in which the research activities on dark matter are concentrated: direct, indirect searches and colliders.
Direct searches investigate collisions between dark matter and experimental targets. It is not a subtle strategy if one thinks about it and it guarantees a wide range of probable WIMPs candidates. In fact, we proved in previous sections that for WIMPs, the relic density is inversely proportional to the non-relativistic annihilation cross section

$$\rho_{DM} \simeq \frac{1}{\sigma_A} \tag{6.0.1}$$

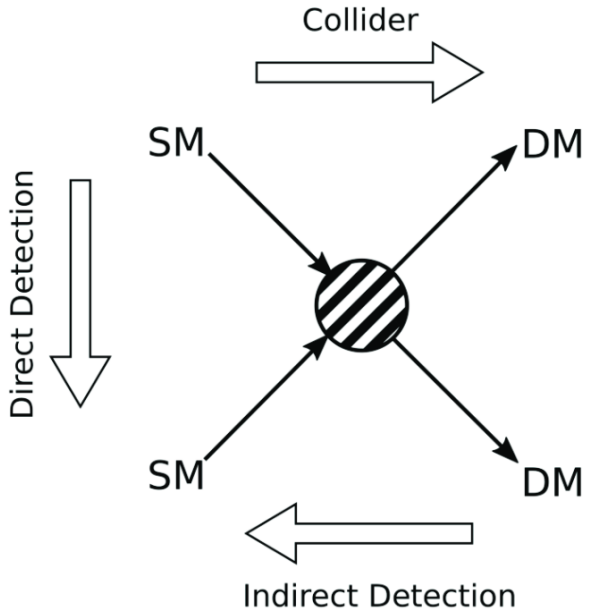

Figure 2.1: This picture is explicative of the three different types of searches we can employ for dark matter. From [38]

so that the event rate would be proportional to the product between this factor and the scattering cross section[21]

$$R \sim \rho\sigma_S \sim \frac{\sigma_S}{\sigma_A}. \tag{6.0.2}$$

This will allow a discrete rate even for WIMPs candidates with a small relic density. In fact, there is a crossing symmetry relating scattering and annihilation cross section, so that even if σ_A is big, the same could be said for σ_S. On the other side, as we will appreciate more in the next section, direct searches are sensitive to uncertainties related to local dark matter halos and are completely insensitive to leptophilic dark matter models in which DM only couples to leptons. Moreover as one can understand, direct detection methods fail whenever DM particles are so light that their signal would not reach the experimental threshold or in the case of a too small σ_S.
Indirect searches look for products of WIMPs annihilations or decay. In particular, dark matter particles that couple with standard model particles, should be revealed through these methods. Of course, when this condition fails to happen this strategy will lose all of its appeals. Anyways these searches are expected to greatly improve in the next years and, as we deepen our knowledge in this sector, we will reach higher sensitivities that will lead us to a clearer picture regarding dark matter and its byproducts.
Finally, colliders are our personal and homemade research lab, where crashes between standard model particles are observed and studied. In the case of a dark matter sector non trivial coupling with SM particles, we would be able to reveal WIMPs through these collisions by observing the missing transverse energy that characterizes them. However hadron colliders are not that sensitive to leptophilic dark matter, but this does not undermine the great importance that this instrument has and the innumerable ways it could serve us, expecially combined with the other two. Let's have a closer look at them all.

7 Direct searches

The first way that comes to mind, when it comes to dark particles to be discovered, is of course to wait for them to crash onto an experimental target and to observe the reaction as a proof of their existence. This technique has its pros, as we can directly observe the fruits of collisions against the detector and attribute them eventually to the presumed dark particle. The point is we must consider the *dark* adjective to be totally characterizing of these particles, as we cannot observe them. Because of this, we study their reaction with the detector. In case a dark particle would be colliding against our target, what we would see is just the target that recoils against what is an invisible particle. We study the recoil energy being deposited inside our target to extract information about the original particle that caused the collision. First of all, we have to recognize that in this kind of experiments, there is going to be a huge background that we need to come to terms with. This is why the totality of experiments considered as direct searches have to be placed underground, in order to protect them from the majority of cosmic rays. There is even an idea of what kind of signal we should get. In fact, it should be just a single hit, and the signals collected should be uniformly distributed in time. This is contrary to what happens with neutrons, particles that tend to interact multiple times with the target [25].

We have introduced in the previous chapter what is roughly the velocity distribution of dark matter in the halo surrounding the Milky Way, and again we reiterate the fact that the local DM density is

$$\rho_{DM} \simeq 0,3\ GeV/cm^3 \tag{7.0.1}$$

in the Standard Halo Model. When we consider DM experiments we must come to terms with DM motion in the galaxy. Although there can't be a preferred direction of motion in the galaxy, we must consider that we, as observers, are continuously in a motion state with respect to the Sun which, in turn, rotates around the center of the galaxy. This has to be taken into account when projecting an experimental apparatus. What is expected is a DM shower, which intensity will be subject to an annual modulation based on the relative motion of the Earth with respect to DM reference frame.
We expect indeed a stronger DM flux incoming towards Earth in the period of May/June and a progressive decrease after in which the flux will eventually touch the lowest point in intensity in the period of November/December.
This is not the only effect that influences the incoming flux though. A competing one would be what is called "gravitational focusing" which is caused by the Sun's gravitational attraction on DM particles, which may pull them away from their direction of motion and basically shift their path towards the Sun. Here, for example, the enhancement in DM flux is perceived at its peak in March, when the Earth is behind the Sun, and at its lowest in September, when the opposite situation arises. The play between the two antagonizing effects is held by DM velocity, in that the slower DM is, the more grip gravitational focusing will exert on it.
In terms of flux, a rough estimate starts when considering

$$n_{DM} = \frac{\rho_{DM}}{m_{DM}} \tag{7.0.2}$$

hence DM flux toward Earth will be

$$\phi_{DM} = n_{DM} v_{DM} = \frac{\rho_{DM}}{m_{DM}} v_{DM} \tag{7.0.3}$$

which, in the case of WIMPs with mass $m_{WIMP} \simeq 100 GeV$ becomes

$$\phi_{DM} = 9 \times 10^4 cm^{-2} s^{-1}. \tag{7.0.4}$$

Not a lot to work with, considering that we started with an extremely small number in ρ_{DM} which is less than 10^{-21} times the density of water! This should make us realize how difficult it is for us to detect these particles.
Now without further ado, let's analyze the details about the experimental apparatus. First, we study a single collision of dark matter against the target of mass M_T in an elastic way.
By imposing the conservation of energy and momentum on the system, one can get to the explicit equation for the recoil energy of the target nucleus

$$E_R = \frac{|\vec{q}|^2}{2M_{nucleus}} = \frac{2\mu^2 v^2 (1 - cos\theta)}{2M_{nucleus}} = \frac{m_\chi^2 M_{nucleus} v^2 (1 - cos\theta)}{(m_\chi + M_{nucleus})^2} \tag{7.0.5}$$

here we made use of $\vec{q}$ as the WIMP's momentum, v as its velocity and μ as the reduced mass of the nucleus-WIMP system.
WIMPs typical velocities are of the order of 300 km/s and for $m_\chi >> M_{nucleus}$ we expect the nucleus recoil to be $E_R \sim M_{nucleus} v^2 \sim 1 - 100\ keV$. The most general picture that allows us to express the rate of WIMPs collisions with the target nucleus is

$$R \simeq \int_{E_{min}}^{E_{max}} \int_{v_{min}}^{v_{max}} \frac{2\rho}{m_\chi} \frac{d\sigma}{d|\vec{q}|} v f(v) dv dE_R \tag{7.0.6}$$

with ρ being dark matter density, σ elastic scattering cross section and $f(v)$ WIMP's velocity distribution. We have already talked about the maximum velocity being the escape one $v_{max} \simeq 650\ km/s$ and with a quick calculus we can estimate $E_{R,max} = \frac{2\mu^2 v^2}{M_{nucleus}}$ to be the maximum recoil energy, so

$$v_{min} = \sqrt{\frac{E_{R,max} M_{nucleus}}{2\mu^2}} \tag{7.0.7}$$

and this means that the detector's energy threshold is what actually discriminates what we can from what we cannot see.
Now two paths open in front of us, depending on the different types of scattering taking place. Dark matter can have indeed spin-dependent or spin-independent interaction with the target. The first case is caused by scalar or vectorial couplings of DM with the nucleus and it can be seen that [44]

$$\frac{d\sigma}{dE_R} = \frac{2m_N}{\pi v^2} [Z f_p + (A - Z) f_n]^2 F^2(q). \tag{7.0.8}$$

Z and A are respectively the atomic number and atomic mass of the nucleus and f_p and f_n are WIMPs couplings to protons and neutrons. In the end, $F(q)$ is a form factor that

accounts for the finite size of the nucleus and is normalized such that $F(0)^2 = 1$. The scattering is coherent and the overall differential cross section is in the end proportional to the nucleus atomic number squared.
The opposite case is represented by spin-dependent scattering which is caused by the axial coupling of dark matter with the nucleus. In this case

$$\frac{d\sigma}{dE_R} = \frac{16 m_N}{\pi v^2} G_F^2 J(J+1) \Lambda^2 F_{SD}^2(q) \tag{7.0.9}$$

with $\Lambda = \frac{1}{J}(a_p < S_p > + a_n < S_n >)$, $a_{p(n)}$ are couplings to proton(neutron) and $< S_{p(n)} >$ the average spin contribution of proton(neutron).
We can see a clear dependence on $J(J+1)$ where J is the total spin of the target. This suggests that this will turn to be a smaller contribution with increasing target dimension. The overall result is that the experimental sensitivity to spin-dependent scatterings will be below that of spin-independent ones.
It is important to notice that the spin-dependent form factor is different from the spin-independent one. Notice also that spin-dependent interaction is not coherent with the nucleus anymore and does not scale as A^2. This results in difficulties in analyzing experimentally spin-dependent interactions.
There is a diverse array of direct detection experiments, and most of them make use of different target materials and techniques. DAMA/LIBRA experiments found in its dataset an annual modulation compatible with the one expected from WIMPs [21]. CoGeNT experiment revealed a modulation and an unexplained rate excess in its data which could belong to WIMPs. These are all examples of experimental situations which could be attributed to WIMPs collisions. It is of crucial importance to compare those results with each other and with the upper bounds already in our possess. With the current experiments we are investigating progressively lower cross section and the idea is to perfect our experiments to keep going in this direction. Eventually, we will reach the *neutrino floor* where the investigated cross section will be undistinguishable from the elastic neutrino cross section. DARWIN experiment is currently working on this and the situation will be clearer once we collect more data with more advanced experiments in the near future.

8 Indirect searches

Here we explore the alternative routes that we can take to unveil the mystery of dark matter. It can be possible to identify dark matter by examining its annihilation products, which we receive here on Earth and are able to detect with the help of our satellites. Of course, dark matter annihilation rate is not what it used to be in the early universe, but this does not mean that the annihilation rate has been nullified in the present time, there can still be byproducts of DM self-interaction coming from places where its density is higher, like for example the center of our galaxy.
In principle, there is plenty of particles in the Standard Model that could be residues of DM annihilations. In the following, we are going to explore some of the most palatable ways we can think about when it comes to indirect detection.

8.1 Indirect detection through photons

Neutral particles in general possess the unique advantage of traveling towards us untouched. They propagate in the space without feeling the influence of magnetic fields and without losing energy. This in turn benefits us of the certainty of their traveling direction and of the energy of the reaction that produced them.
Now we are going to analyze the details of gamma rays originating from DM annihilations, since they carry more information from the start with respect to charged products and, in some cases, they can provide the "smoking gun" for DM annihilations [44].
Since we can express the annihilation rate per DM particle as

$$\sum_i \frac{\rho[r(l,\psi)]}{m_\chi} \times < \sigma_i v > \tag{8.1.1}$$

since there can be multiple annihilation channels. r is the distance between the event and the Galactic center, which in turn depends on l, the line of sight distance and ψ which is the angle observed relative to the direction of the galactic center. If we multiply it by the total number of particles in a volume $dV = l^2 dl d\Omega$, we get a factor of

$$(\sum_i \frac{\rho[r(l,\psi)]}{m_\chi} \times < \sigma_i v >) \times (\frac{\rho[r(l,\psi)]}{2m_\chi}) \tag{8.1.2}$$

with the factor 2 from the two particles involved in the interaction. In the end, we get the photon flux by multiplying this by the number of photons produced at given energy E_γ

$$\frac{d\Phi_\gamma}{dE_\gamma} = \frac{1}{4\pi} \int_{\Delta\Omega} d\Omega \int_{l.o.s.} dl \rho[r(l,\psi)]^2 \sum_i \frac{< \sigma_i v >}{2m_\chi^2} \frac{dN_i}{dE\gamma}. \tag{8.1.3}$$

- We can stack all the astrophysical uncertainties into the factor

$$J = \frac{1}{\Delta\Omega} \int d\Omega \int_{l.o.s.} dl \rho[r(l,\psi)]^2 \tag{8.1.4}$$

  J depends only on the dark matter distribution and it is normalized over an observed solid angle so that a flat halo with a density equal to the one measured in the solar circle, integrated along the line of sight to the galactic center, would give us the value of one. It is important to notice that the larger is J, the better is for DM annihilations. One would have to look for system capable to enhance this factor, like dwarf galaxies which are DM dominated and present very few astrophysical uncertainties compared, for example to the center of our galaxy, despite DM density being higher in the latter case.

- Moving on to the particle physics sector, it can be contained in the factor $\frac{<\sigma v>}{m_\chi^2} \frac{dN}{dE_\gamma}$. Here usually we can pull the cross section out of the integral, ecxept for p-wave processes, amongs all, in which the thermally averaged cross section demonstrate a strong dependence on v.

If we consider the annihilation $\chi\chi \to \gamma X$, where $X = \gamma, Z; H$, we can see that in the non-relativistic limit, the energy conservation condition is written as

$$2m_\chi = E_\gamma + \sqrt{E_\gamma + m_X^2} \longrightarrow E_\gamma \simeq m_X(1 - \frac{m_X^2}{4m_X^2}) \tag{8.1.5}$$

If we consider as final state $\gamma\gamma$, we can clearly see that we obtain a monochromatic energy spectrum, in fact, it would present a monochromatic energy line at the DM mass. In the case of $X = Z$ the line would still be monochromatic, but it would also be shifted towards lower energies.

Such a monochromatic line would be, if observed, astonishing proof of DM existence. Unfortunately, $\gamma\gamma$ production is loop suppressed and with branching ratios 10^{-3}, 10^{-4}, so it is unlikely to be observed.
There are also other possibilities for photon production. In particular, DM annihilations could produce charged leptons or quarks which in turn could emit photons via final state radiation, or in the shower of their decay products. For example pion decay $\pi^0 \to \gamma\gamma$ would consist in a DM proof since the photon energy spectrum would have a cut-off in correspondence of m_χ. It cannot be attributed to DM only tough, since there are also other astrophysical processes that can have the same cut-off which do not involve DM.
We can see, as a final note, that in general the final flux has a strong dependence on the relative velocity of DM particles and on the annihilation cross section in SM particles. The factor $< \sigma v >$ is the same in many models as the one that figures in the relic density formula, so a juicy target would be the WIMP one in which $< \sigma v >= 3 \times 10^{-26}\ cm^3 s^-1$.

8.2 Neutrino searches

The solar system is, as previously stated, in a continuous state of motion with respect to the center of the galaxy and, consequently, to the dark matter reference frame. It can happen, during this motion, that we, as a system, go through dark matter which can scatter with baryonic particles. The scattering can be hard enough to steal a consistent part of dark particles' energy so that they are captured by the huge gravitational field belonging to the Sun [21]. Now, talking about capture rate Γ_C, we can say that it should be proportional to the scattering cross section and to the local DM number density, basing ourselves on previous formulas

$$\Gamma_C \sim \sigma_S n \tag{8.2.1}$$

Time goes by and the number of captured DM particles by the Sun increases $N = \Gamma_C t$ and so does the annihilation rate being proportional to n^2

$$\Gamma_A \sim \sigma_A n^2 \tag{8.2.2}$$

so the number of WIMPs inside the Sun changes with time as

$$\frac{dN}{dt} = \Gamma_C - 2\Gamma_A \tag{8.2.3}$$

The capture rate should be constant in time as the process of capture should not affect the DM density and distribution. Instead, the annihilation rate grows with time, until

some kind of equilibrium is reached when $\Gamma_A = \frac{\Gamma_C}{2}$ and

$$\frac{dn}{dt} = 0. \tag{8.2.4}$$

It can be proved that this equilibrium is reached during the Sun lifetime.
Now the only product of annihilations that can escape from the Sun and reach the Earth are neutrinos. Luckily for us, the ones produced in these types of annihilations are much more energetic than the ones coming from other processes. The best limits in our hands come from IceCube telescope. Moreover, if we consider a situation of equilibrium between capture and annihilation inside the Sun, then the consequent neutrino flux will depend only on the capture rate of WIMPs. This means that the rate will depend only on the scattering cross section. We can see that direct detection experimental results will depend on the same quantity so we can compare both of the measurements. This is a great way to have two different strategies to work in a synergetic manner.

8.3 Anomalous cosmic rays

Charged particles like electrons, positrons, protons and antiprotons can very well be byproducts of WIMPs annihilations. The difference with neutral particles is that in this case, they interact with the galactic magnetic field, hence deviating from their original path and losing energy during their trip toward Earth. Here they present a diffuse spectrum caused by the energy loss while propagating. Several experiments, like PAMELA, are looking for charged particles that could represent a signature of DM presence, like, in the PAMELA case, an abnormal presence of cosmic ray positron fraction above a certain energy threshold, which could be explained by DM annihilations. All the experiments conducted in this field reveal a local source of cosmic rays which can be attributed to Dark Matter. The issue here is how to state that the sole cause of these phenomena is dark matter with absolute certainty, given the fact that there are multiple plausible explanations other than that, like, for example, emission from pulsars.
Positrons and antiprotons are useful to seek because they can be produced in DM annihilation and, on top of it, there is not much antimatter in our Universe, so there is only a handful of processes that can be responsible for their production, one of which is WIMP annihilation. p and $\bar{p}$ have the advantage to propagate for longer distances inside the galaxy over electrons and positrons, which can interact with photons losing energy relatively quickly.
Nevertheless in the years, there has been a consistent development of technologies that would help us to detect such particles. In particular, the birth of balloon experiments has revealed itself as a striking instrument in the search for cosmic positrons, finding an excess over secondary cosmic rays fluxes. This is the case with PAMELA (Payload for Antimatter Matter Exploration and Light-nuclei Astrophysics) which is a satellite with a magnetic spectrometer on itself that reported in 2008 an excess of positron fraction in the 10 to 100 GeV energy range [21]. A rise in the e^+ fraction can be observed over 10 GeV that cannot be explained by collisions of cosmic rays with interstellar medium. The positrons produced in such reactions are expected to have a spectrum that falls quite quickly with energy, so they cannot be the cause of the excess observed by PAMELA. In fact, it is believed that the latter would be either DM annihilation or pulsar.

There has been no observed excess in $\bar{p}$, which excludes the hypothesis of supernova remnants behind the positron excess, and nears our interpretation of dark matter to leptophilic theories, in which DM only couples with leptons. Moreover, there was no endpoint observed in e^+ excess. This is also important because it would have been a hint about DM mass. PAMELA observations combined with HESS, another affine experiment, lead to $m_{DM} \sim few\ TeV$. More at it, DM would be annihilating to 2^{nd} or 3^{rd} generation leptons before the e^+ emission. This happens through the bosonic mediator ϕ, which then decays to $\mu^+\mu^-$ or pions. The reason is that this chain of processes would explain the soft decrease in energy observed in the electron plus positron spectrum by HESS around energies from 1 to 10 TeVs. ϕ is a light particle, hence weakly coupled to baryonic matter. This could very well be that "dark photon" described in some of the most famous theories of dark matter preaching a new and hidden gauge symmetry that completes the standard model gauge group.
There are some problems linked to these theories to explain the data, like the fact that the annihilation rate should be boosted by a factor of 10 to 10^3. A plausible solution would be Sommerfeld enhancement in which the ϕ exchange generates a Yukawa potential which traps the two annihilating particles that in turn form a bound state, hence enhancing the cross section.
Another solution would be just to have a bigger annihilation cross section for WIMPs. Unfortunately this, in turn, would produce a too-small relic abundance for WIMPs, but could be a solution in the case of non-standard pre-BBN cosmology.

9 Collider searches

Colliders offer another main opportunity to search for dark matter. Several colliders aim at revealing dark matter particles through proton, electron or positron collisions. The Standard Model has been, through the years, highly investigated and we are actually in possession of very precise mesurements concerning properties and decays of almost all SM particles. Nevertheless, there remain still some underexplored areas in which dark matter presence could be hidden. In particular Z boson, Higgs boson, top quark or hadrons could still have some small decay rates into pairs of invisible new particles, and in particular into DM candidates, in case their masses were smaller than half the decaying one's.
A source of interest is definetely Higgs boson which can actually be considered a portal for new physics. It has to be noted that Higgs invisible decays are really weakly constrained and in some case, the branching ratio in invisible particles can reach peaks of 26%. This is one of the main reasons extensive searches have been made to collect more data on Higgs decays, it can still exist a coupling between Higgs and a new, maybe dark, particle, hence the name: Higgs portal [2].
Several particle colliders are running and more are about to see the light in the near future. An important example of the former category is LHC, in which protons collide at the center of mass energies up to 13 TeV and it has still not reached its full potential. It offers a high luminosity and can probe particles with mass up to a few TeVs.
On the other hand, we have lepton colliders, like LEP, that have lower luminosity and center-of-mass energy but can provide more precise measurements.
The point with dark matter is that it should be neutral, uncolored and weakly interact-

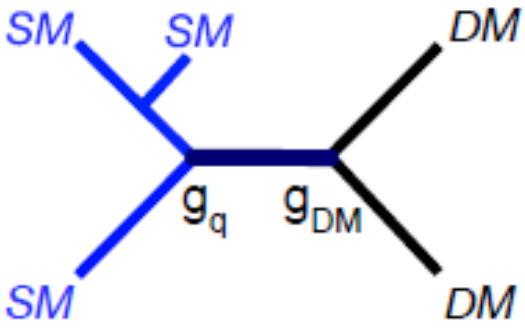

Figure 2.2: Scheme of a mono-X process studied at colliders. From [24]

ing. This means that it can have only very small couplings to QCD, which can be probed thanks to the LHC's high luminosity. Being weakly interacting and neutral, DM collider searches are configured as looking for missing transverse energy in the collision examined. The heavy particles produced in the collision can decay and produce DM particles, then generate significant missing energy. Of course, the specifics of these searches are highly model-dependent.
Other signatures can present very interesting results linked to DM existence. We can indeed study, in the case of DM production, the particles that accompany DM. In this category lye "mono-X searches", where we actually indagate X particle produced in order to extract information about a possible dark particle. The most common search in this case are monojet searches at LHC, where the missing transverse energy recoils against a high energy jet, which is produced as initial state radiation. The complementary search at LEP is monophoton one, in which the missing energy is deduced by the presence of a hard photon.
The limits obtained by studying monophoton and monojet events have been extracted using effective couplings between SM and DM sectors [7]. Examples of this kind of operators are in 2.2 where we can see dark matter and standard model particles together in four points contact interactions, just like Fermi's theory for electroweak interactions before the introduction of W and Z bosons. These operators are valid until the energy of the process lies well below the energy scale characterizing the SM-DM interaction, as is true for all effective field theories.

Effective field theories might be a good instrument that allows us to gather all the fundamental aspects characterizing WIMPs interactions like degrees of freedom and WIMP phenomenology avoiding all the complex detail of a full theory description. The weak point in such a line of reasoning is that at a certain point, as we should know, effective field theories break down, and that can happen if we consider energies corresponding to the scale of DM-SM interaction mediators. Beyond this point, a full theory is necessary in order to describe physics.
A possibility for DM is that the mediator is a standard model particle, or has the same couplings of a standard model boson, like simplified models in which the interaction between DM and SM particle is mediated by a Z boson-like particle. The reason we do not choose SM particles as mediators is that these models are limited by very strong

constraints such as electroweak precision measurements and direct searches. Anyways in the simplified models the interaction between SM and DM particles is determined by the mass of the mediator, its coupling strength to DM g_{DM}, to SM quarks g_q and by DM mass. Usually at LHC are conducted searches using these simplified models with a bosonic mediator with vector or axial coupling and with DM coupling fixed to unity and coupling to quark fixed at specific values [11] [12]. These specific parameters have been chosen so that constraints coming from direct mediator searches are avoided. Let's focus on a Z-like mediator which interacts with DM and quarks only through axial vector couplings. Here colliders can help a great deal in unveiling and study visible decays of the mediator. It is important to notice that there would be, amongst all the possible interactions, the one in which the mediator generated by quark-antiquark or gluon annihilation then decays into di-jets. The decay in jet pairs produces a peculiar signal as there would be an excess in the invariant mass of the two most energetic jets (di-jets) which would be atop the QCD background. These types of searches do not depend strongly on the specific DM models considered and the invariant mass of the two most energetic jets is used as the main observable in the search. Mono-X and dijet searches are used in tandem with these kinds of models as their role is complementary in DM searches. Mono-X searches are more efficient in the region of the parameter space where DM mass is lower than twice the mediator mass, thus allowing the mediator to decay on shell to DM particles. Dijet searches instead are powerful in the region with higher mediator masses and higher DM masses with respect to mono-X searches 2.3. This is because in this region of the parameter space where the mediator decays into DM are suppressed with respect to dijet decays. However, the parameter space is highly dependent on the choice of quark couplings as one would expect. Moreover, if we only consider simple DM models with just a dark matter and one mediator couple to SM particles, only in this case mono-X searches can be considered DM collider searches. If we expand our point of view to include more complex scenarios with a multiplicity of different particles, then we cannot be so sure what we are searching for, as it is increasingly harder to couple the missing energy to dark matter only. This is why, although they can be considered interesting research fields, mono-X searches would hardly lead to DM discovery, if not coupled with other findings in direct detection experiments.

10 Complementarity of WIMPs searches

The methods described in the sections above all provide different informations about dark matter. They can all constrain different aspects concerning dark matter nature and are able to clarify different properties of dark matter interactions. Moreover, they are all susceptible to different kinds of uncertainties, like, amongst all, astrophysical and instrumental. Although it is nearly impossible that we will reach a decisive conclusion on dark matter case only leaning on one of these procedures, they can all work complementary in leading us to unveil this mystery. We can draw a qualitative picture regarding the different experimental strategies that could be summarized as follows:

- Direct detection: this is maybe the simplest and most brutal method we could count on for DM discovery. Thanks to the description we have given above, we can recognize that this method needs delicate care of the low energy background and it

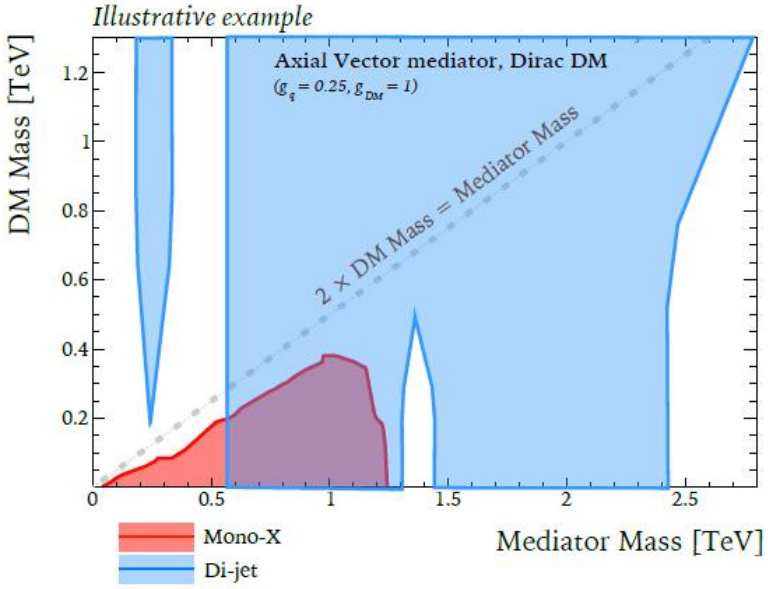

Figure 2.3: Sketch of the constraints on a simplified model of WIMP DM where a particle with axial-vector couplings of 1.0 and 0.25 to DM and SM respectively is exchanged. The constraints from mono-X (exclusion region in red) and dijet DM searches (exclusion region in blue) are shown in the plane of dark matter mass vs. mediator mass. The couplings represented in this sketch and their general features are inspired by LHC dijet and mono-X results. From [24]

is not particularly sensitive to DM that couples to leptons only, but, eventually, it can provide us with crucial information on DM particle mass and its elastic cross section with protons and neutrons.

- Indirect detection is, contrary to direct searches, potentially sensitive to all kinds of DM with all sorts of couplings to SM particles. These types of searches are growing with time in sensitivity, but require a deep understanding of astrophysical background.

- Colliders: like indirect searches are sensitive to a wide variety of DM models. Colliders offer the opportunity to study DM in a highly controlled environment and, in the WIMP scenario, considering the typical WIMP masses and the weak force interactions, we can definetely expect the DM WIMP to be produced at LHC. The downside of collider searches is that even if a dark particle's existence would be probed, still it cannot be established if the newly found particle is stable or cosmologically relevant.

Let's study a toy model in which dark matter interacts with standard model particles through four particles contact interactions [21] [24]. Consider a spin $\frac{1}{2}$ fermion χ that has generation-independent interactions with quark q, gluons g and leptons l:

$$\frac{1}{M_q^2}\bar{\chi}\gamma^\mu\gamma_5\chi\sum_q\bar{q}\gamma^\mu\gamma_5 q + \frac{\alpha_S}{M_g^3}\bar{\chi}\chi G^{a\mu\nu}G^a_{\mu\nu} + \frac{1}{M_l^2}\bar{\chi}\gamma^\mu\chi\sum_l\bar{l}\gamma^\mu l \tag{10.0.1}$$

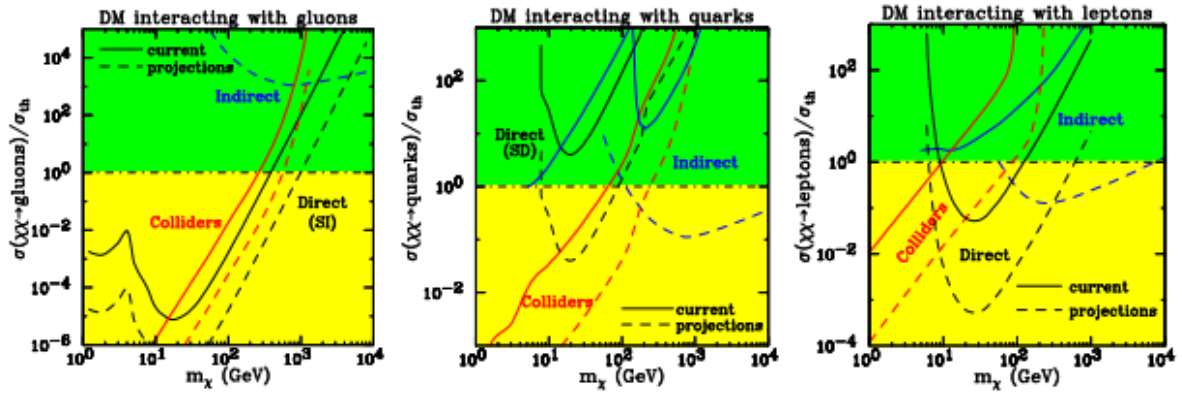

Figure 2.4: DM discovery prospects for direct detection, indirect detection and particle colliders on the cross section $\sigma(\chi\chi \to l, q, g)$ as a function of the WIMP mass. Here $\sigma^{th} = 3 \times 10^{-26} cm^3/s$ is the reference value for the annihilation cross section and it is the value required for a thermal WIMP to account for all of DM. From [24]

Even though there could also be other interactions, the few that we have chosen here are able to express in just a couple of terms, some of DM properties that we have described in the previous sections. For example quark interaction can be easily seen to originate spin-dependent scatterings, while gluon one can create spin-independent scatterings. Moreover M_q,M_l and M_g define the strengths of the interactions and, together with the value m_χ, completely define the theory. The knowledge of these parameters allows us to precisely calculate rates of spin-dependent and spin-independent elastic scattering, DM annihilation rates in quarks, leptons and gluons, together with the DM production rate at colliders.
The annihilation cross section at freeze-out is seen to be completely determinant for the relic density that we observe, so in any of the experiments we perform, we are able to access just a fraction of the complete observed dark matter density Ω_{DM}. If $\sigma_i(M_i)$ is the annihilation cross section for each individual channel for $i = q, g, l$, then we can normalize it to σ^{th} that represents the value required for a thermal WIMP to account for all the DM

$$\frac{\sigma_i(M_i)}{\sigma^{th}} = \frac{f_i}{\Omega_\chi/\Omega_{DM}} \tag{10.0.2}$$

with

$$f_i = \frac{\sigma_i}{\sigma_{total}} \tag{10.0.3}$$

representing the contribution of the singular channel and $\sigma_{total} = \sigma(\chi\chi \to anything)$. If we make the assumption $f_i = 1$, which means that just a single channel is responsible for the total annihilation cross section, we can see that σ^{th} could be the target of our experimental efforts. Indeed if we could get to the point of probing cross section $\sigma_i \sim \sigma^{th}$, we could discover the particle responsible for the totality of dark matter.
This example gives us the opportunity to explore the meaning of complementarity concerning dark matter experiments. Of course, at first glance, we can appreciate the fact that different experiments are sensitive to different couplings between DM and SM particles so that together they can give us a complete picture of DM interactions. Moreover, it is apparent that the outcome that could be achieved through different experimental

paths are also very dependent on DM mass. For example, we can see from the $FIGURE$ that direct searches for dark matter are very effective for masses of the order of 50 GeV and that their power gradually decreases at lower masses, as an effect of detector issues at lower energies.
It is precisely at low masses that colliders take the lead. In fact it can be seen from the picture that in this area, controlled collisions offer the best solution out of the three because they can produce light dark matter particles with really large momenta, so they are the best probes in this type of scenario.
Finally, it is in the high mass range that indirect searches surpass the others in effectiveness. In fact here both direct and colliders searches are out of their reach and indirect detection searches can jump in and make up for their absence. This is a deeper way in which we can really see the complementarity of these three experimental paths.

Chapter 3

Introduction to Z' physics

In the second chapter, we have seen how effective field theory can be employed in the study of dark matter properties. Models like these take advantage of the fact that heavy degrees of freedom are integrated out, resulting in simpler physics. It is apparent that this cannot be an answer to the problem we are dealing with, especially if we are considering collider searches, where the energy scales we investigate are typically near the energy cut-off of our effective field theory. It is in this moment that the alternative of simplified models can be really taken into account. The literature on this is really vast and explored. These models consist of theories in which the Standard Model is extended with a dark matter sector and the mediator between the two is fully present in the particle spectrum of the theory and not integrated out [46] .
We are prone to consider models in which fermionic DM interacts through a bosonic mediator. Of course, this is not the complete solution to the dark matter problem . In fact, these kinds of models do not come free of problems. There are all sorts of unitarity and anomalies issues that we have to deal with. But we will be more clear about this in the next sections.

Moreover, the aim for the grand unification of SM gauge couplings motivate the presence of additional U(1)' symmetries [1], which may appear as relics of larger GUT Lie groups and which could in principle breaks down at energies on the reach of the LHC.

Indeed we start with a gauge group of the kind:

$$G = G_{SM} \otimes U(1)' = SU(3)_c \otimes SU(2)_L \otimes U(1)_Y \otimes U(1)'. \tag{0.0.1}$$

The new Z' boson can be observed in its decay as resonance in di-lepton channel whenever the energy scale at which the symmetry is broken is found at TeV scale. Several theories predict the existence of this new boson, like E_6, $SO(10)$ or left-right symmetric models and these are all GUT realizations.
There are also other things to consider when speaking of simplified models. If the Z' boson mass is generated through a Higgs-like mechanism, the new scalar responsible for the symmetry breaking can play an important role in phenomenology and that will always be omitted in effective field models. Moreover, the condition of anomaly cancellation may

require the presence of new fermions that in turn can be spotted in our searches.
There are several ways to embed dark matter in this scheme [4].

- We extend Standard Model with a new gauge group $U(1)_X$. We charge only dark matter fermions under it while all SM fermions remain singlets. Then we allow the dark matter to couple only to the new Z' boson and not with SM bosons. In turn, Z' will couple with SM fermions through kinetic mixing.
- We employ a new gauge group obtained through lepton number differences like $U(1)_{L_\tau - L_\mu}$ or $U(1)_{L_\tau - L_e}$ or $U(1)_{L_\mu - L_e}$. Of course, these will be anomaly free.
- We use the difference between lepton and baryon numbers $U(1)_{B-L}$. We will see that these models allow the origin of neutrino masses after symmetry breaking. These models are of course anomaly free because of the introduction of right-handed neutrinos which are not contemplated in our version of the Standard Model.

We also embed a new complex scalar field which is heavier than our Higgs and that acquires a Vacuum Expectation Value(VEV) in order to give mass to the Z'.
Some words on the latter models are needed, as they have been extensively studied in the past and there are innumerable versions. In fact, as we said previously, they have the specific advantage of embedding the right-handed neutrinos and promoting an already present SM global symmetry to a local one.
SM has a big disadvantage in not being able to explain the neutrino masses. However today we are practically sure that a non-trivial neutrino mass matrix must be there in order to explain neutrino oscillations that have been observed in the course of history. The problem with the Standard Model is that neutrinos do not have their corresponding right-handed partners there, therefore they cannot acquire mass not even after electroweak symmetry breaking. Neutrino oscillations are of course related to neutrino masses and flavor mixing. A natural way to accommodate all of this could be a type-I seesaw mechanism making use of Majorana right-handed neutrinos. An additional $B - L$ symmetry could be the easiest way to explain neutrino masses through the seesaw mechanism. In fact, in these kinds of models three right-handed neutrinos are introduced with $B - L$ charges equal to -1 and are responsible for anomaly cancellation.

A $B - L$ Higgs boson which is a SM singlet is also added to the theory as we have previously seen [45]. The new Higgs also acquires a $B - L$ charge and gets, of course, a VEV breaking the $B-L$ symmetry. This in turn causes the creation of a $B-L$ boson and the fact that neutrino masses are naturally created through the seesaw mechanism. The mass spectrum of the particles in these theories which consist of the $B - L$ gauge boson, the right-handed neutrinos and $B - L$ Higgs are all dependent on the breaking scale of the new $B - L$ symmetry. If this scale happens to lay in the TeV range, it could very well be probed in the near future thanks to LHC. These simple models suffer a flaw in the sense that, even though we are able to explain neutrino masses, we still lack a dark matter candidate. This can be solved through the very common introduction of an additional Z_2 symmetry. We would assign an odd parity only for one right-handed neutrino, which will play the role of a, thus stable, dark matter particle.

These are the simplest theories one can rely upon aiming to explain dark matter. We will see in the following sections some typical and interesting cases.

1 Z' physics

Of course, there are physical features that are heavily model dependent and we would need to specify the model we are adopting in order to explore the peculiarities that constitute its roots. Fortunately for us, there are some basic features in common among all the physical models that revolve around the Z' boson, according to the classification given in the previous paragraph. Just as a basic reminder, we are considering the following SM extensions [4]:

$$U(1)_X \qquad U(1)_{L_i-L_j} \qquad U(1)_{B-L} \tag{1.0.1}$$

Here we consider models with a Z' spin-1 boson and a dark matter fermion χ with a non-trivial charge under the new group. As we have already begun to see, Z' couplings to SM fermions are of the kind:

$$L_{fermion} = -g_{Z'} j'_\mu Z'^\mu \tag{1.0.2}$$

with

$$\begin{aligned} j'_\mu &= 0 && U(1)_X \\ j'_\mu &= \bar{L}_i\gamma_\mu L_i + \bar{l}_i\gamma_\mu l_i - \bar{L}_j\gamma_\mu L_j - \bar{l}_j\gamma_\mu l_j && U(1)_{L_i-L_j} \\ j'_\mu &= \frac{1}{3}\bar{Q}\gamma_\mu Q + \frac{1}{3}\bar{u_R}\gamma_\mu u_R + \frac{1}{3}\bar{d_R}\gamma_\mu d_R - \bar{L}\gamma_\mu L + \bar{l}\gamma_\mu l && U(1)_{B-L} \end{aligned} \tag{1.0.3}$$

Where naturally Q and L are respectively quarks and lepton doublets, l_i are lepton singlets, d_R and u_R are right-handed quarks.
Now some consideration must be given before introducing dark matter sector. We need dark matter to couple to the new Z' gauge boson. To accomplish this, a Dirac fermion is needed. Moreover, we have to satisfy the specific condition of having no anomalies in our theories. We can avoid adding new conditions to the ones we already have satisfied by employing vector-like charges of DM under the new gauge group. In fact, if we choose $q_{\chi L} = q_{\chi R}$ we will obtain non-chiral fermions and the vector-like couplings to Z' will avoid additional anomalies arising. We remind the reader that the new fermion should be an SM singlet. When all of this comes into play we end up with a dark sector lagrangian of the type:

$$L_{DM} = i\bar{\chi}\ \not{D}\chi - m_\chi\bar{\chi}\chi \tag{1.0.4}$$

where the covariant derivative is naturally obtained as

$$D_\mu = \partial_\mu - ig_{Z'}q_\chi Z'_\mu. \tag{1.0.5}$$

First, let's introduce the lagrangian for the complex scalar that will give mass to the Z' boson thanks to the symmetry breaking:

$$L_{scalar} = \frac{1}{2}(D_\mu S)(D^\mu S)^\dagger + \mu_S^2 S^\dagger S + \frac{\lambda_S}{2}(S^\dagger S)^2 + \lambda_{HS}H^\dagger H S^\dagger S \tag{1.0.6}$$

Now the covariant derivative has the same structure of 1.0.5, with the only exception of introducing a charge q_S for the scalar particle under the new gauge group.
We make use of the fact that Higgs boson will acquire a VEV $< H >= \frac{v}{\sqrt{2}}$ and the complex

scalar will also get a VEV $< S >= \frac{v_S}{\sqrt{2}}$. Moreover, the Higgs boson has in general mixing with S

$$M^2_{HS} = \begin{pmatrix} \lambda_H v^2 & \lambda_{HS} v v_S \\ \lambda_{HS} v v_s & \lambda_S v_S^2 \end{pmatrix} \tag{1.0.7}$$

that can be diagonalized through a unitary transformation

$$\begin{pmatrix} S \\ H \end{pmatrix} \to \begin{pmatrix} c_\alpha & s_\alpha \\ -s_\alpha & c_\alpha \end{pmatrix} \begin{pmatrix} S \\ H \end{pmatrix} \tag{1.0.8}$$

where

$$t_{2\alpha} = \frac{2\lambda_{HS} v v_S}{\lambda_H v^2 - \lambda_S v_S^2} \tag{1.0.9}$$

and $t_{2\alpha} = tan(2\alpha)$

The most general kinetic energy term for the two gauge bosons associated with $U(1)_Y$ and $U(1)'$ includes the kinetic mixing term [42]

$$L_{kin} \to -\frac{c_Y}{4} \hat{B^{\mu\nu}} \hat{B_{\mu\nu}} - \frac{c_{Z'}}{4} \hat{Z'^{\mu\nu}} \hat{Z'_{\mu\nu}} - \frac{c}{2} \hat{B^{\mu\nu}} \hat{Z'_{\mu\nu}} \tag{1.0.10}$$

This does not spoil the gauge invariance, since both field strengths are gauge invariants. One can put the first two terms in canonical form $c_Y = c_{Z'} = 1$ by rescaling the fields and take $c = s_{Z'} = \sin\theta_{Z'}$.
The consequence of this term is that the kinetic term is not canonically normalized:

$$L_{gauge} = -\frac{1}{4} (\hat{B_{\mu\nu}} \qquad \hat{Z'_{\mu\nu}}) \begin{pmatrix} 1 & s_{Z'} \\ s_{Z'} & 1 \end{pmatrix} \begin{pmatrix} \hat{B_{\mu\nu}} \\ \hat{Z'_{\mu\nu}} \end{pmatrix} \tag{1.0.11}$$

So we need first to normalize this and then we will rotate to reach the mass eigenstates, which we will get in a second.
We assume $\sin\theta_{Z'} < 1$, otherwise we will get a theory with a single propagating gauge boson in the case of $\sin\theta_{Z'} = 1$ or a kinetic term with the wrong sign in the case of $\sin\theta_{Z'} > 1$. Now we get to diagonalize the kinetic term with an orthogonal transformation in the two gauge fields. The problem here is that such transformation shifts the hypercharge and, as a consequence, the electromagnetic current. In order to keep what we have already found about the electromagnetic current, we operate the diagonalization by making use of a non-orthogonal transformation:

$$\begin{pmatrix} \hat{B}_\mu \\ \hat{Z}'_\mu \end{pmatrix} = G(\theta_{Z'}) \begin{pmatrix} \hat{B}_\mu \\ \hat{Z}'_\mu \end{pmatrix} = \begin{pmatrix} 1 & -s_{Z'}/c_{Z'} \\ 0 & 1/c_{Z'} \end{pmatrix} \begin{pmatrix} B_\mu \\ Z'_\mu \end{pmatrix} \tag{1.0.12}$$

This way we get a canonically normalized kinetic term.
A consequence of the rotation is that now the fermions couple with the Z' gauge boson through the coupling strength

$$j'_\mu \to \frac{1}{c_{Z'}} j'_\mu - t_{Z'} j^Y_\mu \tag{1.0.13}$$

with j^Y_μ being the hypercharge current.
As an additional consequence, after the normalization, we can get to the mass matrix of the three gauge bosons B_μ, W^3_μ and Z'_μ. Of course, we can diagonalize this mass matrix

through procedures that we already know and arrive at the eigenvalues, the masses of the photon, the Z_{SM} and the new gauge boson Z'. In the following we give an approximated value of the three masses, based on the assumptions $v_S > v$ and $m_{Z'}, m_S > m_Z$.

The masses we find for the vector bosons are

$$\begin{aligned} m_\gamma &= 0 \\ m_Z^2 &= \frac{v^2}{4}(g^2+g'^2)(1-\frac{v^2}{v_S^2}\frac{s_{Z'}^2 g'^2}{8 g_{Z'} q_S^2}) + O(\frac{v^6}{v_S^4}) \\ m_{Z'}^2 &= \frac{g_{Z'}^2 q_S^2 v_S^2}{2c_{Z'}} + \frac{v^2}{4} g'^2 t_{Z'}^2 + O(\frac{v^4}{v_S^2}) \end{aligned} \tag{1.0.14}$$

We started from the mass matrix of the three bosons B_μ, W_μ^3 and Z'_μ. Then we diagonalized it with a combination of two block diagonal rotations, one with mixing angle θ_W and the other with angle θ_3 in the lower right. In fact, we have

$$\begin{aligned} \tan(2\theta_3) &= \frac{2 s_{Z'} c_{Z'} s_W v^2 (g^2+g'^2)}{c_{Z'} v^2 (g^2+g'^2)(1-s_W^2 t_{Z'}^2) - 2 g_{Z'}^2 q_S^2 v_S^2} \\ &= -\frac{2 s_{Z'} c_{Z'} s_W}{2 g_{Z'}^2 q_S^2} \frac{v^2}{v_S^2}(g^2+g'^2) + O(\frac{v^4}{v_S^2}) \end{aligned} \tag{1.0.15}$$

Now if we assume that Higgs VEV and SM gauge couplings are fixed, we can use the measurement with its associated error $m_Z = 91.1876 \pm 0.0021$ to get the constraint

$$\frac{g_{Z'} q_S}{s_{Z'}} v_S \geq 1.3\ TeV \qquad at\ 95\%\ CL \tag{1.0.16}$$

Then, thanks to the mass matrices we obtain after normalization and rotation, we can obtain some sort of comparison between the new complex scalar and the new vector boson mass in the form

$$\frac{m_S}{m_{Z'}} \sim \frac{\sqrt{\lambda_S}}{g_{Z'} q_S / c_{Z'}}. \tag{1.0.17}$$

Now let's write the couplings to fermions and scalars of the mass eigenstates:

$$\begin{aligned} L_{fermion} &= e j_{em} A \\ &- c_w s_3 t_{Z'} e j_{em} Z + (c_3 + s_w s_3 t_{Z'}) \frac{e}{s_w c_w} j_Z Z + \frac{s_3}{c_{Z'}} g_{Z'} j_{Z'} Z \\ &- c_w c_3 t_{Z'} e j_{em} Z' + (s_w c_3 t_{Z'} - s_3) \frac{e}{s_w c_w} j_Z Z' + \frac{c_3}{c_{Z'}} g_{Z'} j_{Z'} Z' \end{aligned} \tag{1.0.18}$$

and

$$\begin{aligned} L_{scalar} &\ni \frac{v}{8}(g^2+g'^2)(c_\alpha H - s_\alpha S) Z_\mu Z^\mu \\ &+ \frac{v}{4} s_w t_{Z'} (g^2+g'^2)(c_\alpha H - s_\alpha S) Z_\mu Z'^\mu \\ &+ \frac{v}{8} s_w^2 t_{Z'}^2 [c_\alpha (g^2+g'^2 + \frac{4 g_{Z'} q_S^2 t_\alpha}{s_w^2 s_{Z'}^2}\frac{v_S}{v}) H - s_\alpha (g^2+g'^2 - \frac{4 g_{Z'} q_S^2 t_\alpha}{s_w^2 s_{Z'}^2}\frac{v_S}{v}) S] Z'_\mu Z'^\mu \end{aligned} \tag{1.0.19}$$

Now it can be seen that in any kind of model, we take into account, there is only a handful of parameters that are relevant in its physics description. In fact, the relevant new parameters we have introduced in the lagrangian are

$$M_\chi, g_{Z'}, m_{Z'}, s_{Z'}, m_S, \lambda_{HS} \tag{1.0.20}$$

We assume that the charges under the new $U(1)'$ gauge group are of order one.
We have seen that the vector and the scalar masses are related. There are models in which the scalar is heavier than the vector $g_{Z'} << \lambda_S < 4\pi$. Here there is a suppression of the interactions of the new Z' with the Standard Model particles. This can lead to the reduction of the annihilation cross section to the point that only in some rare circumstances, like around the pole $m_{Z'} = 2m_\chi$, is possible to obtain an efficient annihilation in the early universe. Of course, even the production cross section at the LHC is affected by this choice of couplings.
The phenomenological aspects of the new Z' boson are determined by its couplings to the Standard Model particles and by $m_{Z'}$. Couplings to SM can arise through kinetic mixing which is proportional to $t_{Z'}$, through mixing to the Z boson with the term s_3 or through the $U(1)'$ charges of fermions with the term $g_{Z'}$.
Finally one can see that S properties are independent of dark matter properties and one can investigate new interesting aspects of interactions by examining the two mediators couplings, like Z'-S-Z coupling.

2 Anomaly-free models

The literature on this argument is really vast. Anomaly-free models have been explored in recent past, bringing us a new knowledge and new constraints in dark matter models. Whenever we decide to extend the Standard Model by including a new Z' vector boson, this operation does not come free of issues, as we have to consider that generally we need additional fermions to erase the anomalies. In fact, as can be seen in the Appendix, the anomalies arise in triangle diagrams, so the condition we have to satisfy is that any triangle diagram coming from a combination of SM gauge field, $U(1)'$ gauge field and graviton should be free of such anomalies [19].
We can summarize the anomaly cancellation conditions in the form of

- $[SU(3)_c^2] \otimes [U(1)']$ which implies $Tr[\{\tau^i, \tau^j\}Y'] = 0$
- $[SU(2)_L^2] \otimes [U(1)']$ which implies $Tr[\{T^i, T^j\}Y'] = 0$
- $[U(1)_Y^2] \otimes [U(1)']$ which implies $Tr[Y^2 Y'] = 0$
- $[U(1)_Y] \otimes [U(1)'^2]$ which implies $Tr[Y Y'^2] = 0$
- $[U(1)_Y^3]$ which implies $Tr[Y'^3] = 0$
- Gauge-gravity, which implies $Tr[Y] = Tr[Y'] = 0$

We shall see that if we adopt models in which there is only one dark fermion χ, in order to satisfy these conditions one would be forced to couple the new Z' to quarks and leptons, thus making it possible to test the theory with LHC searches. Moreover, the new fermion must have vector-like couplings to the Z'. This way the new vector boson theory would

also be within reach of direct searches, making it possible to test the new theory with DM scatterings.
We should see that if we assume a chiral DM fermion, with a purely axial χ-Z' coupling, one would be forced to add additional fermions to the theory and the new vector boson would still be coupled to quarks and leptons.
Anyways one could convert the previous conditions into equations by writing them in the same order as before:

$$\begin{aligned}
3(2Y'_q - Y'_u - Y'_d) &= 0 \\
9Y'_q + 3Y'_l &= 0 \\
2Y'_q - 16Y'_u - 4Y'_d + 6(Y'_l - 2Y'_e) &= 0 \\
6(Y'^2_q - 2Y'^2_u + Y'^2_d) - 6(Y'^2_l - Y'^2_e) &= 0 \\
9(2Y'^3_q - Y'^3_u - Y'^3_d) + 3(2Y'^3_l - Y'^3_e) + Tr_{BSM}(Y'^3) &= 0 \\
9(2Y'_q - Y'_u - Y'_d) + 3(2Y'_l - Y'_e) + Tr_{BSM}(Y') &= 0
\end{aligned} \tag{2.0.1}$$

Here the fermionic $U(1)'$ charges are Y'_i and q and l represent the left-handed quark and lepton doublets respectively. Moreover, we can recognize the right-handed fields in u,d and e, while Tr_{BSM} represents the trace over additional beyond Standard Model fermions. One can clearly see that besides BSM particles, those equations depend only on the charges of the new $U(1)'$ group. There are models in which the new charges Y'_i are taken to be for each fermion proportional to the weak hypercharge Y. Of course, these kinds of models are automatically anomaly free provided that $Tr_{BSM}(Y') = Tr_{BSM}(Y'^3) = 0$. The problem here is that, since the couplings to leptons are non-trivial, these kinds of models result heavily constrained by LHC dilepton searches, so one would need to build models with vanishing lepton couplings.
We can notice a few points even in this preliminary analysis. Let's look at the second equation that imposes $Y'_l = -3Y'_q$. If we want to avoid dilepton constraints, we should put $Y'_l = 0$. This rebounds on quark charges leading to $Y'_q = 0$. When we consider a single Higgs doublet, we obtain the additional condition

$$Y'_H = Y'_q - Y'_u = Y'_d - Y'_q = Y'_e - Y'_l \tag{2.0.2}$$

with Y'_H Higgs $U(1)'$ charge. Here one can see that if we require $Y'_l = 0$ and $Y'_e = 0$ for the same reasons, this implies that also Y'_d and Y'_u are zero. This brings us to the realization that the new vector boson coming from $U(1)'$ symmetry, would not even be produced at tree level if we want to avoid dilepton constraints.
Notice that if the new dark fermion χ is also the only one we add to the Standard Model the last two equations can bring us the information that

$$\begin{aligned}
3(Y'_u - 4Y'_q)^3 + Y'^3_{\chi,L} - Y'^3_{\chi,R} &= 0 \\
3(Y'_u - 4Y'_q) + Y'_{\chi,L} - Y'_{\chi,R} &= 0
\end{aligned} \tag{2.0.3}$$

which have, as the only rational solution,

$$Y'_{\chi,L} = Y'_{\chi,R} \tag{2.0.4}$$

so that the only solution we could employ to add a dark fermionic sector to the standard model is the one where dark matter has only vector-like couplings.

These conclusions were drawn under the assumption that the new charges were generation-independent. This is the simplest hypothesis. However, many models present non universal charges. This choice can be relevant in an experimental environment since it can lead to flavor-changing neutral-currents, some of the most important processes yet to be observed. Hence the non-universality of charges could be very well tested in the near future by the simple observation of these rare processes.
To summarize one can see that if we include only one dark fermion in our model, the latter cannot be leptophobic(vanishing lepton couplings), unless it shows also vanishing quark couplings. The new vector-like fermionic dark matter does not bring any new anomaly equation, instead, they have been already solved by SM particles as can be seen in the Appendix. The problem here is the non-vanishing couplings to lepton and quarks. Dilepton constraints will heavily reduce the parameter space.
It also needs to be taken into account the fact that the DM couplings to the Standard Model particles, where present, must be vectorial. This means that the cross section of DM scattering with the nucleus will not be velocity suppressed. This will in turn enhance the relic density for DM. In conclusion, this kind of model is almost entirely ruled out just by LHC searches.

2.1 Axial dark matter

Now let's say we examine the case of axial dark matter. In these models, dark matter has only axial couplings to the Z'. This way we will be able to lose the constraints coming from direct searches, paying the price of introducing more fermions into the model. Of course, axial dark matter can come into play whenever we decide to build a model where DM is a Majorana particle. In this case, the conditions 2.0.2 are still valid, so the first four equations of 2.0.1 are satisfied. Let's dive more into the equations for anomalies, which are all satisfied but the two below

$$\begin{aligned} 3(Y'_u - 4Y'_q)^3 + \sum_j (Y'^3_{j,L} - Y'^3_{j,R}) = 0 \\ 3(Y'_u - 4Y'_q) + \sum_j (Y'_{j,L} - Y'_{j,R}) = 0 \end{aligned} \tag{2.1.1}$$

Here $Y'_{j,L/R}$ represent the $U(1)'$ charges of left/right component of the new fermion species j.
Of course, we recover what we have already seen previously if we impose $Y'_u = 4Y'_q$ with whatever number of new fermions that have vector-like couplings $Y'_{j,L} = Y'_{j,R}$. If we want to have a non-trivial theory we must involve new fermions in order to cancel anomaly equations, this is clear. So let's consider a fermionic dark matter particle χ chiral with $Y'_{\chi,L} = -Y'_{\chi,R}$ and an additional fermion A singlet under SM and with left and right charges $Y'_{A,L}$ and $Y'_{A,R}$ respectively. After a few mathematical procedures, we can find the solutions

$$\begin{aligned} Y'_{A,L} = -1 \quad , \quad Y'_{A,R} = 1 \\ Y'_{A,L} = 0 \quad , \quad Y'_{A,R} = -1 \quad or \quad Y'_{A,R} = 5/4 \\ Y'_{A,L} = 0 \quad , \quad Y'_{A,R} = -5/4 \quad or \quad Y'_{A,R} = 1 \end{aligned} \tag{2.1.2}$$

These are the only solutions with rational $U(1)'$ charges of the form p/q with $|p,q| \in Z$ and $p,q \leq 100$ we can find in these kinds of models. Indeed there are other solutions, but they imply charged SM leptons, which are not contemplated in our hypothesis. This concludes the proof that there must be at least one additional fermion in order to solve the anomaly equations that could be detected at LHC

2.2 Leptophobic models

By employing the same procedures used above, we consider the case of leptophobic models in which the Z' has vanishing SM lepton couplings. There is plenty of examples of previous models with leptophobic dark matter. However, even in these experimental favored cases, the anomaly equations cannot be looked past. In fact, they impose that a new DM fermion should be accompanied by at least two other fermions that possess non-identical charges. Moreover, at least one of the new fermions should be SM non-singlet. Indeed, at least one of the new fermions introduced must be a doublet under $SU(2)$ in order to have non-trivial solutions to the equations. Furthermore, the new fermions should be subjected to heavy LHC constraints, limiting in a big way their parameter spaces.

3 General solution of anomaly equations

Given the fact that we expect the new $U(1)'$ group to be a byproduct of a greater, non-abelian group that ensures the stability of the theory at high energies, we can always restrict charges to be integers, provided the correct normalization of the gauge couplings. This results in making the anomaly conservation equations as Diophantine ones[17][13]. In fact, suppose we introduce n fermions with non-trivial charges $y_1, ..., y_n$ under a new gauge group $U(1)$. As we said, the new charges can be integers. The two equations that solve the anomaly conditions are

$$y_1^3 + ... + y_n^3 = 0 \tag{3.0.1}$$

for $[U(1)^3]$, and

$$y_1 + ... + y_n = 0 \tag{3.0.2}$$

for the $U(1)$ anomaly cancellation. Before getting started there are few observations that will help us deal with this problem. Of course, if there is a pair of vector-like charges $y_i = -y_k$, then those do not contribute and the number of fermions involved in the equation reduces to $n-2$. From now on then we will consider only fermions which satisfy chirality conditions

$$y_i + y_k \neq 0 \qquad 1 \leq i,k \leq n \tag{3.0.3}$$

We can notice that if we possess a set of charges which are solutions of the two equations above, then we can build another one by just flipping the signs of the charges. Moreover, also charge permutations inside the set we have obtained can bring another set of solutions, more precisely we are able to access to $n! - 1$ sets of solutions just through permutations. This leads us to choose the set of charges in the order of decreasing absolute value of charges, starting with a positive one. We have a canonical set of solution $\{\vec{y} = y_1, ..., y_n\}$ only if

$$y_1 \geq |y_2| \geq ... \geq |y_n| \geq 1 \tag{3.0.4}$$

Now we can also multiply the obtained set of charges by any integer and get another solution. Thus we can consider only coprime sets of charges, in which the greatest common divisor among all charges is 1.
We can also obtain a solution by the composition of two subsets which are already solutions of the two equations. So finally we must consider only coprime and non-composite sets of solutions for the two Diophantine equations. We can call such a solution as a *primitive* solution
If we are able to pull out of the second equation the charge y_n and substitute in the first one, we can get the final equation

$$y_1^3 + ... + y_{n-1}^3 = (y_1 + ... + y_{n-1})^3 \tag{3.0.5}$$

Here we want to find the n charges solutions of this equation such that they depend on at most $n-2$ parameters. Then we need to prove that there is always a choice of parameters such that we can build a primitive solution.
The observation that will lead us to the solution is that, given two sets of integers that satisfy the two equations, $\{\vec{x}\} = \{x_1, ..., x_n\}$ and $\{\vec{z}\} = \{z_1, ..., z_n\}$, we can build another solution by the linear combination of the two we already have, employing cubic polynomial coefficients

$$\{\vec{x}\} \oplus \{\vec{z}\} = (\sum_i^n x_i z_i^2)\{\vec{x}\} - (\sum_i^n x_i^2 z_i)\{\vec{z}\} \tag{3.0.6}$$

The new operation we have introduced, $\oplus$, is called *merger* and satisfies the properties

$$\begin{aligned} \{\vec{x}\} \oplus \{\vec{z}\} &= -\{\vec{z}\} \oplus \{\vec{x}\} \\ \{-\vec{x}\} \oplus \{\vec{z}\} &= \{\vec{x}\} \oplus \{-\vec{z}\} = \{\vec{x}\} \oplus \{\vec{z}\} \end{aligned} \tag{3.0.7}$$

At the end of the merger, we do not know whether or not the final solution will be chiral. In fact, it can be proven that if both $\{\vec{x}\}$ and $\{\vec{z}\}$ are chiral, then the merged set could be vector-like.

3.1 Solution for even n

Here the chiral solution is generated by the two vector-like sets

$$\begin{aligned} \{\vec{v}_+\} &= \{l_1, k_1, ..., k_m, -l_1, -k_1, ..., k_m\} \\ \{\vec{v}_-\} &= \{0, 0, l_1, ..., l_m, -l_1, ..., l_m\} \end{aligned} \tag{3.1.1}$$

and the $n-2$ parameters k_i, l_i with $1 \leq i \leq m$ are integers. We can see that l_1 is the only parameter common in the two sets. The two sets $\{\vec{v}_+\}$ and $\{\vec{v}_-\}$ are vector-like, so they are automatic solutions of the anomaly equations.
We have seen that the merger operation requires cubic polynomial coefficients, these can be found as

$$\begin{aligned} S_+ &= \sum_{i=1}^{m-1} (k_{i+1} - k_i) l_i^2 - (l_1 + k_m) l_m^2 \\ S_- &= k_1^2 l_1 + \sum_{i=2}^{m} k_i^2 (l_i - l_{i-1}) - l_1^2 l_m \end{aligned} \tag{3.1.2}$$

so that at the end of it we obtain the set of charges

$$\begin{aligned}\{\vec{z}\} = \{&l_1 S_+, k_1 S_+, k_2 S_+ + l_1 s_-, ..., k_m S_+ + l_{m-1} S_-, \\ &-l_1 S_+ + l_m S_-, -k_1 S_+ - l_1 S_-, ..., -k_m S_+ - l_m S_-\}\end{aligned} \tag{3.1.3}$$

If we want to find only primitive solutions, then we can divide the set of charges by the gcd. We can see that each solution can be generated by several choices of parameters. In order for the charges to be non zero we should avoid some of the possible parameter values like $l_1, k_1 \neq 0$, $S_+ \neq 0$, $k_2 S_+ \neq -l_1 S_-$ etc.

3.2 Solution for odd n

Here we still have the merger of two vector-like sets

$$\begin{aligned}\{\vec{u}_+\} &= \{0, k_1, ..., k_{m+1}, -k_1, ..., -k_{m+1}\} \\ \{\vec{u}_-\} &= \{l_1, ..., l_m, k_1, 0, -l_1, ..., -l_m, -k_1\}\end{aligned} \tag{3.2.1}$$

with $m = (n-3)/2 \geq 1$. So we still have $n-2$ parameters $k_1, ..., k_{m+1}, l_1, ..., l_m$ with k_1 the only parameter common to both sets.
We then obtain the merger set

$$\begin{aligned}\{\vec{z}\} &= \{\vec{u}_+\} \oplus \{\vec{u}_-\} \\ &= \{l_1 S_-.k_1 S_+ + l_2 S_-, ..., k_{m-1} S_+ + l_m S_- \\ &k_m S_+ + k_1 S_-, k_{m+1} S_+, -k_1 S_+ - l_1 S - -, ..., \\ &-k_m S_+ - l_m S_-, -k_{m+1} S_+ - k_1 S_-\}\end{aligned} \tag{3.2.2}$$

with

$$\begin{aligned}S_+ &= \sum_{i=1}^{m-1} k_i (l_{i+1}^2 - l_i^2) + k_m (k_1^2 - l_m^2) - k_{m+1} k_1^2 \\ S_- &= \sum_{i=1}^{m-1} k_i^2 (l_i - l_{i+1}) + k_m^2 (l_m - k_1) + k_{m+1}^2 k_1\end{aligned} \tag{3.2.3}$$

Like in the even n case, we can express the conditions for non-zero charges and chirality to be $l_1, k_1, k_{m+1} \neq 0$, $S_+ \neq 0$, $k_1 \neq l_m$, $l_i \neq l_{i+1}$, $K_i \neq k_{i+1}$ etc.
The point in both cases is that, once we have obtained the set $\{\vec{z}\}$ in any case, we should be able to show that this is the most general solution for an even(odd) number of fermions. In order to do that the simple strategy is to consider an arbitrary chiral set $\{\vec{q}\}$ which is a solution of the two Diophantine equations and to find $n-2$ integers such that $\{\vec{z}\} \propto \{\vec{q}\}$ up to an overall constant. It is possible to prove that we can always find those $n-2$ integers that satisfy our request.
So to summarize what we have shown in this section, we can say that we started with the problem of finding a solution to the anomaly equations. This turns out to be the solution to two equations, one of which is a cubic Diophantine equation. We have shown that for any number of fermions, whether even or odd, it is always possible to find such a solution in terms of $n-2$ parameters. More at it, it can also be proved that these are the most

general solutions that one could find up to an overall rescaling. In order to do that we have used the *merger* procedure starting from two vectorlike sets, which automatically solve the anomaly equations.
In the following sections we are going to develop and analyze a bunch of models involving the new Z' vector boson and we are going to examine all the peculiar aspects that come with them.

4 Dinamycal inverse seesaw mechanism

Here we examine a model in which we make use of $B-L$ symmetry which is broken by a small parameter [16]. The seesaw mechanism will help us explain the smallness of SM neutrino masses after the spontaneous symmetry breaking of the $B-L$ symmetry. As we have previously seen, the anomaly cancellation condition implies the presence of new fermions, which will account for a new dark sector, charged under $B-L$. We should see some interesting aspects of this model, such as the fact that the Z' boson interacts more with the dark sector than with the Standard Model, thus loosening constraints on the new dark matter relic density.
We start things off with the introduction of two right-handed neutrinos for each SM neutrino. The two right-handed neutrinos will be called N_R and N'_R and will carry lepton numbers 1 and -1 respectively. The mass lagrangian originating is

$$-L = \bar{L}Y_\nu \tilde{H} N_R + \bar{N}^c_R M_N N'_R + \bar{N}'^c_R \mu N'_R + h.c. \tag{4.0.1}$$

Here we can recognize Y_ν to be the neutrino Yukawa matrix, $\tilde{H} = i\sigma_2 H^*$ and L the SM lepton doublet. We can see that the term proportional to M_N will conserve the lepton number, which is broken by two units by the term proportional to μ.
After the right-handed neutrinos are integrated out, we can recover the masses for the active neutrinos as

$$m_\nu \sim v^2 Y_\nu M_N^{-1} \mu (M_N^T)^{-1} Y_\nu^T \tag{4.0.2}$$

If we choose the right-handed neutrinos to be at TeV scale, we can still obtain a Yukawa term close to unity by choosing $\mu \sim O(keV)$. We seek a dynamical explanation for the origin of the μ term, which is the only term that breaks LN, thus it will always be small at all energy scales if we choose it to be. In order to do that, we gauge the $B-L$ symmetry. This symmetry, when spontaneously broken, will generate LN breaking and neutrino masses.
In order to cancel anomalies we have to analyze triangle vertices with three $U(1)_{B-L}$ vertices and the one with gravity and $U(1)_{B-L}$ vertices. The equations we obtain are:

$$\begin{aligned} \sum Q_i = 0 &\implies \sum Q_{iL} - \sum Q_{iR} = 0 \\ \sum Q_i^3 = 0 &\implies \sum Q_{iL}^3 - \sum Q_{iR}^3 = 0 \end{aligned} \tag{4.0.3}$$

4.1 Fermionic sector

Let's introduce our fermionic particles specifying their $B-L$ charges. We have 3 N_R with charge -1, three N'_R with charges $+1$, one χ_R with charge $+5$, one χ_L with charge $+4$ and

one ω with charge +4. This set of particles can be proved to solve the anomaly equations. Moreover, we need to introduce two extra scalars in order to generate the masses of the sterile fermions (besides the right-handed neutrinos) and produce SM neutrino masses. Because of this, we introduce the two scalar fields ϕ_1 and ϕ_2 with charges +1 and +2 respectively. Of course, SM leptons will have $B-L$ charges -1 and SM quarks will have charges 1/3. The most general lagrangian in the neutrino sector we can build with these particles is

$$-L_\nu = \bar{L}Y_\nu\tilde{H}N_R + \bar{N_R^c}M_N N_R' + \phi_2\bar{N_R^c}Y_N N_R + \phi_2^*\bar{N_R'^c}Y_N' N_R' + \phi_1^*\chi_L Y_\chi \bar{\chi_R} + h.c. \quad (4.1.1)$$

The missing $\phi_1^*\bar{\omega}Y_\omega\chi_R$ has been absorbed in the term $\phi_1^*\bar{\chi_L}Y_\chi\chi_R$ through a rotation between ω and χ_L.
We can identify the mass matrix in

$$M = \begin{pmatrix} 0 & Y_\nu\tilde{H} & 0 & 0 & 0 \\ Y_\nu^T\tilde{H}^\dagger & Y_N\phi_2 & M_N & 0 & 0 \\ 0 & M_N^T & Y_N'\phi_2^* & 0 & 0 \\ 0 & 0 & 0 & 0 & Y_\chi\phi_1^* \\ 0 & 0 & 0 & Y_\chi^T\phi_1 & 0 \end{pmatrix} \quad (4.1.2)$$

which is written in the basis $(\nu_L^c, N_R, N_R', \chi_L^c, \chi_R)$. As we can see the parameter μ can be associated with the factor $Y_N'\phi_2^*$. We can also see that ϕ_1 acquires a VEV and, as a consequence, the dark fermion χ gets a mass and the massless fermion ω is created in the dark sector. It can be shown that the contribution of ω to the N_{eff}, or the number of relativistic degrees of freedom in the early universe, is negligible, so it will not have an active impact as far as the results of our measurements are concerned.
We need a $v_2 =< \phi_2 >\sim keV << v$ in order to have a correct TeV inverse seesaw mechanism. Of course, we are considering $v =< H >= 246\, GeV$. More at it, the new Z' boson mass will depend on both ϕ_1 and ϕ_2, so we need absolutely $v_1 =< \phi_1 >\sim TeV$ if we want the Z' mass to be above the electroweak scale. We will show that it is indeed possible to obtain a small v_2 even thou v_1 is on the TeV scale through the coupling $\eta\phi_1^2\phi_2^*$. Then, after all, Higgs-like particles acquire a VEV, we will find ourselves with a particle content of a $B-L$ gauge boson, 3 pseudo-Dirac neutrino pairs, a Dirac fermion at TeV scale(our dark particle) and a massless fermion as well. The dark fermions interact with the Standard Model through Z' coupling. Another source of interaction is via ϕ and Higgs mixing. They represent a viable WIMP candidate and interact more with the Z' boson because of their large charges.

4.2 Scalar sector

We write the scalar potential as

$$\begin{aligned} V = \frac{m_H^2}{2}H^\dagger H + \frac{\lambda_H}{2}(H^\dagger H)^2 + \frac{m_1^2}{2}\phi_1^*\phi_1 + \frac{m_2^2}{2}\phi_2^*\phi_2 + \frac{\lambda_1}{2}(\phi_1^*\phi_1)^2 + \frac{\lambda_2}{2}(\phi_2^*\phi_2)^2 \\ + \frac{\lambda_{12}}{2}(\phi_1^*\phi_1)(\phi_2^*\phi_2) + \frac{\lambda_{1H}}{2}(\phi_1^*\phi_1)(H^\dagger H) + \frac{\lambda_{2H}}{2}(\phi_2^*\phi_2)(H^\dagger H) - \eta(\phi_1^2\phi_2^* + \phi_1^{*2}\phi_2) \end{aligned} \quad (4.2.1)$$

Here we require m_2^2 to be positive and large, so ϕ_2 does not acquire VEV in a classic way as H and ϕ_1 do, but only through the term proportional to η and it will be induced by

v and v_1, so it can be small. We still can make the expansion $\phi_i = (v_i + \phi_i + ia_i)$ and minimize the potential in order to get

$$\begin{aligned} m_H^2 &= -\frac{1}{2}(\lambda_{1H}v_1^2 + \lambda_{2H}v_2^2 + 2\lambda_H v^2) \simeq -\frac{1}{2}(\lambda_{1H}v_1^2 + 2\lambda_H v) \\ m_1^2 &= -\frac{1}{2}(2\lambda_1 v_1^2 + \lambda_{1H}v^2 - 4\sqrt{2}\eta v_2 + \lambda_{12}v_2^2) \simeq -\frac{1}{2}(2\lambda_1 v_1^2 + \lambda_{1H}v^2) \\ m_2^2 &= (\frac{\sqrt{2}\eta}{v_2} - \frac{\lambda_{12}}{2}) - \lambda_2 v_2^2 - \frac{\lambda_{2H}}{2}v^2 \simeq \frac{\sqrt{2}\eta v_1^2}{v_2} \end{aligned} \tag{4.2.2}$$

so we can see that

$$v_2 \simeq \frac{\sqrt{2}\eta v_1^2}{m_2^2} \tag{4.2.3}$$

and, to obtain $v_2 \sim O(keV)$, we could have $m_2 \sim 10\ TeV$, $v_1 \sim 10\ TeV$ and $\eta \sim 10^{-5}\ GeV$.
Now the scalar mass matrix is given by

$$M_0^2 \simeq \begin{pmatrix} \lambda_H v^2 & \lambda_{1H}v_1 v/2 & 0 \\ \lambda_{1H}v_1 v/2 & \lambda_1 v_1^2 & -\sqrt{2}\eta v_1 \\ 0 & -\sqrt{2}\eta v_1 & \eta v_1^2/\sqrt{2}v_2 \end{pmatrix} \tag{4.2.4}$$

The mixing angle between $Re(H^0)$ and $Re(\phi_1^0)$ is constrained to be below 30% by Higgs data [47] . Also, the mixing between new scalars is supposed to be small, given that $\eta << m_2, v_1$, so we can identify the masses of the physical particles

$$\begin{aligned} m_h^2 &= \lambda_H v^2 \\ m_{\phi_1}^2 &= \lambda_1 v_1^2 \\ m_{\phi_2}^2 &= \frac{m_2^2}{2} \end{aligned} \tag{4.2.5}$$

if we consider α_1 and α_2 to be the mixing angles between $h - \phi_1$ and $\phi_1 - \phi_2$ respectively

$$\begin{aligned} \tan(\alpha_1) &\simeq \frac{\lambda_{1H}}{\lambda_1}\frac{v}{2v_1} \\ \tan(\alpha_2) &\simeq 2\frac{v_2}{v_1}. \end{aligned} \tag{4.2.6}$$

If we assume λ_1 and λ_{1H} to be $O(1)$ and v_1 to be on the TeV scale, then we can see that α_1 is small but non-negligible. Moreover we shall notice that the mixing angle between Higgs and a new scalar should only reduce Higgs couplings to SM particles. In fact, we can see that Higgs couplings to SM fermions and bosons result to be

$$k_F = k_V = \cos(\alpha_1) \tag{4.2.7}$$

so we can get the constrain $\cos(\alpha_1) > 0.92$. Moreover, we know that the massless fermion does not couple to a scalar, so we can see that the consequences on Higgs couplings are the only testable Higgs modifications in the model, given that all other particles are heavy. Finally, we can see that α_2 is very small, being proportional to LN breaking VEV and related to the neutrino masses, so its presence will pass undetected.

4.3 Dark matter phenomenology

We have seen how, with this new mechanism, we can obtain two dark fermions, being χ and ω that will constitute our dark sector. We have also seen how ω presence has no influence, being massless and it will just add to the relativistic degrees of freedom in the early universe. It is χ that we are after, being a viable dark matter candidate. In the following, we will just try to speculate the possibility of χ reproducing the correct dark matter relic density.

Relic density

Being a WIMP in the early universe we can consider the dark fermion Z' to be in thermal equilibrium with the primordial plasma due to interactions mediated by Z'. The relevant piece of lagrangian here would be

$$L_{DM} = -g_{BL}\bar{\chi}\gamma^{\mu}(5P_R + 4P_L)\chi Z'_{\mu} + \frac{1}{2}M^2_{Z'}Z'_{\mu}Z'^{\mu} - m_{\chi}\bar{\chi}\chi \tag{4.3.1}$$

where we can get the Z' boson mass after the VEV generation as

$$\begin{aligned} M_{Z'} = g_{BL}\sqrt{v_1^2 + 4v_2^2} \simeq g_{BL}v_1 \\ m_{\chi} = Y_{\chi}\frac{v_1}{2} \end{aligned} \tag{4.3.2}$$

We can extrapolate from this the scattering cross section of $\bar{\chi}\chi \to \bar{f}f$, where f is a fermion, to be at leading order in v:

$$< \sigma v >_{ff} \sim n_c(q_{\chi L} + q_{\chi R})^2 \frac{q_{fL}^2 + q_{fR}^2}{8\pi} \frac{g_{BL}^4 m_{\chi}^2}{(4m_{\chi}^2 - M_{Z'}^2)^2 + \Gamma_{Z'}^2 M_{Z'}^2} + O(v^2) \tag{4.3.3}$$

Here, of course, n_c is the eventual color factor in the final state, q_f are the $B-L$ charges of the final fermions and $q_{\chi R}$ and $q_{\chi L}$ are of course 5 and 4 respectively.
One can estimate also the decay width of the new Z' into two fermions to be

$$\Gamma_{Z'}^{ff} = n_c g_{BL}^2 \frac{\left(6q_{fL}q_{fR}m_f^2 + (q_{fL}^2 + q_{fR}^2)(M_{Z'}^2 - m_f^2)\right)\sqrt{M_{Z'}^2 - 4m_f^2}}{24\pi M_{Z'}^2} \tag{4.3.4}$$

We can obviously see that, whenever $M_{Z'}^2 < m_{\chi}^2$ there is also the possibility of $\bar{\chi}\chi \to Z'Z'$. Moreover the channel $\bar{\chi}\chi \to \phi_1 \to Z'Z'$ is subdominant. The same destiny is shared by the channels $\bar{\chi}\chi \to \phi_1\phi_1$ and $\bar{\chi}\chi \to Z'\phi_1$. In fact, knowing that $m_{\chi} = \frac{Y_{\chi}}{\sqrt{2}v_1}$, $m_{\phi_1} = \sqrt{\lambda_1}v_1$ and $m_{Z'} = g_{BL}v_1$, we can only get subdominant contributions to the relic density. The annihilation channel $\bar{\chi}\chi \to Z'h^0$ is also doomed to fail us.
With this knowledge, we are able to estimate the relic density at the temperature in which $< \sigma v > n_{\chi} \simeq H$ to be

$$\Omega_{\chi}h^2 = \frac{2.5 \times 10^{28} m_{\chi}}{T_{\chi}^{f.o.} M_{PL}^2 \sqrt{g_*} < \sigma v >} \tag{4.3.5}$$

with g_* being the relativistic degrees of freedom at time of freeze-out and M_{PL} is the Planck mass.

Conclusions

We examined the model with the Inverse Seesaw mechanism as a way to generate a dark sector and at the same time to explain the smallness of neutrino masses. Right-handed neutrinos have been added to the standard model in order to erase the anomaly equations and the global SM accidental symmetry $B - L$ has been gauged. This model gives us the possibility to lower the seesaw scale closer with respect to the electroweak scale, thus avoiding the Higgs hierarchy problem. There is a small parameter μ that breaks the $B-L$ symmetry, thus generating the neutrino masses. This very parameter is able to explain the smallness of such masses, being small itself. This mechanism is also able to present us with a viable dark matter candidate , which we named χ and to derive a relic density to be confronted with the present time constraints in our hands.

5 Gauge theory with leptoquarks

This one is interesting because here we still gauge B and L separately [18]. Baryon and lepton numbers will then be broken at low energy scales. The peculiarity here is the introduction of the so-called leptoquarks, particles that possess non-negligible baryon and lepton numbers in order to cancel anomalies and generate masses for all fields. There is also a dark matter candidate in a fermion which is stable due to the spontaneous breaking of the symmetry. Flavor violation is not contemplated in such a model as $\Delta L = \pm 2, \pm 3$ and $\Delta B = \pm 3$ interactions are generated in this theory. The main advantages in this approach are the proven stability of the proton and the possibility to avoid the *large desert* problem that we mentioned above talking about the Higgs hierarchy.
Let's start with the extended version of the Standard Model including baryon and lepton numbers as gauged symmetries

$$G = SU(3) \otimes SU(2)_L \otimes U(1)_Y \otimes U(1)_B \otimes U(1)_L \tag{5.0.1}$$

With the introduction of the right-handed neutrinos, the particle content with their respective charges under the gauge group are

$$\begin{aligned} Q_L \sim (3, 2, \frac{1}{6}, \frac{1}{3}, 0), u_R \sim (3, 1, \frac{2}{3}, \frac{1}{3}, 0) \\ d_R \sim (3, 1, -\frac{1}{3}, \frac{1}{3}, 0), l_L \sim (1, 2, -\frac{1}{2}, 0, 1) \\ \nu_R \sim (1, 1, 0, 0, 1), e_R \sim (1, 1, -1, 0, 1). \end{aligned} \tag{5.0.2}$$

Now the baryonic anomalies can be listed as

$$\begin{aligned} [SU(3)^2] \otimes [U(1)_B], [SU(2)^2] \otimes [U(1)_B], [U(1)_Y^2] \otimes [U(1)_B] \\ [U(1)_Y] \otimes [U(1)_B^2], [U(1)_B], [U(1)_B^3] \end{aligned} \tag{5.0.3}$$

with the only non-zero values in the standard model being

$$[SU(2)^2] \otimes [U(1)_B] = -[U(1)_Y^2] \otimes [U(1)_B] = \frac{3}{2} \tag{5.0.4}$$

For the purely leptonic anomalies we get

$$\begin{aligned} [SU(3)^2] \otimes [U(1)_L], [SU(2)^2] \otimes [U(1)_L], [U(1)_Y^2] \otimes [U(1)_L] \\ [U(1)_Y] \otimes [U(1)_L^2], [U(1)_L], [U(1)_L^3], \end{aligned} \tag{5.0.5}$$

with the only non-zero values in the standard model being

$$[SU(2)^2] \otimes [U(1)_L] = -[U(1)_Y^2] \otimes [U(1)_L] = \frac{3}{2} \tag{5.0.6}$$

plus the mixed anomalies

$$\begin{aligned} [U(1)_B^2] \otimes [U(1)_L], [U(1)_L^2] \otimes [U(1)_B] \\ [U(1)_Y] \otimes [U(1)_L] \otimes [U(1)_B] \end{aligned} \tag{5.0.7}$$

which vanish in the Standard Model.
One of the solutions that come to mind when confronting this problem is Leptoquarks, meaning, for example, particles like $F_L \sim (3, 2, 0, -1, -1)$ or $k_R \sim (3, 1, -\frac{1}{2}, -1, -1)$. Although it is difficult to satisfy both cosmological constraints and to find a model that avoids the large desert problem, there still are some solutions free of anomalies that we can take into consideration. Let's introduce in the table below the fermionic content of our theory, then we will explore the simplest of possibilities that accomplish our wishes.

Field	$SU(3)$	$SU(2)$	$U(1)_Y$	$U(1)_B$	$U(1)_L$
Ψ_L	N	2	Y_1	$B_1 = -\frac{3}{2N}$	$L_1 = -\frac{3}{2N}$
Ψ_R	N	2	Y_1	$B_2 = +\frac{3}{2N}$	$L_2 = +\frac{3}{2N}$
η_R	N	1	Y_2	$B_3 = -\frac{3}{2N}$	$L_3 = -\frac{3}{2N}$
η_L	N	1	Y_2	$B_4 = +\frac{3}{2N}$	$L_4 = +\frac{3}{2N}$
χ_R	N	1	Y_3	$B_5 = -\frac{3}{2N}$	$L_5 = -\frac{3}{2N}$
χ_L	N	1	Y_3	$B_6 = +\frac{3}{2N}$	$L_6 = +\frac{3}{2N}$

So we need to introduce a doublet under $SU(2)$ to cancel the $[SU(2)^2] \otimes [U(1)_B]$ anomaly. Because of this, we need to give our new fermions, the same quantum number of a Standard Model family under $SU(2)$. Of course, our new fermions will be vector-like under SM, so they will have no influence on SM anomalies. Moreover, the $[SU(2)^2] \otimes [U(1)_B]$ condition, gives us the constraint

$$B_1 - B_2 = -\frac{3}{N} \tag{5.0.8}$$

and use $B_1 = -B_2$. For the leptonic version of this, we get

$$L_1 = -L_2 = -\frac{3}{2N}. \tag{5.0.9}$$

If $N \neq 1$ we see that the equation for $[SU(3)^2] \otimes [U(1)_B]$ gives us the condition

$$2(B_1 - B_2) - (B_3 - B_4) - (B_5 - B_6) = 0 \tag{5.0.10}$$

with the help of $B_4 = -B_5$ and $B_5 = -B_6$ we get

$$2B_1 - B_3 - B_5 = 0 \tag{5.0.11}$$

which is solved for

$$B_1 = B_3 = B_5 \tag{5.0.12}$$

For the lepton numbers, the same reasoning brings us the solutions

$$L_4 = -L_3 \qquad and \qquad L_5 = -L_6 \qquad and \qquad L_1 = L_3 = L_5 \tag{5.0.13}$$

For the hypercharge values we obtain solutions for the equation concerning $[U(1)_Y^2] \otimes [U(1)_B]$

$$Y_2^2 + Y_3^2 - 2Y_1^2 = \frac{1}{2} \tag{5.0.14}$$

so we can find the sets of solutions

$$(Y_1, Y_2, Y_3) \in \{(\pm\frac{1}{2}, \pm 1, 0), (\pm\frac{1}{6}, \pm\frac{2}{3}, \pm\frac{1}{3}), (0, \pm\frac{1}{2}, \pm\frac{1}{2})\}. \tag{5.0.15}$$

Anyone of the solutions proposed solves completely all anomaly equations. Moreover, we have different models for different N. The simplest one requires $N = 1$. In these kinds of models, the new fermions do not interact under color forces. The only solution we can choose here is the one with

$$\begin{aligned} Y_1 &= \pm\frac{1}{2} \\ Y_2 &= \pm 1 \\ Y_3 &= 0. \end{aligned} \tag{5.0.16}$$

These fields are the leptoquarks. Their name has nothing to do with leptons or quarks, it stands for their property of possessing both baryon and lepton numbers.

5.1 Lagrangian

The relevant piece of lagrangian here can be written as

$$\begin{aligned} -L = h_1 \bar{\Psi}_L H \eta_R + h_2 \bar{\Psi}_L \tilde{H} \chi_R + h_3 \bar{\Psi}_R H \eta_L + h_4 \bar{\Psi}_R \tilde{H} \chi_L \\ + \lambda_1 \bar{\Psi}_L \Psi_R S_{BL} + \lambda_2 \bar{\eta_R} \eta_L S_{BL} + \lambda_3 \bar{\chi_r} \chi_L S_{BL} \\ + a_1 \bar{\chi_L^c} \chi_L S_{BL} + a_2 \bar{\chi_R^c} \chi_R S_{BL}^\dagger + h.c. \end{aligned} \tag{5.1.1}$$

With

$$S_{BL} \sim (1, 1, 0, -3, -3). \tag{5.1.2}$$

The mass terms for the fermions are generated through the λ_i terms and are vector-like. The terms proportional to a_i allow us to recover Majorana's mass terms through the new field S_{BL}.
We can also create Majorana masses for neutrinos through the seesaw mechanism by just introducing a new Higgs-like field beside the right-handed neutrinos

$$S_L \sim (1, 1, 0, 0, -2) \tag{5.1.3}$$

and have the lagrangian term for this to be

$$-L_\nu = Y_\nu \bar{l_L} \tilde{H} \nu_R + \frac{\lambda_R}{2} \bar{\nu_R^c} \nu_R S_L + h.c. \tag{5.1.4}$$

5.2 Symmetry breaking

The $U(1)_B$ and $U(1)_L$ are broken when S_{BL} acquires a VEV. Instead, when S_L gets his VEV it only influences the breaking of $U(1)_L$. If we make the classical expansions

$$\begin{aligned} S_L &= \frac{1}{\sqrt{2}}(v_L + h_L) + \frac{i}{\sqrt{2}}A_L \\ S_{BL} &= \frac{1}{\sqrt{2}}(v_{BL} + h_{BL}) + \frac{i}{\sqrt{2}}A_{BL} \end{aligned} \tag{5.2.1}$$

so when the two fields acquire VEVs, two fields h_L and h_{BL} are born and mix with the Higgs boson.

5.3 The fermionic sector

After symmetry breaking, we will be left with four neutral and four charged chiral fermions. Notice that our leptoquarks do not couple with baryons or leptons in the Standard Model because they already possess baryon number, so it is impossible to generate flavor violations in these two sectors. Moreover, the lightest of the fermions that we are left with is a viable dark matter candidate, being stable. In fact, its stability is guaranteed by the symmetry breaking.
Notice that we did not have to impose additional discrete symmetries by hand, on the contrary, we are left, after symmetry breaking, with a discrete ζ_2 symmetry as a consequence. All the new fields will be charged under the new symmetry with charge -1 and the Standard Model particles will possess charge $+1$, this will guarantee the difficulty of dark matter decaying into standard model particles, thus its stability.
The right relic density can be achieved in this model and the direct detection constraints can be met under some circumstances. In fact, the dark matter fermion that we obtain Ψ_{LF}, couples to the new gauge bosons Z'_1 and Z'_2 and to the two scalars h_L and h_{BL}. We can obtain what we are after if we find ourselves close to one of these resonances.

5.4 Conclusions

This model proposed two new Z' bosons coming from the two gauged symmetries $U(1)_B$ and $U(1)_L$ and, even though a little beyond the first sections of this chapter, the main physical points are shared and here there is also the presentation of some interesting particles, the leptoquarks, which bring lepton and baryon number together. Moreover, an explanation for the neutrino masses has been given as well with the seesaw mechanism and the introduction of the right-handed neutrinos. The main advantages of this model are the fact that proton decay is not happening, given that the renormalizable operators that cause it do not occur thanks to the formulation of our theory. Moreover, the *large desert* problem has also been solved, given that the two new symmetries are broken at low energies.
It also has to be stressed the fact that the fermion introduced does not bring any source of flavor violation in the standard model and that the lightest of these can be a viable Dark Matter candidate meeting the direct detection constraints and satisfying the correct

relic density.

6 Two portal dark matter

Here we bring to the knowledge a model in which a dark matter candidate is linked to the standard model through two channels: Higgs and a new vector [22]. The peculiarity here is that the dark sector is charged under $U(1)'$ and the SM has a leptophobic interaction with the dark vector boson. Moreover, the contribution to the DM-nucleon elastic scattering starts at one loop, so we are well inside the direct detection constraints provided by LUX and XENON100. More at it the relic density constaraints provided by Planck and WMAP are met. Let's dive straight into it

6.1 The model

Dark matter here has interactions with the Standard Model through two different portals: Higgs and vector. It can be shown that in this way there is no tree level DM scattering off nuclei because the interested Feynman diagrams begin at one loop level. This is why the theory can meet all direct detection constraints. This is on the same line as the velocity-suppressed models. Assume that besides a scalar field that mixes with SM Higgs(Higgs portal), we also have a vector portal interaction, as the dark sector is charged under a new $U(1)'$ symmetry. Moreover, only SM quarks are charged under the new $U(1)'$, but no leptons. This way we have a leptophobic model, which is more in line with the collider constraints. There are three pieces of our complete lagrangian:

$$L = L_{SM} + L_{DM} + L_{int} \tag{6.1.1}$$

Of course, the covariant derivative is modified to include the new boson term. We have already seen this previously, but we will repeat it for simplicity:

$$D_\mu^{SM} \to D_\mu'^{SM} = D_\mu^{SM} - ig'\frac{z}{2}Z'_\mu \tag{6.1.2}$$

where z is the dark charge of the quarks upon which the covariant derivative acts.
The dark matter lagrangian, coupled with a new complex scalar field ϕ is given by

$$L_{DM} = -\frac{1}{4}F'_{\mu\nu}F'^{\mu\nu} + \bar{\chi}(i\gamma^\mu D'_\mu)\chi + (D'_\mu\phi)(D'^\mu\phi)^* - m_\phi^2(\phi\phi^*) - \frac{1}{4}\lambda(\phi\phi^*)^2 \tag{6.1.3}$$

Of course, both fields are charged under the new $U(1)'$ as we can see.
For the dark sector we emply the covariant derivative

$$D'_\mu = d_\mu - ig'\frac{z}{2}Z'_\mu \tag{6.1.4}$$

As we have already hinted in the previous part, none of the leptons couples with the new Z'. Z' is leptophobic, so the interaction lagrangian has a particle content concerning only scalar-Higgs and Z'-quarks interactions

$$L_{int} = -\lambda(\phi\phi^*)(HH^\dagger) + g'\frac{z_{Q_L}}{2}Z'_\mu\bar{Q}_L\gamma^\mu Q_L + g'\frac{z_{u_R}}{2}Z'_\mu\bar{u_R}\gamma^\mu u_R + g'\frac{z_{d_R}}{2}Z'_\mu\bar{d}_r\gamma^\mu d_R \tag{6.1.5}$$

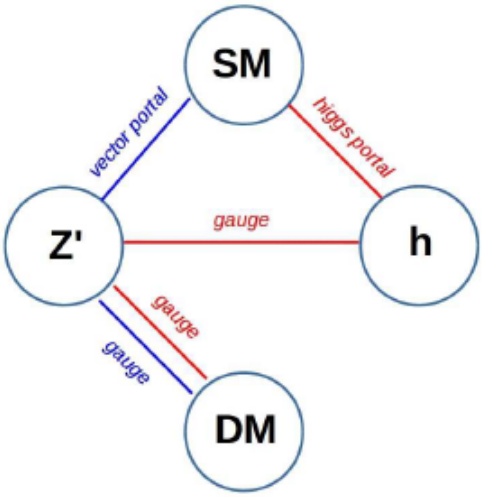

Figure 3.1

Here H is the SM Higgs, Q_L is the left-handed quark doublet, while u_R and d_R are the right-handed quark singlets. Here the couplings z_{Q_L}, z_{u_R} and z_{d_R} are considered to be linked only to the third family of quarks, t and b, as the couplings to light quarks are considered negligible in this type of theory. It is this that allows one-loop contributions to rise and the dark matter scattering off a nucleus to be suppressed.
The anomaly conditions are all met, considering only the third family of quarks to be charged under the new $U(1)'$. Speaking of the t and b quarks here we need to exploit the anomaly equations to find the appropriate charge values to assign. In fact, we get

$$\begin{aligned} z_{Q_L} &= -2 \\ z_{U_R} &= +2 \\ z_{d_R} &= +2 \end{aligned} \tag{6.1.6}$$

which, substituted in the lagrangian above, gives us the interaction

$$L_{int} = -\lambda_1(\phi\phi^*)(HH^\dagger) + g' Z'_\mu \bar{t}\gamma^\mu\gamma^5 t + g' Z'_\mu \bar{b}\gamma^\mu\gamma^5 b. \tag{6.1.7}$$

Here we can see the two portals in the fact that the new scalar interacts with Higgs quadratically and the vector boson interacts with the third family of quarks.
The scalar ϕ interacts with the new gauge boson Z', which in turn interacts with dark matter. The thing to notice here is that there are two mediators between the dark sector and the SM, which are the new scalar ϕ and the new gauge boson. In the figure below there is a simplified scheme of the interactions occurring

Again we stress that the Higgs potential is

$$V_{Higgs} = -\mu_H(HH^\dagger) - \lambda_H(HH^\dagger)^2 \tag{6.1.8}$$

and that it acquires a VEV

$$H = \frac{1}{\sqrt{2}} \begin{pmatrix} 0 \\ v + \tilde{h} \end{pmatrix} \tag{6.1.9}$$

The new scalar acquires a VEV too

$$\phi = v' + \frac{1}{\sqrt{2}}\tilde{h}' \tag{6.1.10}$$

At the moment ϕ get a VEV, the new $U(1)'$ is broken and the gauge boson Z' acquires a mass and it turns out that

$$m_{Z'} = \frac{g'v'}{\sqrt{2}}. \tag{6.1.11}$$

The new scalar presence affects also the Higgs mass, in fact, the two scalars masses are obtained by diagonalization of the mass matrix

$$M = \begin{pmatrix} 2\lambda_H v^2 & \sqrt{2}\lambda_1 v v' \\ \sqrt{2}\lambda_1 v v' & \frac{1}{2}\lambda v'^2 - \frac{1}{2}\lambda_1 v^2 \end{pmatrix} \tag{6.1.12}$$

Here the minimization of potential has brought us the values

$$\begin{aligned} m_\phi^2 &= -\lambda v'^2 - \lambda_1 v^2 \\ \mu_H^2 &= -\lambda_H v^2 - \lambda_1 v'^2. \end{aligned} \tag{6.1.13}$$

Of course, what we have to do now, in order to obtain the physical masses, is to diagonalize the mass matrix. We make use of a rotation with mixing-angle

$$tan(\theta) = \frac{1}{1 + \sqrt{1 + y^2}} \tag{6.1.14}$$

where

$$y = \frac{2m_{\tilde{h}\tilde{h}'}^2}{m_{\tilde{h}}^2 - m_{\tilde{h}'}^2} \tag{6.1.15}$$

and $m_{\tilde{h}\tilde{h}'}$ is the off-diagonal element of the mass matrix.
So we recover the masses of the two scalars

$$\begin{aligned} m_h^2 &= \frac{m_{\tilde{h}}^2 + m_{\tilde{h}'}^2}{2} + \frac{m_{\tilde{h}}^2 - m_{\tilde{h}'}^2}{2}\sqrt{1 + y^2} \\ m_h^2 &= \frac{m_{\tilde{h}}^2 + m_{\tilde{h}'}^2}{2} - \frac{m_{\tilde{h}}^2 - m_{\tilde{h}'}^2}{2}\sqrt{1 + y^2}. \end{aligned} \tag{6.1.16}$$

Of course, we know from our measurements that $m_h = 125\ GeV$. We can also obtain the couplings as a function of the masses we just obtained

$$\begin{aligned} \lambda_H &= \frac{m_{h'}^2 \sin^2(\theta) + m_h^2 \cos^2(\theta)}{2v^2} \\ \lambda &= \frac{m_{h'}^2 \cos^2(\theta) + m_h^2 \sin^2(\theta)}{v^2/2} - \frac{v^2}{v'^2}\lambda_1 \\ \lambda_1 &= \frac{m_h^2 - m_{h'}^2}{2\sqrt{2}vv'}\sin(2\theta). \end{aligned} \tag{6.1.17}$$

The vacuum stability condition imposes that $\lambda_H > 0$, $\lambda v'^2 > \lambda_1 v^2$ and $v'^2(\lambda_H \lambda - 2\lambda_1^2) > v^2 \lambda_1 \lambda_H$.

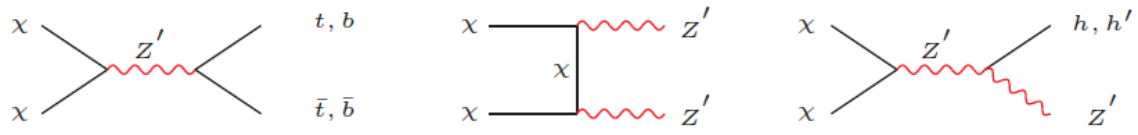

Figure 3.2

6.2 Invisible Higgs decays

It is important to recognize that there are additional decay channels for SM Higgs. Indeed in the case of $m_{Z'} < m_h/2$ there is the possibility of $h \to Z'Z'$ and its estimated decay rate is

$$\Gamma(h \to Z'Z') = \frac{v'^2 g'^4 \sin^2(\theta)}{16\pi m_h}(1 - \frac{4m_{Z'}^2}{m_h^2})^{\frac{1}{2}} \tag{6.2.1}$$

Furthermore if $m_{h'} < \frac{m_h}{2}$ there is also the open channel $h \to h'h'$ with

$$\Gamma(h \to h'h') = \frac{c^2}{128\pi m_h}(1 - \frac{4m_{h'}^2}{m_h^2})^{\frac{1}{2}} \tag{6.2.2}$$

where c is a constant that can be estimated.
The Higgs total decay rate must be modified in

$$\Gamma_{Higgs}^{tot} = \cos^2(\theta)\Gamma_{Higgs}^{SM} + \Theta(m_h - 2m_{Z'})\Gamma(h \to Z'Z') + \Theta(m_h - 2m_{h'})\Gamma(h \to h'h') \tag{6.2.3}$$

where Θ is the step function. Of course, the two channels we have mentioned contribute to the invisible Higgs decays. The theory leverages the fact that there is still room for invisible Higgs decays besides neutrinos. In fact, recent estimates at LHC have

$$BR_{inv} \leq 0.35 \tag{6.2.4}$$

so it is important to have a model in which all invisible decays contribute to the branching ratio in the measure that the limit we just wrote is not surpassed.

6.3 Relic density

The model we investigated showed a dark matter particle able to account for the cold dark matter in the Universe. This is an example of WIMP dark matter of course, so the relic density that we observe today is an effect of the freeze-out mechanism that started from the moment the Hubble radius began to be comparable to the decaying rate. To get the relic density today we would have to solve numerically the Boltzmann equation, just like we stated in the previous chapter. In particular we would have to implement the s-channel processes $\chi\chi \to \bar{b}b, \bar{t}t, Z'h, Z'h'$ and the t and u channels of the process $\chi\chi \to Z'Z'$.

The analysis has been carried and one can show that there are regions of the parameter space that allow for the correct relic density today, considering as independent free variables $m_\chi, m_{h'}, g', v'$ and θ. It appears that there are regions in the parameter space that reproduce correctly the relic density at present time and with DM elastic cross section well below the constraints imposed by LUX and XENON100. It has been observed that said regions are the ones with a small θ, in particular for $\sin\theta = 0.01$. It can be deduced that for dark masses in the range from a few GeV up to 1 TeV this model is able to escape from the direct detection constraints.

6.4 Conclusions

We have presented here a model that exihbits a viable DM candidate and that is able to evade the direct detection constraints. The peculiarity of this model is that there are two portals of communications between the SM and the dark sectors, which are the Higgs and the vector portal. The couplings between the new Z' boson and the light quarks have been assumed negligible, this results in an absence of tree-level interaction, making the DM scattering off a nucleus a one-loop level process.
we have found that this model is able to reproduce the correct relic density of the present-time dark matter for various regions of the parameter space.
One last aspect needs attention. In this model the coupling between dark matter and Z' boson is vectorial and the coupling between Z' and the third quark family is purely axial. Moreover thanks to the new scalar mediator and to the non-universality of Z' coupling to quark families, it is possible to have a spin-independent elastic cross section of dark matter off of nuclei. This is a very important feature that was not present in previous models that employed axial couplings of the Z' to quarks and it can be a tool concerning direct detection searches.

Chapter 4

Unitarity

The concept of unitarity is a powerful tool to implement when looking for bounds in a not completely well-navigated theory. Indeed in the past, we have made use of this theorem to gauge masses and energy scales and, for example, put upper bounds on expected particles, like the Higgs boson, that were forced to respect this rule. We will encounter some example later on in this chapter.
Unitarity constraints come from the conservation of probability. For a state $|\Psi;t\rangle$ at time t, we can translate the conservation of probability in the obligation for the norm of this system to be the same at every instant:

$$\langle\Psi;t|\Psi;t\rangle = \langle\Psi;0|\Psi;0\rangle\,. \tag{0.0.1}$$

Actually, if we expand the state $|\Psi;t\rangle$ in

$$|\Psi;t\rangle = e^{-iHt}\,|\Psi;0\rangle \tag{0.0.2}$$

we can see that the previous equation implies that the Hamiltonian matrix is hermitian $H^\dagger = H$. If we write the matrix S as

$$S = e^{-iHt} \tag{0.0.3}$$

this means that S has to satisfy the requirement

$$S^\dagger S = 1 \tag{0.0.4}$$

so we deduce that the S matrix is unitary. This, even though apparently simple, bears heavy consequences on cross sections and scattering amplitudes for any physical model, and it all comes together into the generalized optical theorem, a milestone in scattering theory.
Let's see that, if we can expand

$$S = 1 + iT \tag{0.0.5}$$

we can also write the unitarity constraint in terms of T matrix in

$$1 = S^\dagger S = (1 - iT^\dagger)(1 + iT) \tag{0.0.6}$$

and

$$i(T^\dagger - T) = T^\dagger T. \tag{0.0.7}$$

Let's look into the T matrix and let's review its ties with the scattering matrix element $M(i \to f) = M_{if}$ from a random initial state to a random final. The relation is

$$\langle i| T |f\rangle = (2\pi)^4 \delta^4(p_i - p_f) M_{if}. \tag{0.0.8}$$

Here instead of going for the usual way of derving the generalized optical theorem, we proceed by analyzing the unitarity constraint in terms of the scattering matrix element. Let's just consider a scattering matrix element $M_{if}(s, \cos\theta)$ where s is the Mandelstam variable identifying the center of mass energy squared and θ is the scattering angle. Now let's have a partial wave expansion. This procedure can be performed in d dimensions and employs the property of the scattering system of being Lorentz symmetric. We decompose the T matrix into a complete set of intermediate states which transform as irreducible representation under the group $SO(1, d-1)$ or, in our case, $SO(1,3)$. In a $2 \to 2$ scattering it is sufficient to characterize the whole system by the two numbers E and J which are respectively energy and the angular momentum in the center of mass frame. It could be noticed actually that the energy dependent factor is not relevant to the scope of our analysis, so we will avoid it. Anyways the partial wave expansion of the T matrix has, of course, a reflection on the scattering matrix element, as they are related by the equation we have just seen. Indeed let's write the J^{th} element of the helicity scattering matrix as

$$M^J_{if} = \frac{1}{32\pi} \beta_{if} \int_{-1}^{1} d\cos\theta d^J_{\mu\mu'}(\theta) M_{if}(s, \cos\theta) \tag{0.0.9}$$

Here $d^J_{\mu\mu'}$ is the J^{th} Wigner function and μ and μ' are the total spins of the initial and final states respectively [41]. Finally, β_{if} is a kinematical factor that can be approximated to unity as high energy scales, which is exactly the study ground for our dark matter models. Notice that the right-hand side of the equation has to be multiplied by a factor of $\frac{1}{\sqrt{2}}$ each, if the initial or the final state particles are identical. Now here is the time when we apply our unitarity constraint to M^J_{if} as

$$Im(M^J_{ii}) = \sum_f |M^J_{if}|^2 = |M^J_{ii}|^2 + \sum_{f \neq i} |M^J_{if}|^2 \geq |M^J_{ii}|^2 \tag{0.0.10}$$

here the sum over f runs of course over all the final states. This result is true for every J and s.
Now this relation has to be satisfied and a violation at tree-level would imply two things: either higher order terms can come into play restoring unitarity or that our theory is not complete and we need new terms that come and rescue us. This is such an easy equation to get and at the same time such a powerful tool that can help us whenever we are dealing with obscure theories about which we are not aware of every detail. The simplified dark matter models belong to this category as we do not know with certainty the whole particle repertoire and we might have missed something truly important in our neediness to have the simplest theory to explain the phenomena. Since it is a law that every scattering system has to respect, this has general importance. In the past physicists have used this tool to discriminate masses of particles or study energy ranges at which

theory would break down as a consequence of a downfall of unitarity. There are various examples of this. A famous one is dated 1977 when Lee, Quigg and Thacker employed the unitarity constraint to draw a conclusion on the Higgs boson mass [43]. That was such an interesting article as they employed techniques in the studies of the two by two scattering process involving weak interactions that we can still take as a model of reasoning today in our quest for dark matter origin as we did. Let's look more specifically at the math involved in the process coming from the relation we have just derived. The condition obtained can be written in the form

$$0 \leq Im(M_{ii}^J) \leq 1 \qquad\qquad |Re(M_{ii}^J)| \leq \frac{1}{2} \tag{0.0.11}$$

and we now know how to operate starting from these two: we are going to restrict the parameter space by eliminating those regions that do not respect unitarity by violating these two relations. Let's carry on with our analysis by studying a system in which both initial and final states have spin zero. In fact, with this particular configuration, we know the Wigner function to be equal to the Legendre polynomials

$$d_{00}^J = P_J(\cos\theta) \tag{0.0.12}$$

In the following, we shall analyze just the contribution coming from the $J = 0$ partial wave, as it is the most important and the one that will give the most stringent constraints. An interesting detail of the Wigner function is that in general $d^0_{\mu\mu'}$ is different from zero only if $\mu = \mu' = 0$ and this is why we can write the helicity scattering matrix element as

$$M_{if}^0 = \frac{1}{64}\beta_{if}\delta_{\mu 0}\delta_{\mu' 0}\int_{-1}^{1} d\cos\theta M_{if}(s,\cos\theta) \tag{0.0.13}$$

and this is the equation we will employ really soon in our study of dark matter models with a Z' mediator. But before ending this section it could be interesting to mention a remarkable application of what we have just seen. Indeed if we go back to the study of weak interaction we will soon stumble upon scattering processes involving four gauge W bosons. The interesting note here comes from the particular shape of the massive boson propagator which is of the kind

$$< W^\mu(k)W^\nu(-k) >= \frac{1}{k^2 - m_W^2}(g^{\mu\nu} - \frac{k^\mu k^\nu}{m_W^2}) \tag{0.0.14}$$

The longitudinal part of the propagator, combined with the longitudinal components of the external vector boson legs, can give a contribution to the overall amplitude which is proportional to $\sqrt{s}$. It is not difficult to imagine that at high energy scales, when $\sqrt{s} \to \infty$, this contribution will break the perturbative unitarity and consequently our theory. In order to correct this, it can be proved that there is plenty of diagrams involving the same external configuration but a Higgs boson exchange that are able to balance the contribution coming from the W boson exchange. Indeed the underlying idea is that the two different types of Feynman diagrams possess the same high-energy behavior and the presence of both is requested in order to make the electroweak theory respect the unitarity bounds that we have seen. This is a simple yet powerful idea that we will employ in our study of dark matter. Anyways the application of the unitary bound of equation

0.0.11 returns an upper bound on Higgs boson mass that can be no greater of 1 TeV. The finding of a Higgs boson with a mass greater than this critical value would signify all of the consequences we already know well. We are going to see more applications of the unitarity to dark matter systems right in the following section.

1 Perturbative unitarity in DM model with Z' mediator

Let's see what happens when we describe dark matter by a Dirac fermion ψ with a mass m_{DM} and represent the Z' boson with a particle of mass $m_{Z'}$ in a lagrangian

$$L = -\sum_{f=q,l,v} Z'^{\mu}\bar{f}[g_f^V\gamma_\mu + g_f^A\gamma_\mu\gamma^5]f - Z'^{\mu}\bar{\psi}[g_{DM}^V\gamma_\mu + g_{DM}^A\gamma_\mu\gamma^5]\psi \tag{1.0.1}$$

This is a simple and general description of dark matter. We have included vector and axial couplings to the new boson, so we are in the most general frame. The point is that just the presence of the new vector boson could, in principle, violate unitarity at high energies. The expression of the Z' propagator is the same as the W one:

$$< Z'^{\mu}(k)Z'^{\nu}(-k) >= \frac{1}{k^2 - m_{Z'}^2}\big(g^{\mu\nu} - \frac{k^\mu k^\nu}{m_{Z'}^2}\big) \tag{1.0.2}$$

As previously stated the dangerous part, concerning unitarity, is the longitudinal one. In fact, it grows with direct proportionality to the four momentum carried by the propagator. This is manifestly a hint that, on high energy scales, this very feature of the new boson would be responsible for the breaking down of our theory. In general the longitudinal part of a vector boson will be dominant at high energies, so we will focus our attention on it during our analysis. Let's have a clear example of the characteristic behavior of the vector boson, which will also be helpful in our future analysis. Let's consider dark matter annihilations, the peculiar behavior of the Z' at high energies will translate into just the term k^μ, which we can contract with the DM current. In formulas, we have a term describing the annihilations that has the form

$$k^\mu\bar{v}(p_2)[g_{DM}^V\gamma_\mu + g_{DM}^A\gamma_\mu\gamma^5]u(p_1) \tag{1.0.3}$$

which corresponds to Figure 4.1

Now we can use the fact that $K = p_1 + p_2$ to write

$$\begin{aligned} k^\mu\bar{v}(p_2)[g_{DM}^V\gamma_\mu + g_{DM}^A\gamma_\mu\gamma^5]u(p_1) &= \bar{v}(p_2)[g_{DM}^V(\not{p}_1 + \not{p}_2) + g_{DM}^A(\not{p}_2\gamma^5 - \gamma^5\not{p}_1)]u(p_1) \\ &= -2g_{DM}^A m_{DM}\bar{v}(p_2)\gamma^5 u(p_1) \end{aligned} \tag{1.0.4}$$

The final result suggests that the propagator has the same behavior as a pseudoscalar with mass $m_{Z'}$ and coupling $2g_{DM}^A\frac{m_{DM}}{m_{Z'}}$. The same is true for quarks and their couplings that are $2g_f^A\frac{m_f}{m_{Z'}}$. We can guess, rightfully so, that unitarity will constraint the fraction

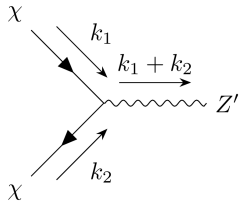

Figure 4.1: Example of tree-level scattering of two dark matter particles into a bosonic propagator carrying four-momentum $k = k_1 + k_2$

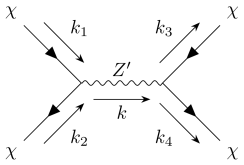

Figure 4.2: Example of a dark matter scattering with a Z' boson propagator

$g_f^A \frac{m_f}{m_{Z'}}$ besides the simple couplings $g^{V,A}$. Now that we have everything in our hands, let's finally look at the way unitarity constraint impacts our theory by applying 0.0.11 to the self-scattering of any two fermions f with a non-trivial axial coupling. Let's look at a scattering process involving two fermions f as initial states and two as final states $f\bar{f} \to f\bar{f}$ with a Z' boson exchange in Figure 4.2. Here

$$M_{ii} = \bar{u}(k_1)(g_f^V \gamma_\mu + g_f^A \gamma_\mu \gamma^5) v(k_2) \frac{1}{k^2 - m_{Z'}^2} (-g^{\mu\nu} + \frac{k^\mu k^\nu}{mZ'^2}) \bar{v}(p_2)((g_f^V \gamma_\mu + g_f^A \gamma_\mu \gamma^5)) u(p_1) \tag{1.0.5}$$

At high energies $K^2 >> m_{Z'}^2$ and the longitudinal part of the propagator dominates, so

$$M_{ii} = \bar{u}(k_1)(g_f^V \gamma_\mu + g_f^A \gamma_\mu \gamma^5) v(k_2) \frac{1}{k^2} (\frac{k^\mu k^\nu}{mZ'^2}) \bar{v}(p_2)((g_f^V \gamma_\mu + g_f^A \gamma_\mu \gamma^5)) u(p_1). \tag{1.0.6}$$

Now we can apply what we have learned a couple of equations above and write

$$M_{ii} = 4 g_f^{2A} m_f^2 \bar{u}(k_1) \gamma^5 v(k_2) \frac{1}{k^2} \frac{1}{m_{Z'}^2} \bar{v}(p_2) \gamma^5 u(p_1) \tag{1.0.7}$$

Now we notice that $k^2 = s$ and that at high energies

$$\bar{u}(k_1)\gamma^5 v(k_2) = \bar{v}(p_2)\gamma^5 u(p_1) \simeq \sqrt{s} \tag{1.0.8}$$

[50]. So now we have

$$M_{ii} = 4 g_f^{2A} m_f^2 \frac{1}{m_{Z'}^2} \tag{1.0.9}$$

And we can calculate

$$M_{ii}^0 = \frac{1}{64\pi} \int_{-1}^{1} d\cos\theta 4 g_f^{2A} m_f^2 \frac{1}{m_{Z'}^2}. \tag{1.0.10}$$

Let's now include the multiplicity factors coming from the exchange of the initial particles, the exchange of the final particles and the exchange of the identical final and initial states,

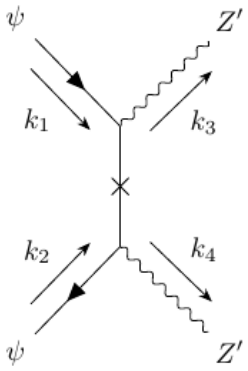

Figure 4.3: t scattering process example. Here the mass insertion in the fermionic line allows the non-trivial result.

which amount to a factor of 8 to get

$$\frac{g_f^{2A} m_f^2}{m_{Z'}^2} \leq \frac{\pi}{2}. \tag{1.0.11}$$

So at the end of our reasoning we obtain, by taking the square root of this relation:

$$m_f \leq \sqrt{\frac{\pi}{2}} \frac{m_{Z'}}{g_f^A}. \tag{1.0.12}$$

That's the end of our calculation. Here is how powerful this tool is: we can obtain an upper bound on the fermion mass just by imposing the unitarity constraint. This is a simple example, but we can employ it with every dark matter model
It is clear that the bound on the fermion mass could have not been obtained only with a non-trivial vector coupling.
Let's take the discussion one step further and analyze what happens if we find ourselves in a scattering process with the new Z' boson as an external leg. If we focus on the scattering process $\psi\bar{\psi} \to Z'_L Z'_L$ in which, of course, we pay attention to the longitudinal Z' component. As we already know from quantum field theory courses, at high momenta, $k^2 >> m_{Z'}^2$, the Z' polarization vector can be approximated by its four-momentum

$$\epsilon_L^\mu(k) = \frac{k^\mu}{m_{Z'}}. \tag{1.0.13}$$

From now on we will use this high-energy behavior in our description. This is why we expect this process to have an energy dependence that grows proportionally to $\frac{s}{m_{Z'}^2}$, thus destroying unitarity at high energies. Here the trick is in the fact that there are two diagrams, t and u, which, with their opposite sign contribution, cancel and get rid of this unwanted behavior. So the s dependence is gone, but with it, the entire contribution of the two diagrams. In order to find a non-zero result we are forced to draw a mass insertion along the fermionic line as we can see in Figure 4.3 . This will also regulate the helicity of the whole diagram. In doing that we are also getting rid of the four moment carried by the fermion and this will lead to an overall $\sqrt{s}$ dependence. Anyways at high

energies we can still employ the same tricks as before and cancel the g^V_{DM} contribution, so the scattering amplitude expression we will get, for the t process, is something like

$$\bar{v}(p_2)[g^A_{DM}\gamma_\nu\gamma^5]\frac{m_{DM}}{t-m^2_{DM}}[g^A_{DM}\gamma_\mu\gamma^5]u(p_1)\frac{k_1^\mu}{m_{Z'}}\frac{k_2^\nu}{m_{Z'}} \tag{1.0.14}$$

Here we have used the Mandelstam variables in the center of mass frame

$$\begin{aligned} s &= (p_1+p_2)^2 = (k_1+k_2)^2 \\ t &= (p_1-k_1)^2 = (p_2-k_2)^2 \\ u &= (p_1-k_2)^2 = (p_2-k_1)^2. \end{aligned} \tag{1.0.15}$$

and the u process has the same expression, only with the u variable in place of t in the denominator of the fermion propagator. The point here is we will get the same contribution from the two diagrams, with the same signs, so we will just employ a multiplicity factor of 2 later on in the calculation.
What happens at high energies in the center of mass frame is that both t and u are proportional to s and an angular contribution. We will just isolate the s contribution at the denominator of the fermion propagator as it is the dominant contribution which will set the dependence of the whole diagram. Then we exploit the growth of both the vector bosons four momenta as $\sqrt{s}$ to cancel the denominator one and use the same technique of the previous example to get a scattering matrix amplitude proportional to

$$(g^A_{DM})^2\sqrt{s}\frac{m_{DM}}{m^2_{Z'}}. \tag{1.0.16}$$

So all in all we will get, after M^0_{ii} calculation, an upper bound of the kind

$$\sqrt{s} \leq \frac{\pi m^2_{Z'}}{(g^A_{DM})^2 m_{DM}}. \tag{1.0.17}$$

Of course there is the problem: when we consider higher energies the theory breaks down. This is an index of the fact that we must consider new physics to come and rescue us as the situation we are in right now with the elements at our disposal does not let us cure unitarity problems by ourselves. This is where the Higgs boson contribution comes in our help. Indeed there is an s diagram Higgs boson exchange that has the same contribution as the one we have just written down. The problem reflects on the Higgs boson mass as it puts an upper limit on it obviously of the form

$$m_s \leq \frac{\pi m^2_{Z'}}{(g^A_{DM})^2 m_{DM}}. \tag{1.0.18}$$

Here is the unitarity in all its might: we can get to an upper bound on the Higgs boson mass by just applying the general methods we have studied in the previous section. That's a sign of a powerful tool.

2 Additional Higgs field

Let's proceed in our journey and consider the dark matter lagrangian combined with another piece containing an additional Higgs [41] field, a complex scalar that will give

mass to our new Z' by symmetry breaking. In the previous section we have seen the need for a new complex scalar coming from the anomaly equation solutions. We have seen how it is almost mandatory to include a new scalar field just to obtain a non-trivial solution of the anomaly equations. So it is coming from numerous sources the request for a new Higgs field. We fulfill the request by including a new piece to our lagrangian which will describe a complex scalar field with the same properties of the Higgs field, but a singlet under $SU(2)_L$. Of course, we need the field to be complex in order to get a $U(1)'$ non-trivial charge.
Our lagrangian, to summarize, will be described by

$$L = L_{SM} + L_{DM} + L'_{SM} + L_S \tag{2.0.1}$$

where the third term describes the interaction between the Standard Model and the new gauge boson and the fourth contains the improved Higgs sector.
Let's see what happens to our dark sector. To start we first mention that it is important to have Z' vectorial couplings vanish in at least one sector. We have talked about it in abundance when treating direct detection constraints so we will not linger on this discussion. Instead, we are just going to assume it right now. For the dark sector one way to obtain vanishing vectorial couplings is to consider a Majorana fermion as the dark matter particle. This will lead to a natural axial coupling between dark matter and the new vector boson. In particular, we are going to consider a fermion whose structure is

$$\psi = \begin{pmatrix} \chi \\ \epsilon\chi^* \end{pmatrix} \tag{2.0.2}$$

where naturally χ is a Weyl spinor. So the property we are making use of here is that under the new $U(1)'$ gauge group the dark matter carries a charge q_{DM} and the whole lagrangian is invariant under the gauge transformation

$$\psi \to \exp\left(ig' q_{DM} \alpha(x) \gamma^5\right) \tag{2.0.3}$$

with g' being the coupling constant of the new gauge group $U(1)'$.
Now about the kinetic term of the new fermion, we can expand the expression for the improved covariant derivative we have talked about in the previous chapter, which will bring the terms

$$L_{kin} = \frac{1}{2}\bar{\psi}(i \not{\partial} - g' q_{DM} \gamma^5 \not{Z'})\psi = \frac{i}{2}\bar{\psi} \not{\partial}\psi - \frac{1}{2} g^A_{DM} Z^{\mu'} \bar{\psi}\gamma^5\gamma_\mu\psi \tag{2.0.4}$$

and $g^A_{DM} = g' q_{DM}$. Now we know that in order to obtain a Majorana mass term it would be impossible just to write it straight from the get-go as the conservation of $U(1)'$ charge would be compromised. Nevertheless, we can obtain a mass term dynamically. This happens simply by spontaneous symmetry breaking. If we choose the new Higgs, which we will refer to as S, with a charge $q_S = -2q_{DM}$, this will lead us naturally to a mass term of the form

$$L_{mass} = -\frac{1}{2} y_{DM} \bar{\psi}(P_L S + P_R S^*)\psi. \tag{2.0.5}$$

It is a Yukawa mass term and of course, P_R and P_L are respectively the left and right propagators. This will allow us to generate a mass for dark matter starting from the $U(1)'$

SSB.
The two new pieces of lagrangian can be written in the following way:

$$L_{DM} = \frac{i}{2}\bar{\psi}\ \not{d}\psi - \frac{1}{2}g^A_{DM}Z^{\mu\prime}\bar{\psi}\gamma^5\gamma_\mu\psi - \frac{1}{2}y_{DM}\bar{\psi}(P_L S + P_R S^*)\psi \tag{2.0.6}$$

and

$$L_S = [(d^\mu + ig_S Z^{\mu\prime}S)]^\dagger[(d^\mu + ig_S Z'_\mu S)] + \mu_s^2 S^\dagger S - \lambda_s(S^\dagger S)^2. \tag{2.0.7}$$

We can easily see how the new Higgs singlet acquires a VEV and gives mass to both dark matter and the Z' boson. If we define

$$S = \frac{1}{\sqrt{2}}(s + w) \tag{2.0.8}$$

where w is the VEV, we can see that, through $g_s = g'q_s = -2g^A_{DM}$, we will come to the equation

$$\begin{aligned} L = \frac{i}{2}\bar{\psi}\ \not{d}\psi - \frac{1}{2}g^A_{DM}Z^{\mu\prime}\bar{\psi}\gamma^5\gamma_\mu\psi - \frac{1}{4}F^{\mu\nu\prime}F'_{\mu\nu} - \frac{m_{DM}}{2}\bar{\psi}\psi - \frac{y_{DM}}{2\sqrt{2}}s\bar{\psi}\psi \\ +\frac{1}{2}m^2_{Z'}Z^{\mu\prime}Z'_\mu + \frac{1}{2}d^\mu s d_\mu s + 2(g^A_{DM})^2 Z^{\mu\prime}Z'_\mu(s^2 + 2sw) + \frac{\mu_s^2}{2}(s+w)^2 - \frac{\lambda_s}{4}(s+w)^4 \end{aligned} \tag{2.0.9}$$

and $F'_{\mu\nu} = d_\mu Z'_\nu - d_\nu Z'_\mu$.
Moreover, we know that

$$m_{DM} = \frac{1}{\sqrt{2}}y_{DM}w \tag{2.0.10}$$

and

$$m_{Z'} \simeq 2g^A_{DM}w \tag{2.0.11}$$

A little thing to notice is that if we decide to charge SM Higgs under $U(1)'$, this will generate an additional contribution to Z' mass. The problem here is that we dispose of the electroweak precision data, a sharp instrument in our hands, which requires this contribution to be very small. So just because of that, we are going to ignore it in the remainder of the discussion as we can safely neglect it right now.
Notice also that we can also safely obtain real masses by requiring y_{DM} and w to be real. This can be achieved through a simple phase redefinition in which S and ψ absorb the complex phases.
Now let's make use of the bound we have obtained and see that the new Higgs boson mass must satisfy the requirement

$$m_s \leq \frac{\pi m^2_{Z'}}{(g^A_{DM})^2 m_{DM}}. \tag{2.0.12}$$

Also, there are other processes that need to be implemented in order to check unitarity. For example the scattering of the kind $ss \to ss$ are such that can influence the scattering amplitude. We are about to examine the scattering of the states $\frac{ss}{\sqrt{2}}$ and $\frac{Z'_L Z'_L}{\sqrt{2}}$ of course in the high energy limit $\sqrt{s} >> m_s >> m_{Z'}$. It is the $J = 0$ partial wave we are after and more specifically M^0_{if}.

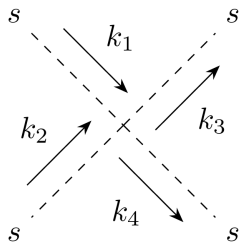

Figure 4.4: A four s vertex.

2.1 $\frac{ss}{\sqrt{2}} \to \frac{ss}{\sqrt{2}}$

Here the Lagrangian element that contributes the most is

$$L = -\frac{\lambda_s}{4} s^4. \tag{2.1.1}$$

Of course, we could also consider loops, but their contribution is not as important at the four-vertex one Figure 4.4. That being said, we need to convert this expression into quantities we could measure or, in some way, that we could have a grasp on. Let's remind ourselves of the formulas

$$\begin{aligned} w^2 &= \frac{\mu_s^2}{2\lambda_s} \\ m_{Z'} &\simeq 2 g_{DM}^A w \\ m_s^2 &= \mu_s^2. \end{aligned} \tag{2.1.2}$$

Let's use these to rewrite the lagrangian term as

$$L = -\frac{m_s^2 (g_{DM}^A)^2}{2 m_{Z'}^2}. \tag{2.1.3}$$

The point here is also to consider, in order to calculate the scattering amplitude of this process, the multiplicity factor. In this particular case, we must employ a factor of 4! and write

$$M_{if} = -12 \frac{m_s^2 (g_{DM}^A)^2}{2 m_{Z'}^2} \tag{2.1.4}$$

and finally

$$M_{if}^0 = \frac{1}{64\pi} \int_{-1}^{1} d\cos\theta M_{if}. \tag{2.1.5}$$

Let's carry out the integration here and obtain eventually

$$M_{if}^0 = -\frac{3}{8\pi} \frac{m_s^2 (g_{DM}^A)^2}{m_{Z'}^2} \tag{2.1.6}$$

This is the result we obtain for this process at high energies. Now we have to consider other processes too. We will see in the following subsection

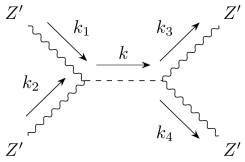

Figure 4.5: Two Z'_L scattering process at tree level.

2.2 $\frac{Z'_L Z'_L}{\sqrt{2}} \to \frac{Z'_L Z'_L}{\sqrt{2}}$

We can see an example of such a process in Figure 4.5. This time we use the results of [43]. In fact, we can apply what is there just by translating it in the case of a new $U(1)'$ symmetry. We can review the reasoning made there just to give a frame of what we are about to see in terms of the result of the scattering amplitude. First of all, among all the graphs, we concentrate only on those that potentially constitute a threat to unitarity, and this appears to be obvious, but saves a lot of time in calculation. Then one should know that there are many possible cancellations among tree-level diagrams so that even though we detect a suspicious behavior at high energies in one graph, it is not trivial that that is going to be the overall dependence of the scattering amplitude, instead, it is possible that that contribution will be erased by an analog in the opposite sign. Indeed we can classify the momentum dependence of tree-level graphs by powers of $\frac{k}{m_{Z'}}$ with k being the four-momentum of the gauge bosons in the center of mass frame. In a tree-level graph with four-boson as external legs, we will have a contribution that will be at worst proportional to $(\frac{k}{m_{Z'}})^4$. As a consequence, in the J partial wave expansion, each graph will contribute with a factor

$$a_J = A(\frac{k}{m_{Z'}})^4 + B(\frac{k}{m_{Z'}})^2 + C. \tag{2.2.1}$$

We can classify the coefficients as A, B and C forces. Every force will be attractive or repulsive depending on the sign of the coefficients. At high energies in the partial wave expansion, all the divergent behaviors are confined in the $J = 0, 1, 2$ partial waves, so we will just examine them. Moreover one can see that there are cancellations between Feynman diagrams in each case of the A forces, and the B forces as well. What happens is that, due to these gauge cancellations, we must consider only the C forces and, in this particular example, the only diagrams that offer a non-trivial contribution at high energies are the s, t and u tree level diagrams.
In this case, the relevant piece of Lagrangian we are considering is

$$L = 4(g^A_{DM})^2 Z^{\mu\prime} Z'_\nu sw \tag{2.2.2}$$

and we are going to employ this to create tree-level diagrams whose contribution is of the type

$$M_{if} = -2\frac{m_s^2 (g^A_{DM})^2}{m^2_{Z'}}(\frac{s}{s-m_s^2} + \frac{t}{t-m_s^2} + \frac{u}{u-m_s^2}) \tag{2.2.3}$$

if we consider the cancellations we were talking about previously.
Then we consider the contribution at $\sqrt{s} \to \infty$ we will see that, by just applying the formula of the previous section,

$$M^0_{if} = -\frac{3}{8\pi}\frac{m_s^2 (g^A_{DM})^2}{m^2_{Z'}} \tag{2.2.4}$$

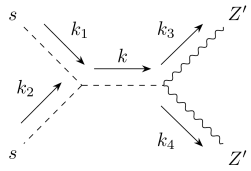

Figure 4.6: Here it is reported a $\frac{ss}{\sqrt{2}} \to \frac{Z'_L Z'_L}{\sqrt{2}}$ process at tree-level.

where we have considered the coefficient and the multiplicities following the same line of reasoning of the previous section. This result was derived on the basis of what we have learned in [43], following the same type of argument as the two situations can be overlapped and the tree-level graphs contributing to the amplitude are the same, with the Standard Model Higgs replaced by the dark Higgs boson. We have just applied the same principle of the crossing symmetries.

2.3 $\frac{ss}{\sqrt{2}} \to \frac{Z'_L Z'_L}{\sqrt{2}}$

For this process, we take also inspiration from [43], as the relevant contribution comes from the tree-level S boson exchange between initial and final states Figure 4.6. The relevant piece of lagrangian is

$$L = 4(g^A_{DM})^2 Z^{\mu\prime} Z'_\nu sw - \frac{\lambda_s}{4}(s^4 + 4s^3 w + 6s^2 w^2 + 4sw^3 + w^4) \tag{2.3.1}$$

and just starting from here we can envision, just like the previous subsection, the contribution coming from the s exchange in tree level diagram describing just the s process. Let's create the scattering amplitude

$$M_{if} = -2(g^A_{DM})^2 m_s^2 \frac{1}{s - m_s^2} \frac{k_1^\mu}{m_{Z'}} \frac{k_{2\nu}}{m_{Z'}} \tag{2.3.2}$$

we make use of the fact that at high energies

$$k_1 \cdot k_2 = \frac{s}{2} \tag{2.3.3}$$

to rewrite

$$M_{if} = -\frac{(g^A_{DM})^2 m_s^2}{m^2_{Z'}} \frac{s}{s - m_s^2} \tag{2.3.4}$$

Now in order to find M^0_{if} we employ the formula we already know and add the contribution of the two final particles exchange and the two initial particles exchange for an overall factor of 4 in order to get

$$M^0_{if} = -\frac{(g^A_{DM})^2 m_s^2}{8\pi m^2_{Z'}} \tag{2.3.5}$$

2.4 $\frac{Z'_L Z'_L}{\sqrt{2}} \to \frac{ss}{\sqrt{2}}$

This process has the same result as the previous one as the elements of the Lagrangian we are considering are exactly the same as before, we have just exchanged initial and final states.

2.5 Scattering matrix

Finally, we can gather all the results we have obtained in the scattering matrix that takes the form, at high energies,

$$\lim_{\sqrt{s}\to\infty} M^0_{if} = -\frac{(g^A_{DM})^2 m_s^2}{8\pi m^2_{Z'}} \begin{pmatrix} 3 & 1 \\ 1 & 3 \end{pmatrix}. \tag{2.5.1}$$

Now the real part of the largest eigenvalue is required to be smaller than $\frac{1}{2}$ by partial wave unitarity. The largest eigenvalue corresponds to the eigenvector $\frac{(ss+Z'_L Z'_L)}{2}$ and thus we obtain as a result

$$m_s \leq \frac{\sqrt{\pi} m_{Z'}}{g^A_{DM}} = \sqrt{4\pi} w \tag{2.5.2}$$

This bound combined with 1.0.12 gives us an enhanced constraint on Higgs boson mass of the kind

$$\sqrt{\pi}\frac{m_{Z'}}{g^A_{DM}} \geq \max[m_s, \sqrt{2} m_{DM}] \tag{2.5.3}$$

3 Complete vector portal theories

Here we skip the part where we analyze the effects of the inclusion of the two new dark sectors in the standard model and we jump directly to the most general solution for dark matter description. Indeed we generalize the argument we were making in the previous section by drawing a UV complete model in which we do not limit ourselves with the numbers of new species introduced. This perspective has the attractive feature of describing the most general model we can think of which includes dark matter and in which its existence is explained dynamically as the product of a symmetry play that we are about to see. Moreover, we are not imposing any kinds of limitations on our theory, instead, we include a generic number of new particles so that our model has the connotation of universality we are aiming for. Moreover, we also bring back to our knowledge what we have learned in the previous chapter in matter of anomalies as we try to build a model which is not just consistent as far as unitarity is concerned, but it has no irregularities in matter of anomalies. We are trying to take the best of both worlds. As far as unitarity goes we are about to use the same techniques we have seen in the previous section, just focused on a more general context, so that what we have experienced will come in our help and will not be neglected. We will see that even in this context unitarity will provide us with important constraints that will have a massive impact and deep consequences as we are about to experience. So let's dive straight into it and introduce, besides our Standard Model description of the elementary particles, an arbitrary number of fermions χ_i and scalars ϕ_j [14]. Moreover, we denote the dark hypercharges of the two different fields as d_{χ_i} and d_{ϕ_j}. Notice that from here on we are going to use a notation in which all SM fermions are left handed Weyl spinors. Indeed we present quark fields as u_i and d_i as a part of a doublet Q_i charged under the weak isospin and their counterparts u^c_i and d^c_i as singlets under the same gauge group. The same is true for lepton doublets L_i and singlets e^c_i where the index i runs over the three SM generations. Speaking of the SM particles, we also charge them under the new gauge group $U(1)'$ with dark hypercharges with the same notation as before, for example, d_Q and d_H etc. As we have done in the

previous chapter we consider only flavor universal dark charges in order to avoid flavor-changing neutral currents that could be dangerous based on our experimental results. Eventually, as it happens in many theories that share the universal frame with this one, the lightest fermion will serve the scope of representing our dark matter candidate $\chi_1 = \chi$. We choose proper DM charges in order to avoid renormalizable couplings like $L_i H \chi$ and respect the stability property dark matter seems to enjoy. Moreover, we can employ, as we have already seen something similar in the model analyzed previously, a Z_2 symmetry in which we only charge the DM fermion with an odd charge and prevent it from unwanted decays. We remind ourselves of our discussion on anomalies and dark hypercharges of the previous chapter enough to say that we are choosing them respecting the constraints

$$\begin{aligned} d_Q + d_d &= -(d_Q + d_u) \\ d_Q + d_d &= d_L + d_e \end{aligned} \tag{3.0.1}$$

in order to ensure gauge invariance for Yukawa terms. This bears as a consequence that the SM Higgs boson has a non-trivial dark hypercharge $d_H = d_Q + d_d$ and it is neutral only if the fermions are vector-like under $U(1)'$. Here we also neglect the kinetic mixing term we introduced at the beginning of the previous chapter as it is not relevant to our discussion. Indeed a kinetic mixing term would come out of a loop process, as we have already seen, while we have already got interaction at tree level between SM and DM semming from the $U(1)'$ gauge group, so it would not be relevant. Moreover, we also neglect fourth-order mixing between scalars and SM Higgs. In fact terms of the type $H^\dagger H \phi_i^\dagger \phi_j$ have been seen not to have a meaningful impact.

4 Lagrangian

After the brief introduction, now we are ready to see more in detail the mathematical formulation of the new model. Indeed we start by introducing the new boson to the Standard Model of particles.
So we introduce a new vector boson in our theory called V^μ which will mediate $U(1)'$ interactions. This reflects in the covariant derivative expression for any particle with a non-trivial charge under $U(1)'$ that becomes

$$D^\mu = D^\mu_{SM} - i g_d d_p q V^\mu \tag{4.0.1}$$

with g_d being the dark coupling of the new symmetry, D^μ_{SM} represents the remaining of the covariant derivative which, for the Standard Model particles can be found in its whole expression in Appendix A, while for the dark fermionic sector coincides with ∂_μ as these are singlets under the Standard Model. Finally, d_p is the dark charge associated with the particle we are taking under exam. We can summarize the dark charges of the particles involved in our model in

Field	l_L	l_L^c	v_L	u_L	d_L	u_L^c	d_L^c	ϕ^+	ϕ^0	χ	ϕ_j
T_3	$-\frac{1}{2}$	0	$\frac{1}{2}$	$\frac{1}{2}$	$-\frac{1}{2}$	0	0	$\frac{1}{2}$	$-\frac{1}{2}$	0	0
Y	$-\frac{1}{2}$	-1	$-\frac{1}{2}$	$\frac{1}{6}$	$\frac{1}{6}$	$\frac{2}{3}$	$-\frac{1}{3}$	$\frac{1}{2}$	$\frac{1}{2}$	0	0
Q	-1	-1	0	$\frac{2}{3}$	$-\frac{1}{3}$	$\frac{2}{3}$	$-\frac{1}{3}$	1	0	0	0
d_p	d_L	$d_{l_L^c}$	d_ν	d_Q	d_Q	d_u	d_d	d_H	d_H	d_χ	d_{ϕ_j}

This has of course deep implications on the standard model lagrangian and the addition brings us a final lagrangian of the type

$$L = L_{SM} + L_{DM} + L'_{SM} + L_S. \tag{4.0.2}$$

Moreover in studying the $U(1)'$ gauge boson V_μ we can see the mass mixing term coming from the Lagrangian element

$$|D_\mu H|^2 \in -g_w g_d d_H v_H^2 Z_\mu^{SM} V^\mu. \tag{4.0.3}$$

Here it is important to keep an eye on all the couplings as $g_w = \sqrt{g_Y^2 + g_2^2}$, g_d is the $U(1)'$ gauge coupling and the SM Higgs VEV is $< H >^T = (0 \quad v_H)$. Now we can see that we can go to the mass basis and look at the mass eigenstates with the rotation

$$\begin{pmatrix} Z_\mu^{SM} \\ V_\mu \end{pmatrix} = \begin{pmatrix} \cos\theta & \sin\theta \\ -\sin\theta & \cos\theta \end{pmatrix} \begin{pmatrix} Z_\mu \\ Z'_\mu \end{pmatrix}. \tag{4.0.4}$$

We have used Z_μ^{SM} as the linear combination of the $SU(2)_L$ and $U(1)_Y$ gauge bosons. In Appendix B there is the procedure on how to obtain the mixing angle θ that we limit ourselves to write here

$$\tan 2\theta = -\frac{4 g_w g_d d_H v_H^2}{4 g_d^2 (d_H^2 v_H^2 + v_\phi^2) - g_w^2 v_H^2} \tag{4.0.5}$$

and $v_\phi^2 = \sum_i d_\phi^2 v_\phi^2$. Let's just mention that electroweak precision tests require $\theta \leq 10^{-3}$. This will be helpful in future calculations.
Now that we have all in our hands, let's see sector after sector how the Standard Model lagrangian is influenced by the brand new boson introduction and what are the consequences as far as dark matter is concerned.

4.1 The dark sector

Let's say we introduce a new fermion to the Standard Model, a Majorana one,

$$\psi = \begin{pmatrix} \chi \\ \epsilon \chi^* \end{pmatrix}. \tag{4.1.1}$$

Now here we are making our steps in the Weyl basis where

$$\gamma^\mu = \begin{pmatrix} 0 & \sigma^\mu \\ \bar{\sigma^\mu} & 0 \end{pmatrix} \tag{4.1.2}$$

and

$$\begin{aligned} \sigma^\mu &= (1, \sigma^i) \\ \bar{\sigma^\mu} &= (1, -\sigma^i). \end{aligned} \tag{4.1.3}$$

Now

$$\gamma^5 = \begin{pmatrix} -\mathbb{1} & 0 \\ 0 & \mathbb{1} \end{pmatrix} \tag{4.1.4}$$

and

$$P_L = \begin{pmatrix} \mathbb{1} & 0 \\ 0 & 0 \end{pmatrix} \qquad P_R = \begin{pmatrix} 0 & 0 \\ 0 & \mathbb{1} \end{pmatrix} \tag{4.1.5}$$

So if we want to consider just the left-handed part, that would be

$$\psi_L = \begin{pmatrix} \chi \\ 0 \end{pmatrix} \qquad and \qquad \bar{\psi_L} = (0, \chi^\dagger) \tag{4.1.6}$$

so now we are ready to write down the kinetic part of the dark sector.
This part is thought to be invariant under the gauge transformation

$$\psi \to \exp\left[i g_d d_\chi \alpha(x) \gamma^5\right] \psi \tag{4.1.7}$$

So

$$L_{DM}^{kin} = \bar{\psi_L}(i \not{D}) \psi_L = (0, \chi^\dagger) i (\not{d} - i g_d d_\chi \gamma^5 \gamma^\mu V_\mu) \begin{pmatrix} \chi \\ 0 \end{pmatrix} \tag{4.1.8}$$

this means that we get the terms

$$L_{DM}^{kin} = i \chi^\dagger \bar{\sigma^\mu} d_\mu \chi + g_d d_\chi \chi^\dagger \bar{\sigma^\mu} \chi V_\mu \tag{4.1.9}$$

Now let's set up a lagrangian for the mass of the dark fermion. Since this is a Majorana fermion and we need only the left-handed part, we need to make sure that it is invariant under the gauge transformation as well. A Majorana mass term would spoil the gauge invariance, this is why we are going to introduce the dark scalar field S which will have as a property

$$d_S = -2 d_\chi \tag{4.1.10}$$

so that the invariance is re-established. We are going to call under the unique name of S the sum of the scalar fields, SM Higgs excluded, that are interacting with the dark sector and whose vev is going to play a part in the generating of Z' mass and dark fermion mass as well

$$S = \sum_j \phi_j. \tag{4.1.11}$$

So we are going to set the term for the mass matrix in the dark sector as

$$L_{DM}^{mass} = -\frac{1}{2} y_{DM} S \chi \chi + h.c \tag{4.1.12}$$

4.2 Dark scalar sector

We have already introduced the scalar field S as the sum of all the ϕ_j, we shall see now what is the lagrangian associated with this field

$$L_S = \sum_j [(d^\mu - i g_d d_{\phi_j} V^\mu)\phi_j]^\dagger [(d_\mu - i g_d d_{\phi_j} V_\mu)\phi_j] + \sum_j \mu^2_{\phi_j} \phi^\dagger_j \phi_j - \sum_j \lambda_{\phi_j} (\phi^\dagger_j \phi_j)^2 \quad (4.2.1)$$

each scalar singlet will acquire a vev $\phi_j = v_{\phi_j} + \frac{\tilde{\phi}_j}{\sqrt{2}}$ so we can see that this will originate the masses for the dark fermion and for the new vector boson

4.3 Visible sector interactions

The term L'_{SM} is generated by keeping in mind the new term in the Higgs covariant derivative and adding a term for the interaction between the new vector boson and the SM fermions. So

$$D_\mu H = (D^{SM}_\mu + i\frac{g_w}{2} Z_\mu - i g_d d_H V_\mu) H \quad (4.3.1)$$

where of course $g_w = \sqrt{g_Y^2 + g_2^2}$ and

$$L'_{SM} = [(D_\mu H)^\dagger (i\frac{g_w}{2} Z_\mu H - i g_d d_H V_\mu H) + h.c] - \sum_{f=q,l,\nu} g_d V^\mu [d_f \bar{f}_L \gamma_\mu f_L] \quad (4.3.2)$$

5 After symmetry breaking

We have to keep in mind that all the scalar fields acquire VEVs. We have seen that

$$H = \begin{pmatrix} 0 \\ v_H + \frac{h}{\sqrt{2}} \end{pmatrix} \qquad and \qquad \phi_j = v_{\phi_j} + \frac{\tilde{\phi}_j}{\sqrt{2}} \quad (5.0.1)$$

with

$$v_H^2 = \frac{\mu^2}{\lambda} \qquad and \qquad v^2_{\phi_j} = \frac{\mu^2_{\phi_j}}{\lambda_{\phi_j}} \quad (5.0.2)$$

Since we are going to work with the sum of scalar fields we can define

$$w = \sum_j v_{\phi_j} \qquad s = \sum_j \tilde{\phi}_j \quad (5.0.3)$$

let's see what this implies for each sector

5.1 Dark fermionic sector

After symmetry breaking, we can find

$$L_{DM}^{kin} = i\chi^{\dagger}\bar{\sigma^{\mu}}d_{\mu}\chi + g_d d_{\chi}\chi^{\dagger}\bar{\sigma^{\mu}}\chi V_{\mu} \tag{5.1.1}$$

and

$$L_{DM}^{mass} = -\frac{1}{2}y_{DM}w\chi\chi - \frac{1}{2\sqrt{2}}y_{DM}s\chi\chi + h.c \tag{5.1.2}$$

so we can see that

$$m_{DM} = y_{DM}w \tag{5.1.3}$$

5.2 Dark scalar sector

We can gather the information from the previous sections into

$$\begin{aligned}\sum_j \frac{1}{2}d^{\mu}\tilde{\phi_j}d_{\mu}\tilde{\phi_j} + \frac{1}{2}(\sum_j 2g_d^2 d_{\phi_j}^2 v_{\phi_j}^2)V_{\mu}V^{\mu} + \frac{1}{2}g_d^2 V_{\mu}V^{\mu}(\sum_j d_{\phi_j}^2 \tilde{\phi_j}^2 + 2\sqrt{2}d_{\phi_j}^2\tilde{\phi_j}v_{\phi_j}) \\ + \sum_j \frac{\mu_{\phi_j}^2}{2}(\tilde{\phi_j} + \sqrt{2}v_{\phi_j})^2 - \frac{\lambda_{\phi_j}}{4}(\tilde{\phi_j} + \sqrt{2}v_{\phi_j})^4\end{aligned} \tag{5.2.1}$$

The important thing to grasp here is the part proportional to $V_{\mu}V^{\mu}$ which constitutes the first half of the new boson mass

5.3 Visible sector interactions

Here after symmetry breaking the term arise

$$\begin{aligned}L'_{SM} &= -\sum_{f=q,l,v} g_d V^{\mu}[d_f \bar{f_L}\gamma_{\mu}f_L] + \frac{g_w^2}{4}(Z_{\mu} - 2\frac{g_d d_H}{g_w}V_{\mu})^2(v_H + \frac{h}{\sqrt{2}})^2 \\ &= -\sum_{f=q,l,v} g_d V^{\mu}[d_f \bar{f_L}\gamma_{\mu}f_L] + \frac{g_w^2}{4}(Z_{\mu} - 2\frac{g_d d_H}{g_w}V_{\mu})^2(v_H^2 + \frac{h^2}{2} + 2\frac{v_H h}{\sqrt{2}})\end{aligned} \tag{5.3.1}$$

Here we can see that finally, we have

$$\begin{aligned}m_Z^2 &= \frac{g_w^2}{2}v_H^2 \\ m_{Z'}^2 &= 2g_d^2(d_H^2 v_H^2 + \sum_j d_{\phi_j}^2 v_{\phi_j}^2)\end{aligned} \tag{5.3.2}$$

there is also a mass mixing term that will be helpful for later

$$m_{ZZ'} = -g_d g_w d_H v_H^2 \tag{5.3.3}$$

5.4 Complete lagrangian

$$\begin{aligned} L = i\chi^\dagger\bar{\sigma^\mu}d_\mu\chi + g_d d_\chi \chi^\dagger\bar{\sigma^\mu}\chi V_\mu - \frac{1}{2}y_{DM}w\chi\chi - \frac{1}{2\sqrt{2}}y_{DM}s\chi\chi \\ + \sum_j \frac{1}{2}d^\mu\tilde{\phi_j}d_\mu\tilde{\phi_j} + \frac{1}{2}(\sum_j 2g_d^2 d_{\phi_j}^2 v_{\phi_j}^2)V_\mu V^\mu + \frac{1}{2}g_d^2 V_\mu V^\mu(\sum_j d_{\phi_j}^2 \tilde{\phi_j}^2 + 2\sqrt{2}d_{\phi_j}^2\tilde{\phi_j}v_{\phi_j}) \\ + \sum_j \frac{\mu_{\phi_j}^2}{2}(\tilde{\phi_j} + \sqrt{2}v_{\phi_j})^2 - \frac{\lambda_{\phi_j}}{4}(\tilde{\phi_j} + \sqrt{2}v_{\phi_j})^4 \\ - \sum_{f=q,l,v} g_d V^\mu[d_f\bar{f}_L\gamma_\mu f_L] + \frac{g_w^2}{4}(Z_\mu - 2\frac{g_d d_H}{g_w}V_\mu)^2(v_H + \frac{h}{\sqrt{2}})^2 \end{aligned} \tag{5.4.1}$$

Let's rotate it by

$$\begin{pmatrix} c_\theta & s_\theta \\ -s_\theta & c_\theta \end{pmatrix} \tag{5.4.2}$$

by means of

$$\begin{pmatrix} Z_\mu^{SM} \\ V_\mu \end{pmatrix} = \begin{pmatrix} c_\theta & s_\theta \\ -s_\theta & c_\theta \end{pmatrix}\begin{pmatrix} Z_\mu \\ Z'_\mu \end{pmatrix} \tag{5.4.3}$$

So to get

$$\begin{aligned} L = i\chi^\dagger\bar{\sigma^\mu}d_\mu\chi - g_d d_\chi\chi^\dagger\bar{\sigma^\mu}\chi s_\theta Z_\mu + g_d d_\chi\chi^\dagger\bar{\sigma^\mu}\chi c_\theta Z'_\mu - \frac{1}{2}y_{DM}w\chi\chi - \frac{1}{2\sqrt{2}}y_{DM}s\chi\chi \\ + \sum_j \frac{1}{2}d^\mu\tilde{\phi_j}d_\mu\tilde{\phi_j} \\ + \frac{1}{2}(\sum_j 2g_d^2 d_{\phi_j}^2 v_{\phi_j}^2)(s_\theta^2 Z^\mu Z_\mu - 2s_\theta c_\theta Z^\mu Z'_\mu + c_\theta^2 Z^{\mu'}Z'_\mu) \\ + \frac{1}{2}g_d^2(\sum_j d_{\phi_j}^2\tilde{\phi_j}^2 + 2\sqrt{2}d_{\phi_j}^2\tilde{\phi_j}v_{\phi_j})(s_\theta^2 Z^\mu Z_\mu - 2s_\theta c_\theta Z^\mu Z'_\mu + c_\theta^2 Z^{\mu'}Z'_\mu) \\ + \sum_j \frac{\mu_{\phi_j}^2}{2}(\tilde{\phi_j} + \sqrt{2}v_{\phi_j})^2 - \frac{\lambda_{\phi_j}}{4}(\tilde{\phi_j} + \sqrt{2}v_{\phi_j})^4 \\ + \sum_{f=q,l,v} g_d[d_f\bar{f}_L\gamma_\mu f_L]s_\theta Z^\mu - \sum_{f=q,l,v} g_d[d_f\bar{f}_L\gamma_\mu f_L]c_\theta Z^{\mu'} \\ + \frac{g_w^2}{4}((c_\theta + 2\frac{g_d d_H}{g_w}s_\theta)^2 Z_\mu Z^\mu)(v_H + \frac{h}{\sqrt{2}})^2 \\ + \frac{g_w^2}{4}((s_\theta - 2\frac{g_d d_H}{g_w}c_\theta)^2 Z'_\mu Z'^\mu + 2(c_\theta + 2\frac{g_d d_H}{g_w}s_\theta)(s_\theta - 2\frac{g_d d_H}{g_w}c_\theta)Z^\mu Z'_\mu)(v_H + \frac{h}{\sqrt{2}})^2 \end{aligned} \tag{5.4.4}$$

Now that the lagrangian is complete and under our control, we can progress from here by studying all the relevant scatterings. In particular, we are going to list and examine here the most relevant, then the others will be consultable in Appendix B.

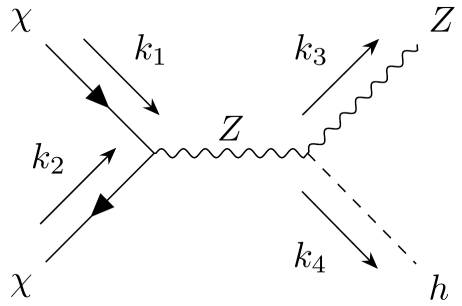

Figure 4.7: S-type process. Z boson propagator

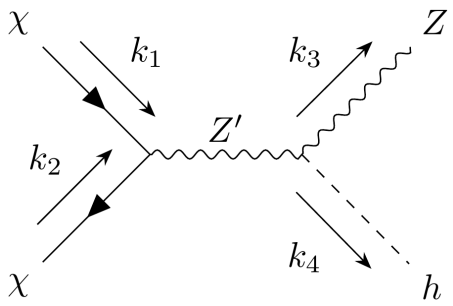

Figure 4.8: S-type process. Z' boson propagator

6 $\chi\chi \to Zh$

Right here we can already see that these kinds of models are susceptibles to the same problems we encountered at the beginning of the chapter, as the longitudinal modes of the vector boson always grow with energies, bringing the danger of breaking unitarity. Here we analyze Majorana DM annihilation $\chi\chi \to Zh$ and look for unitarity breakdown. The reason why we are studying this particular process is that this might be the leading one for relic abundance calculation and indirect detection. The interesting part of Lagrangian is

$$\begin{aligned} L_{\chi\chi\to Zh} = g_d d_\chi \chi^\dagger \bar{\sigma}^\mu \chi(-s_\theta Z_\mu + c_\theta Z'_\mu) + \\ \frac{\sqrt{2}g_w^2}{4} v_H h[(c_\theta + \frac{2g_d d_H}{g_w} s_\theta)^2 Z^\mu Z_\mu + (s_\theta - \frac{2g_d d_H}{g_w} c_\theta)^2 Z'_\mu Z^{\mu'}] \\ +2(c_\theta + \frac{2g_d d_H}{g_w} s_\theta)(s_\theta - \frac{2g_d d_H}{g_w} c_\theta) Z_\mu Z^{\mu'} \end{aligned} \tag{6.0.1}$$

We can already see that the Z' exchange is the leading one for small θ and we can appreciate the two processes in Figure 4.7 and 4.8.

It is clear that the sole Z' exchange will lead to unitarity breakdown. Indeed we can see that $\sigma_{\chi\chi\to Zh}$ with only a Z' exchange approaches a constant value at high energies, thus revealing issues with the theory. Fortunately here comes the diagram with the Z exchange that, if considered, can restore proper high-energy behavior and get rid of all our problems. The neediness to consider the Z exchange diagram comes from the fact that at small θ the two different contributions have potentially the same size as the Z' diagram also disappears for $\theta \to 0$. Indeed we can see that the term containing $ZZ'h$ comes from the mixing term in the Lagrangian and $\tan 2\theta \simeq d_H$. Now in the following of this section, we will demonstrate how it is possible such a cancellation between to apparently unrelated diagrams. First, let's review the interesting quantities we are going to work with as far as unitarity is concerned. Another way of applying the partial waves expansion is to the scattering amplitude of a process. Indeed if we consider two generic states i for initial and f for the final, we can always write its scattering amplitude in terms of partial waves

like

$$M_{if} = 16\pi \sum_{J=0}^{\infty} (2J+1) a_{if}^{J} P_n(\cos\theta) \tag{6.0.2}$$

This is just another way to put what we already know in the matter of wave analysis of a process, but it is better to have all the notable quantities clearly right in front of us before getting to work. The unitarity bounds are the same as before as

$$Re(a_{if}^{J}) \leq \frac{1}{2} \tag{6.0.3}$$

is what is required at high energies. Again this is just a rewriting of what we already know in a different fashion, nothing special or different. Let's cut to the chase and write the full expression for the two M_{if} including the propagators and the external legs

$$\begin{aligned} M^{Z'_L}_{\chi\chi\to Z_L h} = g_d d_\chi v^\dagger(p_2)\bar{\sigma^\mu} u(p_1) c_\theta \frac{\sqrt{2} g_w^2}{2} v_H (c_\theta + \frac{2 g_d d_H}{g_w} s_\theta)(s_\theta - \frac{2 g_d d_H}{g_w} c_\theta) \times \\ \frac{1}{s - m^2_{Z'}} (-g_{\mu\nu} + \frac{k_\mu k_\nu}{m^2_{Z'}}) \epsilon(k_1)^\nu \end{aligned} \tag{6.0.4}$$

and at the high energies we know we can make use of $\epsilon(k_1)^\nu = \frac{k_1^\nu}{m_{Z'}}$.
Instead for the other diagram the full expression is

$$\begin{aligned} M^{Z_L}_{\chi\chi\to Z_L h} = g_d d_\chi v^\dagger(p_2)\bar{\sigma^\mu} u(p_1)(-s_\theta) \frac{\sqrt{2} g_w^2}{2} v_H \times \\ (c_\theta + \frac{2 g_d d_H}{g_w} s_\theta)^2 \frac{1}{s - m^2_{Z'}} (-g_{\mu\nu} + \frac{k_\mu k_\nu}{m^2_{Z'}}) \epsilon(k_1)^\nu \end{aligned} \tag{6.0.5}$$

We want to study the behavior at high energies considering internal and external longitudinal modes of the vector bosons. So first we examine the expression of $M^{Z_L}_{\chi\chi\to Z_L h}$ and see the way it transforms at high energies. We can just isolate the longitudinal part of the propagator and use the expression for the polarization vector of the Z boson to get

$$M^{Z_L}_{\chi\chi\to Z_L h} = g_d d_\chi v^\dagger(p_2)\bar{\sigma^\mu} u(p_1)(-s_\theta) \frac{\sqrt{2} g_w^2}{2} v_H (c_\theta + \frac{2 g_d d_H}{g_w} s_\theta)^2 \frac{1}{s} \frac{k_\mu k_\nu}{m^2_{Z'}} \frac{k_1^\nu}{m_Z} \tag{6.0.6}$$

Now contract k_μ with $\bar{\sigma^\mu}$ and use the identity already proven to obtain a factor of $-2m_\chi$ and contract k_ν with k_1^ν to obtain, at high energies, a factor of $\frac{s}{2}$ so

$$M^{Z_L}_{\chi\chi\to Z_L h} = \frac{\sqrt{2}}{4} g_w^2 g_d d_\chi v^\dagger(p_2)\bar{\sigma^\mu} u(p_1)(-s_\theta) v_H (c_\theta + \frac{2 g_d d_H}{g_w} s_\theta)^2 \frac{-2m_\chi}{m_Z^3} \tag{6.0.7}$$

Use the fact that $d_H = -d_\chi$ with the parametrization chosen

$$M^{Z_L}_{\chi\chi\to Z_L h} = \frac{\sqrt{2}}{2} g_w^2 g_d d_H v^\dagger(p_2)\bar{\sigma^\mu} u(p_1)(-s_\theta) v_H (c_\theta + \frac{2 g_d d_H}{g_w} s_\theta)^2 \frac{m_\chi}{m_Z^3} \tag{6.0.8}$$

Now we have already seen that at high energies $v^\dagger(p_2)\bar{\sigma^\mu} u(p_1) \to \sqrt{s}$. This combined with a multiplicity factor of 2 that comes from the exchange of initial identical particles gives us, for the Z exchange,

$$M^{Z_L}_{\chi\chi\to Z_L h} = \sqrt{2} g_w^2 g_d d_H \frac{v_H m_\chi}{m_Z^3} s_\theta \sqrt{s} (c_\theta + \frac{2 g_d d_H}{g_w} s_\theta)^2. \tag{6.0.9}$$

By following the exact same steps we can conclude that for the diagram containing the Z'_L exchange vector boson

$$M^{Z'_L}_{\chi\chi\to Z_L h} = \sqrt{2} g_w^2 g_d d_H \frac{v_H m_\chi}{m^2_{Z'} m_Z} c_\theta \sqrt{s} (c_\theta + \frac{2 g_d d_H}{g_w} s_\theta)(\frac{2 g_d d_H}{g_w} c_\theta - s_\theta) \tag{6.0.10}$$

So when we approach the sum of the two diagrams we obtain something proportional to

$$M_{\chi\chi\to Z_L h} \propto [\frac{s_\theta}{m_Z^2}(c_\theta + \frac{2 g_d d_H}{g_w} s_\theta) + \frac{c_\theta}{m^2_{Z'}}(\frac{2 g_d d_H}{g_w} c_\theta - s_\theta)]\sqrt{s} \tag{6.0.11}$$

In Appendix A we are going to see precisely how the cancellation works and explain all the details required. Let's just say here that this is possible by writing all the masses involved in the calculation together with the various s_θ and c_θ in terms of the couplings. So that being said we have proved that at high energies the really dangerous terms cancel each other perfectly. This is how unitarity is achieved and why the inclusion of the Z exchange diagram is so crucial for the theory that it absolutely cannot be neglected. This has another consequence though, and it is what we are interested in: the unitarity bounds coming from the application of the rules we have depicted previously in the chapter. We can work out an inverse formula for the expression of a^0_{ij}. In particular, since we are interested in the $J = 0$ partial wave [9]

$$a^0_{ij} = \frac{1}{32\pi} \int_{-1}^{1} d\cos\theta M_{ij}(s, \cos\theta) \tag{6.0.12}$$

that differs from what we have previously calculated from a factor of $\frac{1}{2}$
So how do we calculate a_0 for this kind of process is the crucial question. First, we need to consider the expression for the amplitude of the processes considering just the transverse part of the propagators at high energies:

$$M^{Z'_L}_{\chi\chi\to Z_L h} = -g_d d_\chi v^\dagger(p_2)\bar{\sigma^\mu} u(p_1) c_\theta \frac{\sqrt{2} g_w^2}{2} v_H (c_\theta + \frac{2 g_d d_H}{g_w} s_\theta)(s_\theta - \frac{2 g_d d_H}{g_w} c_\theta)\frac{1}{s}\epsilon(k_1)_\mu \tag{6.0.13}$$

and

$$M^{Z_L}_{\chi\chi\to Z_L h} = -g_d d_\chi v^\dagger(p_2)\bar{\sigma^\mu} u(p_1)(-s_\theta)\frac{\sqrt{2} g_w^2}{2} v_H (c_\theta + \frac{2 g_d d_H}{g_w} s_\theta)^2 \frac{1}{s}\epsilon(k_1)_\mu. \tag{6.0.14}$$

If we sum the two contributions we will obtain something of the form

$$\begin{aligned} M_{\chi\chi\to Z_L h} = -g_d d_\chi v^\dagger(p_2)\bar{\sigma^\mu} u(p_1) c_\theta \frac{1}{s}\sqrt{2}\frac{g_w^2}{2} v_H \times \\ [c_\theta(s_\theta - \frac{2 g_d d_H}{g_w} c_\theta) - s_\theta(c_\theta + \frac{2 g_d d_H}{g_w} s_\theta)](c_\theta + \frac{2 g_d d_H}{g_w} s_\theta)\epsilon(k_1)_\mu \end{aligned} \tag{6.0.15}$$

If we solve the inside of the square brackets we get out of the whole expression, while employing $\epsilon(k_1)_\mu = \frac{(k_1)_\mu}{m_Z}$

$$M_{\chi\chi\to Z_L h} = g_d d_\chi v^\dagger(p_2)\bar{\sigma^\mu} u(p_1)(k_1)_\mu \frac{1}{s}\sqrt{2}\frac{g_w^2}{2} v_H (c_\theta + s_\theta \frac{2 g_d d_H}{g_w})\frac{2 g_d d_H}{g_w}\frac{1}{m_Z} \tag{6.0.16}$$

now see that

$$\int_{-1}^{1} d\cos\theta = \int_{0}^{\pi} \sin\theta d\theta. \tag{6.0.17}$$

Moreover in the center of mass frame, at high energies, we can express

$$(k_1)_\mu = \frac{\sqrt{s}}{2}(1, \cos\theta, 0, \sin\theta) \tag{6.0.18}$$

and $\bar{\sigma^\mu} = (\mathbb{1}, -\sigma^i)$ with σ^i being Pauli matrices. By explicitly contracting $\bar{\sigma^\mu}$ and $(k_1)_\mu$ we can see that only the factor proportional to $\sin\theta$ has a non-vanishing result out of the integration proportional to $\frac{\pi}{2}$ and when all is set and done we get

$$a^0_{\chi\chi\to Z_L h} = \frac{1}{64\pi}\pi g_d d_\chi \sqrt{s}\frac{1}{s}\sqrt{2}\frac{g_w^2}{2}v_H(c_\theta + s_\theta\frac{2g_d d_H}{g_w})\frac{2g_d d_H}{g_w}\frac{1}{m_Z}\frac{\sqrt{s}}{2} \tag{6.0.19}$$

or, simplifying everything

$$a^0_{\chi\chi\to Z_L h} = \frac{\sqrt{2}}{128}\frac{g_w v_H}{m_Z}g_d^2 d_\chi d_H(c_\theta + s_\theta\frac{2g_d d_H}{g_w}). \tag{6.0.20}$$

Now let's apply the bound we have already derived in the small mixing angle limit and obtain

$$g_d|d_\chi d_H|^{\frac{1}{2}} \leq 4\sqrt{2} \tag{6.0.21}$$

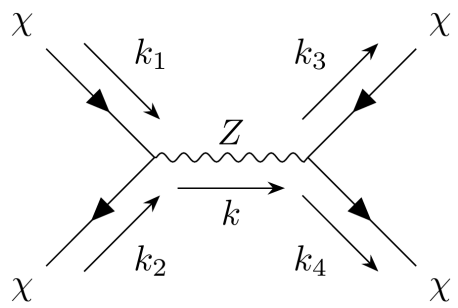

Figure 4.9: S-type process. Vector boson propagator(either Z or Z')

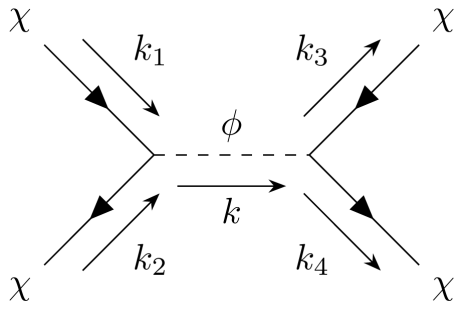

Figure 4.10: S-type process. Dark scalar propagator

7 $\chi\chi \to \chi\chi$

Here we can see from the lagrangian that there are three terms contributing to this process, one with a Z boson exchange, one with a Z' exchange and one with a scalar field ϕ exchange, we can see these respectively in Figure 4.9 and 4.10. Obviously, we can obtain a cumulative scattering amplitude by summing out all the contributions from scalar fields exchange that will be equal, but for now, we examine just one diagram with one scalar ϕ and then we will sum all the contributions. So the scattering amplitudes are respectively

$$\begin{aligned} M^{Z}_{\chi\chi\to\chi\chi} &= -4g_d^2 d_\chi^2 \chi^\dagger \bar{\sigma^\mu} \chi s_\theta^2 \frac{1}{s - m_Z^2}[-g_{\mu\nu} + \frac{k_\mu k_\nu}{m_Z^2}]\chi^\dagger \bar{\sigma^\nu}\chi \\ M^{Z'}_{\chi\chi\to\chi\chi} &= -4g_d^2 d_\chi^2 \chi^\dagger \bar{\sigma^\mu} \chi c_\theta^2 \frac{1}{s - m_Z^2}[-g_{\mu\nu} + \frac{k_\mu k_\nu}{m_{Z'}^2}]\chi^\dagger \bar{\sigma^\nu}\chi \\ M^{\phi_j}_{\chi\chi\to\chi\chi} &= -y_{DM}^2 \chi^\dagger\chi \frac{1}{s - m_{\phi_j}^2}\chi^\dagger\chi \end{aligned} \tag{7.0.1}$$

where all the factors of 4 are multiplicity factors considering the exhange between the two initial particles, the two final and initial and final states exchange.

We see that there is no danger at high energies as

$$k_\mu \chi^\dagger \bar{\sigma^\mu}\chi \to -2m_\chi \chi^\dagger \bar{\sigma^\mu}\chi \tag{7.0.2}$$

Here we have only considered s types diagrams because the t and u ones go to 0 thanks to the same algebra.
At high energies

$$\chi^\dagger \bar{\sigma^\mu}\chi \simeq \chi^\dagger\chi \to \sqrt{s} \tag{7.0.3}$$

thus completely resolving any possible issue stemming from the longitudinal polarization of the vector boson.
Let's see the contribution coming from the longitudinal part of the vector boson propagators:

$$M^{Z_L + Z'_L}_{\chi\chi\to\chi\chi} = -16 m_\chi^2 g_d^2 d_\chi^2 \chi^\dagger \bar{\sigma^\mu}\chi \frac{1}{s}[\frac{s_\theta^2}{m_Z^2} + \frac{c_\theta^2}{m_{Z'}}]\chi^\dagger \bar{\sigma^\nu}\chi \tag{7.0.4}$$

We examine the case in which there is only one dark scalar field, the generalization to n scalar fields comes only with a sum over all the quantities describing them. Here we have

that $d_{\phi_j} = -2d_\chi$ and $m_\chi = y_{DM} v_{\phi_j}$ so this contribution at high energies goes like

$$M^{Z_L+Z'_L}_{\chi\chi\to\chi\chi} = -2y^2_{DM}\chi^\dagger\bar{\sigma^\mu}\chi\frac{1}{s}\chi^\dagger\bar{\sigma^\nu}\chi \tag{7.0.5}$$

which now can be summed to the identical ϕ_j contribution. They both are constants at high energies and will result in

$$M^{Z_L+Z'_L+\phi_j}_{\chi\chi\to\chi\chi} = -3y^2_{DM} \tag{7.0.6}$$

Now from the transverse degrees of freedom for what concerns the a_0 calculation, the longitudinal ones are belittled by the inverse proportionality to the vector boson masses squared. We can sum the two contributions of interests and see that

$$M^{Z_T+Z'_T}_{\chi\chi\to\chi\chi} = g^2_d d^2_\chi \chi^\dagger\bar{\sigma^\mu}\chi\frac{g_{\mu\nu}}{s}\chi^\dagger\bar{\sigma^\nu}\chi \tag{7.0.7}$$

Now this amplitude dominates even on the one coming from the ϕ exchange, it can be seen from electroweak precision data, and at high energies becomes

$$M^{Z_T+Z'_T}_{\chi\chi\to\chi\chi} = -2g^2_d d^2_\chi \tag{7.0.8}$$

So now

$$a_0 = -\frac{1}{32\pi}(3y^2_{DM} + 2g^2_d d^2_\chi) \tag{7.0.9}$$

in which the first contribution dominates.
Being the bound

$$|Re(a_0)| \leq \frac{1}{2} \tag{7.0.10}$$

we can see that we come up with

$$\frac{1}{32\pi}3y^2_{DM} \leq \frac{1}{2} \tag{7.0.11}$$

so

$$y_{DM} \leq 4\sqrt{\frac{\pi}{3}} \tag{7.0.12}$$

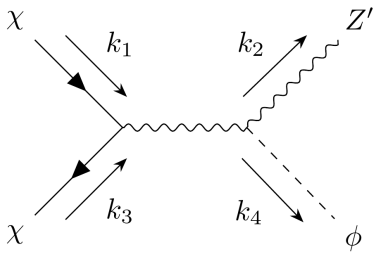

Figure 4.11: S-type process. Vector boson propagator(either Z or Z')

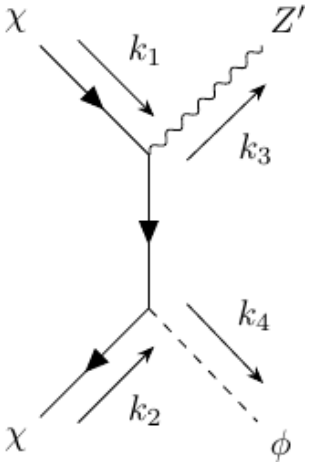

Figure 4.12: T-type process. Fermion propagator

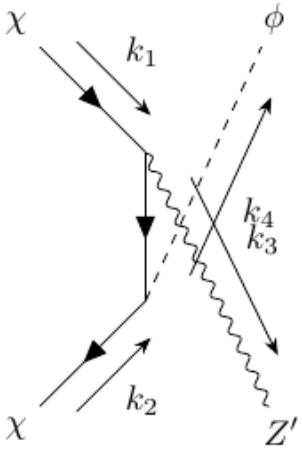

Figure 4.13: U-type process. Fermion propagator

8 $\chi\chi \to Z'\phi$

So here we see the contributions

$$M^{Z}_{\chi\chi\to Z'\phi} = -4\sqrt{2}g_d^3 d^2_{\phi_j} v_{\phi_j} s^2_\theta c_\theta d_\chi \chi^\dagger \bar{\sigma^\mu} \chi \frac{1}{s - m_Z^2}[-g_{\mu\nu} + \frac{(k_1+k_2)_\mu (k_1+k_2)_\nu}{m_Z^2}]\frac{k_{3\mu}}{m_{Z'}} \quad (8.0.1)$$

$$M^{Z'}_{\chi\chi\to Z'\phi} = -4\sqrt{2}g_d^3 d^2_{\phi_j} v_{\phi_j} c^3_\theta d_\chi \chi^\dagger \bar{\sigma^\mu} \chi \frac{1}{s - m_{Z'}^2}[-g_{\mu\nu} + \frac{(k_1+k_2)_\mu (k_1+k_2)_\nu}{m_{Z'}^2}]\frac{k_{3\mu}}{m_{Z'}} \quad (8.0.2)$$

$$M^{\chi}_{\chi\chi\to Z'\phi} = 2\sqrt{2} y_{DM} g_d d_\chi \chi^\dagger \bar{\sigma^\mu} \chi c_\theta [\frac{1}{(\not{k}_1 - \not{k}_3) - m_\chi} + \frac{1}{(\not{k}_1 - \not{k}_4) - m_\chi}]\frac{k_{3\mu}}{m_{Z'}} \quad (8.0.3)$$

where in the last scattering amplitude we have kept track of the T and U type diagrams(They can be seen in Figure 4.11, 4.12 and 4.13).

Let's rearrange the last scattering amplitude in

$$M^{\chi}_{\chi\chi\to Z'\phi} = 2\sqrt{2} y_{DM} g_d d_\chi \chi^\dagger \bar{\sigma^\mu} \chi c_\theta [\frac{(\not{k}_1 - \not{k}_3) + m_\chi}{(k_1 - k_3)^2 - m_\chi^2} + \frac{(\not{k}_1 - \not{k}_4) + m_\chi}{(k_1 - k_4)^2 - m_\chi^2}]\frac{k_{3\mu}}{m_{Z'}} \quad (8.0.4)$$

this way we can see that even the longitudinal polarizations hold a component that is not proportional to $\sqrt{s}$.

Speaking of, we see that if we sum up the contribution coming from the longitudinal degrees of freedom of the first two scattering amplitudes they bring the result, at high energies,

$$M^{Z_L+Z'_L}_{\chi\chi\to Z'\phi} = -8m_\chi\sqrt{2}g_d^3 d^2_{\phi_j} v_{\phi_j} c_\theta d_\chi \frac{1}{s}[\frac{s^2_\theta}{m^2_Z} + \frac{c^2_\theta}{m^2_{Z'}}]\frac{1}{m_{Z'}}[\frac{S + m^2_{Z'} - m^2_\phi}{2}]\sqrt{s} \tag{8.0.5}$$

that becomes

$$M^{Z_L+Z'_T}_{\chi\chi\to Z'\phi} = -2y_{DM}\sqrt{2}g_d c_\theta d_\chi \frac{1}{m_{Z'}}\sqrt{s} \tag{8.0.6}$$

Although this contribution grows at high energies, it is perfectly balanced and destroyed by the same exact contribution coming from the χ exchange diagram which has an opposite sign.
For the transverse degrees of freedom at high energies we have:

$$M^{Z_T+Z'_T}_{\chi\chi\to Z'\phi} = 4\sqrt{2}g_d^3 d^2_{\phi_j} v_{\phi_j} c_\theta d_\chi \chi^\dagger \bar{\sigma^\mu} \chi \frac{k_{3\mu}}{m_{Z'}} \tag{8.0.7}$$

Moreover, we also need to consider the contribution coming from the dark matter exchange, precisely the part proportional to m_χ which is summarized in the formula

$$M^{\chi}_{\chi\chi\to Z'\phi} = 2\sqrt{2}y_{DM}g_d d_\chi \chi^\dagger \bar{\sigma^\mu}\chi c_\theta m_\chi [\frac{1}{(k_1-k_3)^2 - m^2_\chi} + \frac{1}{(k_1-k_4)^2 - m^2_\chi}]\frac{k_{3\mu}}{m_{Z'}}. \tag{8.0.8}$$

We can analyze the two contributions separately. Now first let's rewrite the particle momenta

$$\begin{aligned} k_1^\mu &= \frac{\sqrt{s}}{2}(1,1,0,0) \\ k_2^\mu &= \frac{\sqrt{s}}{2}(1,-1,0,0) \\ k_3^\mu &= \frac{\sqrt{s}}{2}(1,\cos\gamma,0,\sin\gamma) \\ k_4^\mu &= \frac{\sqrt{s}}{2}(1,-\cos\gamma,0,-\sin\gamma) \end{aligned} \tag{8.0.9}$$

and

$$\begin{aligned} T &= -\frac{s}{2}(1-\cos\gamma) \\ U &= -\frac{s}{2}(1+\cos\gamma) \end{aligned} \tag{8.0.10}$$

Now as happened for the $\chi\chi \to Z\phi$ case, the biggest contribution to a_0 from both these terms comes with

$$\chi^\dagger \bar{\sigma^\mu}\chi k_{3\mu} \to \frac{s}{2}\sin\gamma \tag{8.0.11}$$

Now thanks to this we can see that the T exchange term reduces to

$$M^{\chi}_{\chi\chi\to Z'\phi} = -2\sqrt{2}y_{DM}g_d d_\chi c_\theta m_\chi [\frac{\sin\gamma}{1-\cos\gamma}]\frac{1}{m_{Z'}}. \tag{8.0.12}$$

and the U term to

$$M^{\chi}_{\chi\chi\to Z'\phi} = -2\sqrt{2}y_{DM}g_d d_\chi c_\theta m_\chi [\frac{\sin\gamma}{1+\cos\gamma}]\frac{1}{m_{Z'}}. \tag{8.0.13}$$

Now in order to obtain a_0 we shall sum these up with the transverse one and we will end up, in the small angle limit with

$$a_0 = \frac{1}{64\pi}\int_0^\pi 2\sqrt{2}\frac{1}{m_{Z'}}[g_d^3 d_{\phi_j}^2 v_{\phi_j} d_\chi - y_{DM}g_d d_\chi m_\chi(\frac{1}{1-\cos\gamma}+\frac{1}{1+\cos\gamma})]\sin^2\gamma d\gamma \tag{8.0.14}$$

so

$$a_0 = \frac{2\sqrt{2}}{64}\frac{1}{m_{Z'}}[g_d^3 d_{\phi_j}^2 v_{\phi_j} d_\chi \frac{1}{2} - 2y_{DM}g_d d_\chi m_\chi] \tag{8.0.15}$$

Now we exploit the fact that $d_\phi = -2d_\chi$ to impose the bound

$$\sqrt{2}[g_d^3 d_{\phi_j}^2 v_{\phi_j} d_\phi \frac{1}{2} - 2y_{DM}g_d d_\phi m_\chi] \leq 16 m_{Z'} \tag{8.0.16}$$

which will be simplified once we remind ourselves that $m_{Z'} = \sqrt{2}g_d d_\phi v_\phi$ and that $m_\chi = y_{DM}v_\phi$

$$[g_d^2 d_{\phi_j}^2 - 4y_{DM}^2] \leq 32 \tag{8.0.17}$$

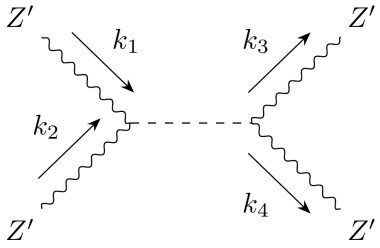

Figure 4.14: S-type process. Scalar propagator

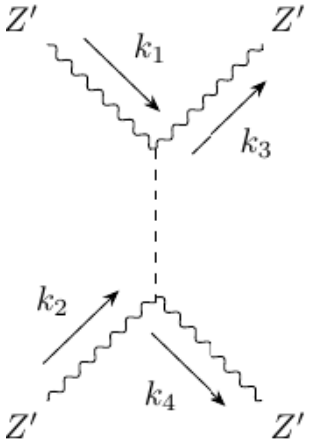

Figure 4.15: T-type process. Scalar propagator

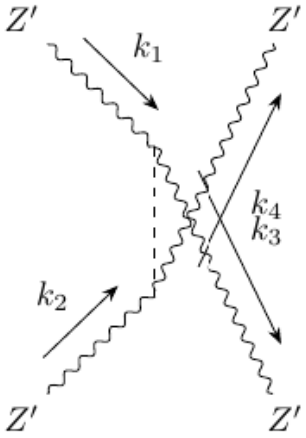

Figure 4.16: U-type process. Scalar propagator

9 $Z'Z' \to Z'Z'$

Here we can write the terms corresponding to this interaction. First we consider one dark scalar field exchange, here we have three diagrams contributing corresponding: S,T and U as they are the Mandelstam variables. We can see the Feynman diagrams in Figures 4.14, 4.15 and 4.16

$$M^{\phi}_{Z'Z'\to Z'Z'} = -4[g_d^2 d^2_{\phi_j}\sqrt{2}v_{\phi_j}c_\theta^2]^2\times \left[\frac{1}{S-m^2_{\phi_j}}(\epsilon_1\cdot\epsilon_2)(\epsilon_3\cdot\epsilon_4)+\frac{1}{T-m^2_{\phi_j}}(\epsilon_1\cdot\epsilon_3)(\epsilon_2\cdot\epsilon_4)+\frac{1}{U-m^2_{\phi_j}}(\epsilon_1\cdot\epsilon_4)(\epsilon_3\cdot\epsilon_2)\right] \tag{9.0.1}$$

to this, one must sum the terms corresponding to the Higgs boson exchange

$$M^{h}_{Z'Z'\to Z'Z'} = -4[\frac{g_w^2}{4}\sqrt{2}v_H(s_\theta - 2\frac{g_d d_H}{g_w}c_\theta)^2]^2\Big[\frac{1}{S-m_h^2}(\epsilon_1\cdot\epsilon_2)(\epsilon_3\cdot\epsilon_4)+ \frac{1}{T-m_h^2}(\epsilon_1\cdot\epsilon_3)(\epsilon_2\cdot\epsilon_4)+\frac{1}{U-m_h^2}(\epsilon_1\cdot\epsilon_4)(\epsilon_3\cdot\epsilon_2)\Big]. \tag{9.0.2}$$

The polarization vectors can be written as

$$\begin{aligned} \epsilon_1^\mu &= \frac{k_1^\mu}{m_{Z'}}+\frac{2m_{Z'}}{T-2m^2_{Z'}}k_3^\mu \qquad & \epsilon_2^\mu &= \frac{k_2^\mu}{m_{Z'}}+\frac{2m_{Z'}}{T-2m^2_{Z'}}k_4^\mu \\ \epsilon_3^\mu &= \frac{k_3^\mu}{m_{Z'}}+\frac{2m_{Z'}}{T-2m^2_{Z'}}k_1^\mu \qquad & \epsilon_4^\mu &= \frac{k_4^\mu}{m_{Z'}}+\frac{2m_{Z'}}{T-2m^2_{Z'}}k_2^\mu \end{aligned} \tag{9.0.3}$$

this ensures that $k_\mu\epsilon^\mu_\lambda = 0$.
Let's write the Mandelstam variables in a generic scattering process:

$$\begin{aligned} S &= (k_1^\mu + k_2^\mu)^2 = (k_3^\mu + k_4^\mu)^2 = 2m^2_{Z'} + 2k_1\cdot k_2 = 2m^2_{Z'} + 2k_3\cdot k_4 \\ T &= (k_1^\mu - k_3^\mu)^2 = (k_2^\mu - k_4^\mu)^2 = 2m^2_{Z'} - 2k_1\cdot k_3 = 2m^2_{Z'} - 2k_2\cdot k_4 \\ U &= (k_1^\mu - k_4^\mu)^2 = (k_2^\mu - k_3^\mu)^2 = 2m^2_{Z'} - 2k_1\cdot k_4 = 2m^2_{Z'} - 2k_2\cdot k_3 \end{aligned} \tag{9.0.4}$$

so there are also the relations

$$\begin{aligned} k_1 \cdot k_2 = k_3 \cdot k_4 &= \frac{S}{2} - m_{Z'}^2 \\ k_1 \cdot k_3 = k_2 \cdot k_4 &= m_{Z'}^2 - \frac{T}{2} \\ k_1 \cdot k_4 = k_2 \cdot k_3 &= m_{Z'}^2 - \frac{U}{2} \end{aligned} \tag{9.0.5}$$

Let's see what happens inside the brackets, in particular, we examine the case in which there is a ϕ scalar exchange, the case with Higgs will be identical apart from a change of notation

$$\begin{aligned} M^{\phi}_{Z'Z' \to Z'Z'} = -4[g_d^2 d_{\phi_j}^2 \sqrt{2} v_{\phi_j} c_\theta^2]^2 \\ \Big[\frac{1}{S - m_{\phi_j}^2}\Big(\frac{(k_1 \cdot k_2)(k_3 \cdot k_4)}{m_{Z'}^4} + \frac{2}{m_{Z'}^2(T - 2m_{Z'}^2)}(k_1 \cdot k_2 + k_3 \cdot k_4)(k_1 \cdot k_4 + k_3 \cdot k_2)\Big) + \\ \frac{1}{T - m_{\phi_j}^2}\Big(\frac{(k_1 \cdot k_3)(k_2 \cdot k_4)}{m_{Z'}^4} + \frac{2}{m_{Z'}^2(T - 2m_{Z'}^2)}(k_1 \cdot k_1 + k_2 \cdot k_2)(k_1 \cdot k_3 + k_2 \cdot k_4)\Big) + \\ \frac{1}{U - m_{\phi_j}^2}\Big(\frac{(k_1 \cdot k_4)(k_2 \cdot k_3)}{m_{Z'}^4} + \frac{2}{m_{Z'}^2(T - 2m_{Z'}^2)}(k_1 \cdot k_2 + k_3 \cdot k_4)(k_1 \cdot k_4 + k_2 \cdot k_3)\Big)\Big] \end{aligned} \tag{9.0.6}$$

Let's look separately at the contributions to that scattering amplitude and start with the leading terms:

$$\frac{1}{S - m_{\phi_j}^2}\frac{(k_1 \cdot k_2)(k_3 \cdot k_4)}{m_{Z'}^4} + \frac{1}{T - m_{\phi_j}^2}\frac{(k_1 \cdot k_3)(k_2 \cdot k_4)}{m_{Z'}^4} + \frac{1}{U - m_{\phi_j}^2}\frac{(k_1 \cdot k_4)(k_2 \cdot k_3)}{m_{Z'}^4} \tag{9.0.7}$$

and transform it into

$$\frac{1}{m_{Z'}^4}\Big[\frac{(\frac{S}{2} - m_{Z'}^2)^2}{S - m_{\phi_j}^2} + \frac{(m_{Z'}^2 - \frac{T}{2})^2}{T - m_{\phi_j}^2} + \frac{(m_{Z'}^2 - \frac{U}{2})^2}{U - m_{\phi_j}^2}\Big] \tag{9.0.8}$$

and expand what is inside the brackets so that it becomes, as an example,

$$\frac{(\frac{S}{2} - m_{Z'}^2)^2}{S - m_{\phi_j}^2} = \frac{\frac{S^2}{4} + m_{Z'}^4 - S m_{Z'}^2}{S}(1 + \frac{m_\phi^2}{S}) = \frac{S}{4} + \frac{m_\phi^2}{4} - m_{Z'}^2 \tag{9.0.9}$$

and the previous expression becomes

$$\frac{1}{m_{Z'}^4}\Big[\frac{S + T + U}{4} + 3(\frac{m_\phi^2}{4} - m_{Z'}^2)\Big] \tag{9.0.10}$$

and we know that

$$S + T + U = 4m_{Z'}^2 \tag{9.0.11}$$

so that we obtain

$$\frac{1}{m_{Z'}^4}\Big[3\frac{m_\phi^2}{4} - 2m_{Z'}^2\Big] \tag{9.0.12}$$

Now for the other terms we have

$$\begin{aligned}
&\frac{1}{S-m_{\phi_j}^2}\Big(\frac{2}{m_{Z'}^2(T-2m_{Z'}^2)}(k_1\cdot k_2+k_3\cdot k_4)(k_1\cdot k_4+k_3\cdot k_2)\Big)+\\
&\frac{1}{T-m_{\phi_j}^2}\Big(\frac{2}{m_{Z'}^2(T-2m_{Z'}^2)}(k_1\cdot k_1+k_2\cdot k_2)(k_1\cdot k_3+k_2\cdot k_4)\Big)+\\
&\frac{1}{U-m_{\phi_j}^2}\Big(\frac{2}{m_{Z'}^2(T-2m_{Z'}^2)}(k_1\cdot k_2+k_3\cdot k_4)(k_1\cdot k_4+k_2\cdot k_3)\Big)
\end{aligned} \tag{9.0.13}$$

that becomes

$$\begin{aligned}
&\frac{1}{S-m_{\phi_j}^2}\Big(\frac{2}{m_{Z'}^2(T-2m_{Z'}^2)}(S-2m_{Z'}^2)(2m_{Z'}^2-U)\Big)+\\
&\frac{1}{T-m_{\phi_j}^2}\Big(\frac{2}{m_{Z'}^2(T-2m_{Z'}^2)}(2m_{Z'}^2)(2m_{Z'}^2-T)\Big)+\\
&\frac{1}{U-m_{\phi_j}^2}\Big(\frac{2}{m_{Z'}^2(T-2m_{Z'}^2)}(S-2m_{Z'}^2)(2m_{Z'}^2-U)\Big)
\end{aligned} \tag{9.0.14}$$

so this becomes

$$\begin{aligned}
&\frac{1}{m_{Z'}^2(T-m_{\phi_j}^2)}\Big(\frac{2}{(S-2m_{Z'}^2)}(-US)\Big)+\\
&\frac{1}{m_{Z'}^2(T-m_{\phi_j}^2)}\Big(\frac{2}{(T-2m_{Z'}^2)}-T2m_{Z'}^2)\Big)+\\
&\frac{1}{m_{Z'}^2(T-m_{\phi_j}^2)}\Big(\frac{2}{(U-2m_{Z'}^2)}(-US)\Big)
\end{aligned} \tag{9.0.15}$$

so what survives is

$$\frac{2}{m_{Z'}^2(T-m_{\phi_j}^2)}\Big(-U-S\Big)=\frac{2}{m_{Z'}^2(T-m_{\phi_j}^2)}\Big(-4m_{Z'}^2+T\Big)=\frac{2}{m_{Z'}^2} \tag{9.0.16}$$

So if we consider both of them we will gather a factor of

$$\frac{3m_\phi^2}{4m_{Z'}^4} \tag{9.0.17}$$

Now as we enter the small angle approximation we can get rid of the scattering amplitude coming from the Higgs boson exchange as it is proportional to d_H and consequently to $\tan 2\theta$ that, as stated, will reach 0. We will only keep the term originating from the dark scalar exchange as

$$a_0=-\frac{1}{32\pi}[g_d^2 d_{\phi_j}^2\sqrt{2}v_{\phi_j}]^2\frac{3m_\phi^2}{m_{Z'}^4}=-\frac{1}{32\pi}\frac{3m_\phi^2}{v_\phi^2} \tag{9.0.18}$$

10 $Z'\phi \to Z'\phi$

For this process, we have again three contributions like the previous ones

$$M^{Z}_{Z'\phi\to Z'\phi} = -4[\sqrt{2}g_d^2 d^2_{\phi_j} v_{\phi_j}]^2 s_\theta^2 c_\theta^2 \Big[\frac{1}{S-m_Z^2}[-\epsilon_1\cdot\epsilon_3 + \frac{(k_1+k_2)_\mu (k_1+k_2)_\nu}{m_Z^2}\epsilon_1^\mu \epsilon_3^\nu] + \frac{1}{T-m_Z^2}[-\epsilon_1\cdot\epsilon_3 + \frac{(k_1-k_3)_\mu (k_1-k_3)_\nu}{m_Z^2}\epsilon_1^\mu \epsilon_3^\nu] + \frac{1}{U-m_Z^2}[-\epsilon_1\cdot\epsilon_3 + \frac{(k_1-k_4)_\mu (k_1-k_4)_\nu}{m_Z^2}\epsilon_1^\mu \epsilon_3^\nu]\Big] \tag{10.0.1}$$

$$M^{Z'}_{Z'\phi\to Z'\phi} = -4[\sqrt{2}g_d^2 d^2_{\phi_j} v_{\phi_j}]^2 c_\theta^4 \Big[\frac{1}{S-m_{Z'}^2}[-\epsilon_1\cdot\epsilon_3 + \frac{(k_1+k_2)_\mu (k_1+k_2)_\nu}{m_{Z'}^2}\epsilon_1^\mu \epsilon_3^\nu] + \frac{1}{T-m_{Z'}^2}[-\epsilon_1\cdot\epsilon_3 + \frac{(k_1-k_3)_\mu (k_1-k_3)_\nu}{m_{Z'}^2}\epsilon_1^\mu \epsilon_3^\nu] + \frac{1}{U-m_{Z'}^2}[-\epsilon_1\cdot\epsilon_3 + \frac{(k_1-k_4)_\mu (k_1-k_4)_\nu}{m_{Z'}^2}\epsilon_1^\mu \epsilon_3^\nu]\Big] \tag{10.0.2}$$

finally the vertex contribution

$$M_{Z'\phi\to Z'\phi} = 4g_d^2 d^2_{\phi_j} c_\theta^2 \epsilon_1\cdot\epsilon_3 \tag{10.0.3}$$

they all can be seen in Figures 4.17,4.18,4.19 and 4.20 here we can use

$$\begin{aligned}\epsilon_1^\mu &= \frac{k_1^\mu}{m_{Z'}} + \frac{2m_{Z'}}{T-2m_{Z'}^2}k_3^\mu \\ \epsilon_3^\mu &= \frac{k_3^\mu}{m_{Z'}} + \frac{2m_{Z'}}{T-2m_{Z'}^2}k_1^\mu\end{aligned} \tag{10.0.4}$$

and

$$\begin{aligned} S = (k_1^\mu + k_2^\mu)^2 = (k_3^\mu + k_4^\mu)^2 = m_{Z'}^2 + m_\phi^2 + 2k_1\cdot k_2 = m_{Z'}^2 + m_\phi^2 + 2k_3\cdot k_4 \\ T = (k_1^\mu - k_3^\mu)^2 = (k_2^\mu - k_4^\mu)^2 = 2m_{Z'}^2 - 2k_1\cdot k_3 = 2m_\phi^2 - 2k_2\cdot k_4 \\ U = (k_1^\mu - k_4^\mu)^2 = (k_2^\mu - k_3^\mu)^2 = m_{Z'}^2 + m_\phi^2 - 2k_1\cdot k_4 = m_{Z'}^2 + m_\phi^2 - 2k_2\cdot k_3 \end{aligned} \tag{10.0.5}$$

Now we can analyze the full contribution coming from the longitudinal part of the bosonic propagator. Indeed we can see that, aligned with what we have already seen, the moment we consider the longitudinal part of the bosonic propagator in the first two amplitudes, and in particular the leading terms, it will appear an anomalous behavior at high energies that will be completely destroyed by the vertex contribution.

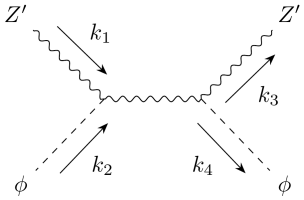

Figure 4.17:
S-type process.
Scalar propagator

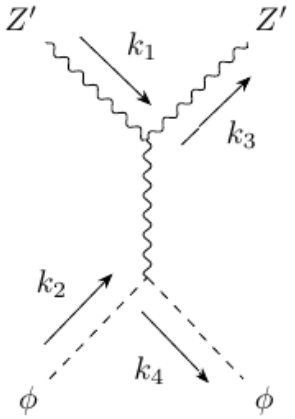

Figure 4.18:
T-type process.
Scalar propagator

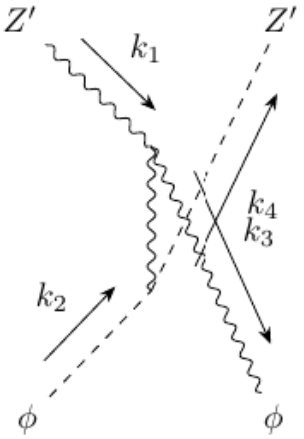

Figure 4.19:
U-type process.
Scalar propagator

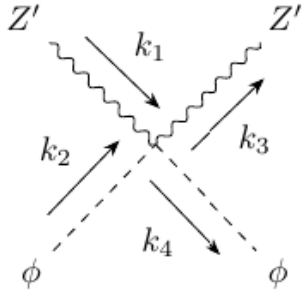

Figure 4.20:
Vertex diagram.

We can analyze this by writing the sum of the leading contributions of the first two scattering amplitudes

$$\begin{aligned} M^{Z_L+Z'_L}_{Z'\phi\to Z'\phi} = -4[\sqrt{2}g_d^2 d^2_{\phi_j} v_{\phi_j}]^2 \frac{1}{m^2_{Z'}} c^2_\theta \Big[\\ (k_1\cdot k_1 + k_2\cdot k_1)(k_1\cdot k_3 + k_2\cdot k_3)[\frac{s^2_\theta}{m^2_Z(S-m^2_Z)} + \frac{c^2_\theta}{m^2_{Z'}(S-m^2_{Z'})}] \\ (k_1\cdot k_1 - k_3\cdot k_1)(k_1\cdot k_3 - k_3\cdot k_3)[\frac{s^2_\theta}{m^2_Z(T-m^2_Z)} + \frac{c^2_\theta}{m^2_{Z'}(T-m^2_{Z'})}] \\ (k_1\cdot k_1 - k_4\cdot k_1)(k_1\cdot k_3 - k_4\cdot k_3)[\frac{s^2_\theta}{m^2_Z(U-m^2_Z)} + \frac{c^2_\theta}{m^2_{Z'}(U-m^2_{Z'})}]\Big] \end{aligned} \tag{10.0.6}$$

Here we can use the series expansion that brings, for example,

$$\frac{1}{S-m^2_Z} = \frac{1}{S}(1+\frac{m^2_Z}{S}) \tag{10.0.7}$$

together with the equations that relate the scalar product of momenta to Mandelstam's variables.

Moreover, we can exploit the fact that

$$S+T+U = 2m^2_{Z'} + 2m^2_\phi. \tag{10.0.8}$$

We also make use of the fact that

$$2g_d^2 d^2_{\phi_j} v^2_{\phi_j}[\frac{s^2_\theta}{m^2_Z} + \frac{c^2_\theta}{m^2_{Z'}}] = 1 \tag{10.0.9}$$

and keep in mind that in the small angle approximation we have $m_{Z'} = \sqrt{2}g_d d_\phi v_\phi$ so the whole contribution, in the small angle approximation. This calculation has been made by employing Mathematica.

The vertex contribution is

$$M_{\phi Z'\to\phi Z'} = 4g_d^2 d^2_{\phi_j} c^2_\theta \epsilon_1\cdot\epsilon_3 = 4g_d^2 d^2_{\phi_j}\frac{k_1\cdot k_3}{m^2_{Z'}} = 4g_d^2 d^2_{\phi_j}\frac{2m^2_{Z'}-T}{2m^2_{Z'}} \tag{10.0.10}$$

so summing the two we obtain

$$M^{Long}_{\phi Z'\to\phi Z'} = -g_d^2 d^2_{\phi_j}\frac{1}{m^2_{Z'}}[-3m^2_{Z'} - \frac{m^2_\phi}{2} - \frac{m^2_{Z'}T^2}{U(T+U)}] \tag{10.0.11}$$

Now including the subleading contributions this becomes

$$M^{Long}_{\phi Z'\to\phi Z'} = -g_d^2 d^2_{\phi_j}\frac{1}{m^2_{Z'}}[-m^2_{Z'} - \frac{m^2_\phi}{2}] \tag{10.0.12}$$

Now in order to calculate a_0 we put all contributions together

$$a_0 = \frac{1}{64\pi}\int_0^\pi d\theta \sin\theta\Big(g_d^2 d_{\phi_j}^2 \frac{1}{m_{Z'}^2}[m_{Z'}^2 + \frac{m_\phi^2}{2}]\Big) \tag{10.0.13}$$

and this gives

$$a_0 = \frac{1}{64\pi v_\phi^2}[m_{Z'}^2 + \frac{m_\phi^2}{2}] \tag{10.0.14}$$

11 $\phi\phi \to Z'Z'$

This process employs the same math as the previous, except for the polarization vectors employed. Here we have

$$\begin{aligned}\epsilon_3^\mu &= \frac{k_3^\mu}{m_{Z'}} + \frac{2m_{Z'}}{T - m_{Z'}^2 - m_\phi^2} k_1^\mu \\ \epsilon_4^\mu &= \frac{k_4^\mu}{m_{Z'}} + \frac{2m_{Z'}}{T - m_{Z'}^2 - m_\phi^2} k_2^\mu\end{aligned} \tag{11.0.1}$$

$$\begin{aligned}S = (k_1^\mu + k_2^\mu)^2 = (k_3^\mu + k_4^\mu)^2 = 2m_\phi^2 + 2k_1 \cdot k_2 = 2m_{Z'}^2 + 2k_3 \cdot k_4 \\ T = (k_1^\mu - k_3^\mu)^2 = (k_2^\mu - k_4^\mu)^2 = m_{Z'}^2 + m_\phi^2 - 2k_1 \cdot k_3 = m_{Z'}^2 + m_\phi^2 - 2k_2 \cdot k_4 \\ U = (k_1^\mu - k_4^\mu)^2 = (k_2^\mu - k_3^\mu)^2 = m_{Z'}^2 + m_\phi^2 - 2k_1 \cdot k_4 = m_{Z'}^2 + m_\phi^2 - 2k_2 \cdot k_3.\end{aligned} \tag{11.0.2}$$

The amplitudes here are the same of the previous one except for the polarization vectors that have to be adjusted to the new scenario

$$\begin{aligned}M^Z_{\phi\phi\to Z'Z'} = -4[\sqrt{2} g_d^2 d_{\phi_j}^2 v_{\phi_j}]^2 s_\theta^2 c_\theta^2 \Big[&\frac{1}{S - m_Z^2}[-\epsilon_3 \cdot \epsilon_4 + \frac{(k_1 + k_2)_\mu (k_1 + k_2)_\nu}{m_Z^2} \epsilon_3^\mu \epsilon_4^\nu] + \\ &\frac{1}{T - m_Z^2}[-\epsilon_3 \cdot \epsilon_4 + \frac{(k_1 - k_3)_\mu (k_1 - k_3)_\nu}{m_Z^2} \epsilon_3^\mu \epsilon_4^\nu] + \\ &\frac{1}{U - m_Z^2}[-\epsilon_3 \cdot \epsilon_4 + \frac{(k_1 - k_4)_\mu (k_1 - k_4)_\nu}{m_Z^2} \epsilon_3^\mu \epsilon_4^\nu] \Big]\end{aligned} \tag{11.0.3}$$

$$\begin{aligned}M^{Z'}_{\phi\phi\to Z'Z'} = -4[\sqrt{2} g_d^2 d_{\phi_j}^2 v_{\phi_j}]^2 c_\theta^4 \Big[&\frac{1}{S - m_{Z'}^2}[-\epsilon_3 \cdot \epsilon_4 + \frac{(k_1 + k_2)_\mu (k_1 + k_2)_\nu}{m_{Z'}^2} \epsilon_3^\mu \epsilon_4^\nu] + \\ &\frac{1}{T - m_{Z'}^2}[-\epsilon_3 \cdot \epsilon_4 + \frac{(k_1 - k_3)_\mu (k_1 - k_3)_\nu}{m_{Z'}^2} \epsilon_3^\mu \epsilon_4^\nu] + \\ &\frac{1}{U - m_{Z'}^2}[-\epsilon_3 \cdot \epsilon_4 + \frac{(k_1 - k_4)_\mu (k_1 - k_4)_\nu}{m_{Z'}^2} \epsilon_3^\mu \epsilon_4^\nu] \Big]\end{aligned} \tag{11.0.4}$$

finally the vertex contribution

$$M_{\phi\phi\to Z'Z'} = 4 g_d^2 d_{\phi_j}^2 c_\theta^2 \epsilon_3 \cdot \epsilon_4 \tag{11.0.5}$$

Again let's take the leading contribution from the longitudinal part of the propagator

$$
\begin{aligned}
M^{Z_L+Z'_L}_{\phi\phi\to Z'Z'} = -4[\sqrt{2}g_d^2 d^2_{\phi_j} v_{\phi_j}]^2 \frac{1}{m^2_{Z'}} c^2_\theta \Big[\\
(k_1\cdot k_3 + k_2\cdot k_3)(k_1\cdot k_4 + k_2\cdot k_4)[\frac{s^2_\theta}{m^2_Z(S-m^2_Z)} + \frac{c^2_\theta}{m^2_{Z'}(S-m^2_{Z'})}] \\
(k_1\cdot k_3 - k_3\cdot k_3)(k_1\cdot k_4 - k_3\cdot k_4)[\frac{s^2_\theta}{m^2_Z(T-m^2_Z)} + \frac{c^2_\theta}{m^2_{Z'}(T-m^2_{Z'})}] \\
(k_1\cdot k_3 - k_4\cdot k_3)(k_1\cdot k_4 - k_4\cdot k_4)[\frac{s^2_\theta}{m^2_Z(U-m^2_Z)} + \frac{c^2_\theta}{m^2_{Z'}(U-m^2_{Z'})}]\Big]
\end{aligned}
\tag{11.0.6}
$$

by making use of

$$
\frac{1}{S-m^2_Z} = \frac{1}{S}(1+\frac{m^2_Z}{S}) \tag{11.0.7}
$$

together with the equations that relate the scalar product of momenta to Mandelstam's variables:

Now the exact counterpart from the vertex contribution is

$$
M_{\phi\phi\to Z'Z'} = 4g_d^2 d^2_{\phi_j} c^2_\theta \epsilon_3\cdot\epsilon_4 = 4g_d^2 d^2_{\phi_j}\frac{k_3\cdot k_4}{m^2_{Z'}} = 4g_d^2 d^2_{\phi_j}\frac{S-2m^2_{Z'}}{2m^2_{Z'}} \tag{11.0.8}
$$

so summing the two we obtain

$$
\begin{aligned}
M^{Long}_{\phi\phi\to Z'Z'} = -g_d^2 d^2_{\phi_j}\frac{1}{m^2_{Z'}}[\frac{m^2_\phi}{2} - m^2_{Z'} + \frac{m^4_\phi + m^2_\phi m^2_{Z'} - m_{Z'}U}{T} + \frac{m^4_\phi + m^2_\phi m^2_{Z'} - m_{Z'}T}{U} + \\
\frac{4m^4_\phi m^2_{Z'} + 8m^2_\phi m^2_{Z'} + 4m^6_{Z'}}{TU}]
\end{aligned}
\tag{11.0.9}
$$

Now let's consider the subleading terms too to gain the expression

$$
M^{Long}_{\phi\phi\to Z'Z'} = g_d^2 d^2_{\phi_j}\frac{1}{m^2_{Z'}}[\frac{m^2_\phi}{2} + m^2_{Z'}] \tag{11.0.10}
$$

All in all, summing all the contributions that we have gathered we obtain

$$
a_0 = \frac{1}{64\pi}\frac{[\frac{m^2_\phi}{2} + m^2_{Z'}]}{v^2_\phi} \tag{11.0.11}
$$

12 Scattering matrix

After all the calculations we end up with the bosonic scattering matrix with the basis $(\frac{\phi\phi}{\sqrt{2}}, \frac{Z'Z'}{\sqrt{2}}, Z'\phi)$ of

$$a_0 = -\frac{m_\phi^2}{64\pi v_\phi^2}\begin{pmatrix} 3 & [1+\frac{2m_{Z'}^2}{m_\phi^2}] & 0 \\ [1+\frac{2m_{Z'}^2}{m_\phi^2}] & 3 & 0 \\ 0 & 0 & -[1+\frac{2m_{Z'}^2}{m_\phi^2}] \end{pmatrix} \tag{12.0.1}$$

13 Benchmark model

Now we set up a benchmark model on the basis of our analysis on unitarity and the one, carried out but now reported here on anomalies. First of all, we add to the SM lagrangian with the notation we have conventionally adopted, three fermion singlets all with $d_{\chi_i} = 1$. There is a number of ways we can originate their mass, but as we have already seen in previous articles, the best one and the most natural and dynamic is through a Majorana mass term coming from a Yukawa interaction with the dark scalars of the theory. Then as we know it is the lightest one among those to rise as a dark matter candidate. SM particles can be chosen to have dark charges $\{d_Q, d_u, d_d, d_L, d_e, d_H\} = \{0, 1, -1, 0, -1, -1\}$ thus making the term $Lh\chi$ renormalizable. This will require us to employ a Z_2 symmetry to keep the dark matter stable. We study only the mass region in which $m_{Z'} > m_\chi \geq 100\ GeV$ and can assume that DM particles only annihilate to SM final particles. The point is here that annihilations to SM fermions are p-wave for a massive Majorana dark matter. This means that the channel Zh can be the leading one in production.
Moreover one can calculate that the Z' exchange diagram has an s-wave cross section. This does not have to confuse us as we have proved that the Z exchange diagram must be absolutely considered to restore unitarity. What happens is a beautiful destructive interference between the two diagrams that leaves the overall cross section p-wave suppressed. This is another perk of our model. One more at it, it can be seen that the only Z' diagram would lead to an inferior relic abundance with respect to the combination of both diagrams. This is another clue that we have to use both processes. Another subtle advantage of the p-wave suppression of DM annihilation to Zh is that this detail makes the whole indirective search argument as ineffective.
If we set $m_\chi = 300\ GeV$ we can also clear the parameter space in the $(m_{Z'}, g_d)$ plane of the unallowed regions. The first thing to do is to cancel the regions where gauge coupling is non-perturbative of course. Then erase the regions where unitarity is broken. The following step is to clear the plane from the region where the mediator width has a size comparable to its mass.
Now reflect on the fact that we have chosen all couplings to SM and DM as universal because of all of the reasons we have outlined previously in the third chapter. This leads to the awareness that the searches for dark matter at LHC will involve a diverse array of complementary decay channels. We know that dilepton constraints are the strongest ones except for the case of a huge mediator mass ($m_{Z'} > 4\ TeV$) where EWPT bounds dominate. So outside this region, we can see that because of the diversity and multiplicity of decay channels, Z' can offer a wide resonance even in the case of perturbative coupling. In the region with $\Gamma_{Z'}$ over 30% of Z' mass dilepton constraints are not effective, so it is necessary to consider other channels like Zh.
We are also in possession of direct detection constraints coming from PandaX-II and PICO that offer similar constraints.

It is important to notice that the region where DM is originated by the standard freeze-out procedure is excluded, but there is a number of alternatives we can explore that are motivated by non-standard cosmology. Another option would be to enhance the dark sector to implement additional annihilation channels.

Chapter 5

Conclusions

As we reach the end of our journey through the mysteries of dark matter it can be helpful to look back at the different stages of our quest as they unfold in front of us revealing the path we have traveled. In the first chapter, we have got to know dark matter since the theorization and we have been able to study deep in detail its influence through different scales. Straight from the get-go I personally reckon this chapter to be crucial in getting the reader acquainted with the style of approach to this as elusive and intriguing enigma. In fact in the second part of the chapter, guilty of our ignorance, we stumbled towards comprehension by cornering dark matter and trying to identify what it *cannot* be. Playing like toddlers, we indeed made some progress towards awareness reaching concrete bounds on properties of dark matter like its mass or stability that definitely helped shape, in a decisive way, our perceptions on this incredibly complex subject.

As a natural consequence of our train of thoughts, we sought a way of conceiving a theory of dark matter that could check all the boxes listed previously. We were capable to discern between hot and cold dark matter and, for the latter, introducing the Boltzmann equation in order to find a relic density that could fit the experimental data. As our first crack at dark matter particle composition, we introduced the framework of Weakly Interacting Massive Particles or WIMPs as they can "miraculously" oblige us with the relic density calculation. Again as a result of our questioning a way to bring to light the truth, we glanced at the modern experimental programs that would help us solve the arcane. Indeed we have touched on the three main experimental areas investigated in present times. The reader has seen how complex and diverse is the experimental scene, but at the same time how these different experimental programs can work together as a sort of symbiosis. In fact, the conclusive part of the chapter shows the synergy of the different procedures that strive towards a breakthrough on the subject and the complementarity of the searches as they can actually serve the scope only when all together consulted in the analysis of a particular model.

The next stage consisted in trying to grasp, at particle level, the actual composition of dark matter. In actuality, the beginning of the chapter is a summary of properties shared by all the models unified by the same motif, which is the presence of a new vector boson

that we have called Z', which constitutes the bridge between Standard Model and dark sector. Indeed here the reader can get acquainted with the mathematics behind all the models that share this peculiar feature. In fact, we have outlined all the common traits of these models and there has been a thorough explanation of how they can be built bearing in mind our intention of building one ourselves. With the Z' physics behind, the major part of this chapter revolves around the concept of anomaly-free dark matter models. Indeed the theme of the chapter here was the search for a general algorithm to generate a solution to the anomaly equations. This is a powerful concept that has been vastly explored in the chapter and constitutes one of the requirements for a model to be consistent. With that being clear, we proceeded on our quest by studying three simplified models of dark matter, each of which possesses a single peculiar characteristic that would help blend the central theme with different and modern questions of particle physics.

Finally, the fourth chapter is the very heart of this master thesis. Unitarity takes over the scene here as we have carefully laid the ground for this as simple as crucial property of the scattering matrix. After an initial dissertation on this peculiar feature followed the section in which we derived important inequalities that all scattering matrices have to satisfy and that originate from unitarity. It is amazing to think that by just using this simple and generic tool, we have been able to draw conclusions on our dark matter model and reach bounds that had not been explored before.
As an *appetizer*, a toy model has been studied with just one dark matter particle, one new vector boson Z' plus a dark scalar enabling us to create mass for the dark sector. Indeed unitarity has been very helpful here in letting us reach bounds first for the new dark scalar mass and then constrain the mass of the vector boson Z'.

The following section is the original part and consists of the setup of a new model, the most general one, with which we do not apply limitations on the particle content of the theory. The lagrangian we have built keeps track of all the possible particles that can be embedded in such an extension of the Standard Model. After the rules of the game were completely set we were free to scrutinize the totality of the processes of scattering that could stem from the particles involved in the model. This study has led to important conclusions on the model we have built. Indeed what we have created is, first and foremost, consistent as far as unitarity goes. This has to be intended in the sense that whatever scattering process one considers, the model shows no breaks when high energies come to play. What can be observed is that in each process considered the different Feynman diagrams, although singularly divergent at high energies, interfere destructively with one another leading to the perfect destruction of all the divergencies. This manifests the importance to consider all the pieces of the puzzle, especially in light of relic density calculation as we have had the pleasure to appreciate in processes such as $\chi\chi \to Zh$. The natural conclusion to the analysis was, of course, the derivation of unitarity bounds from all of the processes considered. The novelty brought here is that the model considered has been developed from scratch and there are no previous records of the results found during the process of analysis. Indeed, just to make some example, processes like $Z'Z' \to Z'Z'$ offer some interesting constraints on the new vector boson mass. Moreover if one considers the scattering $Z'\phi \to Z'\phi$ will realize the constraint present in the combination of the new

vector boson and dark scalar masses.
Taking everything into account we can confidently state that we have reached the main purpose of this master thesis, which was to thoroughly study and analyze dark matter theories with a new vector portal. During our journey we have dug into the subject as deeply as we could and, in the end, we have formulated a model that could be consistent with unitarity claims and looked at all scattering processes that could stem from it. During our investigations we also stumbled upon new limits and constraints on dark matter features, so we are fairly satisfied with that. We humbly thank the reader that has been sticking with us until now and hope that this thesis has shed some light on such an intriguing mystery that is dark matter.

Appendix A

Details on the calculation

In this section, we are going to explain the details of chapter 4, in particular, to explain what we have used to draw the conclusions and see why the high energy behavior of our theory is safe when we employ the Z exchange diagram together with the Z' one. We go straight for what we aim for and start talking about the flavor basis mass matrix. Here we have three masses to consider

$$\begin{aligned} m^2_{Z_F} &= \frac{g_w^2}{2} v_H^2 \\ m^2_{Z'_F} &= 2g_d^2(d_h^2 v_H^2 + v_\phi^2) \\ m_{ZZ'} &= -g_d g_w d_H v_H^2 \end{aligned} \tag{0.0.1}$$

where $m_{ZZ'}$ is the mass term originating from the mixing term between Z and Z' coming from the covariant derivative. Now we can see that the mass matrix term is

$$M^2 = \begin{pmatrix} m^2_{Z_F} & m_{ZZ'} \\ m_{ZZ'} & m^2_{Z'_F} \end{pmatrix} = \begin{pmatrix} a & c \\ c & b \end{pmatrix}. \tag{0.0.2}$$

Now, this mass matrix can be diagonalized through an orthogonal matrix. Thus we pass to the mass basis by diagonalization employing

$$\begin{pmatrix} c_\theta & s_\theta \\ -s_\theta & c_\theta \end{pmatrix}. \tag{0.0.3}$$

And obtain

$$M^2_m = \begin{pmatrix} m^2_Z & 0 \\ 0 & m^2_{Z'} \end{pmatrix}. \tag{0.0.4}$$

In order to obtain a diagonal matrix the rule imposes that

$$\tan 2\theta = \frac{2c}{b-a} \tag{0.0.5}$$

thus obtaining what we saw in Chapter 4. We can work out the formulas

$$s_{2\theta} = \frac{2c}{\sqrt{(b-a)^2 + 4c^2}} \tag{0.0.6}$$

and

$$c_{2\theta} = \frac{b-a}{\sqrt{(b-a)^2+4c^2}} \tag{0.0.7}$$

and finally get

$$m_Z^2 = ac_\theta^2 - 2cs_\theta c_\theta + bs_\theta^2 \tag{0.0.8}$$

and

$$m_{Z'}^2 = as_\theta^2 + 2cs_\theta c_\theta + bc_\theta^2. \tag{0.0.9}$$

Now we have to prove that for

$$M_{\chi\chi\to Z_L h} \propto [\frac{s_\theta}{m_Z^2}(c_\theta + \frac{2g_d d_H}{g_w}s_\theta) + \frac{c_\theta}{m_{Z'}^2}(\frac{2g_d d_H}{g_w}c_\theta - s_\theta)]\sqrt{s} \tag{0.0.10}$$

the term inside the squared brackets vanishes or rearranging

$$s_\theta m_{Z'}^2(c_\theta + \frac{2g_d d_H}{g_w}s_\theta) + c_\theta m_Z^2(\frac{2g_d d_H}{g_w}c_\theta - s_\theta) = 0 \tag{0.0.11}$$

Let's substitute the expression for m_Z^2 and $m_{Z'}^2$ and see that

$$-c(s_\theta^4 + c_\theta^4) + (b - a + \frac{2c^2}{a})s_\theta c_\theta(c_\theta^2 - s_\theta^2) + ss_\theta^2 c_\theta^2(2c - \frac{bc}{a}) = 0 \tag{0.0.12}$$

Now we use first

$$c_\theta^4 + s_\theta^4 = 1 - \frac{s_{2\theta}^2}{2} \tag{0.0.13}$$

and then the expressions that we wrote for $s_{2\theta}$ and $c_{2\theta}$ to obtain

$$-c((b-a)^2 + 4c^2) + 2c^3 + c(b-a)(b - a + \frac{2c^2}{a}) + (2c - \frac{bc}{a})2c^2 \tag{0.0.14}$$

This vanishes after the arithmetics are done. So this proves that the two diagrams perfectly interfere destructively. This is how unitarity is restored and the bad high energy trend is erased.

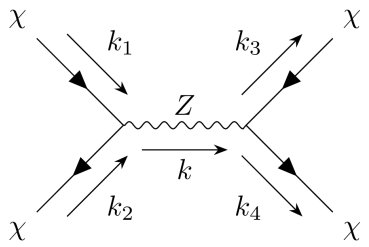

Figure A.1: S-type process. Vector boson propagator

Here in the following, we are going to analyze completely all the possible scattering processes drawn from the Lagrangian from sec. 5 of the fourth chapter. The following process can be summarized by the diagram in the figure.

In the picture, we can see two fermionic lines that represent the initial and final states, connected by a bosonic propagator whose role will be played either by Z or by Z'.

1 $\chi\chi \to \bar{f}_L f_L$

Here there are two contributions too, corresponding to the Z and Z' exchanges. The scattering amplitudes are

$$\begin{aligned} M^{Z}_{\chi\chi\to\bar{f}_L f_L} &= g_d^2 d_\chi d_f s_\theta^2 \chi^\dagger \bar{\sigma^\mu} \chi \frac{1}{s - m_Z^2}[-g_{\mu\nu} + \frac{k_\mu k_\nu}{m_Z^2}]\bar{f}_L \gamma_\mu f_L \\ M^{Z'}_{\chi\chi\to\bar{f}_L f_L} &= g_d^2 d_\chi d_f c_\theta^2 \chi^\dagger \bar{\sigma^\mu} \chi \frac{1}{s - m_{Z'}^2}[-g_{\mu\nu} + \frac{k_\mu k_\nu}{m_{Z'}^2}]\bar{f}_L \gamma_\mu f_L \end{aligned} \tag{1.0.1}$$

we do not see anomalous behaviors at high energies because

$$\begin{aligned} \chi^\dagger \bar{\sigma^\mu} \chi k_\mu &\to -2 m_\chi \chi^\dagger \bar{\sigma^\mu} \chi \\ \bar{f}_L \gamma^\mu f_L k_\mu &\to -2 m_{f_L} \bar{f}_L \gamma^\mu f_L k_\mu \end{aligned} \tag{1.0.2}$$

so this is alright because $\chi^\dagger \bar{\sigma^\mu} \chi \to \sqrt{s}$ and $\bar{f}_L \gamma^\mu f_L \to \sqrt{s}$ at high energy. Now summing the contributions from the transverse degrees of freedom we obtain

$$M^{Z_T + Z'_T}_{\chi\chi\to\bar{f}_L f_L} = -g_d^2 d_\chi d_f \chi^\dagger \bar{\sigma^\mu} \chi \frac{1}{s} \bar{f}_L \gamma^\mu f_L \tag{1.0.3}$$

that becomes

$$M^{Z_T + Z'_T}_{\chi\chi\to\bar{f}_L f_L} = -g_d^2 d_\chi d_f \tag{1.0.4}$$

so

$$a_0 = -\frac{1}{32\pi} \int_0^\pi d\theta \sin\theta g_d^2 d_\chi d_f = -\frac{1}{16\pi} g_d^2 d_\chi d_f \tag{1.0.5}$$

so for the unitarity bound

$$g_d \leq \sqrt{\frac{8\pi}{d_\chi d_f}} \tag{1.0.6}$$

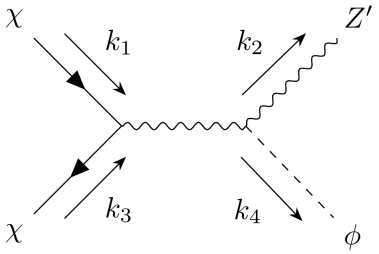

Figure A.2: S-type process

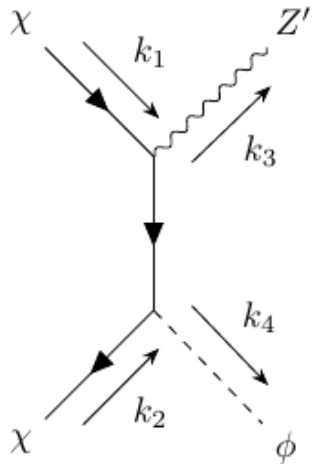

Figure A.3: T-type process

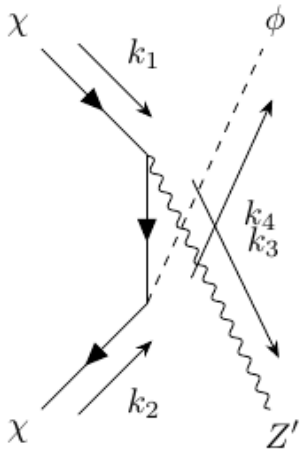

Figure A.4: U-type process

Now the next three sections share the same diagrams

Figure A.2 is a diagram that really all the processes share and represents an exchange of a vector boson which will be either Z or Z' connecting the initial fermionic state with the final one in which a vector boson and a scalar will be present.
The diagrams in Figure A.3 and Figure A.4 will not be a part of the process $\chi\chi \to Z'h$ and will represent respectively the T and U type diagrams where the propagator is exclusively fermionic and more precisely dark matter.

2 $\chi\chi \to Z\phi$

Here we can see that there are three diagrams contributing to the process and are of the same type of the previous scattering. This is why we are going to jump straight into scattering amplitudes right from the bat. First, we will consider the case with one dark scalar field, which will be simpler as far as calculations go. Processes with more fields ϕ will be a generalization of the ones we will look at. So as we have said, let's look at the scattering amplitudes for the three processes

$$\begin{aligned} M^{Z}_{\chi\chi\to Z\phi} &= 2g_d d_\chi \chi^\dagger \bar{\sigma^\mu} \chi s_\theta g_d^2 2\sqrt{2} d^2_{\phi_j} v_{\phi_j} s^2_\theta \frac{1}{s - m_Z^2}[-g_{\mu\nu} + \frac{k_\mu k_\nu}{m_Z^2}]\frac{k_3^\nu}{m_Z} \\ M^{Z'}_{\chi\chi\to Z\phi} &= 2g_d d_\chi \chi^\dagger \bar{\sigma^\mu} \chi c_\theta g_d^2 2\sqrt{2} d^2_{\phi_j} v_{\phi_j} s_\theta c_\theta \frac{1}{s - m_Z^2}[-g_{\mu\nu} + \frac{k_\mu k_\nu}{m_Z^2}]\frac{k_3^\nu}{m_Z} \\ M^{\chi}_{\chi\chi\to Z\phi} &= -\sqrt{2} y_{DM} g_d d_\chi \chi^\dagger \bar{\sigma^\mu} \chi s_\theta [\frac{1}{(\not{k}_1 - \not{k}_3) - m_\chi} + \frac{1}{(\not{k}_1 - \not{k}_4) - m_\chi}]\frac{k_{3\mu}}{m_{Z'}} \end{aligned} \tag{2.0.1}$$

where we have considered for simplicity only one scalar field that we have named ϕ_j. As we have stated previously, for more than one dark scalar field involved in the theory we just generalize the amplitudes by summing on j which will now become a variable representing the number of scalar fields. Anyways first we have to examine how these amplitudes behave at high energies, this is why for the first two we will consider only the longitudinal degrees of freedom, which will be growing proportional with energy. We should remember that

$$\chi^\dagger \bar{\sigma^\mu} \chi k_\mu \to -2 m_\chi \chi^\dagger \bar{\sigma^\mu} \chi \tag{2.0.2}$$

and sum the first two amplitudes at high energies, which will become

$$M^{Z_L + Z'_L}_{\chi\chi\to Z\phi} = 2m_\chi g_d d_\chi \chi^\dagger \bar{\sigma^\mu} \chi s_\theta g_d^2 2\sqrt{2} d^2_{\phi_j} v_{\phi_j} [\frac{s^2_\theta}{m_Z^2} + \frac{c^2_\theta}{m_{Z'}^2}]\frac{p^\nu}{m_Z} k_\nu \tag{2.0.3}$$

now

$$k_3^\nu k_\nu \to \frac{s}{2} \tag{2.0.4}$$

and we know that $\chi^\dagger \bar{\sigma^\mu} \chi \to \sqrt{s}$ so now at high energies we have

$$M^{Z_L + Z'_L}_{\chi\chi\to Z\phi} = m_\chi g_d d_\chi s_\theta g_d^2 2\sqrt{2} d^2_{\phi_j} v_{\phi_j} [\frac{s^2_\theta}{m_Z^2} + \frac{c^2_\theta}{m_{Z'}^2}]\frac{1}{m_Z}\sqrt{s}. \tag{2.0.5}$$

Now one can see that at high energies this grows and threatens to break unitarity. If we go on with our calculation here for a scalar field

$$m_\chi = y_{DM} v_{\phi_j} \tag{2.0.6}$$

and one can show that

$$2 g_d^2 d^2_{\phi_j} v^2_{\phi_j} [\frac{s^2_\theta}{m_Z^2} + \frac{c^2_\theta}{m_{Z'}^2}] = 1 \tag{2.0.7}$$

so

$$M^{Z_L+Z'_L}_{\chi\chi\to Z\phi} = y_{DM} g_d d_\chi s_\theta \sqrt{2} \frac{1}{m_Z} \sqrt{s}. \tag{2.0.8}$$

Let's focus on the diagram mediated by χ and see that at high energies

$$\chi^\dagger \bar{\sigma^\mu} \chi k_\mu \to s \tag{2.0.9}$$

so the whole diagram gives a contribution

$$M^{\chi}_{\chi\chi\to Z\phi} = -g_d d_\chi s_\theta \frac{1}{m_Z} \sqrt{2} y_{DM} \sqrt{s} \tag{2.0.10}$$

which nullifies exactly the previous one so that out theory is safe at high energies.
Now that we have proved that everything is fine at high energies, it's time to extract a contribution to a_0 from these graphs and see what comes out of the unitarity bound. For this scope, we can see that the dominant contribution comes from the transverse degrees of freedom of the first two diagrams, plus we need to consider the contribution coming from the T and U exchanges diagrams. We follow the exact same steps for the process $\chi\chi \to Z'\phi$ and arrive at a value of a_0, which, unfortunately for us, will go to 0 in the small angle approximation, as it will be proportional to s_θ.

3 $\chi\chi \to Z'h$

Here the reasoning is completely the same as the process $\chi\chi \to Zh$ so here we have

$$M^{Z'_L}_{\chi\chi\to Z'_L h} = g_d d_\chi \chi^\dagger \bar{\sigma^\mu} \chi c_\theta \frac{\sqrt{2} g_w^2}{2} v_H (c_\theta + \frac{2 g_d d_H}{g_w} s_\theta)(s_\theta - \frac{2 g_d d_H}{g_w} c_\theta) \frac{1}{s - m^2_{Z'}} (-g_{\mu\nu} + \frac{k_\mu k_\nu}{m^2_{Z'}}) \frac{k_3^\nu}{m_{Z'}} \tag{3.0.1}$$

$$M^{Z_L}_{\chi\chi\to Z'_L h} = g_d d_\chi \chi^\dagger \bar{\sigma^\mu} \chi (-s_\theta) \frac{\sqrt{2} g_w^2}{2} v_H (c_\theta + \frac{2 g_d d_H}{g_w} s_\theta)^2 \frac{1}{s - m^2_{Z'}} (-g_{\mu\nu} + \frac{k_\mu k_\nu}{m^2_{Z'}}) \frac{k_3^\nu}{m_{Z'}} \tag{3.0.2}$$

so we already know that at high energies the sum of the longitudinal contributions goes straight to 0. Then we know already what is the next step of the plan and write the sum of the transverse polarizations of the the vector bosons propagators here that is, at high energies,

$$M^{Z_T + Z'_T}_{\chi\chi\to Z_L h} = g_d d_\chi \chi^\dagger \bar{\sigma^\mu} \chi k_{3\mu} \frac{1}{s} \sqrt{2} \frac{g_w^2}{2} v_H (c_\theta + s_\theta \frac{2 g_d d_H}{g_w}) \frac{2 g_d d_H}{g_w} \frac{1}{m_{Z'}} \tag{3.0.3}$$

so by writing again

$$k_{3\mu} = \frac{\sqrt{s}}{2} (1, \cos\theta, 0, \sin\theta) \tag{3.0.4}$$

we can find out that

$$a^0_{\chi\chi\to Z_L h} = \frac{\sqrt{2}}{128} \frac{g_w v_H}{m_{Z'}} g_d^2 d_\chi d_H (c_\theta + s_\theta \frac{2 g_d d_H}{g_w}). \tag{3.0.5}$$

this goes to 0 in the regime of small angle as $\tan 2\theta \propto d_H$

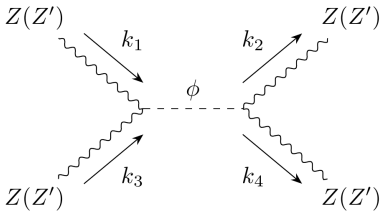

Figure A.5: S-type process of four bosons scattering. The propagator is a scalar particle

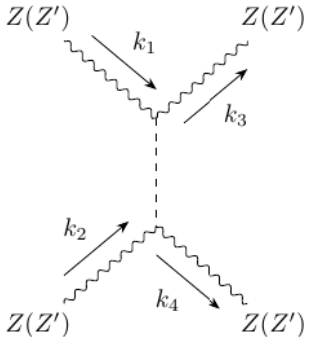

Figure A.6: T-type process

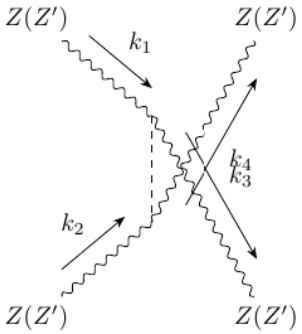

Figure A.7: U-type process

The processes concerning four vector bosons are the same as far as Feynman diagrams go. They all bring three diagrams as S,T and U type processes are involved. Another common property is given by the fact that the propagator is scalar, as we can see in Figure

4 $ZZ \to ZZ'$

We have two contributions as well here:

$$M^{\phi}_{Z'Z'\to Z'Z'} = -4[g_d^2 d^2_{\phi_j}\sqrt{2}v_{\phi_j}]^2 s_\theta^3 c_\theta \times \Big[\frac{1}{S-m^2_{\phi_j}}(\epsilon_1\cdot\epsilon_2)(\epsilon_3\cdot\epsilon_4)+\frac{1}{T-m^2_{\phi_j}}(\epsilon_1\cdot\epsilon_3)(\epsilon_2\cdot\epsilon_4)+\frac{1}{U-m^2_{\phi_j}}(\epsilon_1\cdot\epsilon_4)(\epsilon_3\cdot\epsilon_2)\Big]. \tag{4.0.1}$$

and

$$M^{h}_{Z'Z'\to Z'Z'} = -4[\frac{g_w^2}{4}\sqrt{2}v_H]^2 (c_\theta + 2\frac{g_d d_H}{g_w}s_\theta)^3 (s_\theta - 2\frac{g_d d_H}{g_w}c_\theta)\times \Big[\frac{1}{S-m^2_{h}}(\epsilon_1\cdot\epsilon_2)(\epsilon_3\cdot\epsilon_4)+\frac{1}{T-m^2_{h}}(\epsilon_1\cdot\epsilon_3)(\epsilon_2\cdot\epsilon_4)+\frac{1}{U-m^2_{h}}(\epsilon_1\cdot\epsilon_4)(\epsilon_3\cdot\epsilon_2)\Big]. \tag{4.0.2}$$

We can use the polarization vectors

$$\begin{aligned} \epsilon_1^\mu &= \frac{k_1^\mu}{m_Z}+\frac{2m_Z}{T-2m_Z^2}k_3^\mu \qquad & \epsilon_2^\mu &= \frac{k_2^\mu}{m_Z}+\frac{2m_Z}{T-m_Z^2-m_{Z'}^2}k_4^\mu \\ \epsilon_3^\mu &= \frac{k_3^\mu}{m_Z}+\frac{2m_Z}{T-2m_Z^2}k_1^\mu \qquad & \epsilon_4^\mu &= \frac{k_4^\mu}{m_{Z'}}+\frac{2m_{Z'}}{T-m_Z^2-m_{Z'}^2}k_2^\mu \end{aligned} \tag{4.0.3}$$

We can follow the same procedure as the previous paragraph here.

$$\begin{aligned} S &= (k_1^\mu+k_2^\mu)^2 = (k_3^\mu+k_4^\mu)^2 = 2m_Z^2+2k_1\cdot k_2 = m_Z^2+m_{Z'}^2+2k_3\cdot k_4 \\ T &= (k_1^\mu-k_3^\mu)^2 = (k_2^\mu-k_4^\mu)^2 = 2m_Z^2-2k_1\cdot k_3 = m_Z^2+m_{Z'}^2-2k_2\cdot k_4 \\ U &= (k_1^\mu-k_4^\mu)^2 = (k_2^\mu-k_3^\mu)^2 = m_Z^2+m_{Z'}^2-2k_1\cdot k_4 = 2m_Z^2-2k_2\cdot k_3 \end{aligned} \tag{4.0.4}$$

and of course

$$S+T+U = 3m_Z^2+m_{Z'}^2. \tag{4.0.5}$$

Moreover

$$\begin{aligned} k_1\cdot k_2 &= \frac{S}{2}-m_Z^2 \\ k_3\cdot k_4 &= \frac{S-m_Z^2-m_{Z'}^2}{2} \\ k_1\cdot k_3 &= m_Z^2-\frac{T}{2} \\ k_2\cdot k_4 &= \frac{m_Z^2+m_{Z'}^2-T}{2} \\ k_1\cdot k_4 &= \frac{m_Z^2+m_{Z'}^2-U}{2} \\ k_2\cdot k_3 &= m_Z^2-\frac{U}{2}. \end{aligned} \tag{4.0.6}$$

Now with all that behind and clear, we proceed to examine the content of the brackets. Again just focusing on the part regarding the ϕ exchange, the Higgs one will be the same

$$\begin{aligned}
M_{ZZ\to ZZ'} \propto \Big[\frac{1}{S-m_{\phi_j}^2}\Big(&\frac{(k_1\cdot k_2)(k_3\cdot k_4)}{m_Z^3 m_{Z'}}+\\
&\frac{2}{m_Z m_{Z'}(T-2m_Z^2)}[(k_1\cdot k_2)(k_1\cdot k_4)+(k_2\cdot k_3)(k_3\cdot k_4)]\\
&+\frac{2}{(T-m_Z^2-m_{Z'}^2)}[\frac{m_{Z'}}{m_Z^3}(k_1\cdot k_2)(k_2\cdot k_3)+\frac{1}{m_Z m_{Z'}}(k_1\cdot k_4)(k_3\cdot k_4)]\Big)+\\
\frac{1}{T-m_{\phi_j}^2}\Big(&\frac{(k_1\cdot k_3)(k_2\cdot k_4)}{m_Z^3 m_{Z'}}+\frac{2}{m_Z m_{Z'}(T-2m_{Z'}^2)}[(k_1\cdot k_1)(k_2\cdot k_4)+(k_3\cdot k_3)(k_2\cdot k_4)]\\
&+\frac{2}{(T-m_Z^2-m_{Z'}^2)}[\frac{m_{Z'}}{m_Z^3}(k_2\cdot k_2)(k_1\cdot k_3)+\frac{1}{m_Z m_{Z'}}(k_4\cdot k_4)(k_1\cdot k_3)]\Big)+\\
\frac{1}{U-m_{\phi_j}^2}\Big(&\frac{(k_1\cdot k_4)(k_2\cdot k_3)}{m_Z^3 m_{Z'}}+\frac{2}{m_Z m_{Z'}(T-2m_{Z'}^2)}[(k_1\cdot k_2)(k_1\cdot k_4)+(k_2\cdot k_3)(k_3\cdot k_4)]\\
&+\frac{2}{(T-m_Z^2-m_{Z'}^2)}[\frac{m_{Z'}}{m_Z^3}(k_1\cdot k_2)(k_2\cdot k_3)+\frac{1}{m_Z m_{Z'}}(k_1\cdot k_4)(k_3\cdot k_4)]\Big)\Big]
\end{aligned} \tag{4.0.7}$$

The leading terms are

$$\frac{1}{S-m_{\phi_j}^2}\frac{(k_1\cdot k_2)(k_3\cdot k_4)}{m_Z^3 m_{Z'}}+\frac{1}{T-m_{\phi_j}^2}\frac{(k_1\cdot k_3)(k_2\cdot k_4)}{m_Z^3 m_{Z'}}+\frac{1}{U-m_{\phi_j}^2}\frac{(k_1\cdot k_4)(k_2\cdot k_3)}{m_Z^3 m_{Z'}} \tag{4.0.8}$$

which become

$$\begin{aligned}
\frac{1}{4m_Z^3 m_{Z'}}\Big[&\frac{1}{S}(1+\frac{m_\phi^2}{S})(S-2m_{Z'}^2)(S-m_Z^2-m_{Z'}^2)+\\
&\frac{1}{T}(1+\frac{m_\phi^2}{T})(2m_{Z'}^2-T)(m_Z^2+m_{Z'}^2-T)+\\
&\frac{1}{U}(1+\frac{m_\phi^2}{U})(2m_{Z'}^2-U)(m_Z^2+m_{Z'}^2-U)\Big]
\end{aligned} \tag{4.0.9}$$

so summing all up it gives the contribution

$$\frac{1}{4m_Z^3 m_{Z'}}[3m_\phi^2-2(3m_Z^2+m_{Z'}^2)]. \tag{4.0.10}$$

Now concerning the subleading terms we consider only the first term in the denominator series expansion, as it is the only one that gives a constant contribution:

$$\begin{aligned}
&\frac{2}{m_Z m_{Z'}(T-2m_Z^2)}\Big[\frac{1}{S-m_{\phi_j}^2}\Big((k_1\cdot k_2)(k_1\cdot k_4)+(k_2\cdot k_3)(k_3\cdot k_4)\Big)+\\
&\qquad\frac{1}{T-m_{\phi_j}^2}\Big((k_1\cdot k_1)(k_2\cdot k_4)+(k_3\cdot k_3)(k_2\cdot k_4)\Big)+\\
&\qquad\frac{1}{U-m_{\phi_j}^2}\Big((k_1\cdot k_2)(k_1\cdot k_4)+(k_2\cdot k_3)(k_3\cdot k_4)\Big)\Big]+\\
&\frac{2}{(T-m_Z^2-m_{Z'}^2)}\Big[\frac{1}{S-m_{\phi_j}^2}\Big(\frac{m_{Z'}}{m_Z^3}(k_1\cdot k_2)(k_2\cdot k_3)+\frac{1}{m_Z m_{Z'}}(k_1\cdot k_4)(k_3\cdot k_4)\Big)+\\
&\qquad\frac{1}{T-m_{\phi_j}^2}\Big(\frac{m_{Z'}}{m_Z^3}(k_2\cdot k_2)(k_1\cdot k_3)+\frac{1}{m_Z m_{Z'}}(k_4\cdot k_4)(k_1\cdot k_3)\Big)+\\
&\qquad\frac{1}{U-m_{\phi_j}^2}\Big(\frac{m_{Z'}}{m_Z^3}(k_1\cdot k_2)(k_2\cdot k_3)+\frac{1}{m_Z m_{Z'}}(k_1\cdot k_4)(k_3\cdot k_4)\Big)\Big]+
\end{aligned}\tag{4.0.11}$$

now this can be converted to

$$\begin{aligned}
&\frac{2}{4m_Z m_{Z'}(T-2m_Z^2)}\Big[\frac{1}{S-m_{\phi_j}^2}\Big(-SU-SU\Big)+\\
&\qquad\frac{1}{T-m_{\phi_j}^2}\Big(-2T(m_Z^2+m_{Z'}^2)\Big)+\\
&\qquad\frac{1}{U-m_{\phi_j}^2}\Big(-SU-SU\Big)\Big]+\\
&\frac{2}{4(T-m_Z^2-m_{Z'}^2)}\Big[\frac{1}{S-m_{\phi_j}^2}\Big(\frac{m_{Z'}}{m_Z^3}(-SU)+\frac{1}{m_Z m_{Z'}}(-SU)\Big)+\\
&\qquad\frac{1}{T-m_{\phi_j}^2}\Big(\frac{m_{Z'}}{m_Z^3}(-2Tm_Z^2)+\frac{1}{m_Z m_{Z'}}(-2Tm_{Z'}^2)\Big)+\\
&\qquad\frac{1}{U-m_{\phi_j}^2}\Big(\frac{m_{Z'}}{m_Z^3}(-SU)+\frac{1}{m_Z m_{Z'}}(-SU)\Big)\Big]+
\end{aligned}\tag{4.0.12}$$

so

$$M_{Sub}\propto\frac{m_{Z'}^2+3m_Z^2}{2m_Z^3 m_{Z'}}\tag{4.0.13}$$

so summing the two we gain

$$M_{Lead}+M_{Sub}\propto\frac{3m_\phi^2}{4m_Z^3 m_{Z'}}\tag{4.0.14}$$

Now we ought to calculate a_0. As we already know, for the Higgs exchange case, the proportionality to d_H brings it to 0. This goes also for the dark scalar exchange case, which is proportional to $s-\theta$ and so doomed to annihilate.

5 $ZZ \to Z'Z'$

The procedure is the exact same as the previous section.

$$M^{\phi}_{Z'Z'\to Z'Z'} = -2[g_d^2 d^2_{\phi_j}\sqrt{2}v_{\phi_j}]^2 s_\theta^2 c_\theta^2 \times \Big[\frac{1}{S-m^2_{\phi_j}}(\epsilon_1\cdot\epsilon_2)(\epsilon_3\cdot\epsilon_4)+\frac{1}{T-m^2_{\phi_j}}(\epsilon_1\cdot\epsilon_3)(\epsilon_2\cdot\epsilon_4)+\frac{1}{U-m^2_{\phi_j}}(\epsilon_1\cdot\epsilon_4)(\epsilon_3\cdot\epsilon_2)\Big]. \tag{5.0.1}$$

and

$$M^{h}_{Z'Z'\to Z'Z'} = -2[\frac{g_w^2}{4}\sqrt{2}v_H]^2 (c_\theta + 2\frac{g_d d_H}{g_w}s_\theta)^2 (s_\theta - 2\frac{g_d d_H}{g_w}c_\theta)^2 \times \Big[\frac{1}{S-m^2_{h}}(\epsilon_1\cdot\epsilon_2)(\epsilon_3\cdot\epsilon_4)+\frac{1}{T-m^2_{h}}(\epsilon_1\cdot\epsilon_3)(\epsilon_2\cdot\epsilon_4)+\frac{1}{U-m^2_{h}}(\epsilon_1\cdot\epsilon_4)(\epsilon_3\cdot\epsilon_2)\Big]. \tag{5.0.2}$$

We can use the polarization vectors

$$\begin{aligned} \epsilon_1^\mu &= \frac{k_1^\mu}{m_Z}+\frac{2m_Z}{T-m_Z^2-m_{Z'}^2}k_3^\mu \qquad & \epsilon_2^\mu &= \frac{k_2^\mu}{m_Z}+\frac{2m_Z}{T-m_Z^2-m_{Z'}^2}k_4^\mu \\ \epsilon_3^\mu &= \frac{k_3^\mu}{m_{Z'}}+\frac{2m_{Z'}}{T-m_Z^2-m_{Z'}^2}k_1^\mu \qquad & \epsilon_4^\mu &= \frac{k_4^\mu}{m_{Z'}}+\frac{2m_{Z'}}{T-m_Z^2-m_{Z'}^2}k_2^\mu \end{aligned} \tag{5.0.3}$$

$$\begin{aligned} S &= (k_1^\mu+k_2^\mu)^2 = (k_3^\mu+k_4^\mu)^2 = 2m_Z^2+2k_1\cdot k_2 = 2m_{Z'}^2+2k_3\cdot k_4 \\ T &= (k_1^\mu-k_3^\mu)^2 = (k_2^\mu-k_4^\mu)^2 = m_Z^2+m_{Z'}^2-2k_1\cdot k_3 = m_Z^2+m_{Z'}^2-2k_2\cdot k_4 \\ U &= (k_1^\mu-k_4^\mu)^2 = (k_2^\mu-k_3^\mu)^2 = m_Z^2+m_{Z'}^2-2k_1\cdot k_4 = m_Z^2+m_{Z'}^2-2k_2\cdot k_3 \end{aligned} \tag{5.0.4}$$

and of course

$$S+T+U = 2m_Z^2+2m_{Z'}^2. \tag{5.0.5}$$

Moreover

$$\begin{aligned} k_1\cdot k_2 = k_3\cdot k_4 &= \frac{S}{2}-m_Z^2 \\ k_1\cdot k_3 = k_2\cdot k_4 &= \frac{m_Z^2+m_{Z'}^2-T}{2} \\ k_1\cdot k_4 = k_2\cdot k_3 &= \frac{m_Z^2+m_{Z'}^2-U}{2} \end{aligned} \tag{5.0.6}$$

The factor inside the brackets will be

$$\begin{aligned} M_{ZZ\to Z'Z'} \propto \Big[& \frac{1}{S-m_{\phi_j}^2}\Big(\frac{(k_1\cdot k_2)(k_3\cdot k_4)}{m_Z^2 m_{Z'}^2} \\ & + \frac{2}{T-m_Z^2-m_{Z'}^2}\Big[\frac{(k_1\cdot k_2)(k_1\cdot k_4)+(k_1\cdot k_2)(k_2\cdot k_3)}{m_Z^2} + \\ & \frac{(k_1\cdot k_4)(k_3\cdot k_4)+(k_2\cdot k_3)(k_3\cdot k_4)}{m_{Z'}^2}\Big] \\ & \frac{1}{T-m_{\phi_j}^2}\Big(\frac{(k_1\cdot k_3)(k_2\cdot k_4)}{m_Z^2 m_{Z'}^2} + \frac{2}{T-m_Z^2-m_{Z'}^2}\Big[\frac{(k_2\cdot k_2)(k_1\cdot k_3)+(k_1\cdot k_1)(k_2\cdot k_4)}{m_Z^2} + \\ & \frac{(k_4\cdot k_4)(k_1\cdot k_3)+(k_3\cdot k_3)(k_2\cdot k_4)}{m_{Z'}^2}\Big] \\ & \frac{1}{U-m_{\phi_j}^2}\Big(\frac{(k_1\cdot k_4)(k_2\cdot k_3)}{m_Z^2 m_{Z'}^2} + \frac{2}{T-m_Z^2-m_{Z'}^2}\Big[\frac{(k_1\cdot k_2)(k_1\cdot k_4)+(k_1\cdot k_2)(k_2\cdot k_3)}{m_Z^2} + \\ & \frac{(k_1\cdot k_4)(k_3\cdot k_4)+(k_2\cdot k_3)(k_3\cdot k_4)}{m_{Z'}^2}\Big] \\ & \Big] \end{aligned} \tag{5.0.7}$$

The leading terms are

$$\frac{1}{S-m_{\phi_j}^2}\frac{(k_1\cdot k_2)(k_3\cdot k_4)}{m_Z^2 m_{Z'}^2} + \frac{1}{T-m_{\phi_j}^2}\frac{(k_1\cdot k_3)(k_2\cdot k_4)}{m_Z^2 m_{Z'}^2} + \frac{1}{U-m_{\phi_j}^2}\frac{(k_1\cdot k_4)(k_2\cdot k_3)}{m_Z^2 m_{Z'}^2} \tag{5.0.8}$$

which become

$$\begin{aligned} \frac{1}{4m_Z^2 m_{Z'}^2}\Big[& \frac{1}{S}(1+\frac{m_\phi^2}{S})(S-2m_Z^2)(S-2m_{Z'}^2) + \frac{1}{T}(1+\frac{m_\phi^2}{T})(m_Z^2+m_{Z'}^2-T)^2 + \\ & \frac{1}{U}(1+\frac{m_\phi^2}{U})(m_Z^2+m_{Z'}^2-U)^2\Big] \end{aligned} \tag{5.0.9}$$

that summed give

$$\frac{1}{4m_Z^2 m_{Z'}^2}[3m_\phi^2 - 4(m_Z^2+m_{Z'}^2)]. \tag{5.0.10}$$

The subleading ones are

$$\begin{aligned}\frac{2}{T-m_Z^2-m_{Z'}^2}\Big[\frac{1}{S-m_{\phi_j}^2}\Big(\frac{(k_1\cdot k_2)(k_1\cdot k_4)+(k_1\cdot k_2)(k_2\cdot k_3)}{m_Z^2}+\\ \frac{(k_1\cdot k_4)(k_3\cdot k_4)+(k_2\cdot k_3)(k_3\cdot k_4)}{m_{Z'}^2}\Big)+\\ \frac{1}{T-m_{\phi_j}^2}\Big(\frac{(k_2\cdot k_2)(k_1\cdot k_3)+(k_1\cdot k_1)(k_2\cdot k_4)}{m_Z^2}+\\ \frac{(k_4\cdot k_4)(k_1\cdot k_3)+(k_3\cdot k_3)(k_2\cdot k_4)}{m_{Z'}^2}\Big)+\\ \frac{1}{U-m_{\phi_j}^2}\Big(\frac{(k_1\cdot k_2)(k_1\cdot k_4)+(k_1\cdot k_2)(k_2\cdot k_3)}{m_Z^2}+\\ \frac{(k_1\cdot k_4)(k_3\cdot k_4)+(k_2\cdot k_3)(k_3\cdot k_4)}{m_{Z'}^2}\Big)\Big]\end{aligned} \tag{5.0.11}$$

Let's try to see how they sum

$$\begin{aligned}M_{Sub}\propto\frac{2}{4(T-m_Z^2-m_{Z'}^2)}\Big[\frac{1}{S-m_{\phi_j}^2}\Big(\frac{-2SU}{m_Z^2}+\frac{-2SU}{m_{Z'}^2}\Big)+\\ \frac{1}{T-m_{\phi_j}^2}\Big(\frac{-4T(m_Z^2)}{m_Z^2}+\frac{-4Tm_{Z'}^2}{m_{Z'}^2}\Big)+\\ \frac{1}{U-m_{\phi_j}^2}\Big(\frac{-2SU}{m_Z^2}+\frac{-2SU}{m_{Z'}^2}\Big)\Big]\end{aligned} \tag{5.0.12}$$

So summing them we obtain

$$M_{Sub}\propto\frac{m_Z^2+m_{Z'}^2}{m_Z^2m_{Z'}^2} \tag{5.0.13}$$

and

$$M_{Lead+Sub}\propto\frac{3m_\phi^2}{4m_Z^2m_{Z'}^2} \tag{5.0.14}$$

Unfortunately for us we reach the same conclusions of the sections before as little changes as far as multiplication factors go.

6 $Z'Z' \to Z'Z$

We have

$$M^{\phi}_{Z'Z'\to Z'Z} = -4[g_d^2 d^2_{\phi_j}\sqrt{2}v_{\phi_j}]^2 s_\theta c_\theta^3 \times \Big[\frac{1}{S-m^2_{\phi_j}}(\epsilon_1\cdot\epsilon_2)(\epsilon_3\cdot\epsilon_4)+\frac{1}{T-m^2_{\phi_j}}(\epsilon_1\cdot\epsilon_3)(\epsilon_2\cdot\epsilon_4)+\frac{1}{U-m^2_{\phi_j}}(\epsilon_1\cdot\epsilon_4)(\epsilon_3\cdot\epsilon_2)\Big]. \tag{6.0.1}$$

and

$$M^{h}_{Z'Z'\to Z'Z} = -4[\frac{g_w^2}{4}\sqrt{2}v_H]^2 (c_\theta+2\frac{g_d d_H}{g_w}s_\theta)(s_\theta-2\frac{g_d d_H}{g_w}c_\theta)^3 \times \Big[\frac{1}{S-m^2_{h}}(\epsilon_1\cdot\epsilon_2)(\epsilon_3\cdot\epsilon_4)+\frac{1}{T-m^2_{h}}(\epsilon_1\cdot\epsilon_3)(\epsilon_2\cdot\epsilon_4)+\frac{1}{U-m^2_{h}}(\epsilon_1\cdot\epsilon_4)(\epsilon_3\cdot\epsilon_2)\Big]. \tag{6.0.2}$$

We can use the polarization vectors

$$\begin{aligned} \epsilon_1^\mu &= \frac{k_1^\mu}{m_{Z'}}+\frac{2m_{Z'}}{T-2m^2_{Z'}}k_3^\mu \qquad & \epsilon_2^\mu &= \frac{k_2^\mu}{m_{Z'}}+\frac{2m_{Z'}}{T-m^2_Z-m^2_{Z'}}k_4^\mu \\ \epsilon_3^\mu &= \frac{k_3^\mu}{m_{Z'}}+\frac{2m_{Z'}}{T-2m^2_{Z'}}k_1^\mu \qquad & \epsilon_4^\mu &= \frac{k_4^\mu}{m_{Z}}+\frac{2m_{Z}}{T-m^2_Z-m^2_{Z'}}k_2^\mu \end{aligned} \tag{6.0.3}$$

We can follow the same procedure of the previous paragraph here.

$$\begin{aligned} S &= (k_1^\mu+k_2^\mu)^2 = (k_3^\mu+k_4^\mu)^2 = 2m^2_{Z'}+2k_1\cdot k_2 = m^2_Z+m^2_{Z'}+2k_3\cdot k_4 \\ T &= (k_1^\mu-k_3^\mu)^2 = (k_2^\mu-k_4^\mu)^2 = 2m^2_{Z'}-2k_1\cdot k_3 = m^2_Z+m^2_{Z'}-2k_2\cdot k_4 \\ U &= (k_1^\mu-k_4^\mu)^2 = (k_2^\mu-k_3^\mu)^2 = m^2_Z+m^2_{Z'}-2k_1\cdot k_4 = 2m^2_{Z'}-2k_2\cdot k_3 \end{aligned} \tag{6.0.4}$$

and of course

$$S+T+U = m^2_Z+3m^2_{Z'}. \tag{6.0.5}$$

Moreover

$$\begin{aligned} k_1\cdot k_2 &= \frac{S}{2}-m^2_{Z'} \\ k_3\cdot k_4 &= \frac{S-m^2_Z-m^2_{Z'}}{2} \\ k_1\cdot k_3 &= m^2_{Z'}-\frac{T}{2} \\ k_2\cdot k_4 &= \frac{m^2_Z+m^2_{Z'}-T}{2} \\ k_1\cdot k_4 &= \frac{m^2_Z+m^2_{Z'}-U}{2} \\ k_2\cdot k_3 &= m^2_{Z'}-\frac{U}{2}. \end{aligned} \tag{6.0.6}$$

Now with all that behind and clear, we proceed to examine the content of the brackets. Again just focusing on the part regarding the ϕ exchange, the Higgs one will be the same

$$\begin{aligned}
M_{Z'Z'\to Z'Z} \propto \Big[\frac{1}{S-m_{\phi_j}^2}\Big(&\frac{(k_1\cdot k_2)(k_3\cdot k_4)}{m_Z m_{Z'}^3}+\\
&\frac{2}{m_Z m_{Z'}(T-2m_{Z'}^2)}[(k_1\cdot k_2)(k_1\cdot k_4)+(k_2\cdot k_3)(k_3\cdot k_4)]\\
&+\frac{2}{(T-m_Z^2-m_{Z'}^2)}[\frac{m_Z}{m_{Z'}^3}(k_1\cdot k_2)(k_2\cdot k_3)+\frac{1}{m_Z m_{Z'}}(k_1\cdot k_4)(k_3\cdot k_4)]\Big)+\\
\frac{1}{T-m_{\phi_j}^2}\Big(&\frac{(k_1\cdot k_3)(k_2\cdot k_4)}{m_Z m_{Z'}^3}+\frac{2}{m_Z m_{Z'}(T-2m_Z^2)}[(k_1\cdot k_1)(k_2\cdot k_4)+(k_3\cdot k_3)(k_2\cdot k_4)]\\
&+\frac{2}{(T-m_Z^2-m_{Z'}^2)}[\frac{m_Z}{m_{Z'}^3}(k_2\cdot k_2)(k_1\cdot k_3)+\frac{1}{m_Z m_{Z'}}(k_4\cdot k_4)(k_1\cdot k_3)]\Big)+\\
\frac{1}{U-m_{\phi_j}^2}\Big(&\frac{(k_1\cdot k_4)(k_2\cdot k_3)}{m_Z m_{Z'}^3}+\frac{2}{m_Z m_{Z'}(T-2m_Z^2)}[(k_1\cdot k_2)(k_1\cdot k_4)+(k_2\cdot k_3)(k_3\cdot k_4)]\\
&+\frac{2}{(T-m_Z^2-m_{Z'}^2)}[\frac{m_Z}{m_{Z'}^3}(k_1\cdot k_2)(k_2\cdot k_3)+\frac{1}{m_Z m_{Z'}}(k_1\cdot k_4)(k_3\cdot k_4)]\Big)\Big]
\end{aligned} \tag{6.0.7}$$

The leading terms are

$$\frac{1}{S-m_{\phi_j}^2}\frac{(k_1\cdot k_2)(k_3\cdot k_4)}{m_Z m_{Z'}^3}+\frac{1}{T-m_{\phi_j}^2}\frac{(k_1\cdot k_3)(k_2\cdot k_4)}{m_Z m_{Z'}^3}+\frac{1}{U-m_{\phi_j}^2}\frac{(k_1\cdot k_4)(k_2\cdot k_3)}{m_Z m_{Z'}^3} \tag{6.0.8}$$

which become

$$\begin{aligned}
\frac{1}{4m_Z m_{Z'}^3}\Big[&\frac{1}{S}(1+\frac{m_\phi^2}{S})(S-2m_Z^2)(S-m_Z^2-m_{Z'}^2)+\\
&\frac{1}{T}(1+\frac{m_\phi^2}{T})(2m_Z^2-T)(m_Z^2+m_{Z'}^2-T)+\\
&\frac{1}{U}(1+\frac{m_\phi^2}{U})(2m_Z^2-U)(m_Z^2+m_{Z'}^2-U)\Big]
\end{aligned} \tag{6.0.9}$$

so summing all up it gives the contribution

$$\frac{1}{4m_Z m_{Z'}^3}[3m_\phi^2-2(m_Z^2+3m_{Z'}^2)]. \tag{6.0.10}$$

Now concerning the subleading terms we consider only the first term in the denominator series expansion, as it is the only one that gives a constant contribution:

$$\begin{aligned}
&\frac{2}{m_Z m_{Z'}(T-2m_{Z'}^2)}\Big[\frac{1}{S-m_{\phi_j}^2}\Big((k_1\cdot k_2)(k_1\cdot k_4)+(k_2\cdot k_3)(k_3\cdot k_4)\Big)+\\
&\qquad\frac{1}{T-m_{\phi_j}^2}\Big((k_1\cdot k_1)(k_2\cdot k_4)+(k_3\cdot k_3)(k_2\cdot k_4)\Big)+\\
&\qquad\frac{1}{U-m_{\phi_j}^2}\Big((k_1\cdot k_2)(k_1\cdot k_4)+(k_2\cdot k_3)(k_3\cdot k_4)\Big)\Big]+\\
&\frac{2}{(T-m_Z^2-m_{Z'}^2)}\Big[\frac{1}{S-m_{\phi_j}^2}\Big(\frac{m_Z}{m_{Z'}^3}(k_1\cdot k_2)(k_2\cdot k_3)+\frac{1}{m_Z m_{Z'}}(k_1\cdot k_4)(k_3\cdot k_4)\Big)+\\
&\qquad\frac{1}{T-m_{\phi_j}^2}\Big(\frac{m_Z}{m_{Z'}^3}(k_2\cdot k_2)(k_1\cdot k_3)+\frac{1}{m_Z m_{Z'}}(k_4\cdot k_4)(k_1\cdot k_3)\Big)+\\
&\qquad\frac{1}{U-m_{\phi_j}^2}\Big(\frac{m_Z}{m_{Z'}^3}(k_1\cdot k_2)(k_2\cdot k_3)+\frac{1}{m_Z m_{Z'}}(k_1\cdot k_4)(k_3\cdot k_4)\Big)\Big]+
\end{aligned}\tag{6.0.11}$$

now this can be converted to

$$\begin{aligned}
&\frac{2}{4m_Z m_{Z'}(T-2m_{Z'}^2)}\Big[\frac{1}{S-m_{\phi_j}^2}\Big(-SU-SU\Big)+\\
&\qquad\frac{1}{T-m_{\phi_j}^2}\Big(-2T(m_Z^2+m_{Z'}^2)\Big)+\\
&\qquad\frac{1}{U-m_{\phi_j}^2}\Big(-SU-SU\Big)\Big]+\\
&\frac{2}{4(T-m_Z^2-m_{Z'}^2)}\Big[\frac{1}{S-m_{\phi_j}^2}\Big(\frac{m_Z}{m_{Z'}^3}(-SU)+\frac{1}{m_Z m_{Z'}}(-SU)\Big)+\\
&\qquad\frac{1}{T-m_{\phi_j}^2}\Big(\frac{m_Z}{m_{Z'}^3}(-2Tm_{Z'}^2)+\frac{1}{m_Z m_{Z'}}(-2Tm_Z^2)\Big)+\\
&\qquad\frac{1}{U-m_{\phi_j}^2}\Big(\frac{m_Z}{m_{Z'}^3}(-SU)+\frac{1}{m_Z m_{Z'}}(-SU)\Big)\Big]+
\end{aligned}\tag{6.0.12}$$

so

$$M_{Sub}\propto\frac{3m_{Z'}^2+m_Z^2}{2m_Z m_{Z'}^3}\tag{6.0.13}$$

so summing the two we gain

$$M_{Lead}+M_{Sub}\propto\frac{3m_\phi^2}{4m_Z m_{Z'}^3}\tag{6.0.14}$$

Although this differs from 0 it is of little effect as the proportionality to θ of both the scattering amplitudes dim to 0 the result.

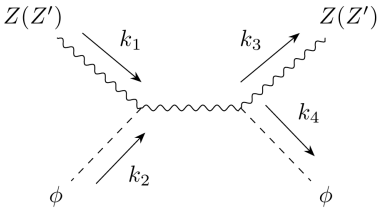

Figure A.8: S-type process

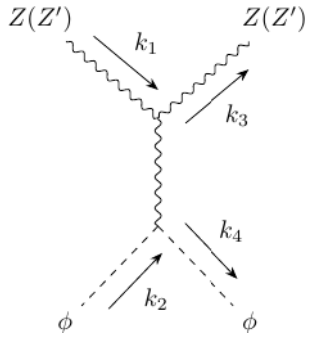

Figure A.9: T-type process

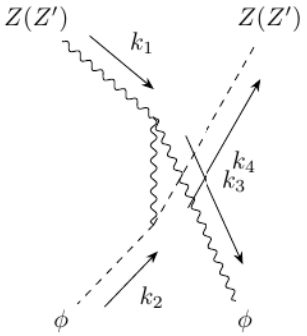

Figure A.10: U-type process

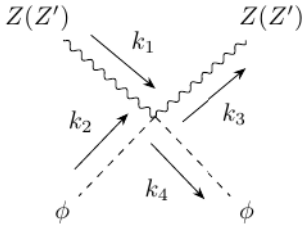

Figure A.11: Vertex interaction

Now the five diagrams that follow do have all the same structure. Indeed we start with the usual three diagrams representing S, T and U processes in which the propagator can be only a vector boson, Z or Z' depending on the case. Then there will be a third additional diagram that will picture a vertex interaction of the four particles with no propagator.

7 $Z\phi \to Z'\phi$

Here we are going to examine the scattering of bosons and scalar fields. For the quantities regarding the scalar field here, we are supposing the existence of only one field, after all the calculations are done it will be easy to generalize to n scalar fields by only summing on the quantities presenting the subscript j.
We go ahead of ourselves as we have seen this game already:

$$\begin{aligned} M^{Z}_{Z\phi\to Z'\phi} = 4[\sqrt{2}g_d^2 d^2_{\phi_j} v_{\phi_j}]^2 s_\theta^3 c_\theta \Big[& \frac{1}{S-m_Z^2}[-\epsilon_1\cdot\epsilon_3 + \frac{(k_1+k_2)_\mu (k_1+k_2)_\nu}{m_Z^2}\epsilon_1^\mu \epsilon_3^\nu] + \\ & \frac{1}{T-m_Z^2}[-\epsilon_1\cdot\epsilon_3 + \frac{(k_1-k_3)_\mu (k_1-k_3)_\nu}{m_Z^2}\epsilon_1^\mu \epsilon_3^\nu] + \\ & \frac{1}{U-m_Z^2}[-\epsilon_1\cdot\epsilon_3 + \frac{(k_1-k_4)_\mu (k_1-k_4)_\nu}{m_Z^2}\epsilon_1^\mu \epsilon_3^\nu]\Big] \end{aligned} \tag{7.0.1}$$

$$\begin{aligned} M^{Z'}_{Z\phi\to Z'\phi} = 4[\sqrt{2}g_d^2 d^2_{\phi_j} v_{\phi_j}]^2 s_\theta c_\theta^3 \Big[& \frac{1}{S-m_{Z'}^2}[-\epsilon_1\cdot\epsilon_3 + \frac{(k_1+k_2)_\mu (k_1+k_2)_\nu}{m_{Z'}^2}\epsilon_1^\mu \epsilon_3^\nu] + \\ & \frac{1}{T-m_{Z'}^2}[-\epsilon_1\cdot\epsilon_3 + \frac{(k_1-k_3)_\mu (k_1-k_3)_\nu}{m_{Z'}^2}\epsilon_1^\mu \epsilon_3^\nu] + \\ & \frac{1}{U-m_{Z'}^2}[-\epsilon_1\cdot\epsilon_3 + \frac{(k_1-k_4)_\mu (k_1-k_4)_\nu}{m_{Z'}^2}\epsilon_1^\mu \epsilon_3^\nu]\Big] \end{aligned} \tag{7.0.2}$$

$$M_{Z\phi\to Z'\phi} = -4g_d^2 d^2_{\phi_j} s_\theta c_\theta \epsilon_1\cdot\epsilon_3 \tag{7.0.3}$$

where we can see that

$$\begin{aligned} \epsilon_1^\mu &= \frac{k_1^\mu}{m_Z} + \frac{2m_Z}{T-(m_Z^2+m_{Z'}^2)}k_3^\mu \\ \epsilon_3^\mu &= \frac{k_3^\mu}{m_{Z'}} + \frac{2m_{Z'}}{T-(m_Z^2+m_{Z'}^2)}k_1^\mu \end{aligned} \tag{7.0.4}$$

Now considering the longitudinal polarization degrees of freedom of the first to diagrams. In particular the leading contributions lead us to the result by addition

$$\begin{aligned} M^{Z_L+Z'_L}_{Z\phi\to Z'\phi} = 4[\sqrt{2}g_d^2 d^2_{\phi_j} v_{\phi_j}]^2 \frac{1}{m_Z m_{Z'}} \Big[& \\ (k_1\cdot k_1 + k_2\cdot k_1)(k_1\cdot k_3 + k_2\cdot k_3)[\frac{s_\theta^3 c_\theta}{m_Z^2(S-m_Z^2)} + \frac{s_\theta c_\theta^3}{m_{Z'}^2(S-m_{Z'}^2)}] & \\ (k_1\cdot k_1 - k_3\cdot k_1)(k_1\cdot k_3 - k_3\cdot k_3)[\frac{s_\theta^3 c_\theta}{m_Z^2(T-m_Z^2)} + \frac{s_\theta c_\theta^3}{m_{Z'}^2(T-m_{Z'}^2)}] & \\ (k_1\cdot k_1 - k_4\cdot k_1)(k_1\cdot k_3 - k_4\cdot k_3)[\frac{s_\theta^3 c_\theta}{m_Z^2(U-m_Z^2)} + \frac{s_\theta c_\theta^3}{m_{Z'}^2(U-m_{Z'}^2)}]\Big] & \end{aligned} \tag{7.0.5}$$

we see that there is an anomalous behavior at high energies. If we consider the vertex scattering amplitude at high energies though we have

$$M_{Z\phi\to Z'\phi} = -4g_d^2 d_{\phi_j}^2 s_\theta c_\theta \frac{k_1 \cdot k_3}{m_Z m_{Z'}} \tag{7.0.6}$$

so for the rules we have already studied, they have the same exact behavior and opposite signs and the two contributions annihilate.
Concerning the subleading contributions one can calculate them and use the equation

$$S + T + U = 2m_\phi^2 + m_Z^2 + m_{Z'}^2 \tag{7.0.7}$$

to prove that they are washed away at high energies.
Now we are ready to examine the contributions coming from the transverse degrees of freedom of the first two scattering amplitudes, those will be dominant for a_0:

$$M_{Z\phi\to Z'\phi}^{Z_T+Z'_T} = -4[\sqrt{2}g_d^2 d_{\phi_j}^2 v_{\phi_j}]^2 s_\theta c_\theta \epsilon_1 \cdot \epsilon_3 [\frac{1}{S} + \frac{1}{T} + \frac{1}{U}]. \tag{7.0.8}$$

We can contract the two four-momentum and obtain

$$M_{Z\phi\to Z'\phi}^{Z_T+Z'_T} = 4[\sqrt{2}g_d^2 d_{\phi_j}^2 v_{\phi_j}]^2 s_\theta c_\theta \frac{T}{2m_Z m_{Z'}} [\frac{1}{S} + \frac{1}{T} + \frac{1}{U}] \tag{7.0.9}$$

and

$$a_0 = \frac{1}{32\pi} \int_0^\pi d\delta \sin(\delta) M(s, \cos(\delta)) \tag{7.0.10}$$

but already here we can see that this quantity is proportional to s_θ so in the end, in the small angle approximation, it will go to 0.
We can see that the same destiny is shared by the subleading contributions of the longitudinal degrees of freedom, as they all acquire a multiplication factor of $s_\theta c_\theta$ and they all go to zero in the small angle approximation

8 $Z\phi \to Z\phi$

Here we have

$$M^{Z}_{Z\phi\to Z\phi} = -4[\sqrt{2}g_d^2 d^2_{\phi_j} v_{\phi_j}]^2 s_\theta^4 \Big[\frac{1}{S-m_Z^2}[-\epsilon_1\cdot\epsilon_3 + \frac{(k_1+k_2)_\mu (k_1+k_2)_\nu}{m_Z^2}\epsilon_1^\mu \epsilon_3^\nu] + \frac{1}{T-m_Z^2}[-\epsilon_1\cdot\epsilon_3 + \frac{(k_1-k_3)_\mu (k_1-k_3)_\nu}{m_Z^2}\epsilon_1^\mu \epsilon_3^\nu] + \frac{1}{U-m_Z^2}[-\epsilon_1\cdot\epsilon_3 + \frac{(k_1-k_4)_\mu (k_1-k_4)_\nu}{m_Z^2}\epsilon_1^\mu \epsilon_3^\nu]\Big] \tag{8.0.1}$$

$$M^{Z'}_{Z\phi\to Z\phi} = -4[\sqrt{2}g_d^2 d^2_{\phi_j} v_{\phi_j}]^2 s_\theta^2 c_\theta^2 \Big[\frac{1}{S-m_{Z'}^2}[-\epsilon_1\cdot\epsilon_3 + \frac{(k_1+k_2)_\mu (k_1+k_2)_\nu}{m_{Z'}^2}\epsilon_1^\mu \epsilon_3^\nu] + \frac{1}{T-m_{Z'}^2}[-\epsilon_1\cdot\epsilon_3 + \frac{(k_1-k_3)_\mu (k_1-k_3)_\nu}{m_{Z'}^2}\epsilon_1^\mu \epsilon_3^\nu] + \frac{1}{U-m_{Z'}^2}[-\epsilon_1\cdot\epsilon_3 + \frac{(k_1-k_4)_\mu (k_1-k_4)_\nu}{m_{Z'}^2}\epsilon_1^\mu \epsilon_3^\nu]\Big] \tag{8.0.2}$$

and then we have a vertex contribution

$$M_{Z\phi\to Z\phi} = 4g_d^2 d^2_{\phi_j} s_\theta^2 \epsilon_1\cdot\epsilon_3 \tag{8.0.3}$$

where ϵ_1 and ϵ_3 can be

$$\begin{aligned}\epsilon_1^\mu &= \frac{k_1^\mu}{m_Z} + \frac{2m_Z}{T-2m_Z^2}k_3^\mu \\ \epsilon_3^\mu &= \frac{k_3^\mu}{m_Z} + \frac{2m_Z}{T-2m_Z^2}k_1^\mu\end{aligned} \tag{8.0.4}$$

here the analysis is carried out in the exact same way we have seen in the previous section. This means that if we consider the contributions coming from the first two amplitudes , specifically, those corresponding with the leading terms on the longitudinal dof of the vector boson propagators, and we sum them, we are going to find an anomalous behavior at high energies that matches perfectly the one from the vertex scattering amplitude, so the two annihilate and we do not have any sort of concern at high energies.
Moreover, the subleading terms have no impact whatsoever, that is also the case.
Now onto the transverse degrees of freedom, we can sum them and obtain a contribution similar to the one of the previous paragraph.

Unfortunately here the contribution is also proportional to s_θ so in the small angle approximation will go to 0 really fast like the one before.
Here we have omitted the contribution coming from the subleading terms of the polarization vector. Indeed, as the previous case showed they too are proportional to s_θ and the contribution goes to 0 as well in the small angle.

9 $Zh \to Z'h$

$$
\begin{aligned}
M^{Z}_{Z\phi\to Z'\phi} = -4[\frac{g_w^2}{4}\sqrt{2}v_H]^2(c_\theta + 2\frac{g_d d_H}{g_w}s_\theta)^3(s_\theta - 2\frac{g_d d_H}{g_w}c_\theta)\times \\
\Big[\frac{1}{S-m_Z^2}[-\epsilon_1\cdot\epsilon_3 + \frac{(k_1+k_2)_\mu(k_1+k_2)_\nu}{m_Z^2}\epsilon_1^\mu\epsilon_3^\nu] + \\
\frac{1}{T-m_Z^2}[-\epsilon_1\cdot\epsilon_3 + \frac{(k_1-k_3)_\mu(k_1-k_3)_\nu}{m_Z^2}\epsilon_1^\mu\epsilon_3^\nu] + \\
\frac{1}{U-m_Z^2}[-\epsilon_1\cdot\epsilon_3 + \frac{(k_1-k_4)_\mu(k_1-k_4)_\nu}{m_Z^2}\epsilon_1^\mu\epsilon_3^\nu]\Big]
\end{aligned}
\tag{9.0.1}
$$

$$
\begin{aligned}
M^{Z'}_{Z\phi\to Z'\phi} = -4[\frac{g_w^2}{4}\sqrt{2}v_H]^2(c_\theta + 2\frac{g_d d_H}{g_w}s_\theta)(s_\theta - 2\frac{g_d d_H}{g_w}c_\theta)^3\times \\
\Big[\frac{1}{S-m_{Z'}^2}[-\epsilon_1\cdot\epsilon_3 + \frac{(k_1+k_2)_\mu(k_1+k_2)_\nu}{m_{Z'}^2}\epsilon_1^\mu\epsilon_3^\nu] + \\
\frac{1}{T-m_{Z'}^2}[-\epsilon_1\cdot\epsilon_3 + \frac{(k_1-k_3)_\mu(k_1-k_3)_\nu}{m_{Z'}^2}\epsilon_1^\mu\epsilon_3^\nu] + \\
\frac{1}{U-m_{Z'}^2}[-\epsilon_1\cdot\epsilon_3 + \frac{(k_1-k_4)_\mu(k_1-k_4)_\nu}{m_{Z'}^2}\epsilon_1^\mu\epsilon_3^\nu]\Big]
\end{aligned}
\tag{9.0.2}
$$

$$
M_{Z\phi\to Z'\phi} = 8(2\frac{g_w^2}{4}(c_\theta + 2\frac{g_d d_H}{g_w}s_\theta)(s_\theta - 2\frac{g_d d_H}{g_w}c_\theta)\frac{1}{4})\epsilon_1\cdot\epsilon_3 \tag{9.0.3}
$$

$$
\begin{aligned}
\epsilon_1^\mu &= \frac{k_1^\mu}{m_Z} + \frac{2m_Z}{T-(m_Z^2+m_{Z'}^2)}k_3^\mu \\
\epsilon_3^\mu &= \frac{k_3^\mu}{m_{Z'}} + \frac{2m_{Z'}}{T-(m_Z^2+m_{Z'}^2)}k_1^\mu
\end{aligned}
\tag{9.0.4}
$$

Now considering the longitudinal polarization degrees of freedom of the first two diagrams. In particular, the leading contributions lead us to the result by addition

$$
\begin{aligned}
M^{Z_L+Z'_L}_{Z\phi\to Z'\phi} = -4[\frac{g_w^2}{4}\sqrt{2}v_H]^2(c_\theta + 2\frac{g_d d_H}{g_w}s_\theta)(s_\theta - 2\frac{g_d d_H}{g_w}c_\theta)\frac{1}{m_Z m_{Z'}}\Big[\\
(k_1\cdot k_1 + k_2\cdot k_1)(k_1\cdot k_3 + k_2\cdot k_3)[\frac{(c_\theta + 2\frac{g_d d_H}{g_w}s_\theta)^2}{m_Z^2(S-m_Z^2)} + \frac{(s_\theta - 2\frac{g_d d_H}{g_w}c_\theta)^2}{m_{Z'}^2(S-m_{Z'}^2)}] \\
(k_1\cdot k_1 - k_3\cdot k_1)(k_1\cdot k_3 - k_3\cdot k_3)[\frac{(c_\theta + 2\frac{g_d d_H}{g_w}s_\theta)^2}{m_Z^2(T-m_Z^2)} + \frac{(s_\theta - 2\frac{g_d d_H}{g_w}c_\theta)^2}{m_{Z'}^2(T-m_{Z'}^2)}] \\
(k_1\cdot k_1 - k_4\cdot k_1)(k_1\cdot k_3 - k_4\cdot k_3)[\frac{(c_\theta + 2\frac{g_d d_H}{g_w}s_\theta)^2}{m_Z^2(U-m_Z^2)} + \frac{(s_\theta - 2\frac{g_d d_H}{g_w}c_\theta)^2}{m_{Z'}^2(U-m_{Z'}^2)}]\Big]
\end{aligned}
\tag{9.0.5}
$$

Again we use expansions of the kind

$$\frac{1}{S-m_Z^2}=\frac{1}{S}(1+\frac{m_Z^2}{S}) \tag{9.0.6}$$

together with the equations that relate scalar product of momenta to Mandelstam's variables:

$$\begin{aligned}M^{Z_L+Z'_L}_{Z\phi\to Z'\phi}=-4[\frac{g_w^2}{4}\sqrt{2}v_H]^2(c_\theta+2\frac{g_d d_H}{g_w}s_\theta)(s_\theta-2\frac{g_d d_H}{g_w}c_\theta)\frac{1}{4m_Z m_{Z'}}\Big[\\ (S+m_Z^2-m_h^2)(S+m_{Z'}^2-m_h^2)[\frac{(c_\theta+2\frac{g_d d_H}{g_w}s_\theta)^2}{m_Z^2 S}(1+\frac{m_Z^2}{S})+\frac{(s_\theta-2\frac{g_d d_H}{g_w}c_\theta)^2}{m_{Z'}^2 S}(1+\frac{m_{Z'}^2}{S})]\\ (T+m_Z^2-m_{Z'}^2)(-T+m_Z^2-m_{Z'}^2)[\frac{(c_\theta+2\frac{g_d d_H}{g_w}s_\theta)^2}{m_Z^2 T}(1+\frac{m_Z^2}{T})+\frac{(s_\theta-2\frac{g_d d_H}{g_w}c_\theta)^2}{m_{Z'}^2 T}(1+\frac{m_{Z'}^2}{T})]\\ (U+m_Z^2-m_h^2)(U+m_{Z'}^2-m_h^2)[\frac{(c_\theta+2\frac{g_d d_H}{g_w}s_\theta)^2}{m_Z^2 U}(1+\frac{m_Z^2}{U})+\frac{(s_\theta-2\frac{g_d d_H}{g_w}c_\theta)^2}{m_{Z'}^2 U}(1+\frac{m_{Z'}^2}{U})]\Big]\end{aligned} \tag{9.0.7}$$

This becomes

$$\begin{aligned}M^{Z_L+Z'_L}_{Z'\phi\to Z'\phi}=-4[\frac{g_w^2}{4}\sqrt{2}v_H]^2(c_\theta+2\frac{g_d d_H}{g_w}s_\theta)(s_\theta-2\frac{g_d d_H}{g_w}c_\theta)\frac{1}{4m_Z m_{Z'}}\\ \Big[[\frac{(c_\theta+2\frac{g_d d_H}{g_w}s_\theta)^2}{m_Z^2}+\frac{(s_\theta-2\frac{g_d d_H}{g_w}c_\theta)^2}{m_{Z'}^2}](S-T+U+2m_Z^2+2m_{Z'}^2-4m_h^2)+(1+4\frac{g_d^2 d_H^2}{g_w^2})\Big]\end{aligned} \tag{9.0.8}$$

now we can exploit the fact that

$$S+T+U=m_Z^2+m_{Z'}^2+2m_h^2 \tag{9.0.9}$$

and see that this reduces to

$$\begin{aligned}M^{Z_L+Z'_L}_{Z'\phi\to Z'\phi}=-4[\frac{g_w^2}{4}\sqrt{2}v_H]^2(c_\theta+2\frac{g_d d_H}{g_w}s_\theta)(s_\theta-2\frac{g_d d_H}{g_w}c_\theta)\frac{1}{4m_Z m_{Z'}}\\ \Big[[\frac{(c_\theta+2\frac{g_d d_H}{g_w}s_\theta)^2}{m_Z^2}+\frac{(s_\theta-2\frac{g_d d_H}{g_w}c_\theta)^2}{m_{Z'}^2}](-2T+3m_Z^2+3m_{Z'}^2-2m_h^2)+(1+4\frac{g_d^2 d_H^2}{g_w^2})\Big]\end{aligned} \tag{9.0.10}$$

We also make use of the fact that

$$\frac{g_w^2 v_H^2}{2}[\frac{(c_\theta+2\frac{g_d d_H}{g_w}s_\theta)^2}{m_Z^2}+\frac{(s_\theta-2\frac{g_d d_H}{g_w}c_\theta)^2}{m_{Z'}^2}]=1 \tag{9.0.11}$$

and the contribution inside the brackets becomes

$$M^{Z_L+Z'_L}_{Z'\phi\to Z'\phi} = -g_w^2(c_\theta + 2\frac{g_d d_H}{g_w}s_\theta)(s_\theta - 2\frac{g_d d_H}{g_w}c_\theta)\frac{1}{4m_Z m_{Z'}} \Big[(-2T + 3m_Z^2 + 3m_{Z'}^2 - 2m_h^2)\Big] \tag{9.0.12}$$

Now the vertex contribution is

$$M_{Z\phi\to Z'\phi} = g_w^2(c_\theta + 2\frac{g_d d_H}{g_w}s_\theta)(s_\theta - 2\frac{g_d d_H}{g_w}c_\theta)\frac{m_Z^2 + m_{Z'}^2 - T}{2m_Z m_{Z'}} \tag{9.0.13}$$

so summing the two we obtain

$$M^{Z_L+Z'_L}_{Z'\phi\to Z'\phi} = -g_w^2(c_\theta + 2\frac{g_d d_H}{g_w}s_\theta)(s_\theta - 2\frac{g_d d_H}{g_w}c_\theta)\frac{1}{4m_Z m_{Z'}} \Big[(m_Z^2 + m_{Z'}^2 - 2m_h^2)\Big] \tag{9.0.14}$$

Moreover the subleading contribution is completely irrelevant at high energies

Now for the transversal degrees of freedom they amount to

$$M^{Z_T+Z'_T}_{Z\phi\to Z\phi} = 4[\frac{g_w^2}{4}\sqrt{2}v_H]^2(c_\theta+2\frac{g_d d_H}{g_w}s_\theta)(s_\theta-2\frac{g_d d_H}{g_w}c_\theta)(1+4\frac{g_d^2 d_H^2}{g_w^2})\epsilon_1\cdot\epsilon_3[\frac{1}{S}+\frac{1}{T}+\frac{1}{U}] \tag{9.0.15}$$

that becomes

$$M^{Z_T+Z'_T}_{Z\phi\to Z\phi} = 4[\frac{g_w^2}{4}\sqrt{2}v_H]^2(c_\theta + 2\frac{g_d d_H}{g_w}s_\theta)(s_\theta - 2\frac{g_d d_H}{g_w}c_\theta)\times (1 + 4\frac{g_d^2 d_H^2}{g_w^2})(\frac{m_Z^2 + m_{Z'}^2 - T}{2m_Z m_{Z'}})[\frac{1}{S} + \frac{1}{T} + \frac{1}{U}] \tag{9.0.16}$$

the only term that survives is the oe proportional to T

$$M^{Z_T+Z'_T}_{Z\phi\to Z\phi} = -12[\frac{g_w^2}{4}\sqrt{2}v_H]^2(c_\theta+2\frac{g_d d_H}{g_w}s_\theta)(s_\theta-2\frac{g_d d_H}{g_w}c_\theta)(1+4\frac{g_d^2 d_H^2}{g_w^2})(\frac{1}{2m_Z m_{Z'}}). \tag{9.0.17}$$

Now in order to calculate a_0 we put all contributions together and go in the small angle approximation. Unfortunately for us, all the contributions are proportional to d_H and, by noticing that $\tan 2\theta \propto d_H$, we can see that they all go to 0 in this regime

10 $Z'h \to Z'h$

For this process we have again three contributions like the previous ones

$$\begin{aligned} M^{Z}_{\phi Z' \to \phi Z'} = -4[\frac{g_w^2}{4}\sqrt{2}v_H(c_\theta + 2\frac{g_d d_H}{g_w}s_\theta)(s_\theta - 2\frac{g_d d_H}{g_w}c_\theta)]^2 \\ \Big[\frac{1}{S-m_Z^2}[-\epsilon_1\cdot\epsilon_3 + \frac{(k_1+k_2)_\mu(k_1+k_2)_\nu}{m_Z^2}\epsilon_1^\mu\epsilon_3^\nu] + \\ \frac{1}{T-m_Z^2}[-\epsilon_1\cdot\epsilon_3 + \frac{(k_1-k_3)_\mu(k_1-k_3)_\nu}{m_Z^2}\epsilon_1^\mu\epsilon_3^\nu] + \\ \frac{1}{U-m_Z^2}[-\epsilon_1\cdot\epsilon_3 + \frac{(k_1-k_4)_\mu(k_1-k_4)_\nu}{m_Z^2}\epsilon_1^\mu\epsilon_3^\nu]\Big] \end{aligned} \tag{10.0.1}$$

$$\begin{aligned} M^{Z'}_{\phi Z' \to \phi Z'} = -4[\frac{g_w^2}{4}\sqrt{2}v_H(s_\theta - 2\frac{g_d d_H}{g_w}c_\theta)^2]^2 \\ \Big[\frac{1}{S-m_{Z'}^2}[-\epsilon_1\cdot\epsilon_3 + \frac{(k_1+k_2)_\mu(k_1+k_2)_\nu}{m_{Z'}^2}\epsilon_1^\mu\epsilon_3^\nu] + \\ \frac{1}{T-m_{Z'}^2}[-\epsilon_1\cdot\epsilon_3 + \frac{(k_1-k_3)_\mu(k_1-k_3)_\nu}{m_{Z'}^2}\epsilon_1^\mu\epsilon_3^\nu] + \\ \frac{1}{U-m_{Z'}^2}[-\epsilon_1\cdot\epsilon_3 + \frac{(k_1-k_4)_\mu(k_1-k_4)_\nu}{m_{Z'}^2}\epsilon_1^\mu\epsilon_3^\nu]\Big] \end{aligned} \tag{10.0.2}$$

finally the vertex contribution

$$M_{Z\phi\to Z'\phi} = 4\frac{g_w^2}{8}(s_\theta - 2\frac{g_d d_H}{g_w}c_\theta)^2\epsilon_1\cdot\epsilon_3 \tag{10.0.3}$$

This one follows the exact same dynamic of the previous one apart form the multiplicity factors. Indeed the final result relies on $\tan 2\theta$ as well as the previous one and this means that is bound to go to 0 in the small angle approximation as well.

11 $Z\phi \to \bar{f}_L f_L$

Here we can see two contributions rising, corresponding to the two vector boson exchanges:

$$M^{Z}_{Z\phi\to\bar{f}_L f_L} = 2g_d^3\sqrt{2}d_{\phi_j}^2 v_{\phi_j}s_\theta^3\frac{1}{s-m_Z^2}[-g_{\mu\nu} + \frac{k_\mu k_\nu}{m_Z^2}]d_f\frac{p_1^\mu}{m_Z}\bar{f}_L\gamma^\nu f_L \tag{11.0.1}$$

and

$$M^{Z'}_{Z\phi\to\bar{f}_L f_L} = 2g_d^3\sqrt{2}d_{\phi_j}^2 v_{\phi_j}s_\theta c_\theta^2\frac{1}{s-m_{Z'}^2}[-g_{\mu\nu} + \frac{k_\mu k_\nu}{m_{Z'}^2}]d_f\frac{p_1^\mu}{m_Z}\bar{f}_L\gamma^\nu f_L \tag{11.0.2}$$

We can see that if we sum up the contributions from the longitudinal degrees of freedom we end up with an expression proportional to $\sqrt{s}$. Unfortunately at tree-level there is no

term that can annihilate that, so processes at one loop level must come and help us correct this behavior. The simplest term that would come to mind is a vertex one, just like we have seen in all previous scattering processes. Indeed if we were in possession of such a term, it would constitute the perfect fit to eliminate longitudinal modes contribution. The reason why this term is not present in our theory is that if we could add that term by hand that would have repercussions on the fermion masses which were accurately measured in the past.

After that is worked out we can analyze what happens to the transverse degrees of freedom as their sum is constant at high energies and corresponds to

$$M^{Z_T+Z'_T}_{Z\phi\to\bar{f}_L f_L} = -2g_d^3\sqrt{2}d^2_{\phi_j}v_{\phi_j}s_\theta\frac{1}{s}d_f\frac{p_1^\mu}{m_Z}\bar{f}_L\gamma_\mu f_L \tag{11.0.3}$$

so that at high energies it becomes

$$M^{Z_T+Z'_T}_{Z\phi\to\bar{f}_L f_L} = g_d^3\sqrt{2}d^2_{\phi_j}v_{\phi_j}s_\theta d_f\frac{1}{m_Z} \tag{11.0.4}$$

and

$$a_0 = \frac{1}{16\pi}\sqrt{2}g_d^3d^2_{\phi_j}v_{\phi_j}s_\theta d_f \tag{11.0.5}$$

that goes to 0 in the small angle approximation

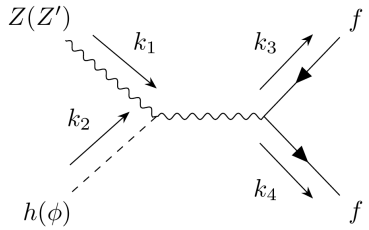

Figure A.12: S diagram. Z/Z' propagator

The next three processes can be all summed up in the diagram above.
Indeed they are all S type processes with a vector boson propagator. Of course, both Z and Z' are going to dress the part resulting in different scattering amplitudes. The initial state is composed of a vector boson and a scalar colliding and the final one is a fermionic line of Standard Model particles.

12 $Zh \to \bar{f}_L f_L$

We have

$$M^Z_{Zh\to\bar{f}_L f_L} = -2\frac{g_w^2}{4}(c_\theta+2\frac{g_d d_H}{g_w}s_\theta)^2 2\sqrt{2}s_\theta v_H g_d d_f \frac{1}{s-m_Z^2}[-g_{\mu\nu}+\frac{k_\mu k_\nu}{m_Z^2}]\frac{p_1^\mu}{m_Z}\bar{f}_L\gamma^\nu f_L \quad (12.0.1)$$

and

$$\begin{aligned} M^{Z'}_{Zh\to\bar{f}_L f_L} &= 2\frac{g_w^2}{4}(c_\theta+2\frac{g_d d_H}{g_w}s_\theta)(s_\theta-2\frac{g_d d_H}{g_w}c_\theta)\times \\ & 2\sqrt{2}c_\theta v_H g_d d_f \frac{1}{s-m_{Z'}^2}[-g_{\mu\nu}+\frac{k_\mu k_\nu}{m_{Z'}^2}]\frac{p_1^\mu}{m_Z}\bar{f}_L\gamma^\nu f_L \end{aligned} \quad (12.0.2)$$

so we can already see that the longitudinal modes will sum up to 0.
Then the transverse ones will contribute to a_0 and will sum up to

$$M^Z_{Zh\to\bar{f}_L f_L} = g_w^2(c_\theta+2\frac{g_d d_H}{g_w}s_\theta)2\sqrt{2}v_H g_d^2 d_f d_H \frac{1}{s}\frac{p_1^\mu}{m_Z}\bar{f}_L\gamma_\mu f_L \quad (12.0.3)$$

so

$$a_0 = \frac{\sqrt{2}}{16\pi}g_w^2(c_\theta+2\frac{g_d d_H}{g_w}s_\theta)v_H g_d^2 d_f d_H \frac{1}{m_Z} \quad (12.0.4)$$

that becomes

$$a_0 = \frac{\sqrt{2}}{16\pi}g_w^2 v_H g_d^2 d_f d_H \frac{1}{m_Z} \quad (12.0.5)$$

and has the bound

$$\sqrt{2}g_w^2 v_H g_d^2 d_f d_H \leq 8\pi m_Z \quad (12.0.6)$$

or

$$g_w^2 v_H g_d d_f d_H \leq 8\pi d_\phi v_\phi \quad (12.0.7)$$

13 $Z'h \to \bar{f}_L f_L$

Here the two contributions are

$$M^{Z}_{Z'h\to\bar{f}_L f_L} = -4\frac{g_w^2}{4}(c_\theta + 2\frac{g_d d_H}{g_w}s_\theta)(s_\theta - 2\frac{g_d d_H}{g_w}c_\theta)\times \\ \sqrt{2}v_H g_d d_f \bar{f}_L\gamma^\mu f_L s_\theta \frac{p_1^\mu}{m_{Z'}}\frac{1}{s-m_Z^2}[-g_{\mu\nu}+\frac{k_\mu k_\nu}{m_Z^2}] \tag{13.0.1}$$

and

$$M^{Z'}_{Z'h\to\bar{f}_L f_L} = 4\frac{g_w^2}{4}(s_\theta - 2\frac{g_d d_H}{g_w}c_\theta)^2\sqrt{2}v_H g_d d_f \bar{f}_L\gamma^\mu f_L c_\theta \frac{p_1^\mu}{m_{Z'}}\frac{1}{s-m_{Z'}^2}[-g_{\mu\nu}+\frac{k_\mu k_\nu}{m_{Z'}^2}] \tag{13.0.2}$$

so we know that the longitudinal part of the propagators is not a problem.
Now onto the transverse modes

$$M^{Z_T+Z'_T}_{Z'h\to\bar{f}_L f_L} = g_w^2(s_\theta - 2\frac{g_d d_H}{g_w}c_\theta)\sqrt{2}v_H g_d d_f \bar{f}_L\gamma_\mu f_L \frac{p_1^\mu}{m_{Z'}}\frac{1}{s}2\frac{g_d d_H}{g_w} \tag{13.0.3}$$

that results in

$$a_0 = -\frac{1}{32\pi}g_w^2(s_\theta - 2\frac{g_d d_H}{g_w}c_\theta)\sqrt{2}v_H g_d d_f \frac{1}{m_{Z'}}2\frac{g_d d_H}{g_w} \tag{13.0.4}$$

in the small angle limit this returns

$$a_0 = \frac{\sqrt{2}}{8\pi}g_d^3 d_H^2 v_H d_f \frac{1}{m_{Z'}} \tag{13.0.5}$$

that yelds the bound

$$g_d^3 d_H^2 v_H d_f \leq \frac{4\pi}{\sqrt{2}}m_{Z'} \tag{13.0.6}$$

or

$$g_d^2 d_H^2 v_H d_f \leq 4\pi d_\phi v_\phi \tag{13.0.7}$$

14 $Z'\phi \to \bar{f}_L f_L$

The argument is the same here of the previous section

$$M^{Z}_{Z\phi\to\bar{f}_L f_L} = 2g_d^3\sqrt{2}d^2_{\phi_j}v_{\phi_j}s^2_\theta c_\theta \frac{1}{s-m_Z^2}[-g_{\mu\nu}+\frac{k_\mu k_\nu}{m_Z^2}]d_f\frac{p_1^\mu}{m_{Z'}}\bar{f}_L\gamma^\nu f_L \tag{14.0.1}$$

and

$$M^{Z'}_{Z\phi\to\bar{f}_L f_L} = 2g_d^3\sqrt{2}d^2_{\phi_j}v_{\phi_j}s_\theta c^3_\theta \frac{1}{s-m_{Z'}^2}[-g_{\mu\nu}+\frac{k_\mu k_\nu}{m_{Z'}^2}]d_f\frac{p_1^\mu}{m_{Z'}}\bar{f}_L\gamma^\nu f_L. \tag{14.0.2}$$

Again we need here contributions at loop-level to destroy the part proportional to the longitudinal degrees of freedom of the boson propagators that grow as $\sqrt{s}$.
When all of that is set and done we can examine the contribution to a_0 coming from the transverse part of the propagator

$$M^{Z_T+Z'_T}_{Z\phi\to\bar{f}_L f_L} = -2g_d^3\sqrt{2}d^2_{\phi_j}v_{\phi_j}c_\theta\frac{1}{s}d_f\frac{p_1^\mu}{m_{Z'}}\bar{f}_L\gamma_\mu f_L \tag{14.0.3}$$

that becomes

$$M^{Z_T+Z'_T}_{Z\phi\to\bar{f}_L f_L} = 2g_d^3\sqrt{2}d^2_{\phi_j}v_{\phi_j}c_\theta d_f\frac{1}{m_{Z'}} \tag{14.0.4}$$

so

$$a_0 = -\frac{\sqrt{2}}{8\pi}g_d^3d^2_{\phi_j}v_{\phi_j}c_\theta d_f\frac{1}{m_{Z'}} = -\frac{1}{8\pi}g_d^2d_\phi d_f c_\theta \tag{14.0.5}$$

so by the formula

$$|Rea_0| \leq \frac{1}{2} \tag{14.0.6}$$

we obtain

$$g_d^2 d_\phi d_f \leq 4\pi \tag{14.0.7}$$

in the small angle approximation

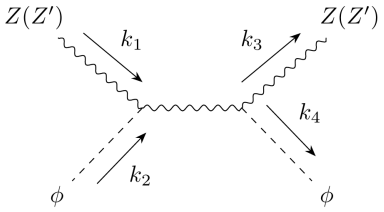

Figure A.13: S-type process

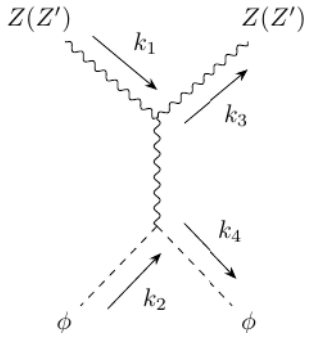

Figure A.14: T-type process

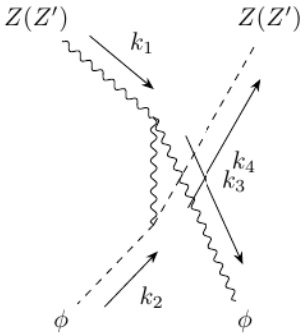

Figure A.15: U-type process

In the last processes we really have two types of diagrams that can be regrouped in one single picture. The difference lies in the propagator, which is going to be either Z or Z'. When that is set we are going to look at S,T and U types processes in which initial and final states are both composed of a vector boson(Z/Z') and a scalar (ϕ/h).

15 $Z\phi \to Zh$

here we pick up the terms

$$\begin{aligned} M^{Z}_{Z\phi\to Zh} = 8g_d^2 d_{\phi_j}^2 v_{\phi_j} s_\theta^2 \frac{g_w^2}{4}(c_\theta + 2\frac{g_d d_h}{g_w}s_\theta)^2 v_H \times \\ \Big[\frac{1}{S-m_Z^2}[-\epsilon_1\cdot\epsilon_3 + \frac{(k_1+k_2)_\mu (k_1+k_2)_\nu}{m_Z^2}\epsilon_1^\mu \epsilon_3^\nu] + \\ \frac{1}{T-m_Z^2}[-\epsilon_1\cdot\epsilon_3 + \frac{(k_1-k_3)_\mu (k_1-k_3)_\nu}{m_Z^2}\epsilon_1^\mu \epsilon_3^\nu] + \\ \frac{1}{U-m_Z^2}[-\epsilon_1\cdot\epsilon_3 + \frac{(k_1-k_4)_\mu (k_1-k_4)_\nu}{m_Z^2}\epsilon_1^\mu \epsilon_3^\nu]\Big] \end{aligned} \tag{15.0.1}$$

and

$$\begin{aligned} M^{Z'}_{Z\phi\to Zh} = -8g_d^2 d_{\phi_j}^2 v_{\phi_j} s_\theta c_\theta \frac{g_w^2}{4}(c_\theta + 2\frac{g_d d_h}{g_w}s_\theta)(s_\theta - 2\frac{g_d d_h s}{g_w}c_\theta) v_H \\ \Big[\frac{1}{S-m_{Z'}^2}[-\epsilon_1\cdot\epsilon_3 + \frac{(k_1+k_2)_\mu (k_1+k_2)_\nu}{m_{Z'}^2}\epsilon_1^\mu \epsilon_3^\nu] + \\ \frac{1}{T-m_{Z'}^2}[-\epsilon_1\cdot\epsilon_3 + \frac{(k_1-k_3)_\mu (k_1-k_3)_\nu}{m_{Z'}^2}\epsilon_1^\mu \epsilon_3^\nu] + \\ \frac{1}{U-m_{Z'}^2}[-\epsilon_1\cdot\epsilon_3 + \frac{(k_1-k_4)_\mu (k_1-k_4)_\nu}{m_{Z'}^2}\epsilon_1^\mu \epsilon_3^\nu]\Big] \end{aligned} \tag{15.0.2}$$

Here

$$\begin{aligned} \epsilon_1^\mu &= \frac{k_1^\mu}{m_Z} + \frac{2m_Z}{T-2m_Z^2}k_3^\mu \\ \epsilon_3^\mu &= \frac{k_3^\mu}{m_Z} + \frac{2m_Z}{T-2m_Z^2}k_1^\mu \end{aligned} \tag{15.0.3}$$

We can already spot some things here based on our experience with previous scattering processes. Indeed if we take both of the contributions coming from the sum of the longitudinal modes of the Z and Z' propagators we obtain something that grows with $\sqrt{s}$. This is not a danger as the sum is proportional to the factor

$$\frac{s_\theta}{m_Z^2}(c_\theta + 2\frac{g_d d_h s}{g_w}s_\theta) - \frac{c_\theta}{m_{Z'}^2}(s_\theta - 2\frac{g_d d_h s}{g_w}c_\theta) = 0 \tag{15.0.4}$$

so that there is no threat at high energies. Of course, this is also true for the subleading terms, as they are proportional to the same factor.

Now for transverse modes, we have that their sum corresponds to

$$M^{Z_T+Z'_T}_{Z\phi\to Zh} = -8g_d^2 d_{\phi_j}^2 v_{\phi_j}\frac{g_w^2}{4}(c_\theta + 2\frac{g_d d_h s}{g_w}s_\theta)2\frac{g_d d_h}{g_w}v_H \epsilon_1\cdot\epsilon_3 s_\theta[\frac{1}{S}+\frac{1}{T}+\frac{1}{U}] \tag{15.0.5}$$

that becomes after the contraction

$$M^{Z_T+Z'_T}_{Z\phi\to Zh} = 8g_d^2 d_{\phi_j}^2 v_{\phi_j}\frac{g_w^2}{4}(c_\theta + 2\frac{g_d d_h s}{g_w}s_\theta)2\frac{g_d d_h}{g_w}v_H \frac{1}{m_Z^2}\frac{3}{4}s_\theta \tag{15.0.6}$$

for the sake of a_0 extraction the part proportional to $\cos\delta$ is negligible and we obtain an expression for a_0 that goes like

$$a_0 = \frac{3}{32\pi} g_d^2 d_{\phi_j}^2 v_{\phi_j} g_w^2 (c_\theta + 2\frac{g_d d_h s}{g_w} s_\theta) \frac{g_d d_h}{g_w} v_H \frac{1}{m_Z^2} s_\theta \tag{15.0.7}$$

Unfortunately, this contribution is proportional to s_θ and goes to 0 in the small angle approximation

16 $Z\phi \to Z'h$

Again we find two contributions here

$$\begin{aligned} M^{Z}_{Z\phi\to Z'h} = 8g_d^2 d^2_{\phi_j} v_{\phi_j} s_\theta^2 \frac{g_w^2}{4}(c_\theta + 2\frac{g_d d_H}{g_w}s_\theta)(s_\theta - 2\frac{g_d d_H}{g_w}c_\theta)v_H \\ \Big[\frac{1}{S-m_Z^2}[-\epsilon_1\cdot\epsilon_3 + \frac{(k_1+k_2)_\mu (k_1+k_2)_\nu}{m_Z^2}\epsilon_1^\mu \epsilon_3^\nu] + \\ \frac{1}{T-m_Z^2}[-\epsilon_1\cdot\epsilon_3 + \frac{(k_1-k_3)_\mu (k_1-k_3)_\nu}{m_Z^2}\epsilon_1^\mu \epsilon_3^\nu] + \\ \frac{1}{U-m_Z^2}[-\epsilon_1\cdot\epsilon_3 + \frac{(k_1-k_4)_\mu (k_1-k_4)_\nu}{m_Z^2}\epsilon_1^\mu \epsilon_3^\nu]\Big] \end{aligned} \tag{16.0.1}$$

and

$$\begin{aligned} M^{Z'}_{Z\phi\to Z'h} = -8g_d^2 d^2_{\phi_j} v_{\phi_j} s_\theta c_\theta \frac{g_w^2}{4}(c_\theta + 2\frac{g_d d_H}{g_w}s_\theta)^2 v_H \\ \Big[\frac{1}{S-m_{Z'}^2}[-\epsilon_1\cdot\epsilon_3 + \frac{(k_1+k_2)_\mu (k_1+k_2)_\nu}{m_{Z'}^2}\epsilon_1^\mu \epsilon_3^\nu] + \\ \frac{1}{T-m_{Z'}^2}[-\epsilon_1\cdot\epsilon_3 + \frac{(k_1-k_3)_\mu (k_1-k_3)_\nu}{m_{Z'}^2}\epsilon_1^\mu \epsilon_3^\nu] + \\ \frac{1}{U-m_{Z'}^2}[-\epsilon_1\cdot\epsilon_3 + \frac{(k_1-k_4)_\mu (k_1-k_4)_\nu}{m_{Z'}^2}\epsilon_1^\mu \epsilon_3^\nu]\Big] \end{aligned} \tag{16.0.2}$$

here again the longitudinal modes are shut down by the factor

$$\frac{s_\theta}{m_Z^2}(c_\theta + 2\frac{g_d d_h s}{g_w}s_\theta) - \frac{c_\theta}{m_{Z'}^2}(s_\theta - 2\frac{g_d d_h s}{g_w}c_\theta) = 0 \tag{16.0.3}$$

And then the contribution coming from the transverse degrees of freedom originates an a_0 term which is unfortunately proportional to s_θ and thus can be neglected.

17 $Z'\phi \to Z'h$

The two scattering amplitudes here are

$$\begin{aligned} M^{Z}_{Z\phi\to Zh} = -8g_d^2 d^2_{\phi_j} v_{\phi_j} s_\theta c_\theta \frac{g_w^2}{4}(c_\theta + 2\frac{g_d d_H}{g_w}s_\theta)(s_\theta - 2\frac{g_d d_H}{g_w}c_\theta)v_H \\ \Big[\frac{1}{S-m_Z^2}[-\epsilon_1\cdot\epsilon_3 + \frac{(k_1+k_2)_\mu (k_1+k_2)_\nu}{m_Z^2}\epsilon_1^\mu \epsilon_3^\nu] + \\ \frac{1}{T-m_Z^2}[-\epsilon_1\cdot\epsilon_3 + \frac{(k_1-k_3)_\mu (k_1-k_3)_\nu}{m_Z^2}\epsilon_1^\mu \epsilon_3^\nu] + \\ \frac{1}{U-m_Z^2}[-\epsilon_1\cdot\epsilon_3 + \frac{(k_1-k_4)_\mu (k_1-k_4)_\nu}{m_Z^2}\epsilon_1^\mu \epsilon_3^\nu]\Big] \end{aligned} \tag{17.0.1}$$

and

$$\begin{aligned} M^{Z'}_{Z\phi\to Zh} = 8g_d^2 d^2_{\phi_j} v_{\phi_j} c_\theta^2 \frac{g_w^2}{4}(s_\theta - 2\frac{g_d d_H}{g_w}c_\theta)^2 v_H \\ \Big[\frac{1}{S-m_{Z'}^2}[-\epsilon_1\cdot\epsilon_3 + \frac{(k_1+k_2)_\mu (k_1+k_2)_\nu}{m_{Z'}^2}\epsilon_1^\mu \epsilon_3^\nu] + \\ \frac{1}{T-m_{Z'}^2}[-\epsilon_1\cdot\epsilon_3 + \frac{(k_1-k_3)_\mu (k_1-k_3)_\nu}{m_{Z'}^2}\epsilon_1^\mu \epsilon_3^\nu] + \\ \frac{1}{U-m_{Z'}^2}[-\epsilon_1\cdot\epsilon_3 + \frac{(k_1-k_4)_\mu (k_1-k_4)_\nu}{m_{Z'}^2}\epsilon_1^\mu \epsilon_3^\nu]\Big] \end{aligned} \tag{17.0.2}$$

With the same tricks as before, we can manage to get rid of the longitudinal modes and of all the possible problems at high energies.
We can use

$$\begin{aligned} \epsilon_1^\mu = \frac{k_1^\mu}{m_{Z'}} + \frac{2m_{Z'}}{T-2m_{Z'}^2}k_3^\mu \\ \epsilon_3^\mu = \frac{k_3^\mu}{m_{Z'}} + \frac{2m_{Z'}}{T-2m_{Z'}^2}k_1^\mu \end{aligned} \tag{17.0.3}$$

The calculations are the exact same as the ones we have already carried out in the previous sections, with the exact same variables. The only difference is placed in massive factors that we can clearly control and substitute thanks to the Mandelstam's variables definitions

$$\begin{aligned} S = (k_1^\mu + k_2^\mu)^2 = (k_3^\mu + k_4^\mu)^2 = m_{Z'}^2 + m_\phi^2 + 2k_1\cdot k_2 = m_{Z'}^2 + m_h^2 + 2k_3\cdot k_4 \\ T = (k_1^\mu - k_3^\mu)^2 = (k_2^\mu - k_4^\mu)^2 = 2m_{Z'}^2 - 2k_1\cdot k_3 = m_\phi^2 + m_h^2 - 2k_2\cdot k_4 \\ U = (k_1^\mu - k_4^\mu)^2 = (k_2^\mu - k_3^\mu)^2 = m_{Z'}^2 + m_h^2 - 2k_1\cdot k_4 = m_{Z'}^2 + m_\phi^2 - 2k_2\cdot k_3 \end{aligned} \tag{17.0.4}$$

Unfortunately for us, this goes exactly like all the ones bearing proportionality to d_H so it will dwindle until it goes to 0 in the small angle approximation.

18 $\phi\phi \to \phi\phi$

Finally, we analyze here the purely dark scalars scattering. The truth is that here the dominant term is purely the vertex one

$$M_{\phi\phi\to\phi\phi} = -\frac{\lambda_\phi}{4} 4! = -6\lambda_\phi \tag{18.0.1}$$

we can rearrange by knowing that $\lambda_\phi = \frac{\mu_\phi^2}{v_\phi^2}$ and that $m_\phi^2 = \mu_\phi^2$. We have incorporated the multiplicity factor due to the fact that the final and initial particles are identycal, we can straight away write

$$a_0 = -\frac{1}{32\pi} 6 \frac{m_\phi^2}{4v_\phi^2} = -\frac{3}{64\pi}\frac{m_\phi^2}{v_\phi^2} \tag{18.0.2}$$

Appendix B

The Standard Model of particles

1 Introduction

In this one, it is our interest to summarize the main points and properties characterizing the standard model of particles. To begin with, as with all models of particle physics, it is of primary importance to specify, such as the gauge group and the matter content. First, we have to consider the fact that the standard model is a theory of particles of spins 0, $\frac{1}{2}$ and 1 which of course are divided into fermions and bosons. Fermions can be regrouped into three generations and they present different properties as they behave differently under SM gauge group.
Speaking of which, SM gauge group G is

$$G = SU(3)_c \otimes SU(2)_L \otimes U(1)_Y. \tag{1.0.1}$$

The matter fields are fermions of spin $\frac{1}{2}$ that are divided into quarks and leptons. Quarks and leptons come into three generations to which we can attach the index $i = 1, 2, 3$. In each generation of quark we can find an up-type u^i and a d-type d^i that respectively show electric charges of $+\frac{2}{3}$ and $-\frac{1}{3}$. This kind of division is followed also in the case of leptons, where we find a lepton with electric charge -1 coupled with a neutrino with no electric charge. This scheme is respected for all fermions, which share identical properties except for their masses
Quarks are organized in triplets of color with index $\alpha = 1, 2, 3$ which from now on we suppress for the sake of notation. Moreover with respect to $SU(2)_L$ the fermions are organized in:

- $SU(2)_L$ doublets $Q^i_L = \begin{pmatrix} u^i_L \\ d^i_L \end{pmatrix}$ and $L^i_L = \begin{pmatrix} v^i_L \\ e^i_L \end{pmatrix}$
- $SU(2)_L$ singlets which are charged under $U(1)_Y$ and so present hypercharge Y. They are U^i_R, d^i_R, e^i_R and v^i_R.

For the generic case of $SU(N)$ from group theory we know that it possesses a number of $N^2 - 1$ generators. This allows us to see that from $SU(3)$ we derive 8 gluons, from $SU(2)_L \otimes U(1)_Y$ we get the electroweak bosons $W^{\pm}$, Z and γ. SM group G is subject to

spontaneous symmetry breaking from which we recover

$$SU(3)_c \otimes SU(2)_L \otimes U(1)_Y \rightarrow SU(3)_c \otimes U(1)_{em} \tag{1.0.2}$$

Thanks to the Higgs mechanism we are able to produce this way masses for all fermions and preserve the photon massless, given that electromagnetism stays a symmetry of this model.
Finally, the last piece of this picture is represented by the Higgs boson ϕ which is a complex scalar of spin 0 and a doublet of the weak isospin.
Thanks to all this information we are able to write the SM lagrangian :

$$\begin{aligned} L_{SM} &= L_{kin}^{gauge} + L_{kin}^{fermion} + L_{kin}^{Higgs} + L_{pot}^{Higgs} + L_{yuk} \\ &= -\frac{1}{4}F_{\mu\nu}F^{\mu\nu} + i\bar{\psi}\gamma^{\mu}D_{\mu}\psi + (D_{\mu}\phi)^{+}D^{\mu}\phi + \mu^2\phi^{+}\phi - \frac{1}{2}\lambda(\phi^{+}\phi)^2 + \bar{\psi}y\phi\psi \end{aligned} \tag{1.0.3}$$

All the masses for fermions and bosons are acquired via Higgs mechanism. The spontaneous symmetry breaking produces a non-trivial vacuum expectation value in which

$$< \phi >= v = 174\ GeV. \tag{1.0.4}$$

This enables the creation of masses for fermions through the Yukawa term.
For the bosons instead, masses are acquired through the same mechanism inside the Higgs kinetic term. In fact, it makes use of the covariant derivative to couple Higgs and electroweak bosons through

$$D_{\mu} = d_{\mu} + gA_{\mu}. \tag{1.0.5}$$

2 $SU(3)_c$

Let's dive some more into the mathematical structure of SM lagrangian [48].Here for the gluons

$$G_{\mu\nu}^{a} = d_{\mu}G_{\nu}^{a} - d_{\nu}G_{\mu}^{a} + g_s f^{abc}G_{\mu,a}G_{\nu,b}. \tag{2.0.1}$$

a is the color index,g_s is the coupling constant and f^{abc} are group structure constants with

$$[T^a, T^b] = if^{abc}T^c \tag{2.0.2}$$

where Ta are the generators of the $SU(3)_c$ group.
The covariant derivative for a generic quark field here has the form

$$D_{\mu}q = (d_{\mu} - ig_s G_{\mu}^{a}T^{a})q \tag{2.0.3}$$

with of course T^a being the group generators in the chosen representation, in the fundamental one they are $T^a = \frac{1}{2}\lambda^a$ with λ^a being the Gell-Mann matrices.

3 $SU(2)_L \otimes U(1)_Y$

For the $SU(2)_L$ group

$$W^a_{\mu\nu} = d_\mu W^a_\nu - d_\nu W^a_\mu + g\epsilon^{abc} W^b_\mu W^c_\nu \qquad (a = 1, 2, 3) \tag{3.0.1}$$

The fundamental representation has $T^a = \frac{\sigma^a}{2}$ with σ^a being the Pauli matrices. ϵ here is the completely antisymmetric tensor. The covariant derivative for a generic left-handed field ψ_L transforming under this representation is

$$D_\mu \psi_L = (d_\mu - igW^a_\mu T^a)\psi_L \tag{3.0.2}$$

For what concerns $U(1)_Y$ we have

$$B_{\mu\nu} = d_\mu B_\nu - d_\nu B_\mu \tag{3.0.3}$$

and the covariant derivative acts here on a generic field ψ as

$$D_\mu \psi = (d_\mu - ig' Y B_\mu)\psi \tag{3.0.4}$$

with Y being the hypercharge of the field which is also connected to the electric charge through the equation

$$Q = T_{3L} + Y \tag{3.0.5}$$

If we rewrite the covariant derivative applied to a left-handed field with hypercharge Y in terms of $W^\pm$, Z^μ and A^μ it can be proved to be

$$D_\mu \psi_L = [d_\mu - i\frac{g}{\sqrt{2}}(\sigma^+ W^+_\mu \sigma^- W_\mu) - ieQA_\mu - i\frac{g}{cos\theta_W}(\frac{\sigma_3}{2} - Q\sin^2\theta_W)Z_\mu)]\psi_L \tag{3.0.6}$$

with the relation

$$g' \cos\theta_W = g \sin\theta_W = e \tag{3.0.7}$$

For a right-handed field

$$D_\mu \psi_R = [d_\mu - ieQA_\mu - i\frac{g}{\cos\theta_W} Q \sin^2\theta_W Z_\mu]\psi_R \tag{3.0.8}$$

So the quantum numbers are

Field	l_L	l_R	v_L	u_L	d_L	u_R	d_R	ϕ^+	ϕ^0
T_3	$-\frac{1}{2}$	0	$\frac{1}{2}$	$\frac{1}{2}$	$-\frac{1}{2}$	0	0	$\frac{1}{2}$	$-\frac{1}{2}$
Y	$-\frac{1}{2}$	-1	$-\frac{1}{2}$	$\frac{1}{6}$	$\frac{1}{6}$	$\frac{2}{3}$	$-\frac{1}{3}$	$\frac{1}{2}$	$\frac{1}{2}$
Q	-1	-1	0	$\frac{2}{3}$	$-\frac{1}{3}$	$\frac{2}{3}$	$-\frac{1}{3}$	1	0

4 The gauge and fermion lagrangian

So for the gauge sector we have

$$L_{gauge} = -\frac{1}{4} G^a_{\mu\nu} G^{a\mu\nu} - \frac{1}{4} W^a_{\mu\nu} W^{a\mu\nu} - \frac{1}{4} B_{\mu\nu} B^{\mu\nu} \tag{4.0.1}$$

For the fermionic part we write here only the kinetic sector, which corresponds to

$$L^{kin}_{Fermion} = \sum_{quarks} i\bar{q}\gamma^\mu D_\mu q + \sum_{\psi_L} i\bar{\psi_L}\gamma^\mu D_\mu \psi_L + \sum_{\psi_R} i\bar{\psi_R}\gamma^\mu D_\mu \psi_R \tag{4.0.2}$$

in which each covariant derivative is obtained through the rules that we have explained above.

5 The Higgs lagrangian

The Higgs doublet is included in the standard model and assumes the form

$$\Phi = \begin{pmatrix} \phi^+ \\ \frac{v+H+i\phi_Z}{\sqrt{2}} \end{pmatrix} \tag{5.0.1}$$

so these terms figure inside the covariant derivative as

$$D_\mu \Phi = [d_\mu - i\frac{g}{\sqrt{2}}(\sigma^+ W^+ + \sigma^- W^-) - ieQA_\mu - i\frac{g}{\cos\theta_W}(\frac{\sigma^3}{2} - Q\sin^2\theta_W)Z_\mu]\Phi \tag{5.0.2}$$

since $Y_\Phi = -\frac{1}{2}$ and for Φ we have that

$$Q = \begin{pmatrix} 1 & 0 \\ 0 & 0 \end{pmatrix} \tag{5.0.3}$$

So as we previously have introduced, the Higgs lagrangian has the form

$$L_{Higgs} = (D_\mu \Phi)^+ (D^\mu \Phi) + \mu^2 \Phi^+ \Phi - \lambda(\Phi^+ \Phi)^2. \tag{5.0.4}$$

One can see after a brief calculus that

$$v^2 = \frac{\mu^2}{\lambda} \qquad m_h^2 = 2\mu^2 \qquad \lambda = \frac{g^2}{8}\frac{m_h^2}{m_W^2} \tag{5.0.5}$$

So if we expand the Lagrangian using the expression that we have written previously for Φ, we find that we recover, after the proper diagonalization, the terms

$$L_{Higgs} = ... + \frac{1}{2}m_Z^2 Z^\mu Z_\mu + m_W^2 W_\mu^+ W^{\mu-} + \ interactions \tag{5.0.6}$$

from this, we are able to recover the expressions for the masses of the electroweak bosons

$$m_W = \frac{1}{2}gv \qquad m_Z = \frac{1}{\cos\theta_W}\frac{1}{2}gv = \frac{1}{\cos\theta_W}m_W. \tag{5.0.7}$$

6 Yukawa lagrangian

This piece of the SM lagrangian combines the Higgs field with the leptons and quarks fields. After the spontaneous symmetry breaking, where the Higgs field acquires a non-trivial vacuum expectation value, it is this very piece of information that gives rise to the masses for fermions. let's see it in more detail writing the form of the Yukawa lagrangian:

$$L_{yukawa} = -\overline{L_L} Y_l \Phi l_R - \overline{Q_L} Y_d \Phi d_R - \overline{Q_L} Y_u \tilde{\Phi} u_R + h.c. \tag{6.0.1}$$

and

$$\tilde{\Phi} = i\sigma_2 \Phi^* = \begin{pmatrix} \frac{v+H-i\phi_Z}{\sqrt{2}} \\ -\phi^- \end{pmatrix} \tag{6.0.2}$$

and Y_l, Y_d and Y_u are 3×3 matrices in the flavor space.
Let's skip to mass basis through the change

$$\begin{aligned} \overline{u_L} &\longrightarrow \overline{u_L} U_{uL}^+ \qquad & \overline{d_L} &\longrightarrow \overline{d_L} U_{dL}^+ \\ u_R &\longrightarrow U_{uR} u_R & d_R &\longrightarrow U_{dR} d_R \end{aligned} \tag{6.0.3}$$

so that we can employ a biunitary transformation to diagonalize the mass matrices, so that they become

$$\begin{aligned} \frac{v}{\sqrt{2}} U_{uL}^+ Y_u U_{uR} &= M_u = diag(m_u, m_c, m_t) \\ \frac{v}{\sqrt{2}} U_{dL}^+ Y_d U_{dR} &= M_d = diag(m_d, m_s, m_b). \end{aligned} \tag{6.0.4}$$

It can be seen that the Higgs coupling to quarks becomes diagonal

$$-L_{Yuk,H} = (1 + \frac{h}{v})[\bar{u} M_u u + \bar{d} M_d d]. \tag{6.0.5}$$

Nothing happens to the couplings with Z^μ and A^μ that continue to be diagonal. The changes occur with the W coupling. In fact, we can see that this piece of lagrangian has the form

$$-L_W = \frac{g}{\sqrt{2}} \bar{u_L} \gamma^\mu d_L W_\mu^+ + h.c. \tag{6.0.6}$$

Given that the two quarks transform with different matrices, they produce a new factor inside this expression when we turn to mass basis:

$$-L_W = \frac{g}{\sqrt{2}} \bar{u_L} V_{CKM} \gamma^\mu d_L W_\mu^+ + h.c. \tag{6.0.7}$$

with

$$V_{CKM} = U_{uL}^+ U_{dL} \tag{6.0.8}$$

being the Cabibbo-Kobayashi-Maskawa matrix.
Moreover, we can see that in SM there are no right-handed neutrinos. This means that neutrinos here can be taken as massless, hence can be rotated in order to balance the transformation of the charged quark needed to diagonalize Y_l. Thus we have in the leptonic sector:

$$Y_l = diag(m_e, m_\mu, m_\tau) \qquad and \qquad V = 1 \tag{6.0.9}$$

7 The complete SM lagrangian

A the end we recover the expression

$$L_{SM} = L_{gauge} + L_{Fermion} + L_{Higgs} + L_{Yukawa} \tag{7.0.1}$$

8 Anomalies

We recognize the crucial importance that symmetries have in quantum theories. We have talked extensively about $SU(3)_c \otimes SU(2)_L \otimes U(1)_Y$ in the previous sections to be the symmetry whose breaking shapes the world that we experience at particle level.
Whenever a symmetry of a classical theory is not anymore a symmetry at quantum level with the same lagrangian, that symmetry is called an anomaly. Now given the importance that we have recognized in symmetries for QFTs, we can understand that anomalies are important as well. We are going to show in the following paragraphs the implications of anomalies in the standard model and how these characterize some of the most important results studied in QFT courses.
In particular, an anomaly has the effect of making the resulting current not conserved. There are theories like QED where the current couples to a massless spin-1 particle. Then we can see that if the current is not conserved, the Ward identity results violated, thus longitudinal polarizations will be produced and unitarity will be violated.
The requirement for the Standard Model to be anomaly free is actually of great importance too, so that it leads to the quantization of the electric charge all by itself in tandem with the quark and lepton charges to be linked.
Let's draw the first line between the two major anomaly categories: gauge anomalies and global anomalies.
As the name suggests, a gauge anomaly requires a gauge boson as part of the symmetry and, on the contrary, a global anomaly does not.
Notice that global anomalies are not a problem. As it appears the Standard Model itself is full of such anomalies and many of them are actually important to explain some observations and do not lead to inconsistencies. For example, the symmetry associated to the baryon number conservation is anomalous. In fact, this symmetry produces, by Noether theorem, the current $J^{\mu}_{baryon} = \sum_i \bar{q}_i \gamma^{\mu} q_i.$, which can be proven to be anomalous. Fortunately, there is no massless spin-1 boson coupling to this current in the Standard Model, so, as we have said, this does not generate inconsistencies, on the contrary, baryon number violation has its relevant importance, as it explains the overabundance of matter over antimatter. We recognize this to be one of the only three conditions imposed by Sakharov in order to explain matter-antimatter asymmetry.
So gauge anomalies are the only problem that can threaten Standard Model's validity. In the following paragraph, we are going to see first the general result linked to the divergence of a current associated to a gauge anomaly.

9 Anomalos gauge symmetries

The history of anomalies is closely related to the pion decay $\pi^0 \to \gamma\gamma$ [49]. The importance of this process and its study lies in the fact that by calculating its rate, we are able also

to grasp the actual color number of quarks $N_c = 3$. In fact, by matching the experimental value we obtain, with the theoretical one we estimated, which depends solely on N_c we are also able to acquire this particular value.
The connection to anomalies lies in the historical difficulty in calculating this particular rate. In 1969, thanks to the recent progress in quantum field theory, the scientists Alder, Bell and Jackiw were able to relate mathematically the calculation of the rate of $\pi^0 \to \gamma\gamma$ to anomalies.
To see this let's first study symmetries in QED lagrangian:

$$\begin{aligned} L_{QED} &= \bar{\psi}(i\not{d} - e\not{A} - m)\psi \\ &= \bar{\psi_L}(i\not{d} - e\not{A})\bar{\psi_L} + \bar{\psi_R}(i\not{d} - e\not{A})\bar{\psi_R} - m\bar{\psi_L}\psi_R - m\bar{\psi_R}\psi_L \end{aligned} \tag{9.0.1}$$

In the massless limit this lagrangian has vector and axial symmetries:

$$\psi \to e^{i\alpha}\psi \qquad \psi \to e^{i\beta\gamma_5}\psi \tag{9.0.2}$$

which produce respectively the vector and axial-vector currents

$$J^\mu = \bar{\psi}\gamma^\mu\psi \qquad J^{\mu 5} = \bar{\psi}\gamma^\mu\gamma_5\psi \tag{9.0.3}$$

Equations of motion imply that

$$d_\mu J^\mu = 0 \qquad d_\mu J^{\mu 5} = 2im\bar{\psi}\gamma_5\psi \tag{9.0.4}$$

so one can see that classically the axial symmetry is only conserved in the massless limit. It can be proven that, including quantum corrections,

$$d_\mu J^{\mu 5} = 2im\bar{\psi}\gamma_5\psi + \frac{e^2}{16\pi^2}\epsilon^{\mu\nu\rho\sigma}F_{\mu\nu}F_{\rho\sigma}. \tag{9.0.5}$$

This result can be obtained by looking at the calculation of the loop diagram shown above for the process $\pi^0 \to \gamma\gamma$.
This result shows that in presence of an electromagnetic field, the axial current cannot be conserved. This happens whether or not we are in the massless limit. So we have that even if $m = 0$, we still have $d_\mu J^{\mu 5} \neq 0$. Instead, we have seen that classically, in the massless limit, $d_\mu J^{\mu 5} = 0$. This behavior can be explained only if the cause of violation was the quantum effects. This means that the axial-vector symmetry is anomalous, based on our previous definition.
What happens in the general case is that we want to see that $d_\mu J^\mu = 0$ and $d_\mu J^{5\mu} = 0$ are still valid when we add quantum corrections. In order to do this we calculate the three point function

$$< J^{\alpha 5}(x)J^\mu(y)J^\nu(z) > \tag{9.0.6}$$

and we verify that

$$\frac{d}{dx^\mu} < J^{\alpha 5}(x)J^\mu(y)J^\nu(z) >= 0 \tag{9.0.7}$$

using Feynman diagrams.
If we move to momentum space this can be translated in

$$p_\mu M_5^{\alpha\mu\nu} = 0 \tag{9.0.8}$$

where the amplitude is given by the formula

$$\begin{aligned} iM_5^{\alpha\mu\nu}(p,q1,q2)(2\pi)^4\delta^4(p-q1-q2) \\ = \int d^4xd^4yd^4ze^{-ipx}e^{iq1y}e^{iq2z} < J^{\alpha 5}(x)J^{\mu}(y)J^{\nu}(z) > \\ = \int d^4xd^4yd^4ze^{-ipx}e^{iq1y}e^{iq2z} < [\psi\bar{(}x)\gamma^{\alpha}\gamma^5\psi(x)][\psi\bar{(}y)\gamma^{\mu}\psi(y)][\psi\bar{(}z)\gamma^{\mu}\psi(z)] > \end{aligned} \tag{9.0.9}$$

After a long and complex mathematical procedure what we get is

$$p_{\alpha}M_5^{\alpha\mu\nu} = \frac{1}{4\pi^2}\epsilon^{\mu\nu\rho\sigma}q1^{\rho}q2^{\sigma} \qquad q_{\mu}^1M_5^{\alpha\mu\nu} = 0 \tag{9.0.10}$$

this reconfirms the fact that the vector current is conserved and the axial current not and corresponds precisely to what we have gained in the previous equation with the new term calculated in the equation for the axial current. In fact, the result obtained correspond to a modification of the axial current by the factor

$$\frac{e^2}{16\pi^2}\epsilon^{\mu\nu\rho\sigma}F_{\mu\nu}F_{\rho\sigma} \tag{9.0.11}$$

It should be noticed that the result obtained is not susceptible to contributions coming from higher order loops, but only from triangle diagrams like the one in FIGURE and that the anomaly is independent of fermion masses and the anomalous term arises in the massless case too.

10 Gauge anomalies in the Standard Model

Here we know that the gauge group is $G = SU(3)_c \otimes SU(2)_L \otimes U(1)_Y$. This produces the three currents J_{μ}^{QCD}, J_{μ}^{weak} and J_{μ}^{Y}. This means that, with the same reasoning as before, we need to check that

$$d_{\mu} < J_{\mu}^j J_{\alpha}^k J_{\nu}^l >= 0 \tag{10.0.1}$$

for j, k, l any of these forces in order for the Standard Model to be anomaly free.
It can be shown that here, like in the QED case, there is a term that needs to be added and that is present even in the massless case, originated by quantum corrections.
In general, when it comes to non-abelian gauge theories, we always obtain conserved currents of the type

$$J_{\mu}^{\alpha} = \sum_{\psi} \bar{\psi}_i T_{ij}^{\alpha}\gamma^{\mu}\psi_j \tag{10.0.2}$$

where T_{ij}^{α} are the generators of the symmetry in the chosen representation.
This means that when we approach the triangle diagrams in calculation, those acquire a factor proportional to T^a. In particular, the two ways momentum can flow, give a result of this kind:

By using our knowledge of the commutators, we can rewrite the expression inside the brackets as

$$tr[T^aT^bT^c] = \frac{1}{2}tr[[T^a,T^b]T^c] + \frac{1}{2}tr[\{T^a,T^b\}T^c] = i\frac{1}{2}T_R f^{abc} + \frac{1}{4}d_R^{abc} \tag{10.0.3}$$

The factor proportional to f^{abc} gives the difference between the two loops and is UV divergent. Although this can be reabsorbed in the renormalization of the $f^{abc}A^a_\mu A^b_\nu d_\mu A^c_\nu$ and gives no contribution. Instead, the contribution from d^{abc}_R is a totally symmetric tensor and is a factor of the kind

$$d^{abc}_R = 2tr[T^a_R\{T^b_R, T^c_R\}] \tag{10.0.4}$$

For $SU(N)$ there is a unique totally symmetric three indices tensor up to a constant, so we can rewrite this contribution as

$$[T^a_R\{T^b_R, T^c_R\}] = A(R)tr[T^a\{T^b, T^c\}] = A(R)d^{abc} \tag{10.0.5}$$

for any representation.
$A(R)$ is the anomaly coefficient and d^{abc} is defined using the fundamental representation so that $A(fund) = 1$. The contribution we obtain is the one that sums the two triangle diagrams.
Consider the case $U(1)^3_Y$, we get a result of the type

$$d_\alpha J^a_\alpha = \big(\sum_{left} A(R_l) - \sum_{right} A(R_r)\big)\frac{g^2}{128\pi^2}d^{abc}\epsilon^{\mu\nu\alpha\beta}F^b_{\mu\nu}F^c_{\alpha\beta} \tag{10.0.6}$$

where we sum over left-handed particles with the anomaly coefficient $A(R_l)$ in their representation R_l and do the same for the right-handed particles. Before proceeding, let's remind ourselves of the charges of the Standard Model particles with respect to the three symmetry groups:

Field	$SU(3)_c$	$SU(2)_L$	$U(1)_Y$	T_3	Q	$Y = Q - T_3$
$L = \begin{pmatrix} v \\ e \end{pmatrix}$	*1*	*2*	$-\frac{1}{2}$	$\begin{pmatrix} +\frac{1}{2} \\ -\frac{1}{2} \end{pmatrix}$	$\begin{pmatrix} 0 \\ -1 \end{pmatrix}$	$\begin{pmatrix} -\frac{1}{2} \\ -\frac{1}{2} \end{pmatrix}$
$Q = \begin{pmatrix} u \\ d \end{pmatrix}$	*3*	*2*	$\frac{1}{6}$	$\begin{pmatrix} +\frac{1}{2} \\ -\frac{1}{2} \end{pmatrix}$	$\begin{pmatrix} \frac{2}{3} \\ -\frac{1}{3} \end{pmatrix}$	$\begin{pmatrix} \frac{1}{6} \\ \frac{1}{6} \end{pmatrix}$
e_R	*1*	*1*	1	0	1	1
u_R	*3*	*1*	$-\frac{2}{3}$	0	$-\frac{2}{3}$	$-\frac{2}{3}$
d_R	*3*	*1*	$\frac{1}{3}$	0	$\frac{1}{3}$	$\frac{1}{3}$

Let's go back to the previous equation. We can see that for $U(1)_Y$ $T^a = 1$ and $d^{abc} = 4$ so

$$d_\mu J^\mu_y = \big(\sum_{left} Y^3_l - \sum_{right} Y^3_r\big)\frac{g'^2}{32\pi^2}d^{abc}\epsilon^{\mu\nu\alpha\beta}B_{\mu\nu}B_{\alpha\beta} \tag{10.0.7}$$

just plugging in the hypercharges, we obtain the desired result

$$(2Y^3_L - Y^3_e - Y^3_v) + 3(2Y^3_Q - Y^3_u - Y^3_d) = 0 \tag{10.0.8}$$

where $Y_L, Y_e, Y_v, Y_Q, Y_u, Y_d$ are the hypercharges of left-handed leptons, right-handed electrons, right-handed neutrinos, left-handed quarks, right-handed up quarks and right-handed down quarks.
For $SU(2)^3$ we can see that the anomalous factor is proportional to $\{\sigma^a, \sigma^b\} = \frac{1}{2}\delta^{ab}\mathbb{1}$ so that $d^{abc} = \delta^{bc}tr(\sigma^a) = 0$, so any $SU(2)^3$ gauge anomaly vanishes.
QCD is non-chiral, so there can never be any $SU(3)^3_{QCD}$ anomaly.
A $SU(N)U(1)^2$ anomaly is proportional to $2tr[T^a\{1,1\}] = 4tr[T^a] = 0$ so it always vanishes. The same is for any anomaly of this kind with a factor of $SU(2)$ or $SU(3)$
We are left with $SU(3)^2U(1)$ and $SU(2)^2U(1)$.
Let's take $SU(3)^2_{QCD}U(1)$. and let's use $tr[T^aT^b] = \frac{1}{2}\delta^{ab}$ which holds for any $SU(N)$. This brings

$$2tr[T^a\{T^b, T^c\}] = 2\delta^{ab}(\sum_{left\ colored} Y_l - \sum_{right\ colored} Y_r) = 2\delta^{ab}(6Y_Q - 3Y_u - 3Y_d) \quad (10.0.9)$$

and plugging in the hypercharges we can see that the result vanishes.
Let's take in examination the case of $SU(2)^2U(1)$, which takes contribution only from left-handed fields:

$$2tr[\sigma^a\{\sigma^b, Y\}] = 2\delta^{ab}\sum_{left} Y_i = 2\delta^{ab}(2Y_L + 6Y_Q) \quad (10.0.10)$$

One can see that left-handed fermion have -3 times the hypercharge of the left-handed quarks, so that the anomaly vanishes.
This ends the demonstration of the fact that all the possible anomalies of the gauge group $G = SU(3)_c \otimes SU(2)_L \otimes U(1)_Y$ vanish.

Bibliography

References

[1] [1]
Elena Accomando et al. *Z', Higgses and heavy neutrinos in $U(1)'$ models: from the LHC to the GUT scale*. Apr. 2017. DOI: 10.1007/JHEP07(2016)086. URL: http://arxiv.org/abs/1605.02910 (visited on 09/07/2022).

[2] [2]
A. Arbey and F. Mahmoudi. "Dark matter and the early Universe: a review". In: *Progress in Particle and Nuclear Physics* **119** (July 2021). DOI: 10.1016/j.ppnp.2021.103865. URL: http://arxiv.org/abs/2104.11488 (visited on 08/04/2022).

[3] [3]
Edward A. Baltz. *Dark Matter Candidates*. Dec. 2004. URL: http://arxiv.org/abs/astro-ph/0412170 (visited on 08/06/2022).

[4] [4]
Martin Bauer et al. "Dark Matter in Anomaly-Free Gauge Extensions". In: *SciPost Physics* **5**.4 (Oct. 2018). DOI: 10.21468/SciPostPhys.5.4.036. URL: http://arxiv.org/abs/1805.01904 (visited on 09/07/2022).

[5] [5]
Gianfranco Bertone and Dan Hooper. "A History of Dark Matter". In: *Reviews of Modern Physics* **90**.4 (Oct. 2018). DOI: 10.1103/RevModPhys.90.045002. URL: http://arxiv.org/abs/1605.04909 (visited on 08/05/2022).

[6] [6]
Gianfranco Bertone, Dan Hooper, and Joseph Silk. "Particle Dark Matter: Evidence, Candidates and Constraints". In: *Physics Reports* **405**.5 (Jan. 2005). DOI: 10.1016/j.physrep.2004.08.031. URL: http://arxiv.org/abs/hep-ph/0404175 (visited on 08/04/2022).

[7] [7]
Oliver Buchmueller, Caterina Doglioni, and Lian-Tao Wang. "Search for dark matter at colliders". In: *Nature Physics* **13**.3 (Mar. 2017). DOI: 10.1038/nphys4054. URL: http://arxiv.org/abs/1912.12739 (visited on 08/08/2022).

[8] [8]
César A. Chacón-Cardona and Rigoberto A. Casas-Miranda. "Millennium Simulation Dark Matter Haloes: Multi-fractal and Lacunarity Analysis with Homogeneity Transition". In: *Monthly Notices of the Royal Astronomical Society*

427.3 (Dec. 2012). DOI: 10.1111/j.1365-2966.2012.22095.x. URL: http://arxiv.org/abs/1209.2637 (visited on 08/05/2022).

[9] [9]
M S Chanowitz, M A Furman, and I Hinchliffe. "WEAK INTERACTIONS OF ULTRA HEAVY FERMIONS (II)". In: ().

[10] [10]
Marco Cirelli. "Dark Matter phenomenology". In: ().

[11] [11]
ATLAS Collaboration. "Search for dark matter produced in association with a hadronically decaying vector boson in pp collisions at $\textbackslashsqrt{s}$=13 TeV with the ATLAS detector". In: *Physics Letters B* **763** (Dec. 2016). DOI: 10.1016/j.physletb.2016.10.042. URL: http://arxiv.org/abs/1608.02372 (visited on 09/12/2022).

[12] [12]
ATLAS Collaboration. "Search for new phenomena in final states with an energetic jet and large missing transverse momentum in pp collisions at $\textbackslashsqrt{s}$=13$ TeV using the ATLAS detector". In: *Physical Review D* **94**.3 (Aug. 2016). DOI: 10.1103/PhysRevD.94.032005. URL: http://arxiv.org/abs/1604.07773 (visited on 09/12/2022).

[13] [13]
Davi B. Costa, Bogdan A. Dobrescu, and Patrick J. Fox. "General solution to the U(1) anomaly equations". In: *Physical Review Letters* **123**.15 (Oct. 2019). DOI: 10.1103/PhysRevLett.123.151601. URL: http://arxiv.org/abs/1905.13729 (visited on 09/07/2022).

[14] [14]
Yanou Cui and Francesco D'Eramo. "Surprises from Complete Vector Portal Theories: New Insights into the Dark Sector and its Interplay with Higgs Physics". In: *Physical Review D* **96**.9 (Nov. 2017). DOI: 10.1103/PhysRevD.96.095006. URL: http://arxiv.org/abs/1705.03897 (visited on 10/21/2022).

[15] [15]
Arnon Dar. *Dark Matter and Big Bang Nucleosynthesis*. Apr. 1995. DOI: 10.1086/176078. URL: http://arxiv.org/abs/astro-ph/9504082 (visited on 08/05/2022).

[16] [16]
Valentina De Romeri et al. "Dark Matter and the elusive $\textbackslashmathbf{Z'}$ in a dynamical Inverse Seesaw scenario". In: *Journal of High Energy Physics* **2017**.10 (Oct. 2017). DOI: 10.1007/JHEP10(2017)169. URL: http://arxiv.org/abs/1707.08606 (visited on 09/07/2022).

[17] [17]
Bogdan A. Dobrescu and Patrick J. Fox. *Diophantine equations with sum of cubes and cube of sum*. Dec. 2020. URL: http://arxiv.org/abs/2012.04139 (visited on 09/07/2022).

[18] [18]
Michael Duerr, Pavel Fileviez Perez, and Mark B. Wise. "Gauge Theory for Baryon and Lepton Numbers with Leptoquarks". In: *Physical Review Letters*

110.23 (June 2013). DOI: 10.1103/PhysRevLett.110.231801. URL: http://arxiv.org/abs/1304.0576 (visited on 09/07/2022).

[19] [19]
John Ellis, Malcolm Fairbairn, and Patrick Tunney. *Anomaly-Free Dark Matter Models are not so Simple*. Aug. 2017. DOI: 10.1007/JHEP08(2017)053. URL: http://arxiv.org/abs/1704.03850 (visited on 09/07/2022).

[20] [20]
Jonathan L. Feng. "Dark Matter Candidates from Particle Physics and Methods of Detection". In: *Annual Review of Astronomy and Astrophysics* **48**.1 (Aug. 2010). DOI: 10.1146/annurev-astro-082708-101659. URL: http://arxiv.org/abs/1003.0904 (visited on 08/04/2022).

[21] [21]
Graciela B. Gelmini. *TASI 2014 Lectures: The Hunt for Dark Matter*. June 2015. URL: http://arxiv.org/abs/1502.01320 (visited on 08/04/2022).

[22] [22]
Karim Ghorbani and Hossein Ghorbani. "Two-portal Dark Matter". In: *Physical Review D* **91**.12 (June 2015). DOI: 10.1103/PhysRevD.91.123541. URL: http://arxiv.org/abs/1504.03610 (visited on 09/07/2022).

[23] [23]
"Heart of darkness; unraveling the mysteries of the invisible universe.." The Free Library. 2013 Ringgold, Inc. 05 Aug. 2022.

[24] [24]
D Hooper, M Kaplinghat, and K Matchev. "Complementarity of Dark Matter Experiments". In: (2013).

[25] [25]
Dan Hooper. *TASI 2008 Lectures on Dark Matter*. Jan. 2009. URL: http://arxiv.org/abs/0901.4090 (visited on 08/04/2022).

[26] [26]
http://cdn.eso.org/images/screen/eso1426b.jpg.

[27] [27]
https://astronomy.swin.edu.au/cms/cpg15x/albums/userpics/rotationcurve1.jpg.

[28] [28]
https://cds.cern.ch/record/2272942/files/figures_lim_WW_AMS.png.

[29] [29]
https://earimediaprodweb.azurewebsites.net/Api/v1/Multimedia/166dd91a-bee3-485e-bd5e-57e79c82713e/Rendition/low-res/Content/Public.

[30] [30]
https://encrypted-tbn0.gstatic.com/images?q=tbn:ANd9GcTlVMmLccS__Rqfp27fyvoS6mMdT

[31] [31]
https://en.wikipedia.org/wiki/Coma_Cluster.

[32] [32]
https://hubblesite.org/files/live/sites/hubble/files/home/resource-gallery/articles/_images/hs-article-0720a-2400x1840.jpg.

[33] [33]
https://images.zapnito.com/uploads/8c67f901884712e601c84a273cc5ee54/c9e6feb3-3a43-4b9b-b68e-672efdf86dc2.png.

[34] [34]
https://i.stack.imgur.com/Qx0Cv.png.
[35] [35]
https://upload.wikimedia.org/wikipedia/commons/0/0b/Planck_satellite_cmb.jpg.
[36] [36]
https://www.esa.int/var/esa/storage/images/esa_multimedia/images/2007/07/the_bullet_clus
2-eng-GB/The_Bullet_Cluster.jpg.
[37] [37]
*https://www.esa.int/var/esa/storage/images/esa_multimedia/images/2013/03/planck_power_*
5-eng-GB/Planck_Power_Spectrum_pillars.jpg.
[38] [38]
https://www.frontiersin.org/files/MyHome%20Article%20Library/453682/453682_Thumb_400
[39] [39]
https://www.researchgate.net/profile/Luis-Padilla-9/publication/328474806/figure/fig1/AS:685097212719115@1540351312825/Temperature-fluctuations-observed-in-the-CMB-using-COBE-WMAP-Planck-data-Gold-et-al.ppm.
[40] [40]
Marco Hufnagel, Kai Schmidt-Hoberg, and Sebastian Wild. "BBN constraints on MeV-scale dark sectors. Part II. Electromagnetic decays". In: *Journal of Cosmology and Astroparticle Physics* **2018**.11 (Nov. 2018). DOI: 10.1088/1475-7516/2018/11/032. URL: http://arxiv.org/abs/1808.09324 (visited on 08/05/2022).
[41] [41]
Felix Kahlhoefer et al. "Implications of unitarity and gauge invariance for simplified dark matter models". In: *Journal of High Energy Physics* **2016**.2 (Feb. 2016). DOI: 10.1007/JHEP02(2016)016. URL: http://arxiv.org/abs/1510.02110 (visited on 10/21/2022).
[42] [42]
Paul Langacker. "The Physics of Heavy Z' Gauge Bosons". In: *Reviews of Modern Physics* **81**.3 (Aug. 2009). DOI: 10.1103/RevModPhys.81.1199. URL: http://arxiv.org/abs/0801.1345 (visited on 09/07/2022).
[43] [43]
Benjamin W. Lee, C. Quigg, and H. B. Thacker. "Weak interactions at very high energies: The role of the Higgs-boson mass". In: *Physical Review D* **16**.5 (Sept. 1977). DOI: 10.1103/PhysRevD.16.1519. URL: https://link.aps.org/doi/10.1103/PhysRevD.16.1519 (visited on 10/21/2022).
[44] [44]
Mariangela Lisanti. "Lectures on Dark Matter Physics". In: *New Frontiers in Fields and Strings*. Jan. 2017. DOI: 10.1142/9789813149441_0007. URL: http://arxiv.org/abs/1603.03797 (visited on 08/04/2022).
[45] [45]
Satomi Okada. *$Z^\textbackslashprime$ portal dark matter in the minimal $B-L$ model*. May 2018. URL: http://arxiv.org/abs/1803.06793 (visited on 09/07/2022).
[46] [46]

Pavel Fileviez Perez et al. "On Anomaly-Free Dark Matter Models". In: *Physical Review D* **100**.1 (July 2019). DOI: 10.1103/PhysRevD.100.015017. URL: http://arxiv.org/abs/1904.01017 (visited on 09/07/2022).

[47] [47]
Tania Robens and Tim Stefaniak. "LHC Benchmark Scenarios for the Real Higgs Singlet Extension of the Standard Model". In: *The European Physical Journal C* **76**.5 (May 2016). DOI: 10.1140/epjc/s10052-016-4115-8. URL: http://arxiv.org/abs/1601.07880 (visited on 09/13/2022).

[48] [48]
Jorge C. Romao and Joao P. Silva. "A resource for signs and Feynman diagrams of the Standard Model". In: *International Journal of Modern Physics A* **27**.26 (Oct. 2012). DOI: 10.1142/S0217751X12300256. URL: http://arxiv.org/abs/1209.6213 (visited on 08/08/2022).

[49] [49]
Matthew D. Schwartz. *Quantum Field Theory and the Standard Model*. 1st ed. Cambridge University Press, Dec. 2013. ISBN: 978-1-108-98503-1 978-1-107-03473-0. DOI: 10.1017/9781139540940. URL: https://www.cambridge.org/core/product/identifier/9781108985031/type/book (visited on 08/08/2022).

[50] [50]
Jing Shu. "Unitarity Bounds for New Physics from Axial Coupling at LHC". In: *Physical Review D* **78**.9 (Nov. 2008). DOI: 10.1103/PhysRevD.78.096004. URL: http://arxiv.org/abs/0711.2516 (visited on 10/21/2022).

[51] [51]
Igor Tkachev. "Cosmology and Dark Matter". In: *CERN Yellow Reports: School Proceedings* (Dec. 2017). DOI: 10.23730/CYRSP-2017-005.259. URL: https://e-publishing.cern.ch/index.php/CYRSP/article/view/444 (visited on 08/06/2022).

[52] [52]
Zwicky, F. Die Rotverschiebung von extragalaktischen Nebeln. Helvetica Physica Acta 6, 110–127 (1933).